

**Modern Video Compression and  
Communications over Wireless Channels:  
From Second to Third Generation Systems,  
WLANs and Beyond**

by

**©L. Hanzo, P.J. Cherriman, J. Streit**  
Department of Electronics and Computer Science,  
University of Southampton, UK

# Contents

<b>Preface and Motivation</b>	<b>1</b>
<b>Acknowledgements</b>	<b>7</b>
<b>Contributors</b>	<b>9</b>
<b>I Transmission Issues</b>	<b>11</b>
<b>1 Communications Theory</b>	<b>13</b>
1.1 Issues in Communications Theory . . . . .	13
1.2 AWGN Channel . . . . .	17
1.2.1 Background . . . . .	17
1.2.2 Practical Gaussian Channels . . . . .	17
1.2.3 Gaussian Noise . . . . .	18
1.3 Information of a Source . . . . .	21
1.4 Entropy . . . . .	22
1.4.1 Maximum entropy of a binary source . . . . .	23
1.4.2 Maximum entropy of a $q$ -ary source . . . . .	25
1.5 Source Coding . . . . .	25
1.5.1 Shannon-Fano Coding . . . . .	26
1.5.2 Huffman coding . . . . .	28
1.6 Entropy of Sources Exhibiting Memory . . . . .	32
1.6.1 Two-State Markov Model for Discrete Sources Exhibiting Memory	32
1.6.2 N-State Markov Model for Discrete Sources Exhibiting Memory	33
1.7 Examples . . . . .	35
1.7.1 Four-state Markov Model for a two-bit quantiser . . . . .	35
1.7.2 Two-state Markov model example . . . . .	36
1.8 Generating Model Sources . . . . .	38
1.8.1 Autoregressive model . . . . .	38
1.8.2 AR model properties . . . . .	39

1.8.3	First-order Markov model . . . . .	40
1.9	Run-length Coding . . . . .	41
1.9.1	Run-length coding principle . . . . .	41
1.9.2	RLC efficiency . . . . .	42
1.10	Transmission via Discrete Channels . . . . .	44
1.10.1	Binary Symmetric Channel Example . . . . .	44
1.10.2	Bayes' Rule . . . . .	46
1.10.3	Mutual information . . . . .	49
1.10.4	Mutual Information Example . . . . .	50
1.10.5	Information loss via imperfect channels . . . . .	51
1.10.6	Error entropy via imperfect channels . . . . .	53
1.11	Capacity of discrete channels . . . . .	59
1.12	Shannon's Channel Coding Theorem . . . . .	61
1.13	Capacity of Continuous Channels . . . . .	64
1.13.1	Practical evaluation of the Shannon-Hartley Law . . . . .	67
1.13.2	Ideal Communications System . . . . .	71
1.14	Shannon's Message for Wireless Channels . . . . .	72
<b>2</b>	<b>The Propagation Environment</b>	<b>75</b>
2.1	The Cellular Concept . . . . .	75
2.2	Radio Wave Propagation . . . . .	79
2.2.1	Background . . . . .	79
2.2.2	Narrow-band fading Channels . . . . .	81
2.2.3	Propagation Pathloss Law . . . . .	82
2.2.4	Slow Fading Statistics . . . . .	84
2.2.4.1	Fast Fading Statistics . . . . .	85
2.2.4.2	Doppler Spectrum . . . . .	91
2.2.4.3	Simulation of Narrowband Fading Channels . . . . .	93
2.2.4.3.1	Frequency-domain fading simulation . . . . .	94
2.2.4.3.2	Time-domain fading simulation . . . . .	94
2.2.4.3.3	Box-Müller Algorithm of AWGN generation . . . . .	95
2.2.5	Wideband Channels . . . . .	96
2.2.5.1	Modelling of Wideband Channels . . . . .	96
<b>3</b>	<b>Convolutional Channel Coding</b>	<b>101</b>
3.1	Brief Channel Coding History . . . . .	101
3.2	Convolutional Encoding . . . . .	102
3.3	State and Trellis Transitions . . . . .	104
3.4	The Viterbi Algorithm . . . . .	106
3.4.1	Error-free hard-decision Viterbi decoding . . . . .	106
3.4.2	Erroneous hard-decision Viterbi decoding . . . . .	109
3.4.3	Error-free soft-decision Viterbi decoding . . . . .	112

**CONTENTS**

<b>4</b>	<b>Block-based Channel Coding</b>	<b>115</b>
4.1	Introduction . . . . .	115
4.2	Finite Fields . . . . .	116
4.2.1	Definitions . . . . .	116
4.2.2	Galois Field Construction . . . . .	119
4.2.3	Galois Field Arithmetic . . . . .	121
4.3	RS and BCH Codes . . . . .	122
4.3.1	Definitions . . . . .	122
4.3.2	RS Encoding . . . . .	124
4.3.3	RS Encoding Example . . . . .	126
4.3.4	Circuits for Cyclic Encoders . . . . .	128
4.3.4.1	Polynomial Multiplication . . . . .	128
4.3.4.2	Shift Register Encoding Example . . . . .	130
4.3.5	RS Decoding . . . . .	133
4.3.5.1	Formulation of the Key-Equations [1–9] . . . . .	133
4.3.5.2	Peterson-Gorenstein-Zierler Decoder . . . . .	138
4.3.5.3	PGZ Decoding Example . . . . .	140
4.3.5.4	Berlekamp-Massey algorithm [1–9] . . . . .	145
4.3.5.5	Berlekamp-Massey Decoding Example . . . . .	151
4.3.5.6	Forney Algorithm . . . . .	155
4.3.5.7	Forney Algorithm Example . . . . .	159
4.3.5.8	Error Evaluator Polynomial Computation . . . . .	161
4.4	RS and BCH Codec Performance . . . . .	164
4.5	Summary and Conclusions . . . . .	166
<b>5</b>	<b>Modulation and Transmission</b>	<b>169</b>
5.1	Modulation Issues . . . . .	169
5.1.1	Choice of Modulation . . . . .	169
5.1.2	Quadrature Amplitude Modulation [10] . . . . .	171
5.1.2.1	Background . . . . .	171
5.1.2.2	Modem Schematic . . . . .	172
5.1.2.2.1	Gray Mapping and Phasor Constellation . . . . .	172
5.1.2.2.2	Nyquist Filtering . . . . .	175
5.1.2.2.3	Modulation and demodulation . . . . .	177
5.1.2.2.4	Data recovery . . . . .	179
5.1.2.3	QAM Constellations . . . . .	179
5.1.2.4	16QAM BER versus SNR Performance over AWGN Channels . . . . .	182
5.1.2.4.1	Decision Theory . . . . .	182
5.1.2.4.2	QAM modulation and transmission . . . . .	184
5.1.2.4.3	16-QAM Demodulation . . . . .	185
5.1.2.5	Reference Assisted Coherent QAM for Fading Channels	188
5.1.2.5.1	PSAM System Description . . . . .	188
5.1.2.5.2	Channel Gain Estimation in PSAM . . . . .	191
5.1.2.5.3	PSAM performance [11] . . . . .	192
5.1.2.6	Differentially detected QAM [10] . . . . .	193

5.1.3	Adaptive Modulation . . . . .	197
5.1.3.1	Background to Adaptive Modulation . . . . .	197
5.1.3.2	Optimisation of Adaptive Modems . . . . .	200
5.1.3.3	Adaptive Modulation Performance . . . . .	202
5.1.3.4	Equalisation Techniques . . . . .	204
5.1.4	Orthogonal Frequency Division Modulation . . . . .	204
5.2	Packet Reservation Multiple Access . . . . .	208
5.3	Flexible Transceiver Architecture . . . . .	210
<b>6</b>	<b>Traffic modelling and multiple access</b>	<b>213</b>
6.1	Video traffic modelling . . . . .	213
6.1.1	Motivation and Background . . . . .	213
6.1.2	Markov Modelling of Video Sources . . . . .	215
6.1.3	Reduced-length Poisson Cycles . . . . .	218
6.1.4	Video Model Matching . . . . .	224
6.2	Multiple Access . . . . .	231
6.2.1	Background . . . . .	231
6.2.2	Classification of multiple access techniques . . . . .	233
6.2.3	Multi-frame packet reservation multiple access . . . . .	235
6.2.3.1	Performance of MF-PRMA . . . . .	236
6.2.4	Statistical Packet Assignment Multiple Access . . . . .	245
6.2.4.1	Statistical Packet Assignment Principles . . . . .	245
6.2.4.2	Performance of the SPAMA Protocol . . . . .	250
6.3	Summary and Conclusions . . . . .	254
<b>7</b>	<b>Co-Channel Interference</b>	<b>255</b>
7.1	Introduction . . . . .	255
7.2	Co-Channel Interference factors . . . . .	256
7.2.1	Effect of fading . . . . .	256
7.2.2	Cell Shapes . . . . .	257
7.2.3	Position of Users and Interferers . . . . .	259
7.3	Theoretical Signal-to-Interference-ratio . . . . .	259
7.4	Simulation Parameters . . . . .	263
7.5	Results for Multiple Interferers . . . . .	266
7.5.1	SIR Profile of Cell . . . . .	266
7.5.2	Signal to noise plus interference ratio (SINR) . . . . .	270
7.5.3	Channel Capacity . . . . .	271
7.6	Results for a Single Interferer . . . . .	276
7.6.1	Simple model for SINR in a single interferer situation . . . . .	277
7.6.2	Effect of SIR and SNR on error rates . . . . .	280
7.6.3	Time varying effects of SIR and SINR . . . . .	283
7.6.4	Effect of Interference on the H.263 videophone system . . . . .	288
7.7	Conclusions . . . . .	292

**CONTENTS**

v

<b>8</b>	<b>Channel Allocation</b>	<b>293</b>
8.1	Introduction . . . . .	293
8.2	Overview of Channel Allocation . . . . .	294
8.2.1	Fixed Channel Allocation . . . . .	296
8.2.1.1	Channel Borrowing . . . . .	297
8.2.1.2	Flexible channel allocation . . . . .	298
8.2.2	Dynamic channel allocation . . . . .	298
8.2.2.1	Centrally Controlled DCA Algorithms . . . . .	301
8.2.2.2	Distributed DCA Algorithms . . . . .	301
8.2.2.3	Locally Distributed DCA Algorithms . . . . .	302
8.2.3	Hybrid channel allocation . . . . .	304
8.2.4	The Effect of Handovers . . . . .	304
8.2.5	The Effect of Transmission Power Control . . . . .	305
8.3	Channel Allocation Simulation . . . . .	305
8.3.1	The Mobile Radio Network Simulator, "Netsim" . . . . .	306
8.3.1.1	Physical Layer Model . . . . .	308
8.3.1.2	Shadow Fading Model . . . . .	309
8.3.2	Channel Allocation Algorithms Investigated . . . . .	310
8.3.2.1	Fixed Channel Allocation Algorithm . . . . .	310
8.3.2.2	Distributed Dynamic Channel Allocation Algorithms . . . . .	311
8.3.2.3	Locally Distributed Dynamic Channel Allocation Algorithms . . . . .	312
8.3.3	Performance Metrics . . . . .	314
8.3.4	Non-Uniform Traffic Model . . . . .	315
8.4	Performance Comparisons . . . . .	316
8.4.1	System Parameters . . . . .	316
8.4.2	Carried Traffic with quality constraints . . . . .	318
8.4.3	Comparing the LOLIA with FCA . . . . .	320
8.4.4	Effect of the "Reuse Distance" Constraint on the LOLIA and LOMIA DCA algorithms . . . . .	322
8.4.5	Comparison of the LOLIA and LOMIA with the LIA . . . . .	324
8.4.6	Interference threshold based distributed DCA algorithms . . . . .	325
8.4.7	Performance comparison of fixed and dynamic channel allocation algorithms using non-uniform traffic distributions . . . . .	327
8.4.8	Effect of shadow fading on the FCA, LOLIA and LOMIA . . . . .	330
8.4.9	Effect of shadow fading frequency and standard deviation on the LOLIA . . . . .	331
8.4.10	Effect of shadow fading standard deviation on FCA and LOLIA . . . . .	333
8.4.11	SINR profile across cell area . . . . .	335
8.4.12	Overview of Results . . . . .	338
8.5	Conclusions . . . . .	341
<b>9</b>	<b>Video Over Second Generation Mobile Systems</b>	<b>345</b>
9.1	The Wireless Communications Scene . . . . .	345
9.2	Global System of Mobile Communications - GSM . . . . .	348
9.2.1	Introduction to GSM . . . . .	348

9.2.2	Overview of GSM . . . . .	351
9.2.3	Logical and Physical Channels in GSM . . . . .	352
9.2.4	Speech and Data Transmission in GSM . . . . .	353
9.2.5	Transmission of Control Signals in GSM . . . . .	358
9.2.6	Synchronisation Issues in GSM . . . . .	363
9.2.7	Gaussian Minimum Shift Keying in GSM . . . . .	364
9.2.8	Wideband Channel Models in GSM . . . . .	365
9.2.9	Adaptive Link Control in GSM . . . . .	366
9.2.10	Discontinuous Transmission in GSM . . . . .	369
9.2.11	Summary of GSM Features . . . . .	369
<b>10</b>	<b>Third-generation CDMA Systems</b>	<b>371</b>
10.1	Introduction . . . . .	371
10.2	Basic CDMA System . . . . .	372
10.2.1	Spread Spectrum Fundamentals . . . . .	372
10.2.1.1	Frequency Hopping . . . . .	373
10.2.1.2	Direct Sequence . . . . .	374
10.2.2	The Effect of Multipath Channels . . . . .	377
10.2.3	RAKE receiver . . . . .	380
10.2.4	Multiple Access . . . . .	384
10.2.4.1	Downlink Interference . . . . .	385
10.2.4.2	Uplink Interference . . . . .	386
10.2.4.3	Gaussian Approximation . . . . .	389
10.2.5	Spreading Codes . . . . .	390
10.2.5.1	<i>m</i> -sequences . . . . .	391
10.2.5.2	Gold Sequences . . . . .	392
10.2.5.3	Extended <i>m</i> -sequences . . . . .	393
10.2.6	Channel Estimation . . . . .	393
10.2.6.1	Downlink Pilot Assisted Channel Estimation . . . . .	394
10.2.6.2	Uplink Pilot Symbol-assisted channel estimation . . . . .	395
10.2.6.3	Pilot Symbol Assisted Decision-Directed Channel Estimation . . . . .	396
10.2.7	Summary . . . . .	398
10.3	Third Generation Systems . . . . .	399
10.3.1	Introduction . . . . .	399
10.3.2	UMTS/IMT-2000 Terrestrial Radio Access . . . . .	401
10.3.2.1	Characteristics of UTRA/IMT-2000 . . . . .	402
10.3.2.2	Transport Channels . . . . .	405
10.3.2.3	Physical Channels . . . . .	407
10.3.2.3.1	UTRA Physical Channels . . . . .	408
10.3.2.3.2	IMT-2000 Physical Channels . . . . .	411
10.3.2.4	Service Multiplexing and Channel Coding in UTRA/IMT-2000 . . . . .	415
10.3.2.4.1	Mapping Several Speech Services to the Physical Channels in FDD Mode . . . . .	417

CONTENTS

vii

10.3.2.4.2	Mapping a 2.048 Mbps Data Service to the Physical Channels in TDD Mode . . . . .	420
10.3.2.5	Variable Rate and Multicode Transmission in UTRA/IMT-2000 . . . . .	422
10.3.2.6	Spreading and Modulation . . . . .	422
10.3.2.6.1	Orthogonal Variable Spreading Factor Codes in UTRA/ IMT-2000 . . . . .	423
10.3.2.6.2	Uplink Spreading and Modulation . . . . .	426
10.3.2.6.3	Downlink Spreading and Modulation . . . . .	428
10.3.2.7	Random Access . . . . .	429
10.3.2.8	Power Control . . . . .	431
10.3.2.8.1	Closed Loop Power Control in UTRA/IMT-2000 . . . . .	431
10.3.2.8.2	Open Loop Power Control During the Mobile Station's Access . . . . .	432
10.3.2.9	Cell Identification . . . . .	433
10.3.2.10	Handover . . . . .	435
10.3.2.10.1	Intra-frequency Handover or Soft Handover . . . . .	435
10.3.2.10.2	Inter-frequency Handover or Hard Handover . . . . .	436
10.3.2.11	Inter-cell Time Synchronization in the UTRA/ IMT-2000 TDD mode . . . . .	437
10.3.3	The cdma2000 Terrestrial Radio Access . . . . .	437
10.3.3.1	Characteristics of cdma2000 . . . . .	439
10.3.3.2	Physical Channels in cdma2000 . . . . .	440
10.3.3.3	Service Multiplexing and Channel Coding . . . . .	442
10.3.3.4	Spreading and Modulation . . . . .	443
10.3.3.4.1	Downlink Spreading and Modulation . . . . .	444
10.3.3.4.2	Uplink Spreading and Modulation . . . . .	446
10.3.3.5	Random Access . . . . .	448
10.3.3.6	Handover . . . . .	450
10.3.4	Performance Enhancement Features . . . . .	451
10.3.4.1	Adaptive Antennas . . . . .	451
10.3.4.2	Multiuser Detection/Interference Cancellation . . . . .	451
10.3.4.3	Transmit Diversity . . . . .	452
10.3.4.3.1	Time Division Transmit Diversity . . . . .	452
10.3.4.3.2	Orthogonal Transmit Diversity . . . . .	452
10.3.5	Summary of 3G Systems . . . . .	452
10.4	Non-Coherent $M$ -ary Modulated CDMA . . . . .	453
10.4.1	Background . . . . .	453
10.4.2	Fundamentals of $M$ -ary Orthogonal Modulation . . . . .	454
10.4.3	Fundamentals of $M$ -ary CDMA . . . . .	456
10.4.3.1	System Model . . . . .	456
10.4.3.1.1	The Transmitter Model . . . . .	456
10.4.3.1.2	Channel Model . . . . .	459
10.4.3.1.3	The Receiver Model . . . . .	460
10.4.3.2	Performance Analysis . . . . .	464



10.4.3.2.1	Noise analysis . . . . .	465
10.4.3.2.2	Self-interference analysis . . . . .	465
10.4.3.2.3	MAI analysis . . . . .	466
10.4.3.2.4	Decision Statistic and Error Probability . . . . .	466
10.4.3.3	Bandwidth Efficiency in $M$ -ary modulated CDMA . . . . .	469
10.4.3.4	Numerical Simulation Results . . . . .	469
10.4.4	RNS-based Orthogonal Modulation . . . . .	475
10.4.4.1	Residue Number System - An Overview . . . . .	477
10.4.4.1.1	Background . . . . .	477
10.4.4.1.2	Decimal-to-residue conversion . . . . .	478
10.4.4.1.3	Residue-to-decimal conversion . . . . .	480
10.4.4.1.3.1	Chinese Remainder Theorem . . . . .	480
10.4.4.1.3.2	Mixed Radix Conversion . . . . .	481
10.4.4.1.4	Redundant Residue Number System . . . . .	482
10.4.4.1.4.1	Conversion by discarding . . . . .	483
10.4.4.2	RNS-based Modulation Basics . . . . .	483
10.4.4.2.1	Transmitter Model . . . . .	484
10.4.4.2.2	Receiver Model . . . . .	485
10.4.4.2.3	Performance Analysis . . . . .	487
10.4.4.2.4	Simulation results . . . . .	490
10.4.5	Summary . . . . .	496
10.5	Chapter Summary . . . . .	497
10.6	Mathematical Derivations . . . . .	497
10.6.1	Derivation of Equations 10.65 and 10.65 . . . . .	497
10.6.1.1	In-phase channel . . . . .	497
10.6.1.2	Quadrature channel . . . . .	499
10.6.2	Derivation of Equation 10.79 . . . . .	499
 <b>II Video Systems based on Proprietary Video Codecs</b>		<b>501</b>
 <b>11 Fractal Image Codecs</b>		<b>503</b>
11.1	Fractal Principles . . . . .	503
11.2	One Dimensional Fractal Coding . . . . .	506
11.2.1	Fractal Codec Design . . . . .	510
11.2.2	Fractal Codec Performance . . . . .	511
11.3	Error sensitivity and Complexity . . . . .	515
11.4	Summary and Conclusions . . . . .	517
 <b>12 Very Low Bitrate DCT Codecs and Multimode Videophone Transceivers</b>		<b>519</b>
12.1	Video Codec Outline . . . . .	519
12.2	The Principle of Motion Compensation . . . . .	521
12.2.1	Distance measures . . . . .	525
12.2.2	Motion Search algorithms . . . . .	526
12.2.2.1	Full or Exhaustive Motion Search . . . . .	527
12.2.2.2	Gradient Based Motion Estimation . . . . .	528

CONTENTS

ix

12.2.2.3	Hierarchical or Tree Search . . . . .	529
12.2.2.4	Subsampling search . . . . .	530
12.2.2.5	Post-processing of motion vectors . . . . .	531
12.2.2.6	Gain-Cost Controlled Motion Compensation . . . . .	531
12.2.3	Other Motion Estimation Techniques . . . . .	533
12.2.3.1	Pel-Recursive Displacement Estimation . . . . .	534
12.2.3.2	Grid Interpolation Techniques . . . . .	534
12.2.3.3	MC using higher order transformations . . . . .	534
12.2.3.4	MC in the transform domain . . . . .	535
12.2.4	Conclusion . . . . .	535
12.3	Transform Coding . . . . .	537
12.3.1	One-dimensional Transform Coding . . . . .	537
12.3.2	Two-dimensional Transform Coding . . . . .	538
12.3.3	Quantiser Training for Single Class DCT . . . . .	541
12.3.4	Quantiser Training for Multi Class DCT . . . . .	542
12.4	The Codec Outline . . . . .	544
12.5	Initial Intra Frame Coding . . . . .	547
12.6	Gain-Controlled Motion Compensation . . . . .	547
12.7	The MCER Active / Passive Concept . . . . .	548
12.8	Partial Forced Update . . . . .	549
12.9	The Gain/Cost Controlled Inter Frame Codec . . . . .	551
12.9.1	Complexity Considerations and Reduction Techniques . . . . .	553
12.10	The Bit Allocation Strategy . . . . .	554
12.11	Results . . . . .	555
12.12	DCT-codec performance under erroneous conditions . . . . .	557
12.12.1	Bit sensitivity . . . . .	558
12.12.2	Bit-sensitivity of Codec I and II . . . . .	560
12.13	DCT-based Low-rate Video Transceivers . . . . .	561
12.13.1	Choice of Modem . . . . .	561
12.13.2	Source-matched Transceiver . . . . .	562
12.13.2.1	System 1 . . . . .	562
12.13.2.1.1	System Concept . . . . .	562
12.13.2.1.2	Sensitivity-matched Modulation . . . . .	563
12.13.2.1.3	Source Sensitivity . . . . .	563
12.13.2.1.4	Forward Error Correction . . . . .	563
12.13.2.1.5	Transmission Format . . . . .	564
12.13.2.2	System 2 . . . . .	565
12.13.2.2.1	Automatic Repeat Request . . . . .	567
12.13.2.3	Systems 3-5 . . . . .	571
12.14	System Performance . . . . .	571
12.14.1	Performance of System 1 . . . . .	571
12.14.2	Performance of System 2 . . . . .	578
12.14.2.1	FER Performance . . . . .	578
12.14.2.2	Slot Occupancy Performance . . . . .	578
12.14.2.3	PSNR Performance . . . . .	579
12.14.3	Performance of Systems 3-5 . . . . .	579

12.15	Summary and Conclusions . . . . .	580
<b>13</b>	<b>Very Low Bitrate VQ Codecs and Multimode Videophone Transceivers</b>	<b>583</b>
13.1	Introduction . . . . .	583
13.2	The Codebook Design . . . . .	583
13.3	The Vector Quantiser Design . . . . .	587
13.3.1	Mean and Shape Gain Vector-Quantisation . . . . .	590
13.3.2	Adaptive Vector Quantisation . . . . .	592
13.3.3	Classified Vector Quantisation . . . . .	594
13.3.4	Algorithmic Complexity . . . . .	594
13.4	Performance under erroneous conditions . . . . .	596
13.4.1	Bit allocation strategy . . . . .	596
13.4.2	Bit sensitivity . . . . .	598
13.5	VQ-based Low-rate Video Transceivers . . . . .	599
13.5.1	Choice of Modulation . . . . .	599
13.5.2	Forward Error Correction . . . . .	600
13.5.3	Architecture of System 1 . . . . .	601
13.5.4	Architecture of System 2 . . . . .	602
13.5.5	Architecture of Systems 3-6 . . . . .	604
13.6	System Performance . . . . .	605
13.6.1	Simulation Environment . . . . .	605
13.6.2	Performance of Systems 1 and 3 . . . . .	607
13.6.3	Performance of Systems 4 and 5 . . . . .	609
13.6.4	Performance of Systems 2 and 6 . . . . .	610
13.7	Summary and Conclusions . . . . .	610
<b>14</b>	<b>Quad-Tree Based Codecs</b>	<b>613</b>
14.1	Introduction . . . . .	613
14.2	Quad-Tree Decomposition . . . . .	614
14.3	Quad-Tree Intensity Match . . . . .	617
14.3.1	Zero-order Intensity Match . . . . .	617
14.3.2	First-order Intensity Match . . . . .	618
14.3.3	Decomposition Algorithmic Issues . . . . .	619
14.4	Model-based Parametric Enhancement . . . . .	622
14.4.1	Eye and mouth detection . . . . .	623
14.4.2	Parametric Codebook Training . . . . .	626
14.4.3	Parametric Encoding . . . . .	626
14.5	The Enhanced QT Codec . . . . .	628
14.6	Performance and Considerations under erroneous conditions . . . . .	629
14.6.1	Bit Allocation . . . . .	630
14.6.2	Bit Sensitivity . . . . .	632
14.7	QT-codec based Video Transceivers . . . . .	632
14.7.1	Channel Coding and Modulation . . . . .	632
14.7.2	QT-based Transceiver Architectures . . . . .	634
14.8	QT-based Video-transceiver Performance . . . . .	636
14.9	Summary of QT-based Video Transceivers . . . . .	641

**CONTENTS**

xi

14.10 Summary of Low-rate Codecs/Transceivers . . . . . 642

**III High-Resolution Image Coding 647**

Introduction and Video Formats . . . . . 649

**15 Low Complexity Techniques 655**

15.1 Differential Pulse Code Modulation . . . . . 655  
 15.1.1 Basic Differential Pulse Code Modulation . . . . . 655  
 15.1.2 Intra/Inter-frame Differential Pulse Code Modulation . . . . . 657  
 15.1.3 Adaptive Differential Pulse Code Modulation . . . . . 659  
 15.2 Block Truncation Coding . . . . . 659  
 15.2.1 The Block Truncation Algorithm . . . . . 660  
 15.2.2 Block Truncation Codec Implementations . . . . . 662  
 15.2.3 Intra-frame Block Truncation Coding . . . . . 662  
 15.2.4 Inter-frame Block Truncation Coding . . . . . 665  
 15.3 Subband Coding . . . . . 667  
 15.3.1 Perfect Reconstruction Quadrature Mirror Filtering . . . . . 668  
 15.3.1.1 Analysis Filtering . . . . . 668  
 15.3.1.2 Synthesis Filtering . . . . . 671  
 15.3.1.3 Practical QMF Design Constraints . . . . . 673  
 15.3.2 Practical Quadrature Mirror Filters . . . . . 675  
 15.4 Run-length based intra-frame subband coding . . . . . 679  
 15.4.1 Max-Lloyd based subband coding . . . . . 682  
 15.5 Summary and Conclusions . . . . . 686

**16 High-Resolution DCT Coding 689**

16.1 Introduction . . . . . 689  
 16.2 The Intra-frame Quantiser Training . . . . . 689  
 16.3 Motion Compensation for High Quality Images . . . . . 694  
 16.4 Inter-frame DCT Coding . . . . . 700  
 16.4.1 Properties of the DCT transformed MCER . . . . . 700  
 16.4.2 Joint motion compensation and residual encoding . . . . . 707  
 16.5 The Proposed Codec . . . . . 709  
 16.5.1 Motion Compensation . . . . . 710  
 16.5.2 The Inter / Intra DCT codec . . . . . 712  
 16.5.3 Frame Alignment . . . . . 712  
 16.5.4 Bit Allocation . . . . . 716  
 16.5.5 The Codec Performance . . . . . 716  
 16.5.6 Error Sensitivity and Complexity . . . . . 717  
 16.5.7 Conclusions . . . . . 719

**IV Video Systems based on Standard Video Codecs 723**

**17 H.261 reconfigurable videophone 725**

17.1 Introduction . . . . . 725

17.2	The H.261 video coding standard . . . . .	725
17.2.1	Overview . . . . .	725
17.2.2	Source Encoder . . . . .	726
17.2.3	Coding Control . . . . .	729
17.2.4	Video multiplex coder . . . . .	730
17.2.4.1	Picture Layer . . . . .	730
17.2.4.2	Group of Blocks Layer . . . . .	731
17.2.4.3	Macro block (MB) Layer . . . . .	733
17.2.4.4	Block Layer . . . . .	734
17.2.5	Simulated coding statistics . . . . .	736
17.2.5.1	Fixed-quantiser coding . . . . .	736
17.2.5.2	Variable Quantiser coding . . . . .	738
17.3	Effect of Transmission Errors . . . . .	740
17.3.1	Error Mechanisms . . . . .	740
17.3.2	Error Control Mechanisms . . . . .	742
17.3.2.1	Background . . . . .	742
17.3.2.2	Intra-frame Coding . . . . .	744
17.3.2.3	Automatic Repeat Request . . . . .	744
17.3.2.4	Re-configurable Modulations Schemes . . . . .	744
17.3.2.5	Combined Source/Channel Coding . . . . .	745
17.3.3	Error Resilience of the H.261 Codec . . . . .	746
17.3.4	Error Recovery . . . . .	746
17.3.5	Effects of Errors . . . . .	746
17.3.5.1	Qualitative Error Effects . . . . .	747
17.3.5.2	Quantitative Error Effects . . . . .	749
17.3.5.2.1	Errors in an INTRA-coded frame . . . . .	750
17.3.5.2.2	Errors in an INTER-coded frame . . . . .	752
17.3.5.2.3	Errors in Quantiser indices . . . . .	755
17.3.5.2.4	Errors in an INTER-coded frame with mo- tion vectors . . . . .	757
17.3.5.2.5	Errors in an INTER-coded frame at low rate . . . . .	758
17.4	A Wireless Reconfigurable Videophone . . . . .	761
17.4.1	Introduction . . . . .	761
17.4.2	Objectives . . . . .	761
17.4.3	Bitrate Reduction of the H.261 Codec . . . . .	762
17.4.4	Investigation of macroblock size . . . . .	762
17.4.5	Error correction coding . . . . .	766
17.4.6	Packetisation algorithm . . . . .	766
17.4.6.1	Encoding History List . . . . .	767
17.4.6.2	Macroblock compounding . . . . .	767
17.4.6.3	End of frame effect . . . . .	770
17.4.6.4	Packet transmission feedback . . . . .	771
17.4.6.5	Packet truncation and compounding algorithms . . . . .	771
17.5	H.261 Videophone System Performance . . . . .	772
17.5.1	System Architecture . . . . .	772
17.5.2	System Performance . . . . .	776

**CONTENTS**

xiii

17.6 Summary . . . . .	782
<b>18 Comparison of the H.261 and H.263 codecs</b>	<b>785</b>
18.1 Introduction . . . . .	785
18.2 The H.263 coding algorithms . . . . .	788
18.2.1 Source Coder . . . . .	788
18.2.1.1 Prediction . . . . .	788
18.2.1.2 Motion Compensation and Transform Coding . . . . .	788
18.2.1.3 Quantisation . . . . .	789
18.2.2 Video multiplex coder . . . . .	789
18.2.2.1 Picture Layer . . . . .	791
18.2.2.2 Group of Blocks Layer . . . . .	791
18.2.2.3 H.261 Macroblock Layer . . . . .	792
18.2.2.4 H.263 Macroblock Layer . . . . .	793
18.2.2.5 Block Layer . . . . .	797
18.2.3 Motion compensation . . . . .	798
18.2.3.1 H.263 motion vector predictor . . . . .	799
18.2.3.2 H.263 sub-pixel interpolation . . . . .	800
18.2.4 H.263 negotiable options . . . . .	801
18.2.4.1 Unrestricted motion vector mode . . . . .	801
18.2.4.2 Syntax based arithmetic coding mode . . . . .	803
18.2.4.2.1 Arithmetic coding [12] . . . . .	803
18.2.4.3 Advanced prediction mode . . . . .	805
18.2.4.3.1 Four motion vectors per macroblock . . . . .	806
18.2.4.3.2 Overlapped motion compensation for lumiance . . . . .	806
18.2.4.4 P-B frames mode . . . . .	808
18.3 Performance Results . . . . .	811
18.3.1 Introduction . . . . .	811
18.3.2 H.261 Performance . . . . .	812
18.3.3 H.261/H.263 Performance Comparison . . . . .	815
18.3.4 H.263 Codec Performance . . . . .	818
18.3.4.1 Grey-Scale versus Colour comparison . . . . .	819
18.3.4.2 Comparison of QCIF resolution colour video . . . . .	821
18.3.4.3 Coding performance at various resolutions . . . . .	824
18.4 Conclusions . . . . .	829
<b>19 H.263 mobile videophone system</b>	<b>833</b>
19.1 Introduction . . . . .	833
19.2 H.263 in a mobile environment . . . . .	833
19.2.1 Problems of using H.263 in a mobile environment . . . . .	833
19.2.2 Possible solutions for using H.263 in a mobile environment . . . . .	834
19.2.2.1 Coding video sequences only with Intra frames . . . . .	835
19.2.2.2 Automatic repeat requests . . . . .	835
19.2.2.3 Multi-mode modulation schemes . . . . .	835
19.2.2.4 Combined Source/Channel Coding . . . . .	836

19.3	Error resilient videophone design . . . . .	837
19.3.1	Introduction . . . . .	837
19.3.2	Controlling the bitrate . . . . .	838
19.3.3	Employing FEC codes in the videophone system . . . . .	840
19.3.4	Transmission packet structure . . . . .	841
19.3.5	Coding parameter history list . . . . .	842
19.3.6	The packetisation algorithm . . . . .	844
19.3.6.1	Operational scenarios of the packetising algorithm . . . . .	844
19.4	H.263-based Video System Performance . . . . .	846
19.4.1	System Environment . . . . .	846
19.4.2	Performance Results . . . . .	847
19.4.2.1	Error-free transmission results . . . . .	847
19.4.2.2	Effect of packet dropping on image quality . . . . .	849
19.4.2.3	Image quality versus channel quality without ARQ . . . . .	850
19.4.2.4	Image quality versus channel quality with ARQ . . . . .	851
19.4.3	Comparison of H.263 and H.261 based systems . . . . .	851
19.4.3.1	Performance with antenna diversity . . . . .	853
19.4.3.2	Performance over DECT channels . . . . .	856
19.5	Transmission Feedback . . . . .	863
19.5.1	ARQ issues . . . . .	867
19.5.2	Implementation of transmission feedback . . . . .	868
19.5.2.1	Majority logic coding . . . . .	868
19.6	Conclusions . . . . .	873
<b>20</b>	<b>Error-rate based Power Control</b>	<b>875</b>
20.1	Background . . . . .	875
20.2	Power Control Algorithm . . . . .	875
20.3	Performance of the Power Control . . . . .	880
20.3.1	Frame Error Rate Performance . . . . .	882
20.3.2	Signal-to-Interference Ratio Performance . . . . .	882
20.3.3	SINR performance . . . . .	886
20.4	Multi-Mode Performance . . . . .	886
20.5	Average Transmission Power . . . . .	889
20.6	Parameter Optimisation . . . . .	893
20.6.1	Joint Optimisation of IPC and DPC parameters . . . . .	895
20.6.2	Joint Optimisation of NEF and NFE . . . . .	897
20.6.3	Joint Optimisation of IPSS and DPSS . . . . .	899
20.6.4	Conclusions from optimising the power control algorithm parameters . . . . .	900
20.7	Performance at various speeds . . . . .	901
20.7.1	Power control results for pedestrians . . . . .	901
20.7.2	Channel Fading . . . . .	904
20.7.3	Tracking of slow fading . . . . .	906
20.7.4	Power control error . . . . .	907
20.8	Multiple Interferers . . . . .	911
20.8.1	Frame Error Rate Performance . . . . .	911

**CONTENTS**

**xv**

20.8.2	Further effects of power control on system performance . . . . .	913
20.9	Conclusions . . . . .	915
<b>21</b>	<b>Adaptive Video Systems</b>	<b>917</b>
21.1	Adaptive QAM-based Wireless Videophony . . . . .	917
21.1.1	Introduction . . . . .	917
21.1.2	Adaptive Video Transceiver . . . . .	919
21.1.3	Burst-by-Burst Adaptive Videophone Performance . . . . .	922
21.1.4	Switching Thresholds . . . . .	930
21.1.5	Turbo-coded video performance . . . . .	932
21.1.6	Conclusions . . . . .	935
21.2	A UMTS-like Video-phone System . . . . .	937
21.2.1	Motivation and Video Transceiver Overview . . . . .	937
21.2.2	Multi-mode Video System Performance . . . . .	940
21.2.3	Burst-by-Burst adaptive videophone system . . . . .	945
21.2.4	Conclusions . . . . .	948
21.3	H.263/OFDM-based Video Systems . . . . .	949
21.3.1	Background . . . . .	949
21.3.2	System Overview . . . . .	951
21.3.2.1	The WATM System . . . . .	956
21.3.2.2	The UMTS-type Framework . . . . .	958
21.3.3	The Channel Model . . . . .	959
21.3.4	Video-related System Aspects . . . . .	960
21.3.4.1	Video parameters of the WATM system . . . . .	960
21.3.4.2	Video parameters of the UMTS scheme . . . . .	964
21.3.5	System Performance . . . . .	965
21.3.6	Conclusions . . . . .	968
21.4	Adaptive Turbo-coded OFDM-based Video Telephony . . . . .	969
21.4.1	Motivation and Background . . . . .	969
21.4.2	Burst-by-burst Adaptive Video Transceiver . . . . .	972
21.4.3	AOFDM Modem Mode Adaptation and Signalling . . . . .	972
21.4.4	AOFDM Subband BER Estimation . . . . .	973
21.4.5	Video Compression and Transmission Aspects . . . . .	973
21.4.6	Comparison of subband-adaptive OFDM and fixed mode OFDM transceivers . . . . .	974
21.4.7	Subband-adaptive OFDM transceivers having different target bitrates . . . . .	978
21.4.8	Time-variant target bitrate OFDM transceivers . . . . .	983
21.4.9	Summary and Conclusions . . . . .	994
21.5	Video Broadcasting to Mobile Receivers . . . . .	994
21.5.1	Background and Motivation . . . . .	994
21.5.2	MPEG-2 Bit Error Sensitivity . . . . .	995
21.5.3	DVB Terrestrial Scheme . . . . .	1006
21.5.4	Channel Model . . . . .	1008
21.5.5	Data Partitioning Scheme . . . . .	1009
21.5.6	Performance of Data Partitioning Scheme . . . . .	1017



---

21.5.7 Performance of the DVB Terrestrial Scheme Employing Non-hierarchical Transmission . . . . .	1025
21.5.8 Performance of the DVB Terrestrial Scheme Employing Hierarchical Transmission . . . . .	1028
21.5.9 Conclusions and Future Work . . . . .	1033
21.6 Satellite-based Video Broadcasting . . . . .	1033
21.6.1 Background and Motivation . . . . .	1033
21.6.2 DVB Satellite Scheme . . . . .	1034
21.6.3 Channel Model . . . . .	1035
21.6.4 The blind equalisers . . . . .	1036
21.6.5 Performance of the DVB Satellite Scheme . . . . .	1038
21.6.6 Conclusions and Future Work . . . . .	1050
<b>Glossary</b>	<b>1053</b>
<b>Bibliography</b>	<b>1061</b>

# Preface and Motivation

## The Wireless Multimedia Communications Scene

Against the backdrop of the emerging third - generation wireless personal communications standards and broad-band access network standard proposals, this book is dedicated to a range of topical wireless video communications aspects. *The transmission of multimedia information over wireline based links* can now be considered a mature area, where a range of interactive and distributive services are offered by various providers right across the globe, such as Integrated Services Digital Network (ISDN) based H.261/H.263 assisted video telephony, video on demand services using the Motion Pictures Expert Group (MPEG) video compression standards, multimedia electronic mail, cable television and radio programmes, etc. *A range of interactive mobile multimedia communications services are also realistic in technical terms* at the time of writing and their variety, quality as well as market penetration is expected to exceed that of the wireline oriented services during the next few years.

*The wireless multimedia era is expected to witness a tremendous growth with the emergence of the third-generation (3G) personal communications networks (PCN) and wireless asynchronous transfer mode (WATM) systems*, which constitute a wireless extension of the existing ATM networks. All the three global 3G PCN standard proposals, which originate from the USA, Europe and Japan are based on Code Division Multiple Access (CDMA) and are capable of transmitting at bitrates in excess of 2 Mbps. Furthermore, the European proposal was also designed to support multiple simultaneous calls and services. The WATM solutions often favour Orthogonal frequency Division Multiple Access (OFDM) as their modulation technique and indeed, the imminent so-called Broadband Access Network (BRAN) standard also advocates OFDM. A range of WATM video aspects and mobile digital video broadcast (DVB) issues are also reviewed in Part IV of the book.

Research is also well under way towards the definition of a whole host of new modulation and signal processing techniques and a further trend is likely to dominate this new era, namely **the merger of wireless multimedia communications, multimedia consumer electronics and multimedia computer technologies**. These trends are likely to hallmark the community's future research in the forthcoming years. This book is naturally limited in terms of its coverage of these aspects, simply due to space limitations. We endeavoured, however, to provide the reader with a broad range of applications examples, which are pertinent to scenarios, such as transmitting low-latency interactive video as well as distributive or broadcast video signals over the existing second generation (2G) wireless systems, 3G arrangements and the forthcoming fourth generation systems. We also characterised the video performance of a

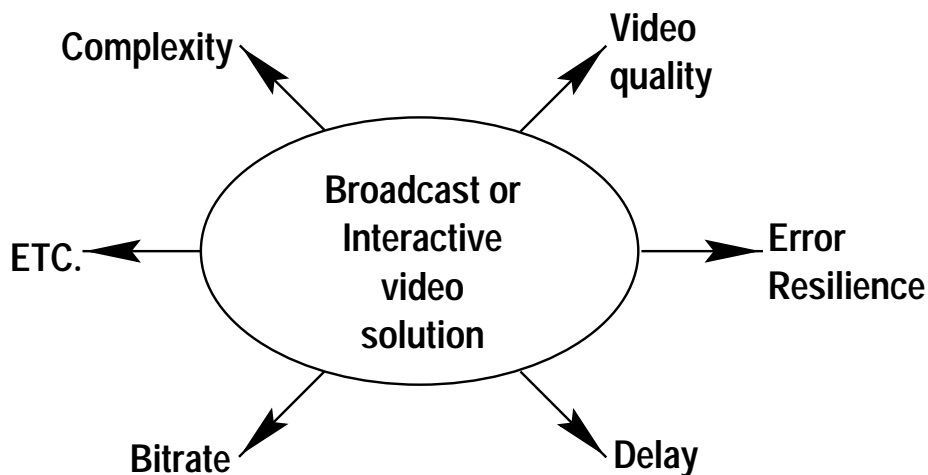


**Figure 1:** Contradictory system design requirements of various video communications systems

range of high bitrate Local Area Network (LAN) type systems as well as various video broadcast systems, transmitting broad-cast quality video signals to mobile receivers both within the home and farther afield - to demanding bussiness customers on the move.

**These enabling technologies facilitate a whole host of wireless services, such as video telephony, electronic commerce, city guide, Internet access for games, electronic mail and web browsing. Further attractive applications can be found in wireless in-home networks, DVB reception in busses, trains, cars, on board of ships, etc - for example using multi-media laptop PCs. Again, the books does not delve in the area of specific applications, it rather offers a range of technical solutions, which are applicable to various propagation and application environments.**

*We hope that the book offers you a range of interesting topics, sampling - 'hopefully without gross aliasing errors' - the current state-of-the-art in the associated enabling technologies. In simple terms, finding a specific solution to a distributive or interactive video communications problem has to be based on a compromise in terms of the inherently contradictory constraints of video quality, bitrate, delay, robustness against channel errors, and the associated implementational complexity, as suggested by Figure 1. Analysing these trade-offs and proposing a range of attractive solutions to various video communications problems is the basic aim of this book. Below we attempt to raise your interest in this book by providing a brief guided tour of its topics.*

## Video Over Wireless Systems

Over the past decade second generation (2G) wireless systems have been installed right across the globe and in some countries about a third of the population possesses

a mobile telephone. These systems typically exhibit a higher spectral efficiency than their analogue counterparts and offer a significantly wider range of services, such as data, fax, email, short messages, high-speed circuit switched data, etc. However, due to their relatively low bitrates the provision of interactive wireless videotelephony has been hindered. Potentially there are two different options for transmitting video over the 2G systems, namely over their data channel, or - provided that the standards can be amended accordingly - by allocating an additional speech channel for video transmissions. Considering the latter option first, the low-rate speech channel of the 2G systems constrains the achievable bitrate to such low values that the spatial video resolution supported is limited to  $174 \times 144$ -pixel so-called Quarter Common Intermediate Format (QCIF) or to the  $128 \times 96$ -pixel Sub-QCIF (SQCIF) at a 5-10 frames/s video frame scanning rate.

The range of standard video formats are summarised in Table 1, along with their uncompressed bitrates at frame scanning rates of both at 10 and 30 frames/sec for both grey and colour video signals. This table indicates the extremely wide range of potential bitrate requirements. Clearly, the higher resolution formats can only be realistically used for example in the context of high-rate WATM systems.

The so-called Cordless Telephone (CT) schemes of the second generation typically have a 32 kbit/s speech rate, which is more readily amenable to interactive video telephony. For the sake of supporting a larger video frame size, such as the  $352 \times 288$ -pixel Common Intermediate Format (QCIF), higher bitrates must be supported, which is possible over the DECT system upon linking a number of slots at a rate in excess of 500 kbps.

By contrast, the data channel of the 2G systems can often offer a higher data rate, than that of the speech channel, for example by linking a number of time-slots, as it was proposed in the so-called Digital European Cordless Telecommunications (DECT) scheme or in the high-speed circuit switched data (HSCSD) mode of the Global System of Mobile communications known as GSM. CT schemes typically refrain from invoking channel coding, since they typically operate over benign channels and hence they do not employ channel interleavers, which is advantageous in video delay terms, but disadvantageous in terms of error resilience. The data transmission mode of cellular systems, however, typically exhibits a high so-called interleaving delay, which assists in increasing the system's robustness against channel errors. This is advantageous in terms of reducing the channel-induced video impairments, but may result in 'lip-synchronisation' problems between the speech and video output signals.

Both the speech and data channels of the 2G systems tend to support a fixed constant bitrate. However, the existing standard video codecs, such as the H.263 and MPEG2 codecs, generate a time-variant bitrate. This is, because they endeavour to reduce the bitrate to near the lowest possible bitrate constituted by the so-called entropy of the source signal. Since this is achieved by invoking high-compression variable-length coding schemes, their time-variant bitstream becomes very sensitive against transmission errors. In fact a single transmission error may potentially render the video quality of an entire video frame unacceptable. Hence the existing standard-based video codecs, such as the H.263 and MPEG2 schemes require efficient system-level transport solutions, in order to address the above mentioned deficiencies. This issue will be discussed in more depth in Part IV of the book. An alternative solution

Video Format	Luminance dimensions	No. of Pels per frame	Uncompressed bitrate (Mbit/s)			
			10 frame/s		30 frame/s	
			Grey	Colour	Grey	Colour
SQCIF	128 x 96	12 288	0.983	1.47	2.95	4.42
QCIF	176 x 144	25 344	2.03	3.04	6.09	9.12
CIF	352 x 288	101 376	8.1	12.2	24.3	36.5
4CIF	704 x 576	405 504	32.4	48.7	97.3	146.0
16CIF	1408 x 1152	1 622 016	129.8	194.6	389.3	583.9
CCIR 601	720 x 480	345 600	27.65	41.472	82.944	124.416
HDTV 1440	1440 x 960	1 382 400	110.592	165.888	331.776	497.664
HDTV	1920 x 1080	2 073 600	165.9	248.832	497.664	746.496

SQCIF: Sub-Quarter Common Intermediate Format  
 QCIF: Quarter Common Intermediate Format  
 CIF: Common Intermediate Format  
 HDTV: High Definition Television

**Table 1:** Various video formats and their uncompressed bitrate. Upon using compression 10-100 times lower average bit rates are realistic.

is invoking constant-rate proprietary video codecs, which - to a degree - sacrifice compression efficiency for the sake of an increased robustness against channel errors. This philosophy was pursued in Part II of the book, which relies on much of the compression and communications theory, as well as on the various error correction coding and transmission solutions presented in Part I.

At the time of writing the standardisation of three third generation (3G) systems is approaching completion in Europe, the United States and in Japan. These systems - which are characterised in Part I of the book, along with their 2G counterparts - were designed to further enrich the range of services supported and they are more amenable to interactive wireless videotelephony, for example, than their 2G counterparts. This book aims to propose a range of video system solutions bridging the evolutionary avenue between the second and third generation systems.

Part I of the book provides an overview of the whole range of associated transmission aspects of the various video systems proposed and investigated. Specifically, Chapter 1 summarises the necessary background on information-, compression- and communications theory. This is followed by Chapter 2, which is dedicated to the characterisation of wireless channels. The impairments inflicted by these channels can be counteracted by the channel codecs of Chapters 3 and 4. Various modulation and transmission schemes are the topic of Chapter 5. We then provide a discourse on video traffic modelling and evaluate the proposed model's performance in the context of various statistical multiplexing and multiple access schemes in Chapter 6. The effects of co-channel interferences - which constitute the most dominant performance limiting factor of multiple access based cellular systems - are characterised in Chapter 7. Dynamic channel allocation schemes - which rely on the knowledge of the co-channel interference and the multiple access scheme employed - are the topic of Chapter 8. The video transmission capabilities of 2G wireless systems are discussed in Chapter 9. These elaborations are followed by an indepth treatise on various CDMA schemes in Chapter 10, including a variety of novel so-called residual number system based CDMA schemes and on the global 3G CDMA proposals, which concludes Part I of the book.

Part II is dedicated to a host of fixed, but arbitrarily programmable rate video codecs based on fractal coding, on the discrete cosine transform (DCT), on vector quantised (VQ) codecs and quad-tree based codecs. These video codecs and their associated quadrature amplitude modulated (QAM) video systems are portrayed in Chapters 11-14. Part III of the book is dedicated to high-resolution video coding, encompassing Chapters 15 and 16.

Part IV is constituted by Chapters 17-21, which are dedicated to the characterisation of the H.261 and H.263 video codecs, constituting one of the most important representative of the family of state-of-the-art hybrid DCT codecs. Hence the associated findings of these chapters can be readily applied in the context of other hybrid DCT codecs, such as the MPEG family, including the MPEG2 and MPEG4 codecs. Chapters 17-21 also portray the interactions of these hybrid DCT video codecs with reconfigurable multimode QAM transceivers. The book is concluded by Chapter 21, which offers a range of system design studies related to wideband burst-by-burst adaptive TDMA/TDD, OFDM and CDMA interactive as well as distributive mobile video systems and their performance characterisation over highly dispersive transmis-

sion media.

## Motivation

The rationale of this book was outlined above from a technical perspective. **Another important motivation of the book is to bring together two seemingly independent research communities, namely the video compression and the wireless communications communities by bridging the philosophical difference between them.** These philosophical differences are partially based on the contradictory requirements portrayed and discussed in the context of Figure 1. Specifically, whilst a range of exciting developments have taken place in both the image compression and wireless communications communities, most of the video compression research was cast in the context of wire-line based communications systems, such as ISDN and ATM links, for example. These communications systems typically exhibit a low bit error rate (BER) and low so-called packet or cell loss rate. For example, ATM systems aim for a cell-loss rate of  $10^{-9}$ . Hence the error resilience requirements of the video codecs were extremely relaxed.

In the increasingly pervasive wireless era, however, such extreme transmission integrity requirements are simply unrealistic, since they would impose unreasonable constraints on the design of wireless systems, such as for example WATM systems. For example, the ATM cell-loss rate of  $10^{-9}$  could only be maintained over wireless links at a high implementational cost, potentially invoking Automatic Repeat Requests (ARQ). ARQs, however, would increase the system delay, potentially precluding real-time interactive video communications, unless innovative design principles are invoked. Again, all these trade-offs are the subject of this book.

Part I of the book aims for providing sufficient background for readers requiring an overview in wireless communications, potentially for example video compression experts. Part II assumes a sound knowledge of the issues treated in Part I of the book, whilst offering an effortless introduction to the associated video compression aspects. Hence wireless experts may skip Part I and commence reading Part II of the book. Part III is exclusively on video compression. Hopefully readers from both the video compression and wireless communications communities will find Part IV of the book informative and fun to read, since it integrates the knowledge base of both fields, aiming to design improved video systems.

Again, it is our hope that the book underlines the range of contradictory system design trade-offs in an unbiased fashion and that you will be able to glean information from it, in order to solve your own particular wireless video communications problem, but most of all that you will find it an enjoyable and relatively effortless reading, providing you with intellectual stimulation.

*Lajos Hanzo*

## Acknowledgements

The book has been written by the staff in the Electronics and Computer Science Department at the University of Southampton. We are indebted to our many colleagues who have enhanced our understanding of the subject. These colleagues and valued friends, too numerous all to be mentioned, have influenced our views concerning various aspects of wireless multimedia communications and we thank them for the enlightenment gained from our collaborations on various projects, papers and books. We are grateful to J. Brecht, Jon Blogh, Marco Breiling, M. del Buono, Clare Brooks, Stanley Chia, Byoung Jo Choi, Joseph Cheung, Peter Fortune, Lim Dongmin, D. Didascalou, S. Ernst, Eddie Green, David Greenwood, Hee Thong How, Thomas Keller, W.H. Lam, C.C. Lee, M.A. Nofal, Xiao Lin, Chee Siong Lee, Tong-Hooi Liew, Matthias Muenster, V. Roger-Marchart, Redwan Salami, David Stewart, Jeff Torrance, Spiros Vlahoyiannatos, William Webb, John Williams, Jason Woodard, Choong Hin Wong, Henry Wong, James Wong, Lie-Liang Yang, Bee-Leong Yeap, Mong-Suan Yee, Kai Yen, Andy Yuen and many others with whom we enjoyed an association.

We also acknowledge our valuable associations with the Virtual Centre of Excellence in Mobile Communications, in particular to its Chief Executive, Dr. Tony Warwick, Dr. Keith Baughan and other members of its Executive Committee. Our sincere thanks are also due to the EPSRC, UK; Dr. Joao Da Silva, Dr Jorge Pereira and other colleagues from the Commission of the European Communities, Brussels; Andy Wilton, Luis Lopes and Paul Crichton from Motorola ECID, Swindon, UK for sponsoring some of our recent research.

We feel particularly indebted to Chee Siong Lee for his invaluable help with proof-reading the manuscript. Finally, our sincere gratitude is due to the numerous authors listed in the Author Index - as well as to those, whose work was not cited due to space limitations - for their contributions to the state-of-the-art, without whom this book would not have materialised.

*Lajos Hanzo*





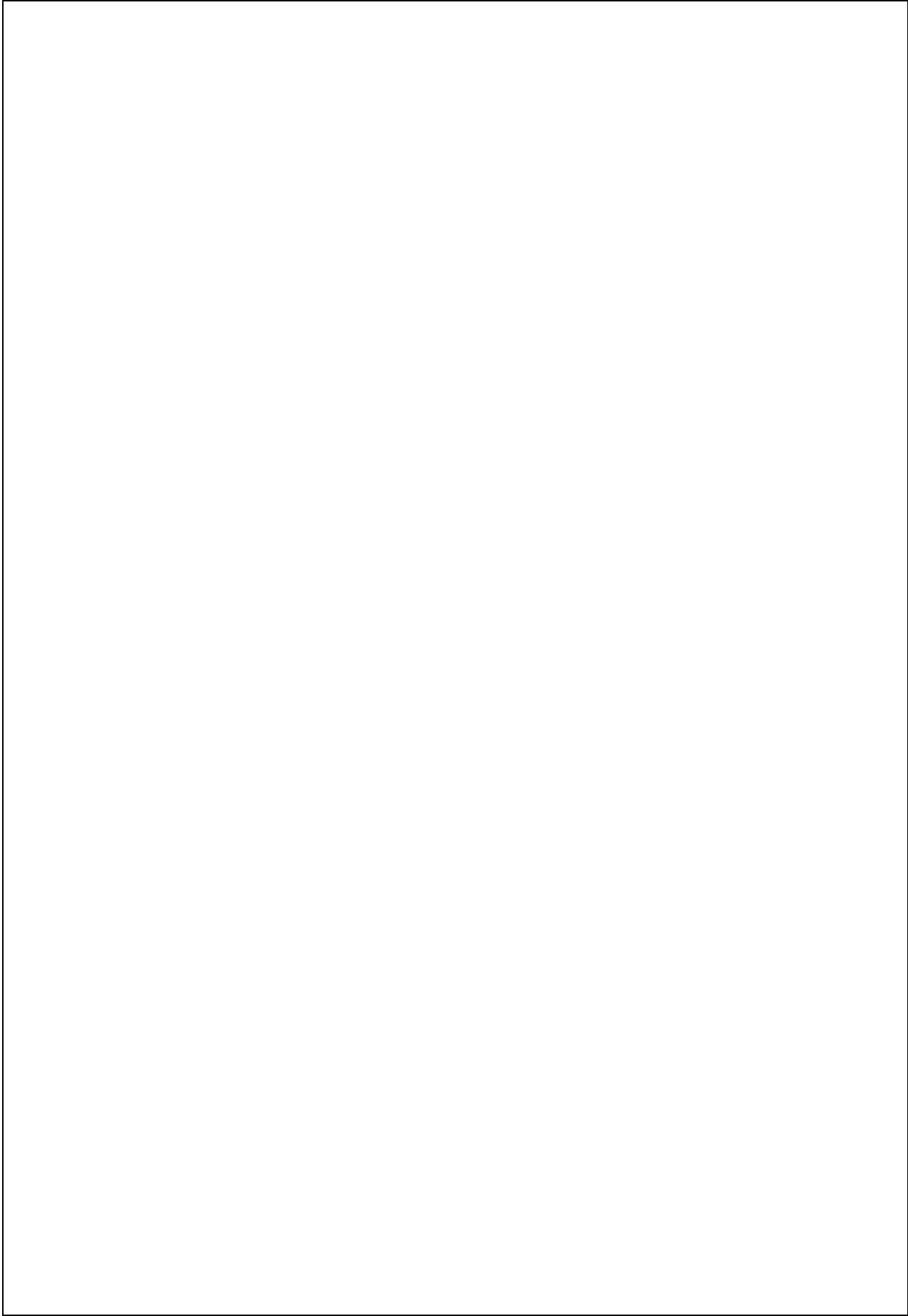
# Contributors

**Chapter 10: Yen Kai, Lie-Liang Yang, L. Hanzo**

**Chapter 20: P. Cherriman, L. Hanzo, T. Keller, E.L. Kuan, C.S. Lee, C.H. Wong**

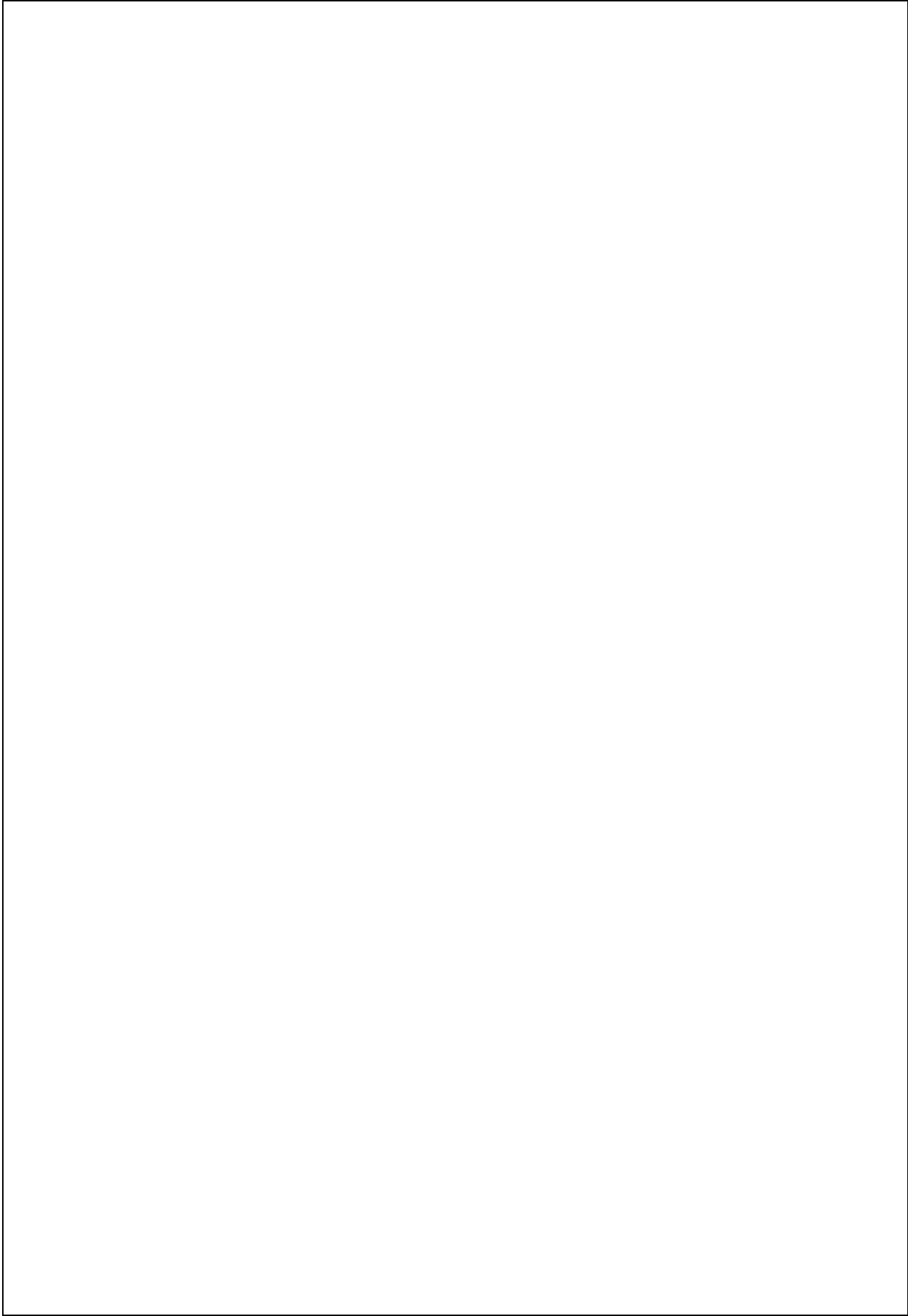


**Part I**  
**Transmission Issues**



**Part II**

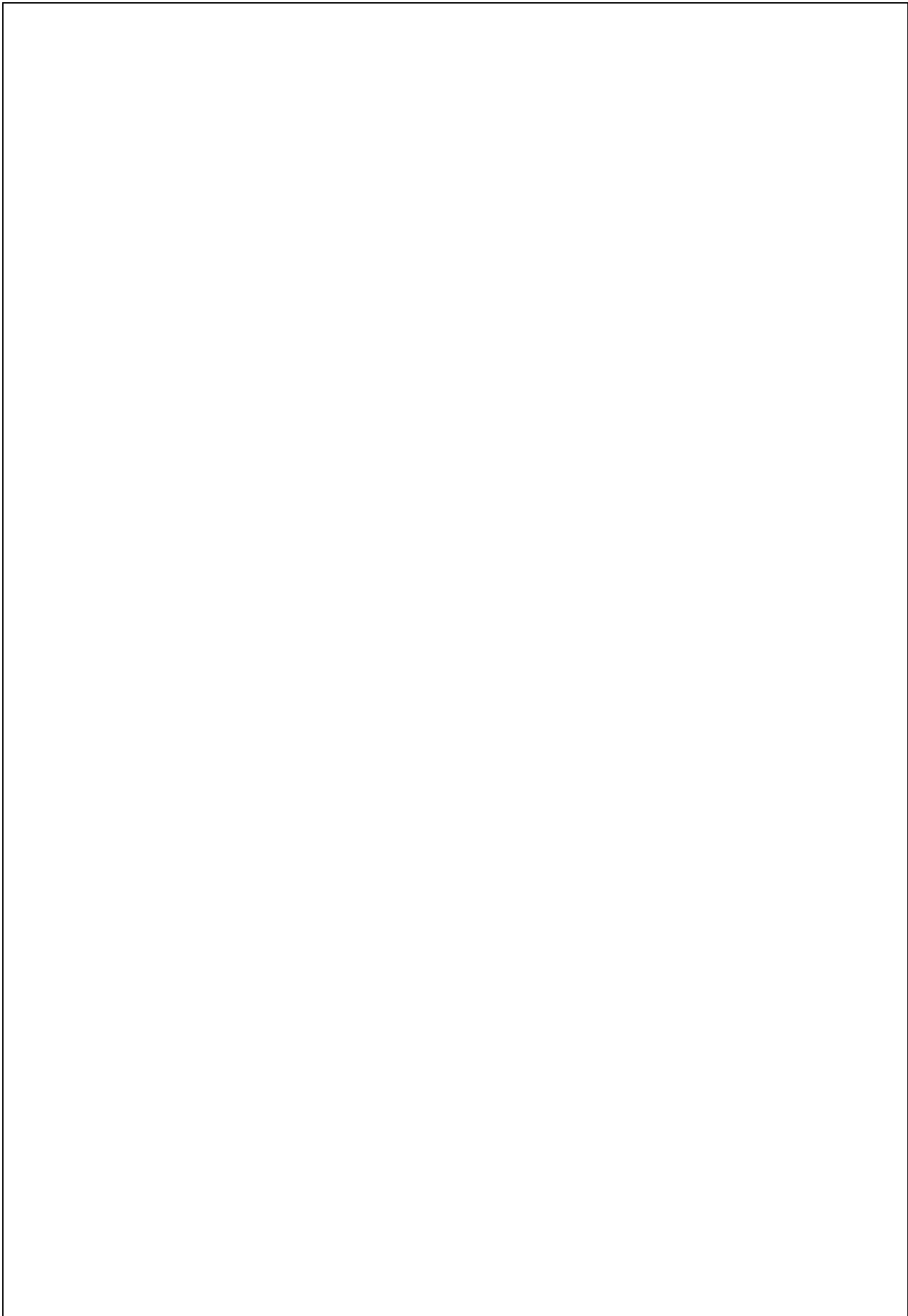
**Video Systems based on  
Proprietary Video Codecs**



**Part IV**

**Video Systems based on  
Standard Video Codecs**





# Chapter 21

## Adaptive Single-carrier, Multi-carrier and CDMA based Video Systems

P.J. Cherriman, L. Hanzo, T. Keller,  
Ee-Lin Kuan, C.S. Lee, C.H. Wong

### 21.1 Wideband Burst-by-burst Adaptive QAM-based Wireless Videophony<sup>1 2</sup>

#### 21.1.1 Introduction

In contrast to our previous chapters, where we used statically reconfigurable narrow-band multimode modems, in this chapter we will consider a range of dynamically or near-instantaneously reconfigurable modems. These near-instantaneously reconfigurable transceivers are also often referred to as burst-by-burst adaptive modems, which were discussed in some depth in Chapter 5. Their philosophy is that a higher-order modulation mode is invoked, when the channel quality is favourable, in order to increase the system's bits per symbol capacity and conversely, a more robust lower order modulation scheme is employed, when the channel exhibits inferior channel quality, in order to improve the mean Bit Error Ratio (BER) performance. A practical scenario, where adaptive modulation can be applied is, when a reliable, low-delay

---

<sup>1</sup>This section is based on

**P. Cherriman, C.H. Wong, L. Hanzo:** Wideband Burst-by-burst Adaptive H.263-assisted Wireless Video Telephony; submitted to IEEE Tr. on CSVT, 1999

<sup>2</sup>©1999 IEEE. Personal use of this material is permitted. However, permission to reprint/republish this material for advertising or promotional purposes or for creating new collective works for resale or redistribution to servers or lists, or to refuse any copyrighted component of this work in other works must be obtained from IEEE.

feedback path is created between the transmitter and receiver, for example by superimposing the estimated channel quality perceived by the receiver on the reverse-direction messages of a duplex interactive channel. The transmitter then adjusts its modem mode according to this perceived channel quality.

Recent developments in adaptive modulation over a narrow-band channel environment have been pioneered by Webb and Steele [126], where the modulation adaptation was utilized in a Digital European Cordless Telephone - like (DECT) system. The concept of variable rate adaptive modulation was then further developed by Sampei *et al* [564], showing promising advantages, when compared to fixed modulation in terms of spectral efficiency, BER performance and robustness against channel delay spread. In another paper, the numerical upper bound performance of adaptive modulation in a slow Rayleigh flat-fading channel was evaluated by Torrance *et al* [101] and subsequently, the optimization of the switching threshold levels using Powell minimization was proposed in order to achieve a targeted performance [102]. In addition, adaptive modulation was also studied in conjunction with channel coding and power control techniques by Matsuoka *et al* [585] as well as Goldsmith and Chua [130, 586].

In the narrow-band channel environment, the quality of the channel was determined by the short term Signal to Noise Ratio (SNR) of the received burst, which was then used as a criterion in order to choose the appropriate modulation mode for the transmitter, based on a list of switching threshold levels,  $l_n$  [101, 126, 564, 587]. However, in a wideband environment, this criterion is not an accurate measure for judging the quality of the channel, where the existence of multi-path components produces not only power attenuation of the transmission burst, but also intersymbol interference. Subsequently, a new criterion has to be defined to estimate the wideband channel quality in order to choose the appropriate modulation scheme.

In addition, the wideband channel-induced degradation is combated not only by the employment of adaptive modulation but also by equalization. In following this line of thought, we can formulate a two-step methodology in mitigating the effects of the dispersive wideband channel. In the first step, the equalization process will eliminate most of the intersymbol interference based on a Channel Impulse Response (CIR) estimate derived using the channel sounding midamble and consequently, the signal to noise and residual interference ratio at the output of the equalizer is calculated.

We found that the residual channel-induced inter-symbol-interference (ISI) at the output of the decision feedback equaliser (DFE) is near-Gaussian distributed and that if there are no decision feedback errors, the pseudo-SNR at the output of the DFE,  $\gamma_{dfe}$  can be calculated as [588]:

$$\begin{aligned} \gamma_{dfe} &= \frac{\text{Wanted Signal Power}}{\text{Residual ISI Power} + \text{Effective Noise Power}} \\ &= \frac{E \left[ |S_k \sum_{m=0}^{N_f-1} C_m h_m|^2 \right]}{\sum_{q=-(N_f-1)}^{-1} E \left[ |f_q S_{k-q}|^2 \right] + N_o \sum_{m=0}^{N_f-1} |C_m|^2}. \end{aligned} \tag{21.1}$$

where  $C_m$  and  $h_m$  denotes the DFE's feed-forward coefficients and the channel impulse response, respectively. The transmitted signal and the noise spectral density

is represented by  $S_k$  and  $N_o$ . Lastly, the number of DFE feed-forward coefficients is denoted by  $N_f$ . By utilizing the pseudo-SNR at the output of the equalizer, we are ensuring that the system performance is optimised by employing equalization and adaptive quadrature amplitude modulation [10] (AQAM) in a wideband environment according to the following switching regime:

$$\text{Modulation Mode} = \begin{cases} BPSK & \text{if } \gamma_{DFE} < f_1 \\ 4QAM & \text{if } f_1 < \gamma_{DFE} < f_2 \\ 16QAM & \text{if } f_2 < \gamma_{DFE} < f_3 \\ 64QAM & \text{if } \gamma_{DFE} > f_3, \end{cases} \quad (21.2)$$

where  $f_n, n = 1...3$  are the pseudo-SNR thresholds levels, which are set according to the system's integrity requirements.

Having reviewed the background of burst-by-burst adaptive modems, we now focus our attention on video issues. Färber, Steinbach and Girod at Erlangen University contrived various error-resilient H.263-based schemes [589], Sadka, Eryurtlu and Kondoz [590] from Surrey University proposed various improvements to the H.263 scheme. The philosophy of our proposed schemes follows that of the narrowband, statically configured multimode system introduced in [189], employing an adaptive rate control and packetisation algorithm, supporting constant Baud-rate operation. **In this section we employed wideband burst-by-burst adaptive modulation, in order to quantify the video performance benefits of such systems.** It is an important element of the system that when the BCH codes protecting the video stream are overwhelmed by the plethora of transmission errors, we refrain from decoding the video packet in order to prevent error propagation through the reconstructed frame buffer [189]. Instead, these corrupted packets are dropped and the reconstructed frame buffer will not be updated, until the next packet replenishing the specific video frame area arrives. The associated video performance degradation is fairly minor for packet dropping or frame error rates (FER) below about 5%. These packet dropping events are signalled to the remote decoder by superimposing a strongly protected one-bit packet acknowledgement flag on the reverse-direction packet, as outlined in [189].

This section is structured as follows. Subsection 21.1.2 introduces the video transceiver parameters, which is followed by Subsection 21.1.3, focusing on the video performance analysis of the proposed burst-by-burst adaptive system. Lastly, Subsection ch-switch characterises the effects of the adaptive modem mode switching thresholds on the system's video performance.

### 21.1.2 Adaptive Video Transceiver

In this section we used 176x144 pixel QCIF-resolution, 30 frames per sec scanned video sequences encoded at bitrates resulting in high perceptual video quality. Table 21.1 shows the modulation- and channel parameters employed. The COST207 [324] four-path typical urban (TU) channel model was used and its impulse response is portrayed in Figure 21.1. We used the Pan-European FRAMES proposal [591] as the basis for our wideband transmission system, the frame structure of which is shown in Figure 21.2. Employing the FRAMES Mode A1 (FMA1) so-called non-spread data burst

Parameter	Value
Carrier Frequency	1.9GHz
Vehicular Speed	30mph
Doppler frequency	85Hz
Norm. Doppler freq.	$3.27 \times 10^{-5}$
Channel type	COST 207 Typical Urban (see Figure 21.1)
No. of imp. resp. taps	4
Data modulation	Adaptive QAM (BPSK, 4-QAM, 16-QAM, 64-QAM)
Receiver type	Decision Feedback Equalizer Number of Forward Filter Taps = 35 Number of Backward Filter Taps = 7

Table 21.1: Modulation and channel parameters

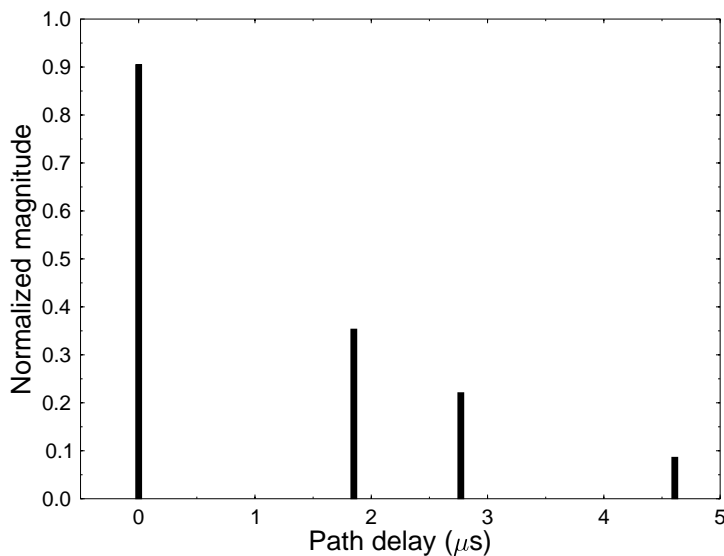
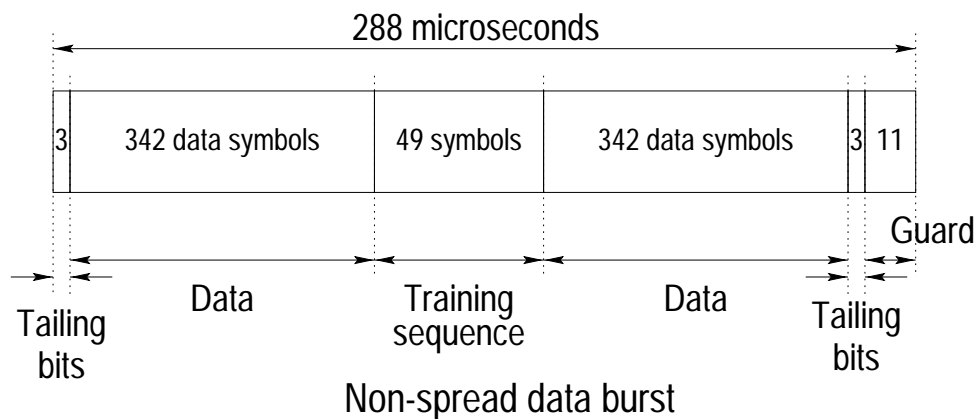


Figure 21.1: Normalized channel impulse response for the COST 207 [324] four-path Typical Urban channel.

mode required a system bandwidth of 3.9MHz, when assuming a modulation excess bandwidth of 50%. A range of other system parameters are shown in Table 21.2.

The proposed video transceiver is based on the H.263 video codec [182], which was the subject of Chapters 18 and 19. The video coded bitstream was protected by binary Bose-Chaudhuri-Hocquenghem (BCH) coding, as discussed in Chapter 4 [9] combined with an intelligent burst-by-burst adaptive wideband multi-mode Quadrature Amplitude Modulation (QAM) modem, which was considered in depth in Chap-



**Figure 21.2:** Transmission burst structure of the FMA1 non-spread data burst mode of the FRAMES proposal [591]

Features	Value
Multiple access	TDMA
No. of Slots/Frame	16
TDMA frame length	4.615ms
TDMA slot length	288 $\mu$ s
Data Symbols/TDMA slot	684
User Data Symbol Rate (KBd)	148.2
System Data Symbol Rate (MBd)	2.37
Symbols/TDMA slot	750
User Symbol Rate (KBd)	162.5
System Symbol Rate (MBd)	2.6
System Bandwidth (MHz)	3.9
Eff. User Bandwidth (kHz)	244

**Table 21.2:** Generic system features of the reconfigurable multi-mode video transceiver, using the non-spread data burst mode of the FRAMES proposal [591] shown in Figure 21.2.

Features	Multi-rate System			
Mode	BPSK	4QAM	16QAM	64QAM
Bits/Symbol	1	2	4	6
FEC	Near Half-rate BCH			
Transmission bitrate (kbit/s)	148.2	296.4	592.8	889.3
Unprotected bitrate (kbit/s)	75.8	151.7	303.4	456.1
Effective Video-rate (kbit/s)	67.0	141.7	292.1	446.4
Video fr. rate (Hz)	30			

**Table 21.3:** Operational-mode specific transceiver parameters

ter 5 [10]. The adaptive QAM scheme was configurable either under network control or under transceiver control, in order to operate as a 1, 2, 4 and 6 bits/symbol scheme, while maintaining a constant signalling rate. This allowed us to support an increased throughput expressed in terms of the average number of bits per symbol, when the instantaneous channel quality was high, leading ultimately to an increased video quality in a constant bandwidth.

The transmitted bitrate for all four modes of operation is shown in Table 21.3. The unprotected bitrate before approximately half-rate BCH coding is also shown in the table. The actual useful bitrate available for video is slightly less, than the unprotected bitrate due to the required strongly protected packet acknowledgement information and packetisation information. The effective video bitrate is also shown in the table.

### 21.1.3 Burst-by-Burst Adaptive Videophone Performance

The proposed burst-by-burst adaptive modem maximizes the system capacity available by using the most appropriate modulation mode for the current instantaneous channel conditions. We found that the pseudo-SNR at the output of the channel equaliser was an adequate channel quality measure in our burst-by-burst adaptive wide-band modem. Figure 21.3 demonstrates how the burst-by-burst adaptive modem changes its modulation modes every transmission burst, ie every 4.615 ms, based on the fluctuating pseudo-SNR. The right-hand-side vertical axis indicates the associated number of bits per symbol.

By changing to more robust modulation schemes automatically, when the channel quality is reduced allows the packet loss ratio, or synonymously, the FER, to be reduced, which results in increased perceived video quality. In order to judge the benefits of burst-by-burst adaptive modulation we considered two scenarios. In the first scheme the adaptive modem always chose the perfectly estimated AQAM modulation mode, in order to provide a maximum upper bound performance. In the second scenario the modulation mode was based upon the perfectly estimated AQAM modulation mode for the previous burst, which corresponded to a delay of one Time

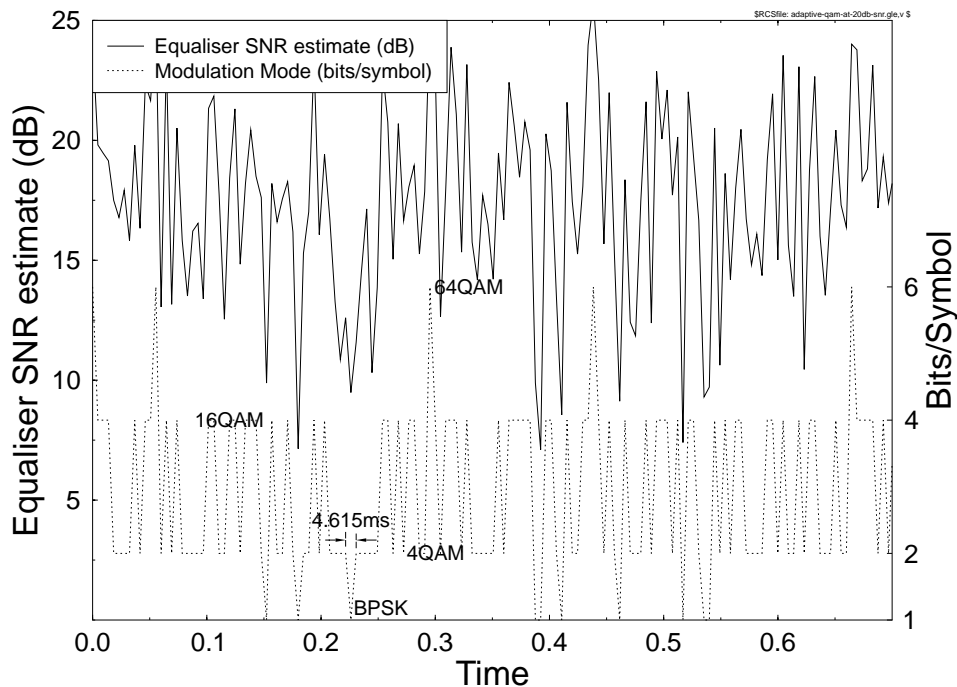


**Figure 21.3:** Adaptive burst-by-burst modem in operation for an average channel SNR of 20dB, where the modulation mode switching is based upon the SNR estimate at the output of the equaliser, using the channel parameters defined in Table 21.1.

Division Multiple Access (TDMA) frame duration of 4.615ms. This second scenario represents a practical burst-by-burst adaptive modem, where the one-frame channel quality estimation latency is due to superimposing the receiver's perceived channel quality on a reverse-direction packet, for informing the transmitter concerning the best mode to be used.

The probability of the adaptive modem using each modulation mode for a particular average channel SNR is portrayed in Figure 21.4 in terms of the associated modem mode probability density functions (PDFs). It can be seen at high channel SNRs that the modem mainly uses the 64QAM modulation mode, while at low channel SNRs the BPSK mode is the most prevalent one.

Figure 21.5 shows the transmission FER (or packet loss ratio) versus channel SNR for the 1, 2, 4 and 6 bit/symbol fixed modulation schemes, as well as for the ideal and for the one-frame delayed realistic scenarios using the burst-by-burst adaptive QAM (AQAM) modem. A somewhat surprising fact is [592] - which is not explicitly shown here due to lack of space - that at low SNRs AQAM can maintain a lower BER than BPSK, since under inferior instantaneous channel conditions it exhibits the corresponding BPSK BER, but the average number of transmitted AQAM bits is



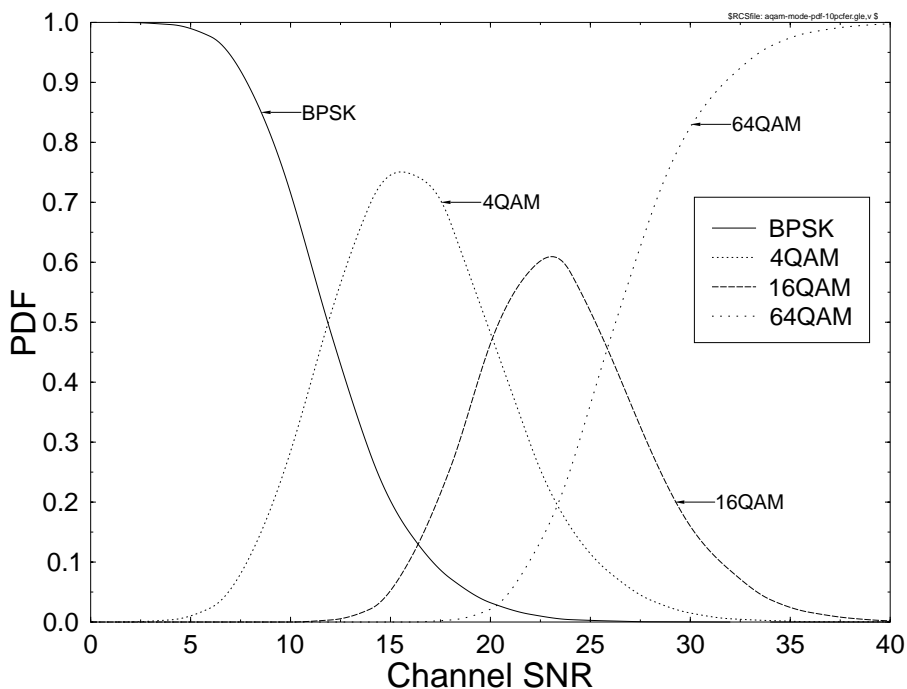


**Figure 21.4:** PDF of the adaptive modem being in a particular modulation mode versus channel SNR.

higher than that of BPSK, resulting in a reduced average AQAM BER. At high SNRs the AQAM BER curve asymptotically joins the 64QAM BER curve, since 64QAM is the predominant mode used. The associated FER curve obeys similar tendencies in terms of having the BPSK and 64QAM FER curves as asymptotes at low and high SNRs, respectively. However - in contrast to the BER - the AQAM FER cannot be lower than that of BPSK, since the same number of frames is transmitted in both cases. The substantial advantage of AQAM is that due to its higher number of bits/symbol the number bits transmitted per frame is higher, resulting in an increased video quality.<sup>3</sup> The FER curves are portrayed on a logarithmic scale in Figure 21.6, where - for the sake of comparison - we also showed the associated FER curve for statically reconfigured modem modes switching at 5% transmission FER, as it will be detailed below.

Explicitly, the statically reconfigured modem was invoked in Figure 21.6 as a benchmarker, in order to indicate, how a system would perform, which cannot act on the basis of the near-instantaneously varying channel quality. As it can be inferred

<sup>3</sup>We note here that the associated performance results typically degrade upon increasing the Doppler frequency and improve upon reducing it, since the effects of channel estimation latency become less significant. This phenomenon was quantified in [592]

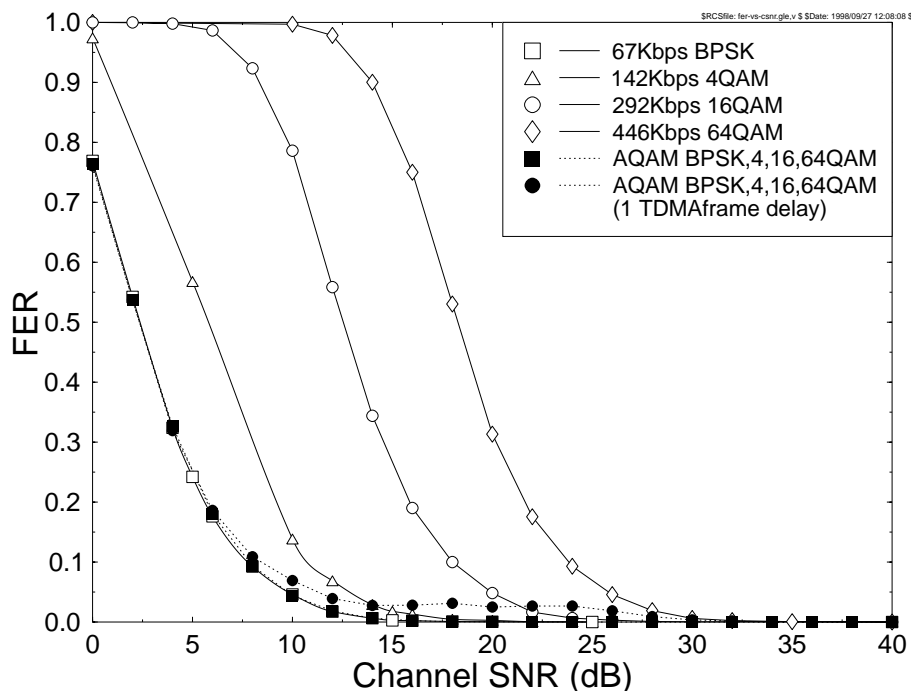


**Figure 21.5:** Transmission FER (or packet loss ratio) versus Channel SNR comparison of the four fixed modulation modes (BPSK, 4QAM, 16QAM, 64QAM) and that of the adaptive burst-by-burst modem (AQAM). AQAM is shown with a realistic one TDMA frame delay between channel estimation and mode switching, and also with a zero delay version for indicating the upper bound performance. The channel parameters were defined in Table 21.1.

from Figure 21.6, such a statically reconfigured transceiver switches its mode of operation from a lower-order modem mode, such as for example BPSK to a higher-order mode, such as 4QAM, when the channel quality has improved sufficiently for the 4QAM mode's FER to become lower than 5 % upon reconfiguring the transceiver in this 4QAM mode. Again - as seen also in Figure 21.5 earlier on a non-logarithmic scale - Figure 21.6 clearly shows on a logarithmic scale that the 'one-frame channel estimation delay' AQAM modem manages to maintain a similar FER performance to the fixed rate BPSK modem at low SNRs, although we will see in Figure 21.7 that AQAM provides increasingly higher bitrates, reaching four times higher values than BPSK for high channel SNRs, where the employment of 64QAM is predominant. In this high SNR region the FER curve asymptotically approaches the 64QAM FER curve for both the realistic and the ideal AQAM scheme, although this is not visible in the figure for the ideal scheme, since this occurs at SNRs outside the range of Figure 21.6. Again, the reason for this performance discrepancy is the occasionally misjudged channel quality estimates of the realistic AQAM scheme. Additionally,

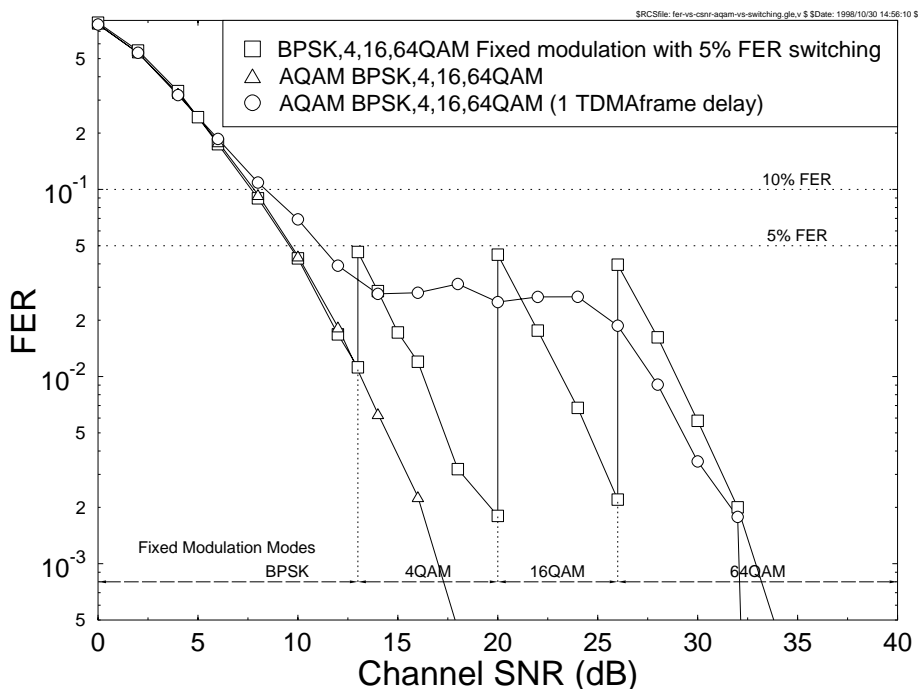


**Figure 21.6:** Transmission FER (or packet loss ratio) versus Channel SNR comparison of the four fixed modulation modes (BPSK, 4QAM, 16QAM, 64QAM) with 5% FER switching and adaptive burst-by-burst modem (AQAM). AQAM is shown with a realistic one TDMA frame delay between channel estimation and mode switching, and a zero delay version is included as an upper bound. The channel parameters were defined in Table 21.1.

Figure 21.6 indicates that the realistic AQAM modem exhibits a near-constant 3% FER at medium SNRs. The issue of adjusting the switching thresholds in order to achieve the target FER will be addressed in detail in Section 21.1.4 and the thresholds invoked will be detailed with reference to Table 21.4. Suffice to say at this stage that the average number of bits per symbol - and potentially also the associated video quality - can be increased upon using more aggressive switching thresholds. However, this results in an increased FER, which tends to decrease the video quality, as it will be discussed in Section 21.1.4.

A comparison of the effective video bitrate versus channel SNR is shown in Figure 21.7 for the four fixed modulation schemes, and the ideal and realistic AQAM modems. The effective video bitrate is the average bitrate provided by all the successfully transmitted video packets. It should be noted that the realistic AQAM modem has a slightly lower throughput, since sometimes the incorrect modulation mode is chosen, which may result in packet loss. At very low channel SNRs the throughput bitrate converges to that of the fixed BPSK mode, since the AQAM modem is almost

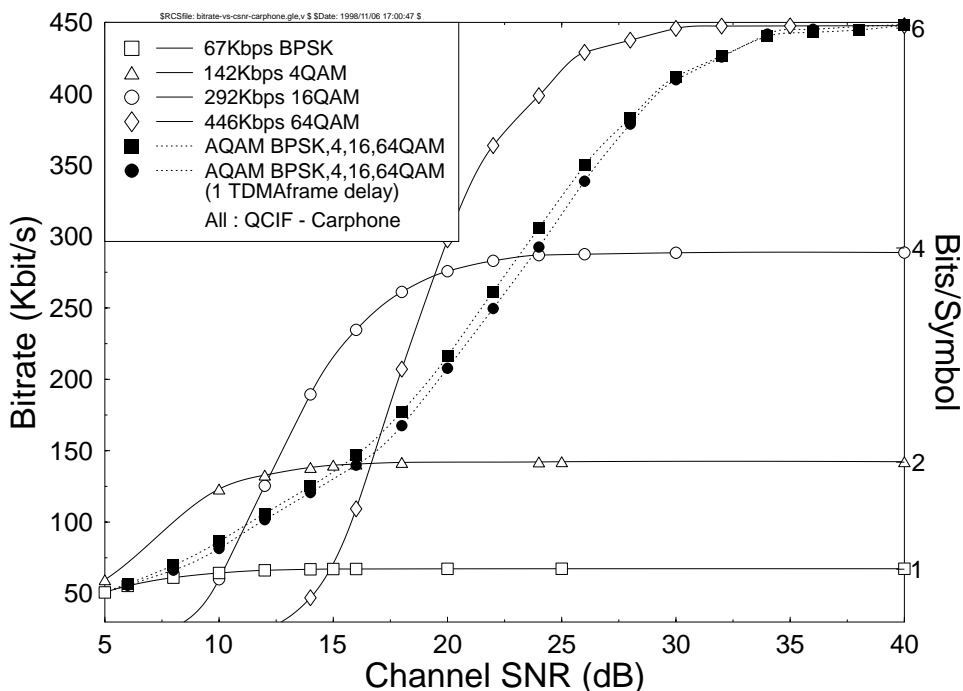


**Figure 21.7:** Video bitrate versus channel SNR comparison of the four fixed modulation modes (BPSK, 4QAM, 16QAM, 64QAM) and adaptive burst-by-burst modem (AQAM). AQAM is shown with a realistic one TDMA frame delay between channel estimation and mode switching, and also as a zero delay version for indicating the upper bound. The channel parameters were defined in Table 21.1.

always in the BPSK mode at these SNRs, as demonstrated in Figure 21.4.

Having shown the effect of the burst-by-burst adaptive modem on the transmission FER and effective bitrate, let us now demonstrate these effects on the decoded video quality, measured in terms of the Peak Signal-to-Noise Ratio (PSNR). Figure 21.8 shows the decoded video quality in terms of PSNR versus channel SNR for both the ideal and realistic adaptive modem, and for the four modes of the statically configured multi-mode modem. It can be seen that the ideal adaptive modem, which always selects the perfect modulation modes, has a better or similar video quality for the whole range of channel SNRs. For the statically configured multi-mode scheme the video quality degrades, when the system switches from a higher-order to a lower-order modulation mode. The ideal adaptive modem however smoothes out the sudden loss of video quality, as the channel degrades. The non-ideal adaptive modem has a slightly lower video quality performance, than the ideal adaptive modem, especially at medium SNRs, since it sometimes selects the incorrect modulation mode due to the estimation delay. This can inflict video packet loss and/or a reduction of the effective

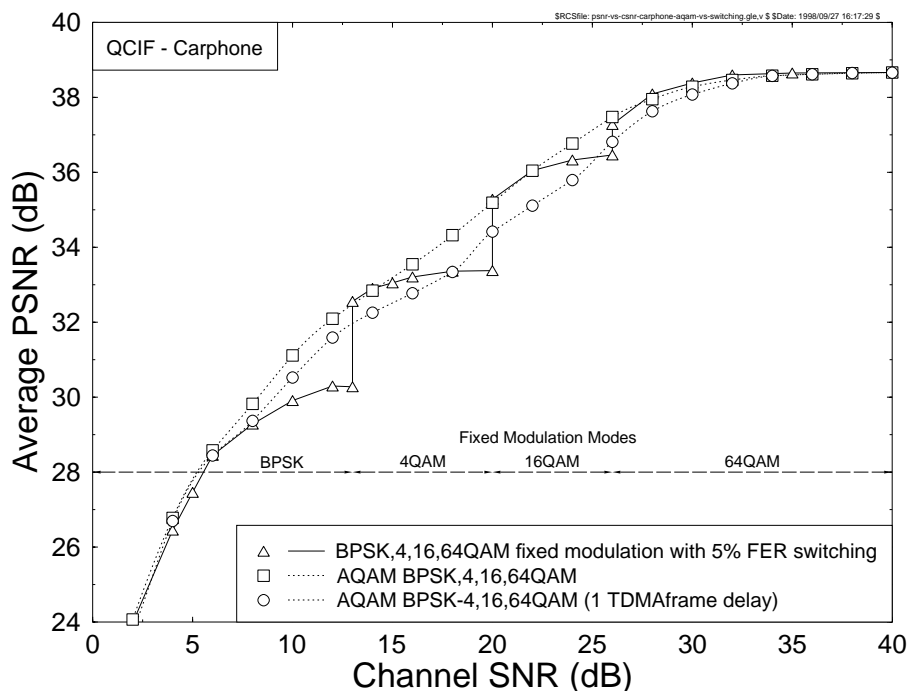


**Figure 21.8:** Decoded video quality (PSNR) versus channel SNR comparison of the four fixed modulation modes (BPSK, 4QAM, 16QAM, 64QAM) with 5% transmission FER switching and that of the adaptive burst-by-burst modem (AQAM). AQAM is shown with a realistic one TDMA frame delay between channel estimation and mode switching, and a zero delay version for indicating the upper bound. The channel parameters were defined in Table 21.1.

video bitrate, which in turn reduces the video quality.

The difference between the ideal burst-by-adaptive modem, using ideal channel estimation and the non-ideal, realistic burst-by-burst adaptive modem, employing a non-ideal delayed channel estimation can be seen more clearly in Figure 21.9 for a range of video sequences. Observe that at high and low channel SNRs the video quality performance is similar for the ideal and non-ideal adaptive modems. This is because the channel estimation delay has little effect, since at low or high channel SNRs the adaptive modem is in either BPSK or 64QAM mode for the majority of the time. More explicitly, the channel quality of a transmission frame is almost always the same as that of the next, and hence the delay has little effect at low and high SNRs.

The video quality versus channel quality trade-offs can be more explicitly observed in Figure 21.10. This figure portrays the decoded video quality in PSNR versus the packet loss ratio or transmission FER. The ideal and practical adaptive modem performance is plotted against that of the four fixed modulation schemes in the figure. It

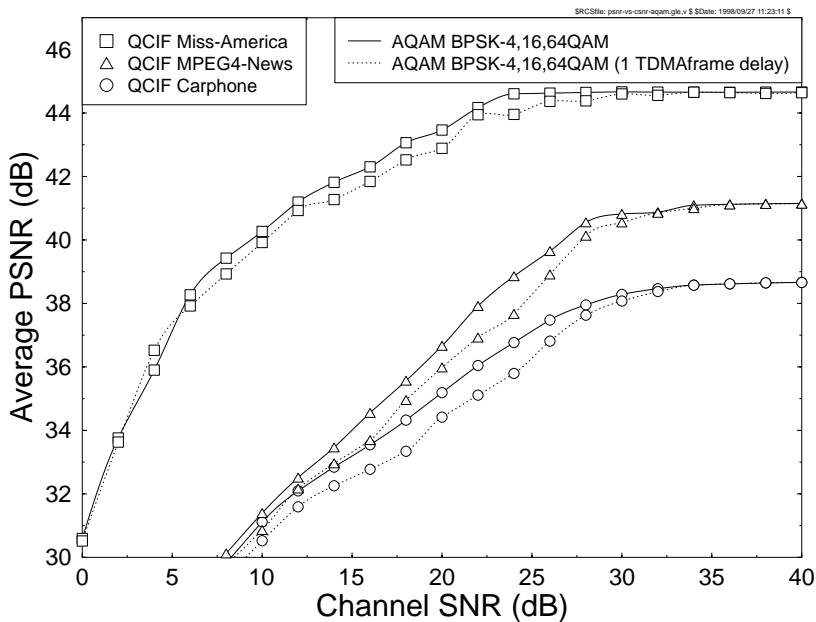


**Figure 21.9:** Decoded video quality (PSNR) versus channel SNR for the adaptive burst-by-burst modem (AQAM). AQAM is shown with a realistic one TDMA frame delay between channel estimation and mode switching, and a zero delay version indicating the upper bound. Results are shown for three video sequences using the channel parameters that were defined in Table 21.1.

can be seen that the adaptive modems' video quality degrades from that achieved by the error-free 64QAM modem towards the BPSK modem performance as the packet loss ratio increases. The practical adaptive modems' near constant FER performance of 3% at medium SNRs can be clearly seen in the figure, which is associated with the reduced PSNRs of the various modem modes, while having only minor channel error-induced impairments. In order to augment the interpretation of this figure we note that although the objective video quality of the various fixed QAM modes expressed in PSNR appears to be higher than that of the AQAM schemes, the associated perceived video quality of AQAM is significantly more pleasing. This is because the channel-induced PSNR degradation is significantly more objectionable than the PSNR reduction imposed by invoking the inherently lower-bitrate, lower-quality but more robust AQAM modes. Again, the philosophy here was that the AQAM scheme maintained the required near-constant target FER, which was necessary for high perceived video quality at the cost of invoking reduced-rate, but more robust modem modes under hostile channel conditions.

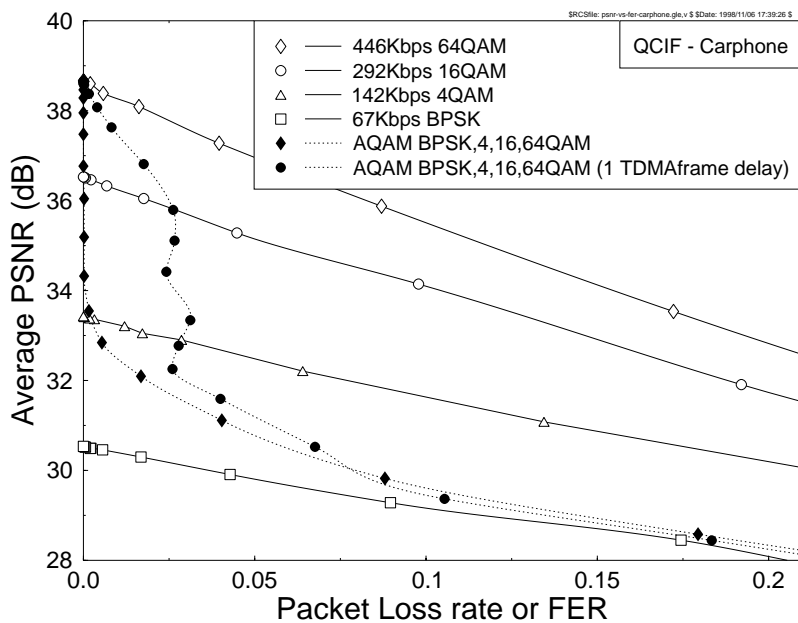


**Figure 21.10:** Decoded video quality (PSNR) versus transmission FER (or packet loss ratio) comparison of the four fixed modulation modes (BPSK, 4QAM, 16QAM, 64QAM) and that of the adaptive burst-by-burst modem (AQAM). AQAM is shown with a realistic one TDMA frame delay between channel estimation and mode switching, and a zero delay version indicating the upper bound. The channel parameters were defined in Table 21.1.

	BPSK	4QAM	16QAM	64QAM
Standard	<10dB	≥10dB	≥18dB	≥24dB
Conservative	<13dB	≥13dB	≥20dB	≥26dB
Aggressive	<9dB	≥9dB	≥17dB	≥23dB

**Table 21.4:** SINR estimate at output of the equaliser required for each modulation mode in the proposed burst-by-burst adaptive modem, ie. switching thresholds

### 21.1.4 Switching Thresholds

The burst-by-burst adaptive modem changes its modulation modes based on the fluctuating channel conditions expressed in terms of the SNR at the equaliser's output. The set of switching thresholds used in all the previous graphs is the "Standard" set shown in Table 21.4, which was determined on the basis of the required channel SINR for maintaining the specific target video FER.

In order to investigate the effect of different sets of switching thresholds, we defined two new sets of thresholds, a more conservative set, and a more aggressive set, employing less robust, but more bandwidth-efficient modem modes at lower SNRs. The

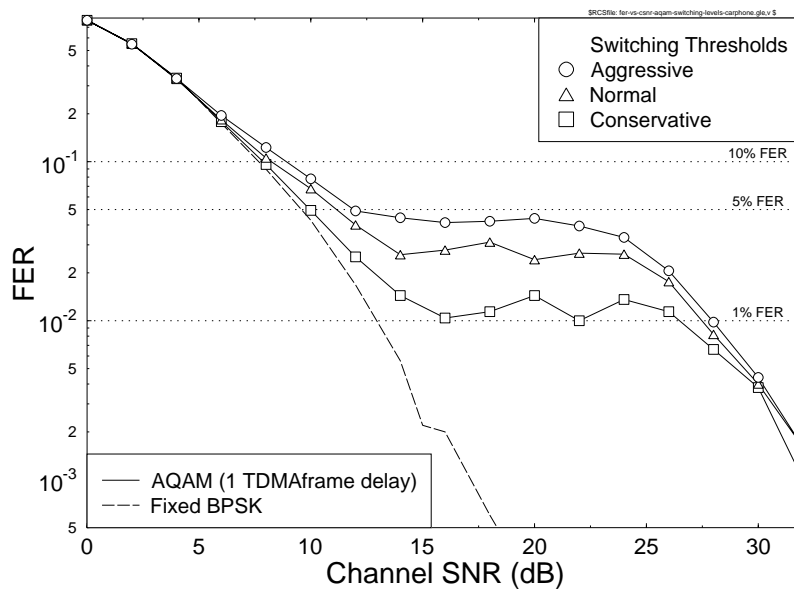


**Figure 21.11:** Transmission FER (or packet loss ratio) versus Channel SNR comparison of the fixed BPSK modulation mode and the adaptive burst-by-burst modem (AQAM) for the three sets of switching thresholds described in Table 21.4. AQAM is shown with a realistic one TDMA frame delay between channel estimation and mode switching. The channel parameters were defined in Table 21.1.

more conservative switching thresholds reduced the transmission FER at the expense of a lower effective video bitrate. The more aggressive set of thresholds increased the effective video bitrate at the expense of a higher transmission FER.

The transmission FER performance of the realistic burst-by-burst adaptive modem, which has a one TDMA frame delay between channel quality estimation and mode switching is shown in Figure 21.11 for the three sets of switching thresholds of Table 21.4. It can be seen that the more conservative switching thresholds reduce the transmission FER from about 3% to about 1% for medium channel SNRs. The more aggressive switching thresholds increase the transmission FER from about 3% to 4-5%. However, since FERs below 5% are not objectionable in video quality terms, this FER increase is an acceptable compromise for a higher effective video bitrate. The effective video bitrate for the realistic adaptive modem with the three sets of switching thresholds is shown in Figure 21.12. The more conservative set of switching thresholds reduces the effective video bitrate but also reduces the transmission FER. The aggressive switching thresholds, increase the effective video bitrate, but also increase the transmission FER. Therefore the optimal switching thresholds should be set such that the transmission FER is deemed acceptable in the range of channel SNRs considered.



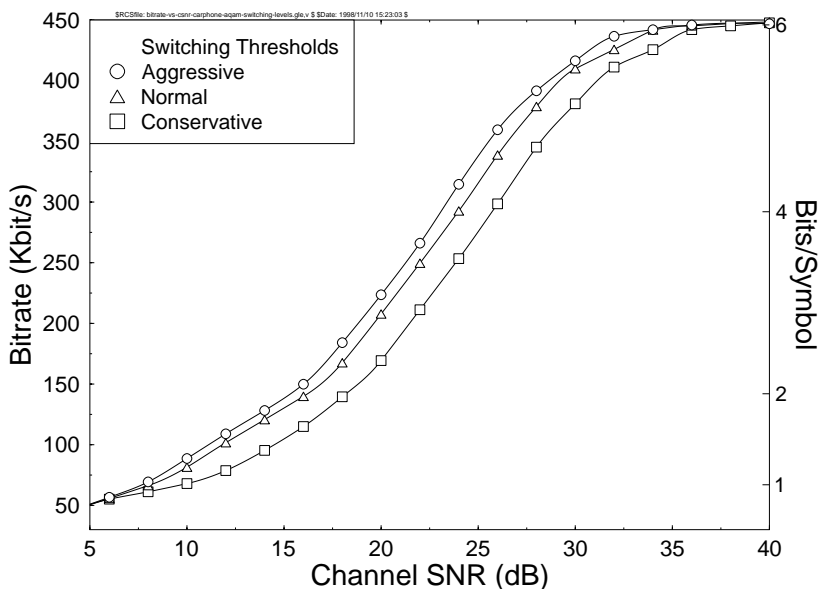


**Figure 21.12:** Video bitrate versus channel SNR comparison for the adaptive burst-by-burst modem (AQAM) with a realistic one TDMA frame delay between channel estimation and mode switching for the three sets of switching thresholds as described in Table 21.4. The channel parameters were defined in Table 21.1.

We note that the switching thresholds can be adjusted for example using Powell's optimisation for uncoded transmissions [?], in order to achieve the required target BER. However, the coded AQAM system's BER/FER performance is not analytically tractable and hence no closed-loop optimisation was invoked - the thresholds were adjusted experimentally. We note furthermore that instead of the equaliser's pseudo-SNR we also investigated using the channel codec's BER estimates for controlling the switching process, which resulted in a similar system performance. Let us now consider the performance improvements achievable, when employing powerful turbo codecs.

### 21.1.5 Turbo-coded video performance

In this subsection we demonstrate the additional performance gains that are achievable, when turbo coding is used in preference to BCH coding. The generic system parameters of the turbo-coded reconfigurable multi-mode video transceiver are the same as those used in the BCH-coded version summarised in Table 21.2. Turbo-coding schemes are known to perform best in conjunction with square-shaped turbo interleaver arrays and their performance is improved upon extending the associated interleaving depth, since then the two constituent encoders are fed with more inde-

Features	Multi-rate System			
Mode	BPSK	4QAM	16QAM	64QAM
Bits/Symbol	1	2	4	6
FEC	Half-Rate Turbo coding with CRC			
Transmission bitrate (kbit/s)	140.4	280.8	561.6	842.5
Unprotected bitrate (kbit/s)	66.3	136.1	275.6	415.2
Effective Video-rate (kbit/s)	60.9	130.4	270.0	409.3
Video fr. rate (Hz)	30			

**Table 21.5:** Operational-mode specific turbo-coded transceiver parameters

pendent data. This ensures that the turbo decoder can rely on two quasi-independent data streams in its efforts to make as reliable decisions, as possible. A turbo interleaver size of  $18 \times 18$  was chosen, requiring 324 bits for filling the interleaver. The required so-called recursive systematic convolutional component codes had a coding rate of  $1/2$  and a constraint length of  $K = 3$ . After channel coding the transmission burst length became 648 bits, which allowed the decoding of all AQAM transmission bursts independently. The operational-mode specific transceiver parameter are shown in Table 21.5, and should be compared to the corresponding BCH-coded parameters of Table 21.3.

The turbo-coded parameters result in a 10% lower effective throughput bitrate compared to BCH-coding under error-free conditions. However, we will show that under error-impaired conditions the turbo coding performance becomes better, resulting in a reduced video packet loss ratio. This reduced video packet loss ratio results in an increased effective throughput for a wide range of channel SNRs. Figure 21.13 shows the effective throughput video bitrate versus channel SNR for the proposed AQAM modem using either BCH or turbo coding, when the delay between the channel quality estimate and mode switching of the AQAM modem was one TDMA frame duration.

At high channel SNRs and virtually error-free conditions the BCH-coded modem slightly outperforms the turbo-coded modem in throughput bitrate terms, which were 446 and 409Kbps respectively. However as the channel quality degrades the lower packet loss ratio performance of the turbo-coded AQAM modem results in a higher effective throughput bitrate below channel SNRs of about 28dB.

The associated FER or video packet loss ratio (PLR) performance versus channel SNR is shown in Figure 21.14.

The BCH-coded and turbo-coded AQAM modems exhibit similarly shaped FER performance curves, both of which obey a similar FER performance curve to that of the corresponding 64QAM modem mode at high SNRs, whilst at low SNRs the FER curve follows that of the BPSK modem mode. For medium channel SNRs the FER performance curve becomes near-constant, since the modem modes are adaptively adjusted, in order to maintain the required target FER. Observe, however that the turbo coded AQAM modem requires approximately a 3dB lower channel SNR for

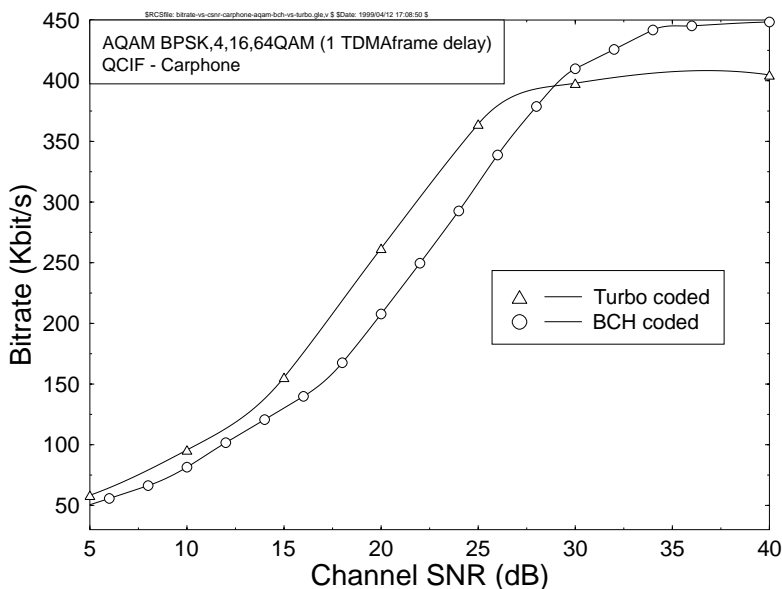


**Figure 21.13:** Effective throughput video bitrate versus channel SNR comparison of the adaptive burst-by-burst modems (AQAM) using either BCH or turbo coding. The AQAM modems have a one TDMA frame delay between channel estimation and mode switching. The channel parameters were defined in Table 21.1.

achieving the required FER target. Hence, if the minimum acceptable video packet loss ratio is shown by the 5% limit drawn in the figure, the turbo-coded modem can maintain the required PLR for channel SNRs in excess of 8dB, while the BCH-coded modem requires channel SNRs in excess of 11dB.

Having shown that the turbo-coded AQAM modem outperforms the BCH coded modem in terms of video packet loss performance, which results in a higher effective throughput video bitrate for all except very high channel SNRs, we demonstrate the associated effects on the video quality expressed in terms of the PSNR. Figure 21.15 shows the PSNR video quality versus channel SNR for the AQAM modems using either BCH or turbo coding. The higher throughput of the BCH coded modem at high channel SNRs results in a slight advantage over the turbo coded modem in terms of PSNR. However, the reduced video packet loss ratio of the turbo coded modem below channel SNRs of 30dB resulted in a higher effective throughput, increasing the video quality of the turbo coded modem. In conclusion, we have shown that the more complex turbo coded AQAM modem outperformed the BCH coded modem, since it reduced the video packet loss ratio and hence increased both the effective throughput and the video quality for all but high channel SNRs.

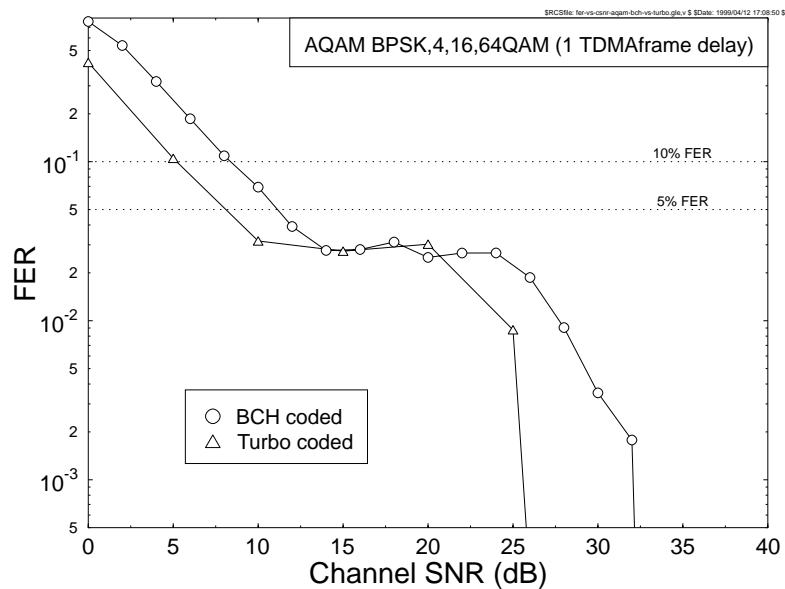


**Figure 21.14:** Transmission FER (or packet loss ratio) versus channel SNR comparison of the adaptive burst-by-burst modem (AQAM) using the standard switching thresholds of Table 21.4, and either BCH or turbo coding. The channel parameters were defined in Table 21.1 and again, there was a one TDMA frame delay between channel estimation and mode switching.

### 21.1.6 Conclusions

In this section we have proposed a wideband bursts-by-burst adaptive modem, which employs the mean squared error at the output of the the channel equaliser as the quality measure for controlling the modem modes. Furthermore, we have quantified the achievable video performance gains due to employing the proposed wideband bursts-by-burst adaptive modem. When our adaptive packetiser is used in conjunction with the adaptive modem, it continually adjusts the video codec's target bitrate, in order to exploit the instantaneous bitrate capacity provided by the adaptive modem.

We have also shown that a burst-by-burst adaptive modem exhibits a better performance, than a statically configured multi-mode scheme. The delay between the channel estimation and modulation mode switching was shown to have a considerable effect on the performance achieved by the adaptive modem. This performance penalty can be mitigated by reducing the modem mode switching latency. However, at low vehicular speeds, i.e. at low Doppler frequencies the switching latency is less crucial and the practical adaptive modem can achieve a performance that is close to that of the ideal adaptive modem benefiting from instantaneous modem mode switching, which we used to quantify the expected upper-bound performance. We have also demonstrated, how the transmission FER performance is affected by chang-

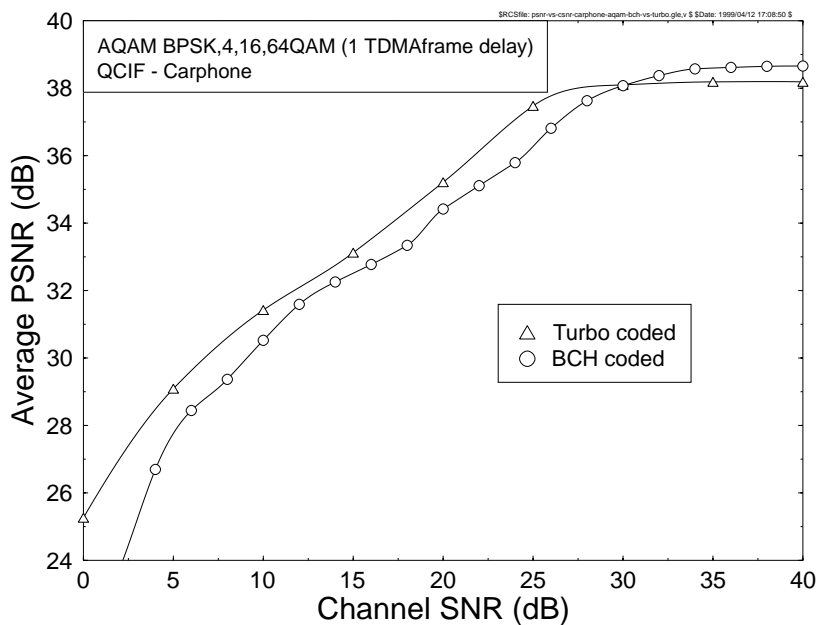


**Figure 21.15:** Decoded video quality (PSNR) versus transmission FER (or packet loss ratio) comparison of the realistic adaptive burst-by-burst modems (AQAM) using either BCH or turbo coding. The channel parameters were defined in Table 21.1.

ing the switching thresholds. Therefore the system can be tuned to the required FER performance using appropriate switching thresholds. Our future work will be concentrated on improving the system performance by invoking more complex turbo coding schemes.

Motivated by the recent dominance of CDMA-based wireless systems - such as the UMTS, IMT-2000 and cdma2000 systems - in the next section we embark on studying the video performance of various joint-detection based multi-user wireless videophone systems.

## 21.2 A UMTS-like Video-phone System: Turbo-coded Burst-by-burst Adaptive Joint - detection CDMA/H.263 Based Videophony<sup>4 5</sup>

### 21.2.1 Motivation and Video Transceiver Overview

While the third-generation wireless communications standards are still evolving at the time of writing, they became sufficiently mature for the equipment designers and manufacturers to complete the design of prototype equipment. One of the most important service tested in the field-trials of virtually all dominant players in the field is interactive video telephony at various bitrates and video qualities. Motivated by these events the goal of this section is to quantify the expected video performance of a UMTS-like videophone scheme, whilst also providing an outlook to more powerful burst-by-burst adaptive transceivers of the near-future.

In this study we transmitted 176x144 pixel Quarter Common Intermediate Format (QCIF) and 128x96 pixel Sub-QCIF (SQCIF) video sequences at 10 frames/s using a reconfigurable Time Division Multiple Access / Code Division Multiple Access (TDMA / CDMA) transceiver, which can be configured as a 1, 2 or 4 bit/symbol scheme. The H.263 video codec [182] exhibits an impressive compression ratio, although this is achieved at the cost of a high vulnerability to transmission errors, since a run-length coded stream is rendered undecodable by a single bit error. In order to mitigate this problem, when the channel codec protecting the video stream is overwhelmed by the transmission errors, we refrain from decoding the corrupted video packet in order to prevent error propagation through the reconstructed video frame buffer [189]. We found that it was more beneficial in video quality terms, if these corrupted video packets were dropped and the reconstructed frame buffer was not updated, until the next video packet replenishing the specific video frame area was received. The associated video performance degradation was found perceptually unobjectionable for packet dropping- or transmission frame error rates (FER) below about 5%. These packet dropping events were signalled to the remote decoder by superimposing a strongly protected one-bit packet acknowledgement flag on the reverse-direction packet, as outlined in [189]. Bose-Chaudhuri-Hocquenghem (BCH) [9] and turbo error correction codes [28] were used and again, the CDMA transceiver was capable of transmitting 1, 2 and 4 bits per symbol, where each symbol was spread using a low spreading factor (SF) of 16, as seen in Table 21.6. The associated parameters will be addressed in more depth during our further discourse. Employing a low spreading factor of 16 allowed us to improve the system's multi-user performance with the aid of joint-detection techniques [340]. We note furthermore that the implementation of the joint detection receivers is independent of the number of bits per symbol associated with the modulation mode used, since the receiver

<sup>4</sup>This section is based on P. Cherriman, E.L. Kuan, L. Hanzo: Burst-by-burst Adaptive Joint-detection CDMA/H.263 Based Video Telephony, submitted to IEEE Tr. on CSVT, 1999

<sup>5</sup>©1999 IEEE. Personal use of this material is permitted. However, permission to reprint/republish this material for advertising or promotional purposes or for creating new collective works for resale or redistribution to servers or lists, or to refuse any copyrighted component of this work in other works must be obtained from IEEE.

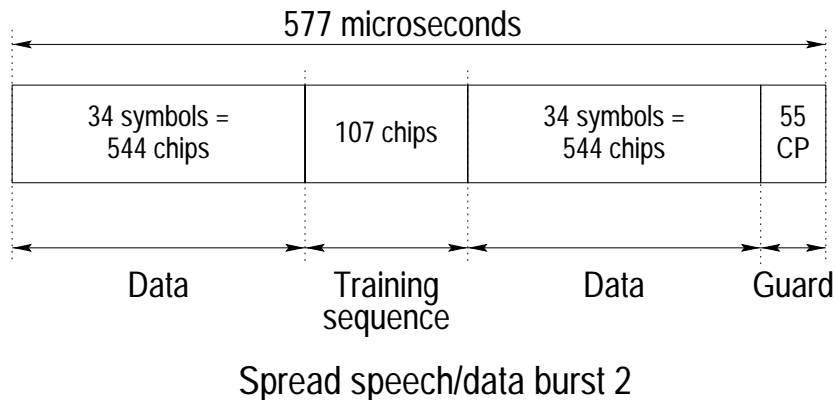


**Figure 21.16:** Transmission burst structure of the FMA1 spread speech/data mode 2 of the FRAMES proposal [591]

simply inverts the associated system matrix and invokes a decision concerning the received symbol, irrespective of how many bits per symbol were used. **Therefore, joint detection receivers are amenable to amalgamation with the above 1, 2 and 4 bit/symbol modem, since they do not have to be reconfigured each time the modulation mode is switched.**

In this performance study we used the Pan-European FRAMES proposal [591] as the basis for our CDMA system. The associated transmission frame structure is shown in Figure 21.16, while a range of generic system parameters are summarised in Table 21.6. In our performance studies we used the COST207 [324] seven-path bad urban (BU) channel model, whose impulse response is portrayed in Figure 21.17.

Our initial experiments compared the performance of a whitening matched filter (WMF) for single user detection and the Minimum mean square error block decision feedback equalizer (MMSE-BDFE) for joint multi-user detection. These simulations were performed using 4-level Quadrature Amplitude Modulation (4QAM), invoking both binary BCH [9] and turbo coded [28] video packets. The associated bitrates are summarised in Table 21.7. The transmission bitrate of the 4QAM modem mode was 29.5Kbps, which was reduced due to the approximately half-rate BCH or turbo coding, plus the associated video packet acknowledgement feedback flag error control [593] and video packetisation overhead to produce effective video bitrates of 13.7Kbps and 11.1Kbps, respectively. A more detailed discussion on the video packet acknowledgement feedback error control and video packetisation overhead will be provided in Section 21.2.2 with reference to the convolutionally coded multi-mode investigations.

Figure 21.18 portrays the bit error ratio (BER) performance of the BCH coded video transceiver using both matched filtering and joint detection for 2–8 users. The bit error ratio is shown to increase, as the number of users increases, even upon employing the MMSE-BDFE multi-user detector (MUD). However, while the matched filtering receiver exhibits an unacceptably high BER for supporting perceptually unimpaired video communications, the MUD exhibits a far superior BER performance.

When the BCH codec was replaced by the turbo-codec, the bit error ratio per-

Parameter	
Multiple access	TDMA/CDMA
Channel type	COST 207 Bad Urban
Number of paths in channel	7
Normalised Doppler frequency	$3.7 \times 10^{-5}$
CDMA spreading factor	16
Spreading sequence	Random
Frame duration	4.615 ms
Burst duration	577 $\mu$ s
Joint detection CDMA receiver	Whitening matched filter (WMF) or Minimum mean square error block decision feedback equalizer (MMSE-BDFE)
No. of Slots/Frame	8
TDMA frame length	4.615ms
TDMA slot length	577 $\mu$ s
TDMA slots/Video packet	3
Chip Periods/TDMA slot	1250
Data Symbols/TDMA slot	68
User Data Symbol Rate (kBd)	14.7
System Data Symbol Rate (kBd)	117.9

**Table 21.6:** Generic system parameters using the Frames spread speech/data mode 2 proposal [591]

Features	BCH coding	Turbo coding
Modulation	4QAM	
Transmission bitrate (kbit/s)	29.5	
Video-rate (kbit/s)	13.7	11.1
Video framerate (Hz)	10	

**Table 21.7:** FEC-protected and unprotected BCH and Turbo coded bitrates for the 4QAM transceiver mode



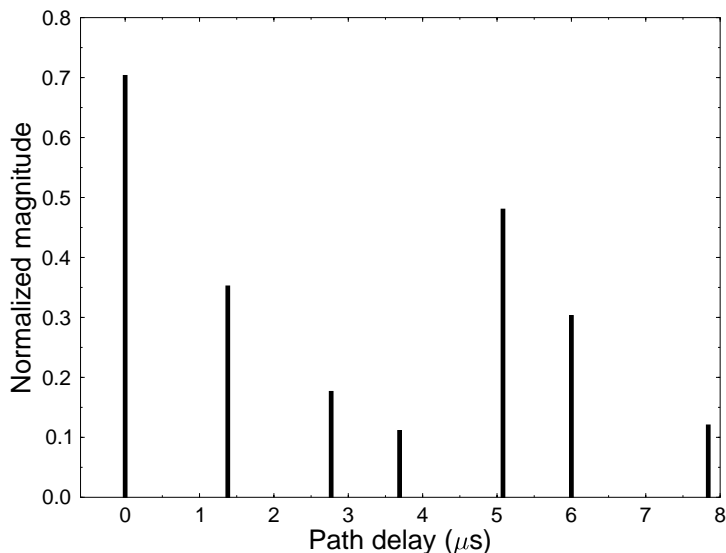


**Figure 21.17:** Normalized channel impulse response for the COST 207 [324] seven-path Bad Urban channel.

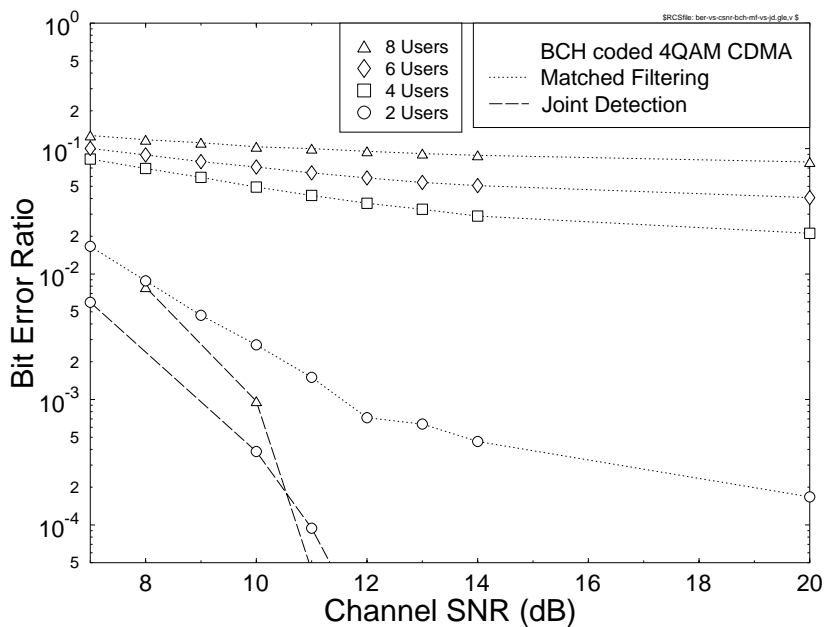
formance of both matched filtering and the MUD receiver improved, as shown in Figure 21.19. However, as expected, matched filtering was still outperformed by the joint detection scheme for the same number of users. Furthermore, the matched filtering performance degraded rapidly for more than two users.

Figure 21.20 shows the video packet loss ratio (PLR) for the turbo coded video stream using matched filtering and joint detection for 2–8 users. The figure clearly shows that the matched filter was only capable of meeting the target packet loss ratio of 5% for upto four users, when the channel SNR was in excess of 11dB. However, the joint detection algorithm guaranteed the required video packet loss ratio performance for 2–8 users in the entire range of channel SNRs shown. Furthermore, the 2-user matched-filtered PLR performance was close to the 8-user MUD PLR.

### 21.2.2 Multi-mode Video System Performance

Having shown that joint detection can substantially improve our system's performance, we investigated the performance of a multi-mode convolutionally coded video system employing joint detection, while supporting two users. The associated convolutional codec parameters are summarised in Table 21.8.

Below we now detail the video packetisation method employed. The reader is reminded that the number of symbols per TDMA frame was 68 according to Table 21.6. In the 4QAM mode this would give 136 bits per TDMA frame. However, if we transmitted one video packet per TDMA frame, then the packetisation overhead would absorb a large percentage of the available bitrate. Hence we assembled



**Figure 21.18:** BER versus channel SNR 4QAM performance using BCH coded 13.7Kbps video, comparing the performance of matched filtering and joint detection for 2-8 users.

Features	Multi-rate System		
Mode	BPSK	4QAM	16QAM
Bits/Symbol	1	2	4
FEC	Convolutional Coding		
Transmitted bits/packet	204	408	816
Total bitrate (kbit/s)	14.7	29.5	58.9
FEC-coded bits/packet	102	204	408
Assigned to FEC-coding (kbit/s)	7.4	14.7	29.5
Error detection per packet	16 bit CRC		
Feedback bits / packet	9		
Video packet size	77	179	383
Packet header bits	8	9	10
Video bits/packet	69	170	373
Unprotected video-rate (kbit/s)	5.0	12.3	26.9
Video framerate (Hz)	10		

**Table 21.8:** Operational-mode specific transceiver parameters for the proposed multi-mode system

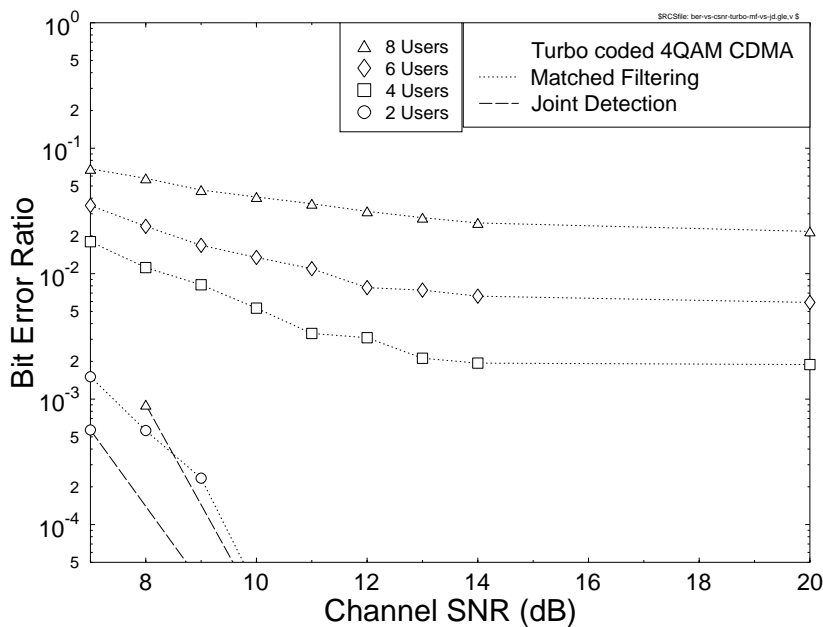


**Figure 21.19:** BER versus channel SNR 4QAM performance using turbo-coded 11.1Kbps video, comparing the performance of matched filtering and joint detection for 2–8 users.

larger video packets, thereby reducing the packetisation overhead and arranged for transmitting the contents of a video packet over three consecutive TDMA frames, as indicated in Table 21.6. Therefore each protected video packet consists of  $68 \times 3 = 204$  modulation symbols, yielding a transmission bitrate of between 14.7 and 38.9 Kbps for BPSK and 16QAM, respectively. However, in order to protect the video data we employed half-rate, constraint-length nine convolutional coding, using octal generator polynomials of 561 and 753. The useful video bitrate was further reduced due to the 16-bit Cyclic Redundancy Checking (CRC) used for error detection and the nine-bit repetition-coded feedback error flag for the reverse link. This results in video packet sizes of 77, 179 and 383 bits for each of the three modulation modes. The useful video capacity was finally further reduced by the video packet header of between 8 and 10 bits, resulting in useful or effective video bitrates ranging from 5 to 26.9 Kbps in the BPSK and 16QAM modes, respectively.

The proposed multi-mode system can switch amongst the 1, 2 and 4 bit/symbol modulation schemes under network control, based upon the prevailing channel conditions. As seen in Table 21.8, when the channel is benign, the unprotected video bitrate will be approximately 26.9Kbps the 16QAM mode. However, as the channel quality degrades, the modem will switch to the BPSK mode of operation, where the video bitrate drops to 5Kbps, and for maintaining a reasonable video quality, the video resolution has to be reduced to SQCIF (128x96 pels).

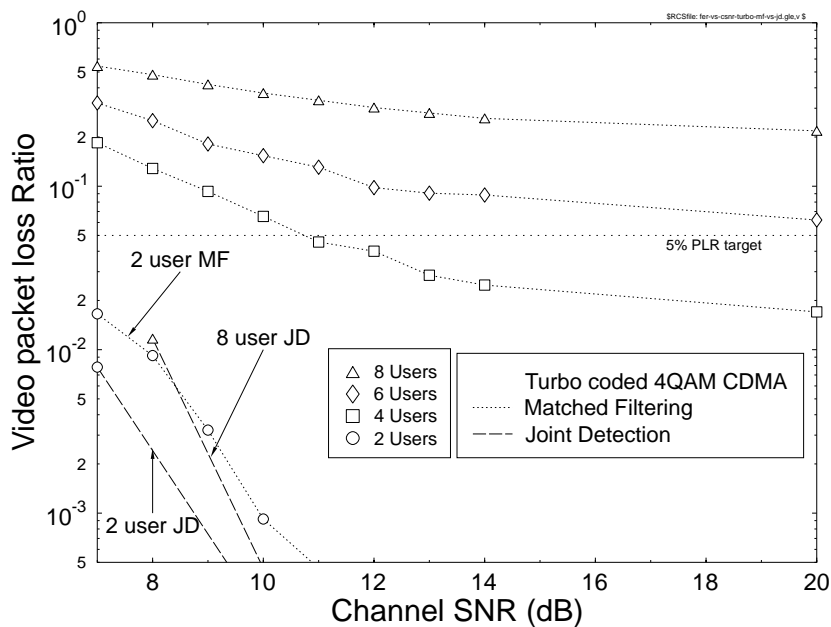


**Figure 21.20:** Video packet loss ratio versus channel SNR for the turbo-coded 11.1 Kbps video stream, comparing the performance of matched filtering and joint detection for 2–8 users.

Figure 21.21 portrays the packet loss ratio for the multi-mode system, in each of its modulation modes for a range of channel SNRs. It can be seen in the figure that above a channel SNR of 14dB the 16QAM mode offers an acceptable packet loss ratio of less than 5%, while providing an unprotected video rate of about 26.9Kbps. If the channel SNR drops below 14dB, the multi-mode system is switched to 4QAM and eventually to BPSK, when the channel SNR is below 9dB, in order to maintain the required quality of service, which is dictated by the packet loss ratio. The figure also shows the acknowledgement feedback error ratio (FBER) for a range of channel SNRs, which has to be substantially lower, than the video PLR itself. This requirement is satisfied in the figure, since the feedback errors only occur at extremely low channel SNRs, where the packet loss ratio is approximately 50%, and it is therefore assumed that the multi-mode system would have switched to a more robust modulation mode, before the feedback acknowledgement flag can become corrupted.

The video quality is commonly measured in terms of the peak-signal-to-noise-ratio (PSNR). Figure 21.22 shows the video quality in terms of the PSNR versus the channel SNRs for each of the modulation modes. As expected, the higher throughput bitrate of the 16QAM mode provides a better video quality. However, as the channel quality degrades, the video quality of the 16QAM mode is reduced and hence it becomes beneficial to switch from the 16QAM mode to 4QAM at an SNR of about 14dB, as it was suggested by the packet loss ratio performance of Figure 21.21. Although

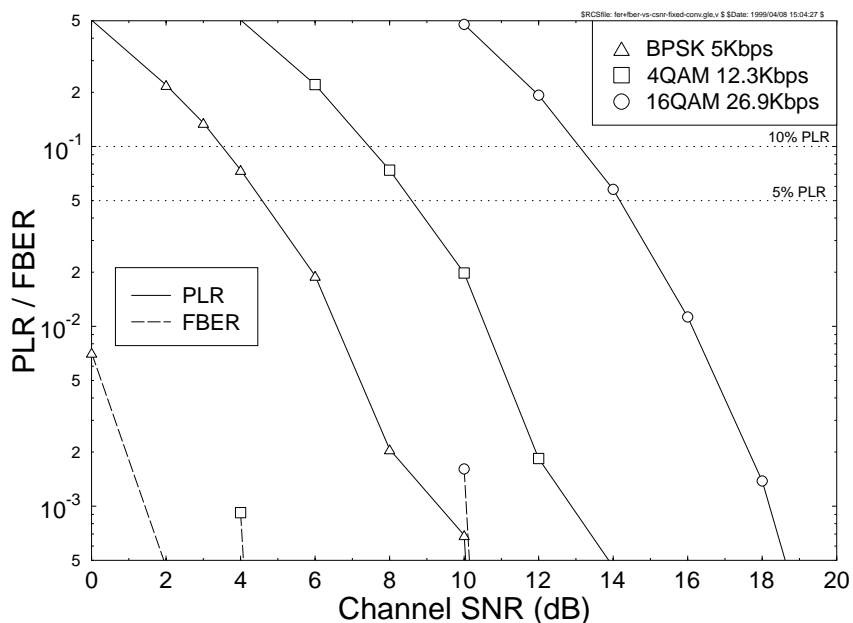


**Figure 21.21:** Video packet loss ratio (PLR) and feedback error ratio (FBER) versus channel SNR for the three modulation schemes of the 2-user multi-mode system using joint detection.

the video quality expressed in terms of PSNR is superior for the 16QAM mode in comparison to the 4QAM mode at channel SNRs in excess of 12dB, however, due to the excessive PLR the perceived video quality appears inferior in comparison to that of the 4QAM mode, even though the 16QAM PSNR is higher for channel SNRs in the range of 12–14dB. More specifically, we found that it was beneficial to switch to a more robust modulation scheme, when the PSNR was reduced by about 1dB with respect to its unimpaired PSNR value. This ensured that the packet losses did not become subjectively obvious, resulting in a higher perceived video quality and smoother degradation, as the channel quality deteriorated.

The effect of packet losses on the video quality quantified in terms of PSNR is portrayed in Figure 21.23. The figure shows, how the video quality degrades, as the PLR increases. It has been found that in order to ensure a seamless degradation of video quality as the channel SNR reduced, it was the best policy to switch to a more robust modulation scheme, when the PLR exceeded 5%. The figure clearly shows that a 5% packet loss ratio results in a loss of PSNR, when switching to a more robust modulation scheme. However, if the system did not switch until the PSNR of the more robust modulation mode was similar, the perceived video quality associated with the originally higher rate, but channel-impaired stream became inferior.

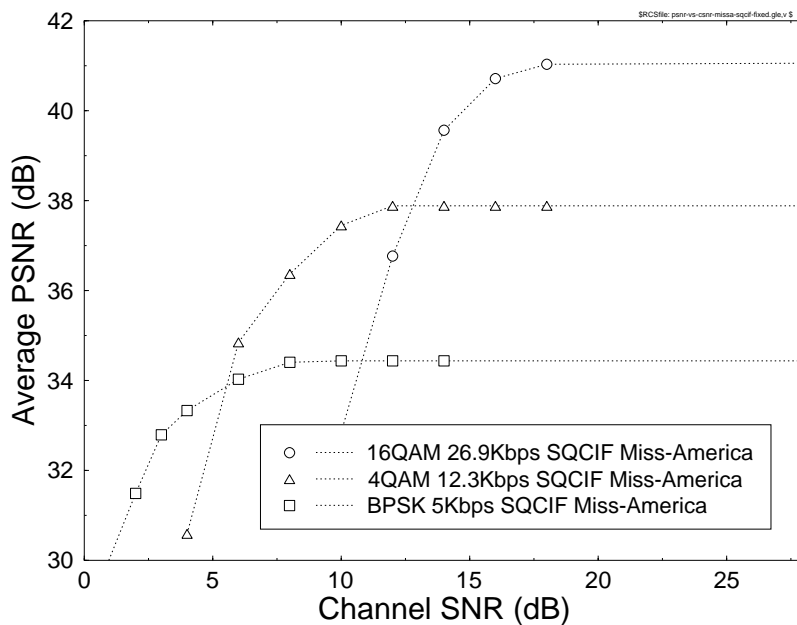


**Figure 21.22:** Decoded video quality (PSNR) versus channel SNR for the modulation modes of BPSK, 4QAM and 16QAM supporting 2-users with the aid of joint detection. These results were recorded for the Miss-America video sequence at SQCIF resolution (128x96 pels).

### 21.2.3 Burst-by-Burst adaptive videophone system

A burst-by-burst adaptive modem, maximizes the system's throughput by using the most appropriate modulation mode for the current instantaneous channel conditions. Figure 21.24 exemplifies, how a burst-by-burst adaptive modem changes its modulation modes based on the fluctuating channel conditions. The adaptive modem uses the SINR estimate at the output of the joint-detector to estimate the instantaneous channel quality, and hence to set the modulation mode.

The probability of the adaptive modem using each modulation mode for a particular channel SNRs is portrayed in Figure 21.25. It can be seen at high channel SNRs that the modem mainly uses the 16QAM modulation mode, while at low channel SNRs the BPSK mode is most prevalent.

The advantage of dynamically reconfigured burst-by-adaptive modem over the statically switched multi-mode system previously described, is that the video quality is smoothly degraded as the channel conditions deteriorate. The switched multi-mode system results in more sudden reductions in video quality, when the modem switches to a more robust modulation mode. Figure 21.26 shows the throughput bitrate of the dynamically reconfigured burst-by-burst adaptive modem, compared to the three modes of the statically switched multi-mode system. The reduction of

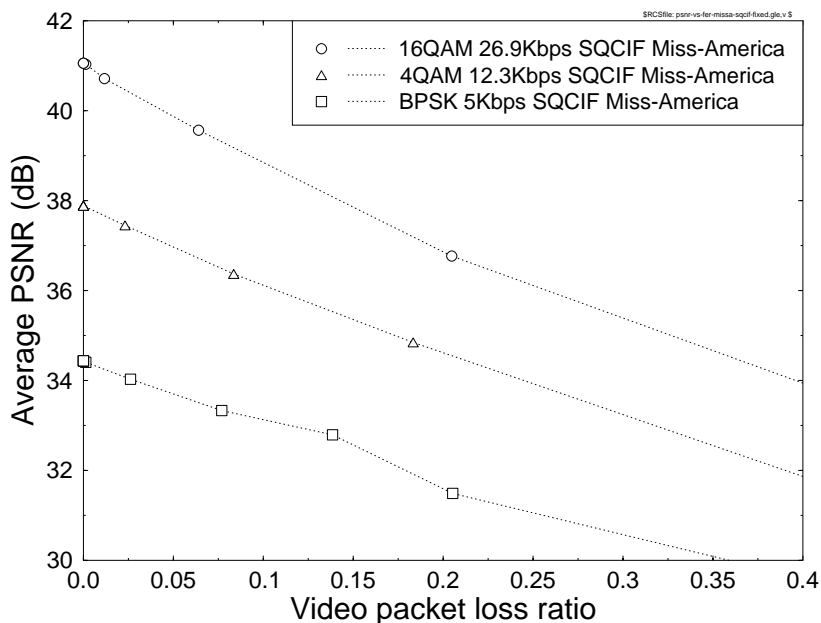


**Figure 21.23:** Decoded video quality (PSNR) versus video packet loss ratio for the modulation modes of BPSK, 4QAM and 16QAM, supporting 2-users with the aid of joint detection. The results were recorded for the Miss-America video sequence at SQCIF resolution (128x96 pels).

the fixed modem modes' effective throughput at low SNRs is due to the fact that under such channel conditions an increased fraction of the transmitted packets have to be dropped, reducing the effective throughput. The figure shows the smooth reduction of the throughput bitrate, as the channel quality deteriorates. The burst-by-burst modem matches the BPSK mode's bitrate at low channel SNRs, and the 16QAM mode's bitrate at high SNRs. The dynamically reconfigured burst-by-burst adaptive modem characterised in the figure perfectly estimates the prevalent channel conditions although in practice the estimate of channel quality is not perfect and it is inherently delayed. However, we have shown in the previous section 21.1 on wideband video transmission that non-perfect channel estimates result in only slightly reduced performance, when compared to perfect channel estimation.

The smoothly varying throughput bitrate of the burst-by-burst adaptive modem translates into a smoothly varying video quality as the channel conditions change. The video quality measured in terms of the average peak signal to noise ratio (PSNR) is shown versus the channel SNR in Figure 21.27 in contrast to that of the individual modem modes. The figure demonstrates that the burst-by-burst adaptive modem provides equal or better video quality over a large proportion of the SNR range shown than the individual modes. However, even at channel SNRs, where the adaptive modem has a slightly reduced PSNR, the perceived video quality of the adaptive

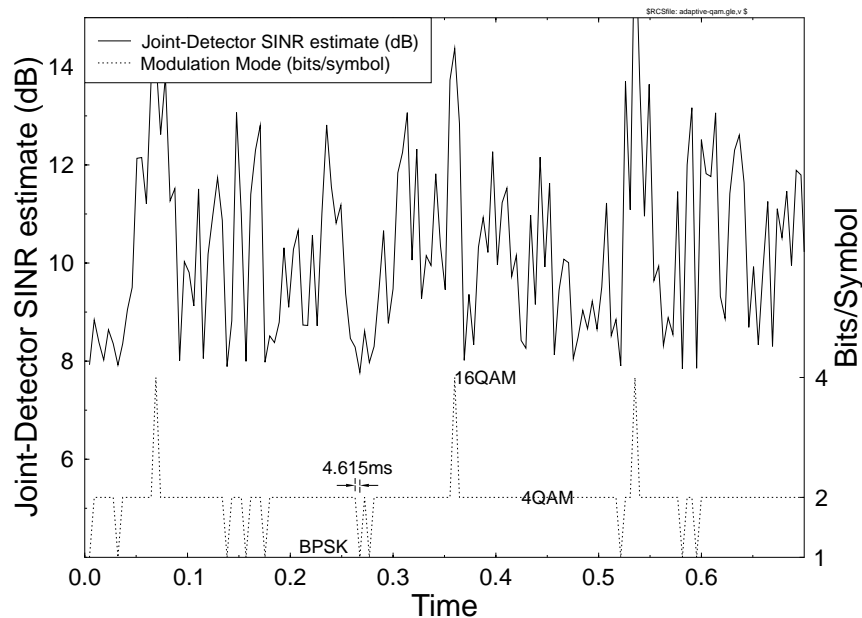


**Figure 21.24:** Example of modem mode switching in a dynamically reconfigured burst-by-burst modem in operation, where the modulation mode switching is based upon the SINR estimate at the output of the joint-detector.

modem is better since the video packet loss rate is far lower, than that of the fixed modem modes.

Figure 21.28 shows the video packet loss ratio versus channel SNR for the three fixed modulation modes and the burst-by-burst adaptive modem with perfect channel estimation. Again the figure demonstrates that the video packet loss ratio of the adaptive modem is similar to that of the fixed BPSK modem mode, however the adaptive modem has a far higher bitrate throughput, as the channel SNR increases. The burst-by-burst adaptive modem gives an error performance similar to that of the BPSK mode, but with the flexibility to increase the bitrate throughput of the modem, when the channel conditions improve. If imperfect channel estimation is used, the throughput bitrate of the adaptive modem is reduced slightly. Furthermore, the video packet loss ratio seen in Figure 21.28 is slightly higher for the AQAM scheme due to invoking higher-order modem modes, as the channel quality increases. However we have shown in our previous report on wideband video transmission [594] that it is possible to maintain the video packet loss ratio within tolerable limits for the range of channel SNRs considered.

The interaction between the video quality measured in terms of PSNR and the video packet loss ratio can be more clearly seen in Figure 21.29. The figure shows that the adaptive modem slowly degrades the decoded video quality from that of the error free 16QAM fixed modulation mode, as the channel conditions deteriorate. The



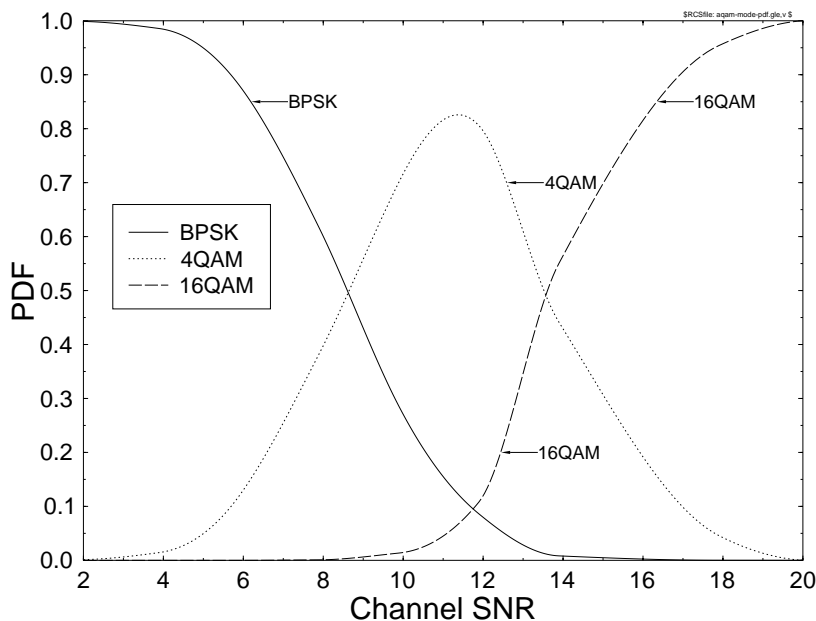


Figure 21.25: PDF of the various adaptive modem modes versus channel SNR.

video quality degrades from the error-free 41dB PSNR, while maintaining a near-zero video packet loss ratio, until the PSNR drops below about 36dB PSNR. At this point the further reduced channel quality inflicts an increased video packet loss rate and the video quality degrades more slowly. The PSNR versus packet loss ratio performance then tends toward that achieved by the fixed BPSK modulation mode. However the adaptive modem achieved better video quality than the fixed BPSK modem even at high packet loss rates.

#### 21.2.4 Conclusions

In conclusion, the proposed joint-detection assisted burst-by-burst adaptive CDMA-based video transceiver substantially outperformed the matched-filtering based transceiver. The transceiver guaranteed a near-unimpaired video quality for channel SNRs in excess of about 5 dB over the COST207 dispersive Rayleigh-faded channel. The benefits of the multimode video transceiver clearly manifest themselves in terms of supporting un-impaired video quality under time-variant channel conditions, where a single-mode transceiver's quality would become severely degraded by channel effects. The dynamically reconfigured burst-by-burst adaptive modem gave better perceived video quality due to its more graceful reduction in video quality, as the channel conditions degraded, than a statically switched multi-mode system.

Following our discussions on joint-detection assisted CDMA-based burst-by-burst adaptive interactive video telephony, in the next two sections we will concentrate

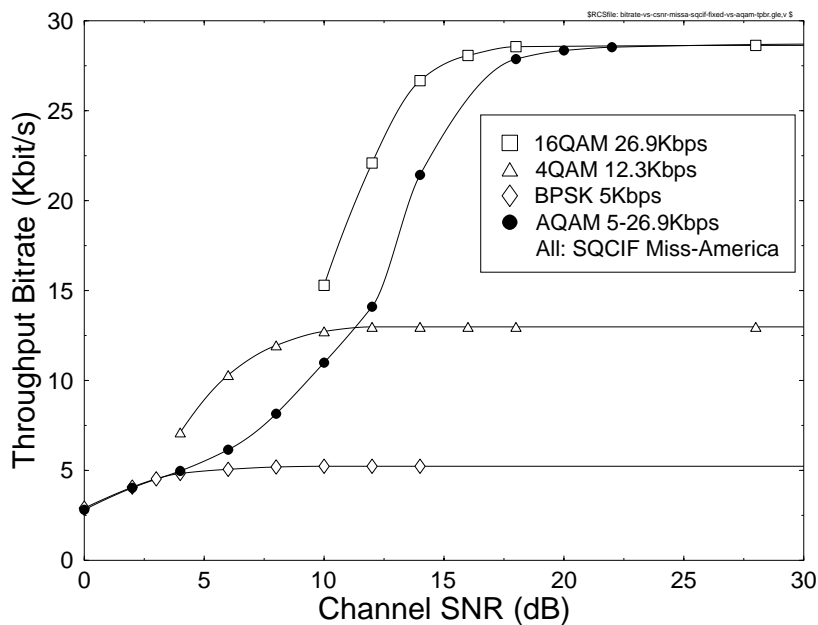


**Figure 21.26:** Throughput bitrate versus channel SNR comparison of the three fixed modulation modes (BPSK, 4QAM, 16QAM) and the adaptive burst-by-burst modem (AQAM), both supporting 2 users with the aid of joint detection.

on a range multi-carrier modems, while the last section of this chapter will consider distributive broadcast video transmission, based also on multi-carrier modems.

## 21.3 H.263/OFDM-based Video Systems for Frequency-selective Wireless Networks<sup>6 7</sup>

### 21.3.1 Background

In our previous video systems, so-called single-carrier or serial modems were used. In recent years the so-called multi-carrier orthogonal frequency division multiplex (OFDM) or parallel modems have also received considerable attention, especially in distributive, or synonymously, in broadcasting systems. In this section we will show that OFDM systems are also attractive in interactive video telephony.

<sup>6</sup>This section is based upon: P. Cherriman, T. Keller, and L. Hanzo, "Orthogonal frequency division multiplex transmission of H.263 encoded video over highly frequency-selective wireless networks." IEEE Transactions on Circuits and Systems for Video Technology, Aug. 1999 [595].

<sup>7</sup>©1999 IEEE. Personal use of this material is permitted. However, permission to reprint/republish this material for advertising or promotional purposes or for creating new collective works for resale or redistribution to servers or lists, or to refuse any copyrighted component of this work in other works must be obtained from IEEE.

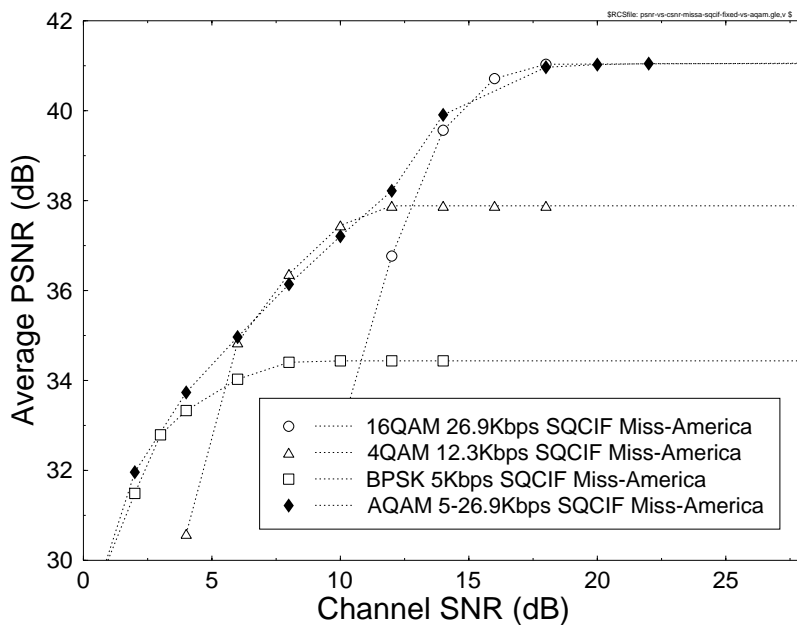


**Figure 21.27:** Average decoded video quality (PSNR) versus channel SNR comparison of the fixed modulation modes of BPSK, 4QAM and 16QAM, and the burst-by-burst adaptive modem. Both supporting 2-users with the aid of joint detection. These results were recorded for the Miss-America video sequence at SQCIF resolution (128x96 pels).

A rudimentary introduction to OFDM was provided in Chapter 5. OFDM was originally proposed by Chang in 1966 [?], where instead of estimating the wide-band dispersive channel's impulse response, as in conventional equalised serial modems [10], the channel is rendered non-dispersive by splitting the information to be transmitted into a high number of parallel, low-rate, non-dispersive channels [10]. In this case, there is no need to estimate the channel's impulse response, since for the low-rate subchannels it can be considered non-dispersive. Over the past three decades this technique has been regularly revisited by a number of researchers [?, 155, 156, 158, 162, 596]. Despite its conceptual elegance, until recently its employment has been mostly limited to military applications due to implementation difficulties. However, it has recently been adopted as the new pan-European digital audio broadcasting (DAB) standard [167], and digital terrestrial television broadcast DTTB standard [168] - now known as (DVB-T) - as well as for a range of other high-rate applications, such as 155 Mbps wireless Asynchronous Transfer Mode (WATM) local area networks. These wide-ranging applications underline the significance of OFDM modems as an alternative technique to conventional serial modems with channel equalisation, in order to combat signal dispersion [?, 155, 156, 158, 162, 596].

The outline of this section is as follows. In Section 21.3.2 the ability of the H.263

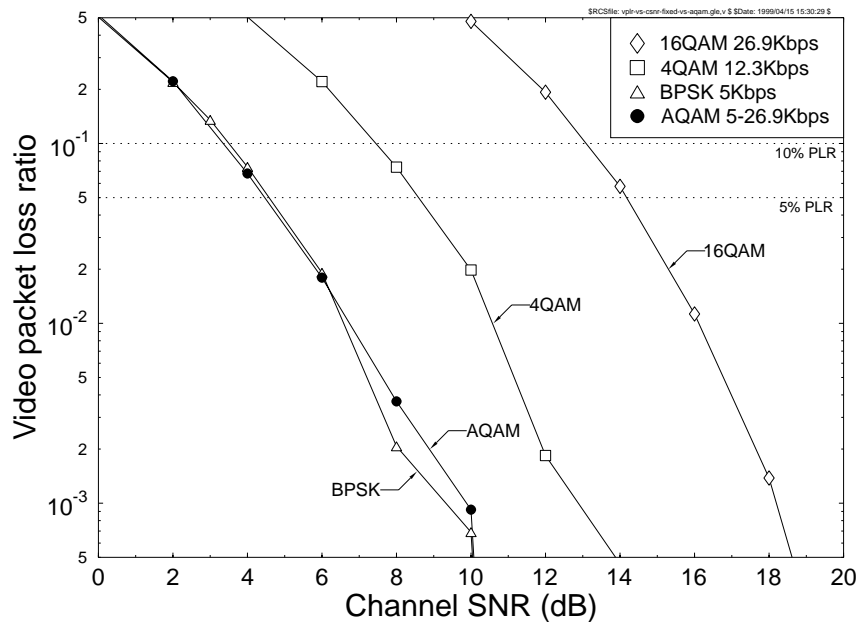


**Figure 21.28:** Video packet loss ratio (PLR) versus channel SNR for the three modulation schemes of the multi-mode system, compared to the burst-by-burst adaptive modem. Both systems sustain 2-users using joint detection.

codec to support a wide range of video services is analysed. Sections 21.3.2.1 and 21.3.2.2 provide an overview of the two proposed systems, while Section 21.3.3 characterises the propagation environment of both our UMTS-like and WATM-oriented systems. Section 21.3.4 is concerned with the system's video aspects and the overall system performance is evaluated in Section 21.3.5.

The image quality versus bitrate performance of the H.263 codec for various image resolutions, frame rates and video sequences was analysed in the corresponding earlier Sections. The video sequences used in this section are summarised in Table 21.9. We note, however that for cellular and cordless systems only SQCIF and QCIF resolutions are realistic in terms of their minimum required bitrates, while for higher-rate local area networks CIF, 4CIF and 16CIF resolutions cater for substantially increased video quality. Let us commence our discourse with a brief system overview.

### 21.3.2 System Overview

In order to explore the range of potential applications for our H.263 / OFDM system, we will investigate two different schemes. Specifically, a higher-rate wireless asynchronous transfer mode (WATM) system will be studied in Section 21.3.2.1 and a lower-rate cellular type system will be investigated in Section 21.3.2.2.

Both proposed wireless system's schematic follows the structure of Figure 21.30

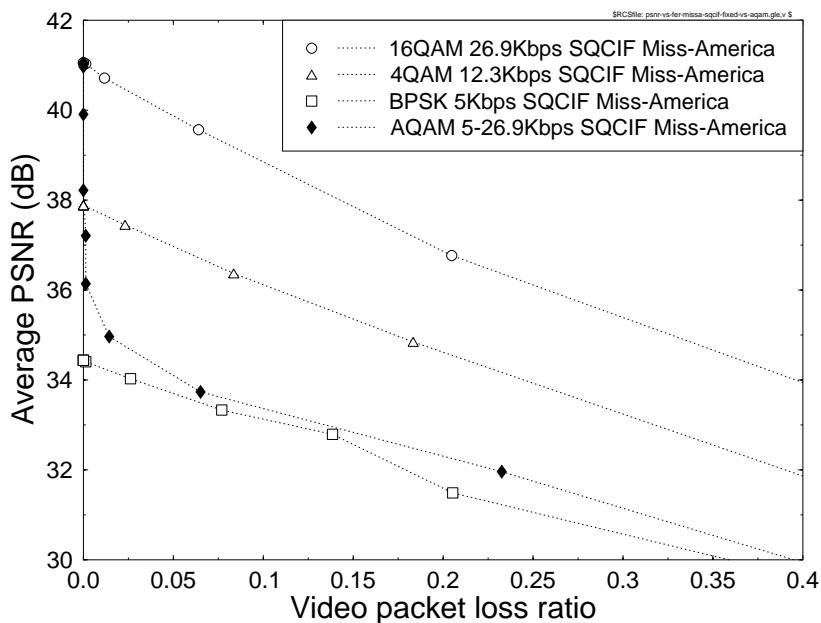


**Figure 21.29:** Decoded video quality (PSNR) versus video packet loss ratio comparison of the fixed modulation modes of BPSK, 4QAM and 16QAM, and the burst-by-burst adaptive modem. Both supporting 2-users with the aid of joint detection. These results were recorded for the Miss-America video sequence at SQCIF resolution (128x96 pels).

Video Clip	Size	Frame/s	Colour
Miss America	QCIF	10, 30	Grey
Miss America	SQCIF, QCIF, CIF	10, 30	Colour
Carphone	QCIF	10, 30	Colour
Suzie	SQCIF, QCIF, 4CIF	10, 30	Colour
Football	4CIF	10, 30	Colour
Mall	16CIF	10, 30	Colour

CIF: 288 × 352 pixel Common Intermediate Format  
 QCIF: 144 × 176 pixel Quarter CIF  
 SQCIF: 96 × 128 pixel Sub-QCIF  
 4CIF: 576 × 704 pixel 4×CIF  
 16CIF: 1152 × 1408 pixel 16×CIF

**Table 21.9:** Video sequences used for H.263 simulations

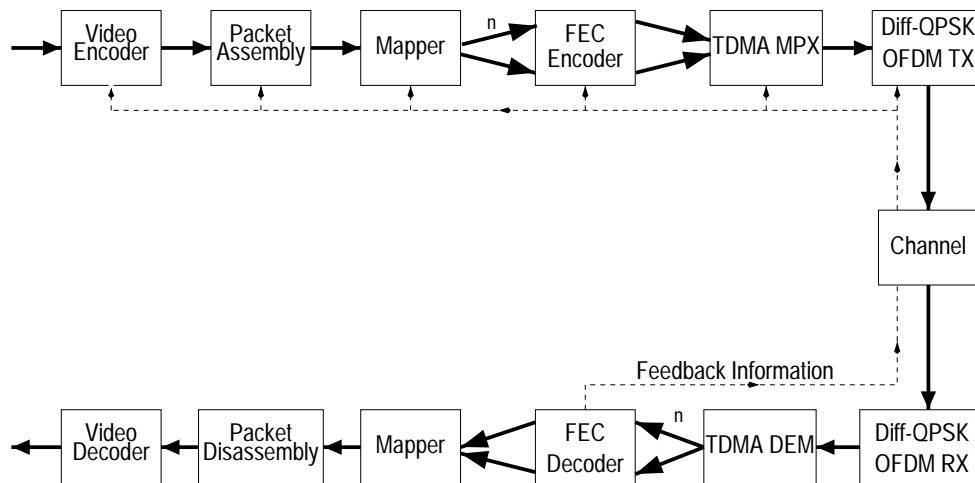
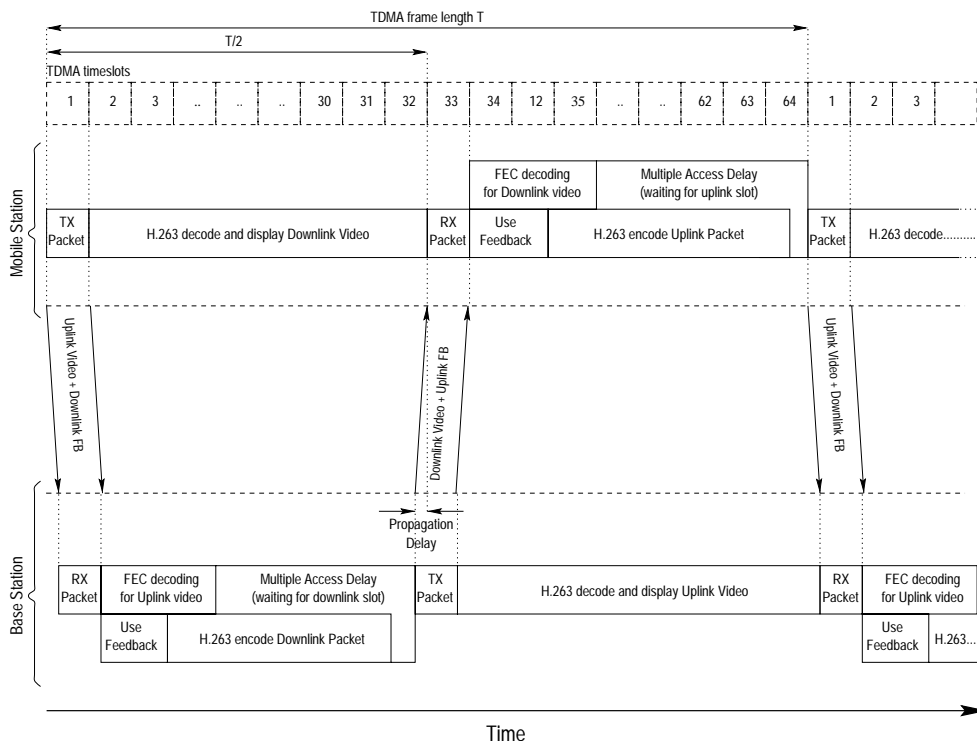


Figure 21.30: H.263/OFDM Video Transceiver Schematic

and both support interactive videophone calls. The video signal is compressed using the H.263 video compression standard [182]. As argued before, the H.263 standard achieves high compression ratios, however the resulting bitstream is extremely sensitive to channel errors. This sensitivity to channel errors is not a serious problem over benign wireline-based channels, such as conventional ATM links, but it is an impediment, when used over wireless networks. There have been several solutions suggested in the literature for overcoming this using Automatic Repeat Request (ARQ) [555], dual-level coding [184] and the use of a feedback channel [185]. A range of further robust video schemes were proposed in [188, 189, 473, 501, 597].

As seen in Figure 21.30, our system uses a feedback channel, in order to inform the encoder of the loss of previous packets, as in the case of our single-carrier video systems. As before, we do not retransmit the corrupted packets, since this would reduce the system's teletraffic capacity by occupying additional transmission slots, while increasing the video delay. We have shown before that simply dropping the corrupted packets at both the local and remote decoder results in an extremely high error resilience, in particular in high frame-rate systems, where 30 frames/s high-rate transmissions are facilitated. The rationale behind this is that un-updated video frame segments can only persist at 30 fps for 33 ms. This allows for the reconstruction frame buffer contents of the local and remote decoders to remain identical, which is essential for preventing error propagation through the reconstructed frame buffer. Then, when the instantaneous channel quality improves, the corrupted picture segments of the reconstructed frame buffers are replenished with more up-to-date video information. Similarly to our single-carrier videophone systems, the feedback channel is implemented by superimposing the packet dropping request on the reverse link, as shown in Figure 21.31. This figure shows, how the feedback acknowledgement is implemented in the context of the proposed Time Division Multiple Access (TDMA), Time Division Duplex (TDD) system using 32 timeslots, where one video packet was



**Figure 21.31:** Transmission feedback timing diagram showing the feedback signalling superimposed on the reverse channel video datastream. The tasks that need to be performed in each time interval are shown for both the mobile station and the basestation.

transmitted in each TDD frame. A number of further interesting details concerning the system's operation become explicit by studying the Figure in more depth, which we have to refrain from here due to lack of space.

As demonstrated by Figure 21.30, the H.263 encoded bitstream is passed to the packet assembly block, which was detailed in section 19.3.6. The packetiser's function is to assemble the video packets for transmission, taking into account the packet acknowledgement feedback information. The packet disassembly block of Figure 21.30 ensures that always an error-free H.263 bitstream is output to the video decoder, discarding any erroneously received packet and using only error-free packets to update the reconstructed frame buffer. Since the transmission packets contain typically fractions of video macroblocks at the beginning and end of the packets, a corrupted packet implies that the previously received partial macroblocks have to be discarded. The loss of the packet is then signalled via the feedback channel to the video encoder and packet assembly blocks.

The lost macroblocks are not re-transmitted, but strongly error protected acknowledgement flags are inserted into the video bitstream to signify the macroblocks that have not been updated. This requires one bit per lost macroblock in the next

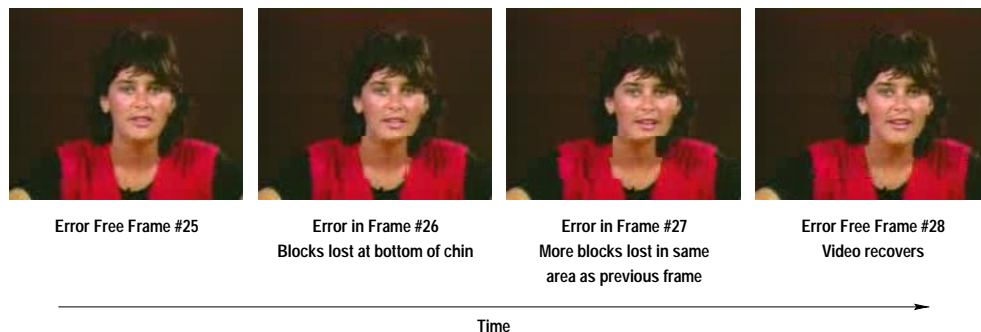


**Figure 21.32:** Typical expected video quality of the proposed video transceiver for 16Kbit/s at 10fps, for a frame error rate (or packet dropping rate) of 5%. This figure also shows the error recovery and concealment used in frames 26 and 27.

reverse-direction packet of the given user. The decoded video stream is error-free, although certain parts of some video frames may be 'frozen' for a frame duration due to lost packets. These areas will usually be updated in the next video frame, and the effect of the lost packet will be no longer visible. Again, this packet loss has a prolonged effect for 100 ms at 10 fps, which is more preceivable than the losses at 30 fps. These operations were also indicated earlier in the context of Figure 21.31, while aspects of the acknowledgement flag protection and the associated probability of correct acknowledgement flag reception are quantified in Figure 19.22 on page 870 and in Figure 21.41, which will be discussed at a later stage. An example of a typical scenario, portraying the error-free frame 25, a lost block in frame 26, which is not updated during frame 27, but finally replenished in frame 28, as shown in Figure 21.32.

The packetised video stream is then Forward Error Correction (FEC) coded, mapped to the allocated TDMA timeslot and transmitted using Differential Quaternary Phase Shift Keying (D-QPSK) between adjacent sub-carriers of the Orthogonal Frequency Division Multiplex (OFDM) scheme employed [10]. Again, it is important to strongly protect the binary acknowledgement flag from transmission errors, which prevents the remote decoder from updating the local reconstruction buffer, if the received packet was corrupted. Following a range of considerations, we opted for using a repetition-code, which was superimposed on the forthcoming reverse-direction packet in the proposed Time Division Duplex (TDD) scheme of Table 21.10. The repetition-coded flag is then Majority Logic Decision (MLD) decoded at the receiver. The probability of correct decoding of the 5, 9, 18, and 27 bit majority logic codes was numerically evaluated for the range of bit error rates 0% to 50% using a random error distribution in Figure 19.22 on page 870. On the basis of the results we opted for using the strongest MLD code of MLD(27,1,13), repeating the flag 27 times, which was hence able to correct up to 13 transmission errors or a channel BER of about 50 %.

In the next Section we briefly consider the specific system parameters used, which closely resemble those proposed by the Pan-European Wireless Asynchronous Transfer Mode (WATM) consortium referred to as Median.



Feature	Value
TDMA/TDD frame length	171 $\mu$ s
Slots/Frame	64 (62 useable)
Slot length	2.667 $\mu$ s
OFDM carriers	512 (511 used)
Modulation	Differential-QPSK
Coded Bits/slot	1022 bits
FEC (1/2 rate)	BCH(255,131,18)
Pre-FEC bits/slot	524 bits
System Bandwidth	225MHz
System Symbol rate (symbols/sec)	186 $\times$ 10 <sup>6</sup>
Normalised Doppler Frequency	1.235 $\times$ 10 <sup>-5</sup>

**Table 21.10:** Summary of the Median-like WATM System Parameters ©IEEE, Cherriman, Keller, Hanzo, 1998, [595]

### 21.3.2.1 The WATM System

The system employed in our experiments resembles the ACTS MEDIAN WATM proposal, operating in the 60GHz band utilising OFDM as modulation technique [10]. The MEDIAN-like WATM system parameters are listed in Table 21.10. Channel access in the MEDIAN WATM system is based on Time Division Multiple Access / Time Division Duplex (TDMA / TDD) frames having a duration of 170.7 $\mu$ s. This frame is split into 64 time-slots of 2.667 $\mu$ s duration. Two of these time slots are reserved for networking functions, leaving 62 for useful information transfer.

In order to avoid implementationally complex equalisation at the FEC-coded sampling rate, OFDM is employed as the proposed baseband modulation technique [10]. Again, a rudimentary introduction to OFDM was provided in Chapter 5. Differential Quaternary Phase Shift Keying (D-QPSK) between adjacent sub-carriers is used as frequency-domain modulation scheme. If all 512 sub-carriers are used, with one subcarrier being used as phase reference, then 1022 bits can be transmitted using a single OFDM symbol. Figure 21.33 portrays the Median WATM frame- and slot-structure. Each time-slot contains one OFDM symbol, preceded by a cyclic extension of 64 samples in order to combat interference in wideband channels [10]. The role of the quasi-periodic cyclic extension of the time-domain OFDM symbol is to generate a waveform, which appears to be periodic for the duration of the bandlimited channel's memory. Although this time-domain signal-segment may become interfered due to channel dispersion and transients, the useful information-related segment remains intact. A cyclic post-amble is also appended to the OFDM data samples in order to simplify symbol timing synchronisation [598]. For our simulations, all 512 sub-carriers per OFDM symbol were actively used, resulting in the maximum throughput of 1022 bits per OFDM symbol.

Variable bit rate users can be accommodated by allocating groups of time-slots per frame, as seen in Table 21.11 in case of high-rate users or by skipping time frames in case of low-rate users. The shaded area of Figure 21.34 defines the 'payload' of a TDMA frame in the 4CIF scenario of the Table and hence this 'payload' must be

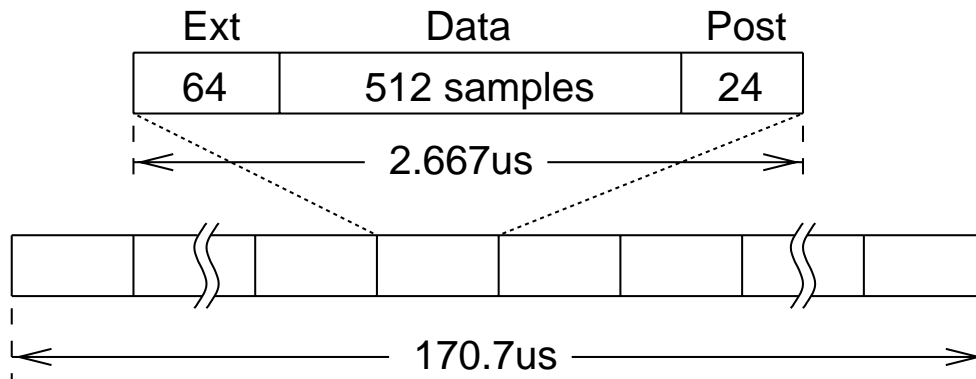
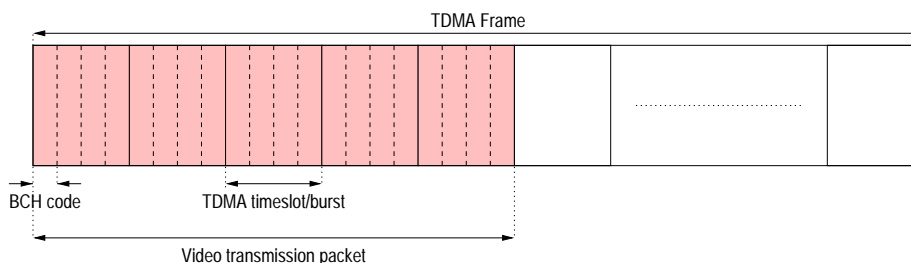


**Figure 21.33:** Schematic plot of the ACTS MEDIAN WATM frame structure. A time frame contains 64 timeslots of  $2.667\mu\text{s}$  duration. Each timeslot holds the data samples of a 512 point IFFT OFDM symbol, 64 samples of the cyclic extension and a cyclic postamble of 24 samples ©IEEE, Cherriman, Keller, Hanzo, 1998, [595]



- Rate of BCH code overloading is the BCH error rate.
- Rate of at least one BCH code in each TDMA timeslot/burst becomes overloaded is TDMA burst error rate.
- Rate of at least one BCH code in each video transmission packet becomes overloaded is Frame error rate (FER) or packet error rate.

**Figure 21.34:** Stylised TDMA frame structure for the WATM system transmitting 4CIF resolution video, where each video transmission packet is formed using 5 timeslots and 20 BCH codewords per active TDMA frame and each timeslot contains 4 BCH codewords ©IEEE, Cherriman, Keller, Hanzo, 1998, [595]

received error-freely. If it is corrupted, this event is defined as a TDMA frame error and the relative frequency of these events defines the transmission frame error rate (FER) of the system. As seen in Figure 21.34 and Table 21.11, in this case we need five time-slots for supporting the associated 10.2 Mbps video rate, but other video resolutions require a different number of time slots. Their FER is defined on the basis of the success or failure of all the slots of a specific video user in a TDMA frame, since in this regime we cannot selectively re-transmit the payload of each timeslot due to having only one acknowledgement flag per TDMA frame per user. This results in larger video frame sections remaining un-updated due to the increased payload per TDMA frame at high video rates. Again, the required number of slots per TDMA

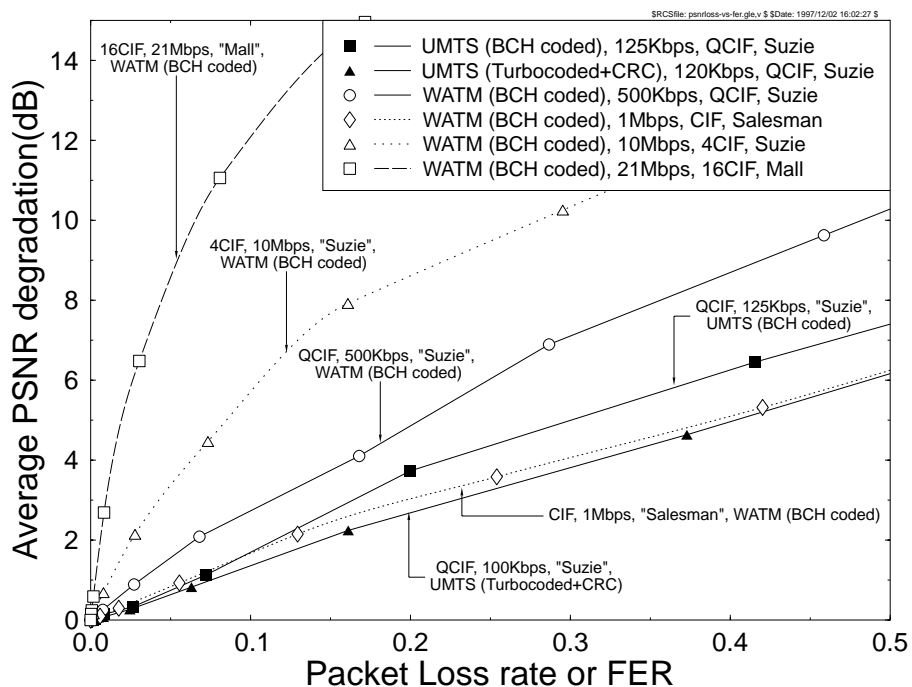


**Figure 21.35:** PSNR degradation versus video packet loss rate or transmission frame error rate for the scenarios described in Tables 21.11 and 21.12 ©IEEE, Cherri-man, Keller, Hanzo, 1998, [595]

frame for each video mode was summarised for the various modes in Table 21.11, while reference [599] proposed an efficient statistical multiplexing scheme for variable-rate scenarios, where the number of slots can be varied on a frame-by-frame basis. The associated PSNR degradation of the various user scenarios of Table 21.11 were quantified in Figure 21.35, where the more dramatic PSNR degradation of the larger video frame sizes becomes explicit for any given transmission frame error rate.

### 21.3.2.2 The UMTS-type Framework

The alternative transmission scheme used in our investigations was partially inspired by the ACTS FRAMES [600,601] Mode 1 Universal Mobile Telecommunications System (UMTS) proposal, which entails a time frame structure of 4.615ms, split into eight timeslots of 577 $\mu$ s duration each. However, instead of using the originally proposed Direct Sequence Code Division Multiple Access (DS-CDMA) scheme with a chip-rate of 2.17Mchips/s, we have employed 1024-subcarrier OFDM, as is it shown in Figure 21.36. Hence we refer to this system as a Frames-like scheme. The modified timeslot contains a 1024-sample OFDM symbol, which is preceded by a cyclic extension of 168 samples length and followed by a guard interval of 60 samples. In order to

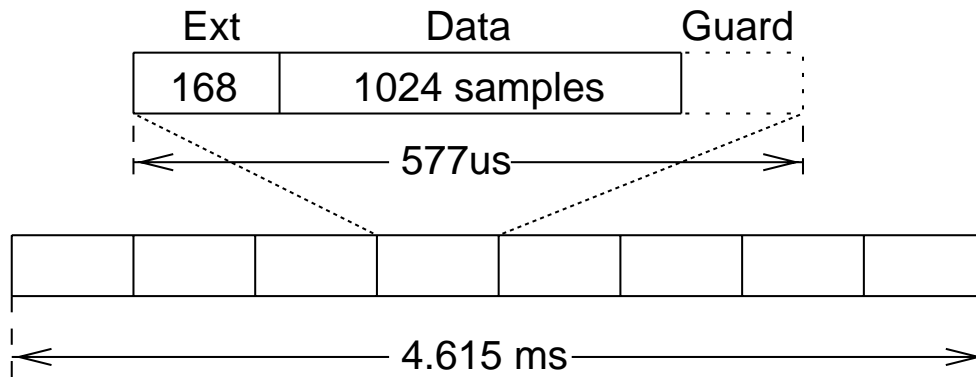


**Figure 21.36:** Schematic plot of the ACTS FRAMES Mode 1-like frame structure as used in this paper. A timeslot of 4.615ms duration is split into eight timeslots of 577μs. Each timeslot holds a 1024 point IFFT OFDM symbol with a cyclic extension of 168 samples ©IEEE, Cherriman, Keller, Hanzo, 1998, [595]

maintain the Frames UMTS bandwidth of 1.6MHz, the 1024 subcarrier OFDM symbol contains 410 unused, so-called virtual subcarriers and 614 information bearer subcarriers, therefore reducing the bandwidth to 1.3MHz and allowing for a modulation excess bandwidth within the band of 1.6MHz. Let us now consider the corresponding channel models in the next section.

### 21.3.3 The Channel Model

The channel model employed for the WATM system experiments was a five-path, Rayleigh fading indoors channel. The impulse response shown in Figure 21.37 was obtained by ray-tracing for a  $100 \times 100\text{m}^2$  hall or warehouse environment and every path in the impulse response was faded independently according to a Rayleigh fading narrow band channel with a normalised Doppler frequency of  $f'_d = 1.235 \cdot 10^{-5}$ , corresponding to the 60 GHz propagation frequency and a worst-case indoor speed of 30 mph. We note that normalisation of  $f'_d$  was carried out with respect to the OFDM symbol duration, which was constituted by 1024 transmitted samples, rather than relative to the 1024 times shorter original sample duration.

A transmission rate of 155 Mbps was used, which is applicable to Wireless Asynchronous Transfer Mode (WATM) systems. A 7-path channel, corresponding to the four walls, ceiling and floor plus the line-of-sight (LOS) path was employed. The LOS path and the two reflections from the floor and ceiling were combined into one single path in the impulse response. The worst-case impulse response associated with the highest path length and delay spread was experienced in the farthest corners of the hall, which was determined using inverse second power law attenuation and the speed of light for the computation of the path delays. The corresponding frequency response was plotted in Figure 21.38 for our 512-channel system, as a function of both the time-domain OFDM symbol index and frequency-domain subchannel index. Observe the very hostile frequency selective fading in the figure, which is efficiently combated by

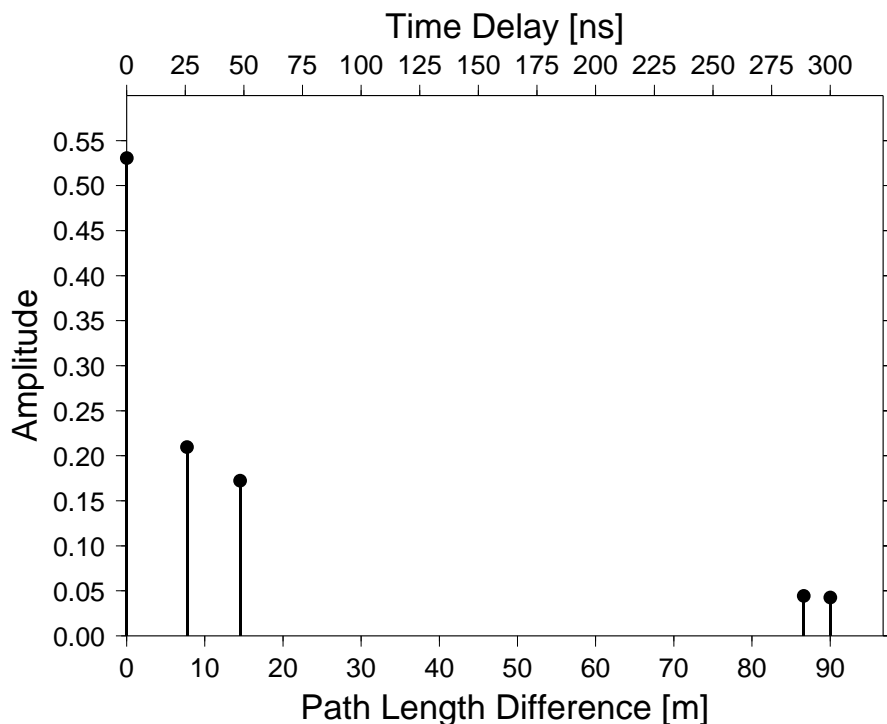


**Figure 21.37:** WATM five-path impulse response ©IEEE, Cherriman, Keller, Hanzo, 1998, [595]

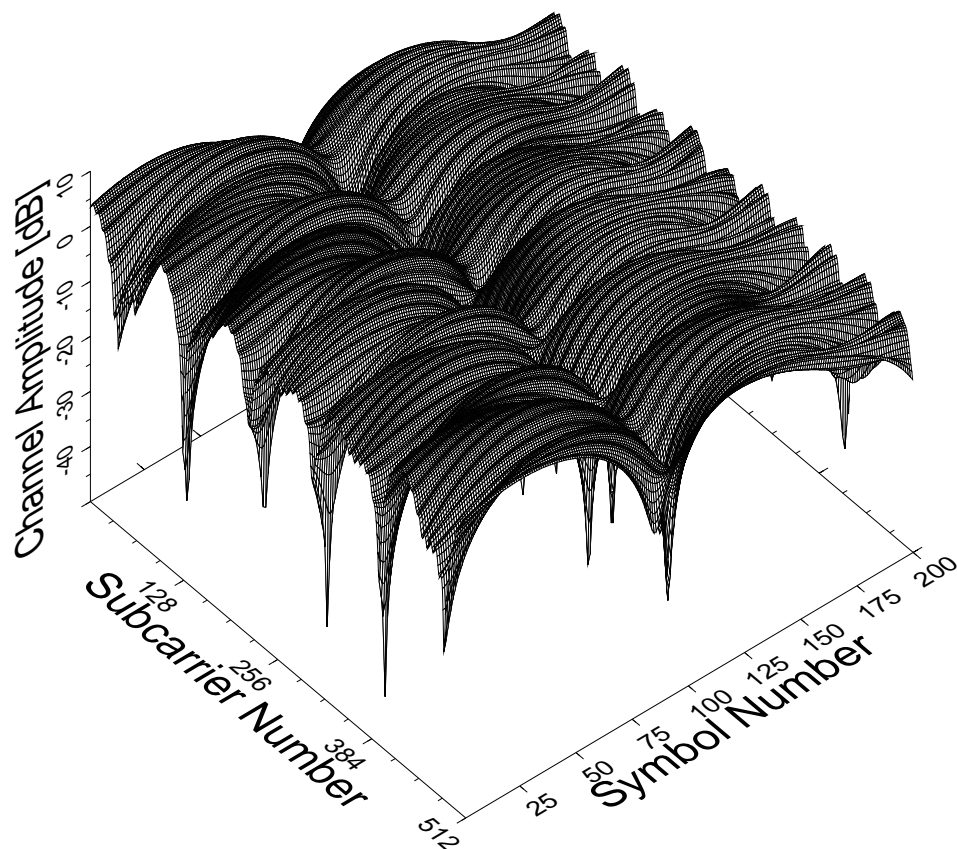
the OFDM modem, since for each of the 512 narrow subchannels the channel can be considered more or less flat fading. The residual frequency-domain subchannel transfer function 'tilt' or distortion can be equalised using a simple frequency-domain pilot-assisted equaliser, where known pilot symbols are inserted periodically in the OFDM spectrum and the channel's frequency domain transfer function is linearly interpolated and equalised between them.

The channel model used for the UMTS-type system experiments was based on a COST 207 [324] Bad Urban conformant seven-path impulse response shown in Figure 21.39. Again, each of the impulses was faded independently according to a Rayleigh narrow band fading channel with a normalised Doppler frequency of  $f'_d = 89.39\text{Hz}/2.17\text{MHz} = 4.12 \cdot 10^{-5}$ , where the carrier frequency and vehicular velocity were set to 2 GHz and 30 mph, respectively.

### 21.3.4 Video-related System Aspects

#### 21.3.4.1 Video parameters of the WATM system

Our high-rate WATM system constitutes an ideal medium for high resolution video transmission. In order to assess the system's ability to support various application scenarios, we investigated four different resolution video systems, ranging from QCIF



GMT Nov 26 14:23 430

**Figure 21.38:** Frequency response of the 512-subcarrier WATM OFDM system at 155 Mbps  
©IEEE, Cherriman, Keller, Hanzo, 1998, [595]

to 16CIF frame formats, as seen in Table 21.11. The video packetizer operated most efficiently, when the transmission packet generation rate per TDMA frame was neither too high nor too low. If the packet-generation rate per TDMA frame is too high, each packet may contain less than a whole macroblock, leading to an increased buffering in the de-packetizer [189]. If the packet generation rate is too low, then each packet contains a high number of macroblocks, and therefore when a transmission packet is corrupted, a large proportion of the video frame is lost. Therefore the packet generation rate for each video resolution was adjusted experimentally, taking into account that as the video resolution was increased four-fold, corresponding to increasing the video resolution for example from QCIF to CIF, the number of macroblocks per TDMA frame or per time unit was increased by the same factor, resulting in a corresponding increase in terms of the packet generation rate. These aspects

Feature	Video Resolution			
	QCIF	CIF	4CIF	16CIF
Luminance resolution (pixels)	176x144	352x288	704x576	1408x1152
Chrominance Resolution (pixels)	88x72	176x144	352x288	704x576
Packet separation (in No. of TDMA frames)	30	6	1.5	1
Packet rate (packets/s)	195	975	3900	5448
Bits/Timeslot	1022	1022	1022	1022
Timeslots per active TDMA frame	5	2	5	7
Bits per active TDMA frame (packet size)	5110	2044	5110	7154
Channel Bitrate	1Mbps	2Mbps	20Mbps	41.8Mbps
FEC	20×BCH(255,131,18)	8×BCH(...)	20×BCH(...)	28×BCH(...)
Pre-FEC Bits per active TDMA frame	2620	1048	2620	3668
Pre-FEC Bitrate	511Kbps	1Mbps	10.2Mbps	21.5Mbps
Feedback control bits	26	24	26	29
H.263 Packetisation header bits	13	12	13	14
Video bits per active TDMA frame	2581	1012	2581	3625
Useful Video Bitrate	503Kbps	1Mbps	10Mbps	21.2Mbps

**Table 21.11:** Summary of video parameters for the WATM system ©IEEE, Cherriman, Keller, Hanzo, 1998, [595]

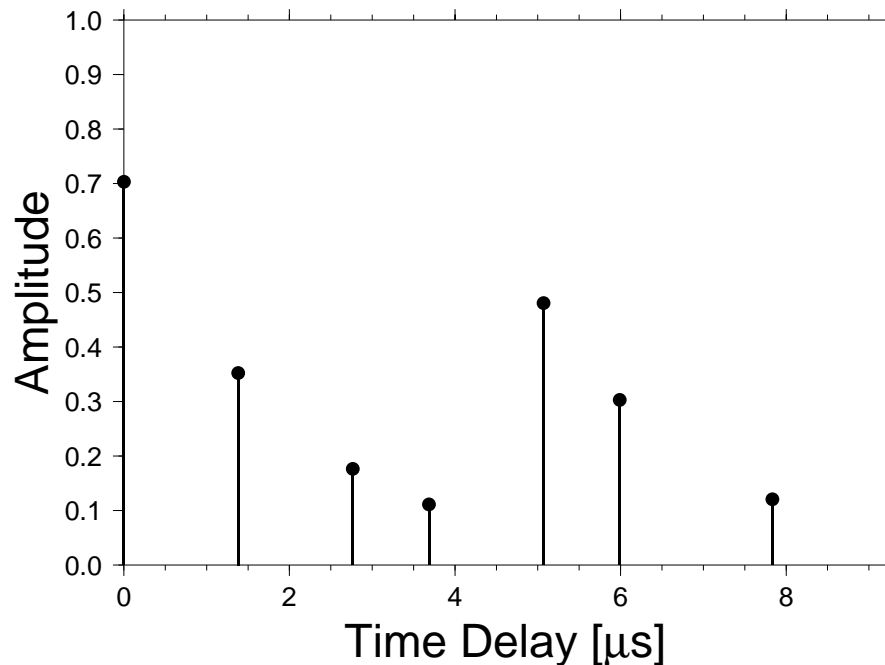


Figure 21.39: COST 207 Bad Urban compliant impulse response, used for the UMTS [324]

were discussed in the context of defining the FER at the end of Section 21.3.2.1. The multiplier factor associated with the BCH codewords in Table 21.11 indicates the number of the BCH codewords per TDMA frame, which are jointly acknowledged by one protected feedback flag bit.

Again, the packet generation rate for each of the four video resolutions used is shown in Table 21.11 in terms of both the number of TDMA frames between video packets or, synonymously, the TDMA packet separation, as well as in terms of packets per second, which are matched to the bitrate requirement of each mode. For example, for QCIF resolution video, the packet generation rate is 195 per second, which corresponds to one packet every 30 TDMA frames. After setting the packet generation rates for each video mode, the video target bitrates were set to give high quality video for the majority of video sequences. As mentioned previously, the OFDM system can transmit 1022 bits in every timeslot. Hence for the QCIF mode, with one timeslot every 30 TDMA frames, the channel bitrate would be  $1022 \times 195 = 200Kbit/s$ . Upon using half-rate channel coding, the video bitrate is constrained to  $100Kbit/s$ . Since we required around  $500Kbit/s$  for high quality QCIF video for a wide range of video sequences, we decided to use 5 timeslots once every 30 TDMA frames, which corresponded to 20 BCH(255,131,18) codewords, as seen in Table 21.11. The corresponding 4CIF frame structure was illustrated in Figure 21.34. Therefore the channel bitrate became  $5 \times 1022 \times 195 = 1Mbit/s$ , providing a bitrate of  $500Kbit/s$  for video



source coding. The interested reader is referred to our web page<sup>8</sup> for some examples of coded sequences, which can be viewed using an MPEG player.

For the WATM investigations we decided to use binary Bose-Chaudhuri-Hocquenghem (BCH) block coding [602], since it is capable of both error correction and error detection. For all the modes we used the near half-rate code of BCH(255,131,18). The corresponding pre-FEC bitrates for the various modes are shown in Table 21.11. In conjunction with this channel coding scheme, the pre-FEC bitrate for the QCIF mode is 511Kbit/s.

The videophone system requires some additional overhead for its operation, since the feedback information for the reverse link is concatenated with the information packet, requiring a maximum of 29 additional bits/packet. In addition, the H.263 packetisation adds a header to each packet [189], which is dependent on the number of bits in each packet and for our system, this header was between 12-14 bits per packet. Therefore, the number of useful video source bits in each packet used for video transmission was about 40 bits less than the actual number of bits/packet. The corresponding useful video source bitrate for each of the modes is shown in Table 21.11, which was 503Kbit/s for QCIF resolution video, when taking into account the above-mentioned transmission overheads.

#### 21.3.4.2 Video parameters of the UMTS scheme

Our UMTS-type scheme was also designed for a range of bitrates and services. We opted for using the so-called high bitrate slot type, of which there can be a maximum of eight in each TDMA frame, since  $8 \times 577\mu s = 4.615ms$ . The OFDM system designed for this scenario contained 614 active information subcarriers and 410 passive virtual subcarriers and after allocating one subcarrier as the reference for the differential decoder, it conveyed 1224 bits per timeslot. This yields a channel bitrate of 265Kbit/s or approximately 130Kbit/s before half rate FEC coding. This bitrate is suitable for high-quality QCIF video or lower quality CIF video. Hence we limited our investigations to QCIF resolution. Additionally, we invoked two different types of channel coding, BCH blocks codes [602], and turbo coding [28], which were also specified in Table 21.12. Since our system also required an error detection facility, the use of block codes is convenient due to their inherent error correction and detection capabilities. The parameters for the UMTS-type scheme are summarised in Table 21.12. Since turbo coding cannot provide error detection, to this effect a 16-bit Cyclic Redundancy Checking (CRC) code was used. Given the 1224 bits/slot 'payload' per TDMA frame, before channel coding the number of bits per TDMA frame was constrained to 618 for BCH coding and 594 for turbo coding. Half-rate turbo coding was used, however, two termination bits per slot were required for the convolutional encoders. Therefore the number of pre-FEC bits per transmission packet was  $1224/2 - 2(\text{termination}) - 16(\text{CRC}) = 594$ . This led to a pre-FEC bitrate of 134Kbit/s for BCH coding and 129Kbit/s for turbo coding. The additional system overhead required 27 bits per packet for the reverse link's acknowledgement flag and 11 bits for the H.263 packetisation header [189]. This led to a video bitrate of 126Kbit/s for BCH coding and 120Kbit/s for turbo coding. Having highlighted

<sup>8</sup><http://www-mobile.ecs.soton.ac.uk/peter/robust-h263/robust.html>

Feature	Value	
	BCH coding	Turbo Coding
Modulation	Differential-QPSK	
TDMA frame length	4.615ms	
Slots/Frame	8	
Slot length	577 $\mu$ s	
OFDM carriers	1024 (612 used + 2 pilots)	
System Bandwidth	1.6MHz	
System Symbol rate (symbols/sec)	2.17 $\times$ 10 <sup>6</sup>	
Normalised Doppler Frequency	4.267 $\times$ 10 <sup>-5</sup>	
Coded Bits/slot	1224 bits	
Feedback control bits	27	
H.263 Packetisation header bits	11	
Channel Coding ( $\approx$ 1/2 rate)	4 $\times$ BCH(255,131,18) + 2 $\times$ BCH(127,64,10) + BCH(63,30,6)	Turbo Coding using 612 bit random interleaver + 16bit CRC
Pre-FEC Bits per timeslot	618	594
Pre-FEC Bitrate	134Kbit/s	129Kbit/s
Video bits per timeslot (FEC)	580	556
Useful Video Bitrate (FEC)	126Kbit/s	120Kbit/s

**Table 21.12:** Summary of UMTS-like Parameters ©IEEE, Cherriman, Keller, Hanzo, 1998, [595]

the salient video-specific system features, let us now consider the achievable system performance in the next section.

### 21.3.5 System Performance

Figure 21.40 portrays the bit error rate (BER) performance of both candidate systems over the wideband channels characterised by the impulse responses shown in Figures 21.37 and 21.39, respectively. It is interesting to observe that since the number of subcarriers was sufficiently high in both systems for narrow-band subchannel conditions to prevail, the modem BER curves are fairly similar, irrespective of the different Doppler frequencies. Nevertheless, the slightly lower uncoded BER of the UMTS-type scheme manifested itself in a further improved FEC-decoded BER. Lastly, as expected, the similar-rate turbo codec outperformed the BCH codec in terms of BER.

Figure 21.41 portrays the FER and the acknowledgement flag Feed-back Error Rate (FBER) performance of both systems. Despite the BER differences of the systems, their FER performances are fairly similar. This indicates that the UMTS-like scheme's lower average BER actually results in a similar FER, despite its lower in-burst BER, when a BCH codeword was overwhelmed by an excessive number of channel errors. However, the lowest in-burst BER of the turbo codec translated in a substantially reduced acknowledgement flag feedback error rate after MLD decoding.

Figure 21.42 shows the video quality in terms of the average Peak-Signal-to-Noise-Ratio (PSNR) versus the channel SNR for QCIF resolution video transmitted over the WATM scheme. The figure shows the video quality of a range of video sequences from the highly motion active "Foreman" and "Carphone" sequences to the lower-activity "Miss America" sequence, which is more amenable to compression. For all the video sequences the PSNR starts to drop, when the channel SNR falls below about 20dB. Due to lack of space the frame error rate (FER) versus channel Signal-to-Noise Ratio (CSNR) performance of the system is not explicitly characterised in this treatise, but our records show that the frame error rate around this CSNR value is about 3%. The corresponding visual quality appears unimpaired and the effects of transmission

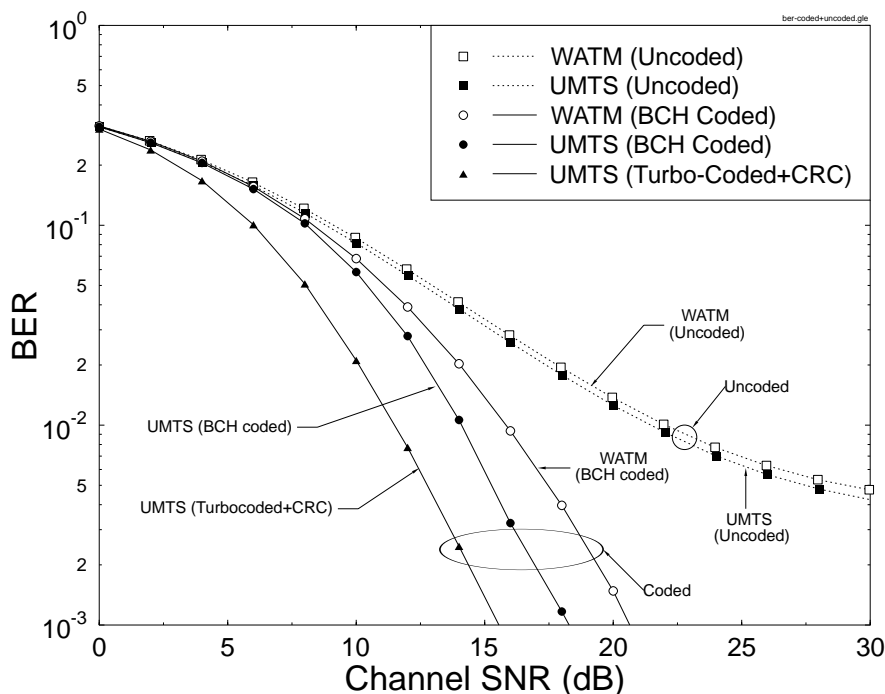


**Figure 21.40:** Uncoded channel BER and channel-decoded BER of the WATM and UMTS systems over the wideband channels characterised by the impulse responses shown in Figures 21.37 and 21.39, respectively ©IEEE, Cherriman, Keller, Hanzo, 1998, [595]

packet dropping do not become evident for CSNRs in excess of 16dB. At a channel SNR of 16dB the frame error rate is 17%. However, the effects of this packet loss are only becoming 'just noticeable' at a CSNR of 16dB. The effect of the packet loss is that parts of the picture are 'frozen', but usually for only one video frame duration of about 30ms at 30 frames/s, which is not sufficiently long for these artifacts to become objectionable. However, if the part of the picture that was lost contains a moving object, the effect of the loss of the packet becomes more obvious. Therefore, for more motion active sequences, the effect of packet loss is more pronounced.

In order to portray the expected system performance in other application scenarios, where higher video quality is expected, in Figure 21.43 we portrayed the average PSNR versus channel SNR performance for a range of video resolutions from CIF to 16xCIF HDTV quality. At CIF resolution the 'Miss America' sequence was encoded at both 500kbps and 1Mbps. For 4CIF resolution the 'Suzie' sequence was encoded at 2 and 10Mbps, while for 16CIF resolution the 'Mall' video clip was transmitted at 3 and 21 Mbps. This figure shows results for using multiple timeslots per active TDMA frame, as suggested by Table 21.11, down to just a single timeslot per active

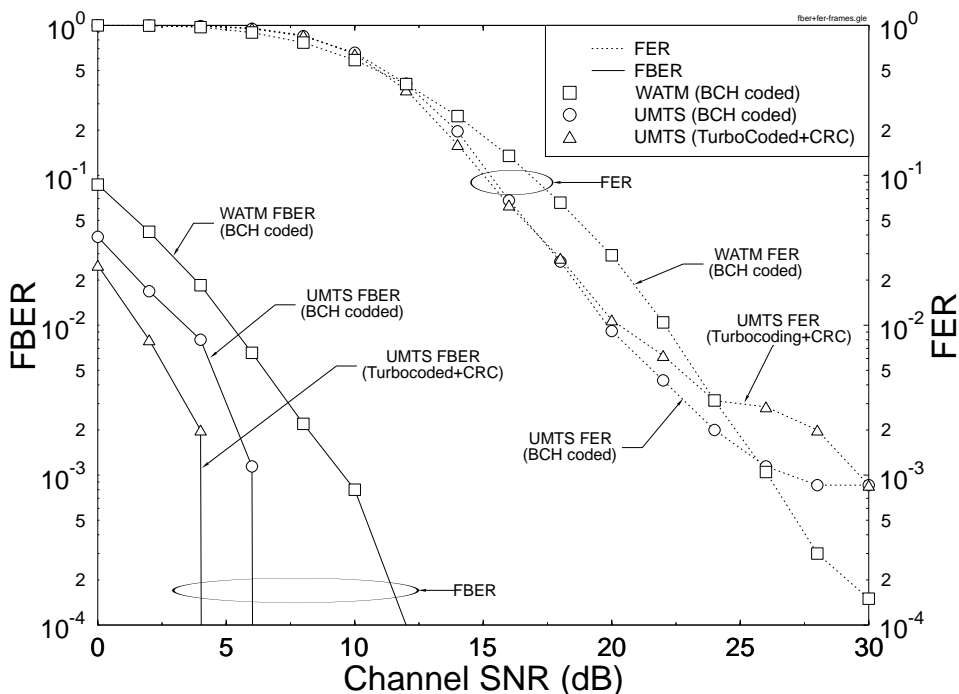


**Figure 21.41:** FER and FBER after channel decoding versus channel SNR for the WATM system using BCH codes, and for the UMTS-type scheme using BCH codes or Turbo Coding plus CRC over the wideband channels characterised by the impulse responses shown in Figures 21.37 and 21.39, respectively. The WATM results are typical and are shown for the CIF mode of operation ©IEEE, Cherriman, Keller, Hanzo, 1998, [595]

TDMA frame. Notice that the high and low bitrate modes for each resolution seem to converge to a similar PSNR, when the channel SNR is low, which is a consequence of the higher PSNR degradations inflicted by a given FER in high-resolution modes due to their larger packet size, as seen in Table 21.11 and Figure 21.35.

The 16CIF scenarios seem to be more vulnerable to packet loss. This is because the packet generation rate is not four times that of the 4CIF simulations and therefore each 16CIF video packet contains approximately 2.5 times more macroblocks per transmission packet than the CIF and 4CIF resolution video packets. Hence the effect of packet loss is more noticeable and this is manifested in the faster reduction of the PSNR, as the channel SNR degrades.

Focusing our attention on the UMTS-like scheme, since the FER of the turbo coded scheme in Figure 21.41 was not substantially lower than that of the BCH coded arrangement, the corresponding video PSNR performances are also quite similar, as evidenced by Figures 21.44 and 21.45. This is a consequence of the system's high error resilience. Hence in practical systems the added complexity of turbo coding may

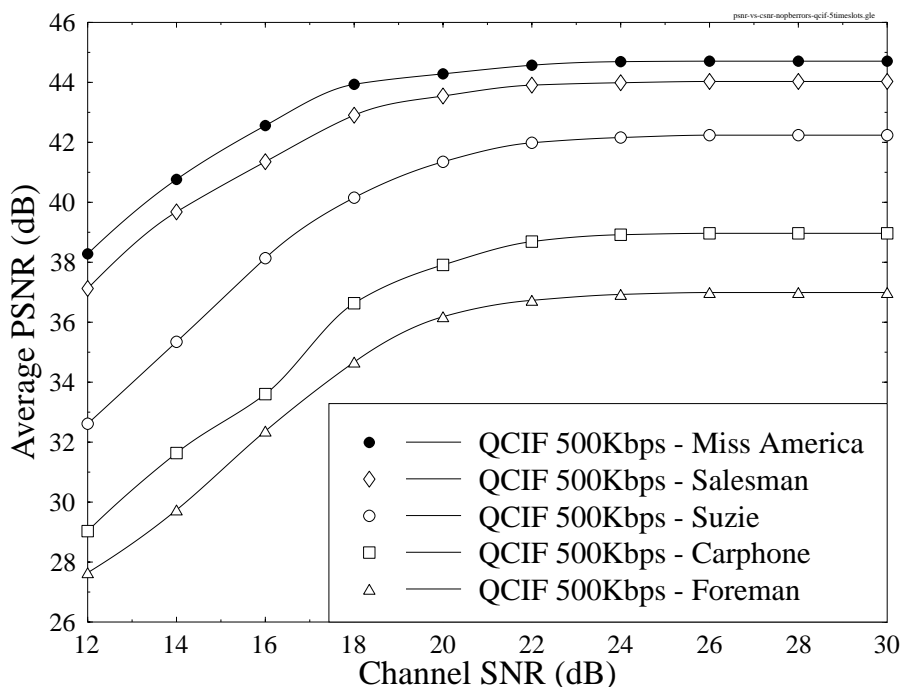


**Figure 21.42:** QCIF video quality in PSNR versus channel SNR at 500Kbit/s and 30fps over the WATM System, for various video sequences, using the impulse response of Figure 21.37 ©IEEE, Cherriman, Keller, Hanzo, 1998, [595]

not be justified. A similar-rate WATM performance curve is also shown in the figure.

### 21.3.6 Conclusions

In this section the expected video performance of a WATM and that of a UMTS-type system was quantified in a variety of applications scenarios, using a range of video resolutions and bitrates. The high-efficiency H.263 video codec was employed to compress the video signal. The video formats used were summarised in Table 21.11 along with their associated target bitrate figures. The proposed system ensures robust video communications using the WATM and the UMTS-type framework in a highly dispersive Rayleigh-fading environment. Even at a vehicular speed of 30mph, the system requires channel SNRs in excess of only about 16dB for near-unimpaired video transmission. Despite the different propagation conditions, the BER and FER modem performance of both systems was quite similar. Furthermore, due to the high error-resilience of the video system, the increased complexity of the turbo codec was not justified in video performance terms, although the acknowledgement flag FBER was significantly reduced.

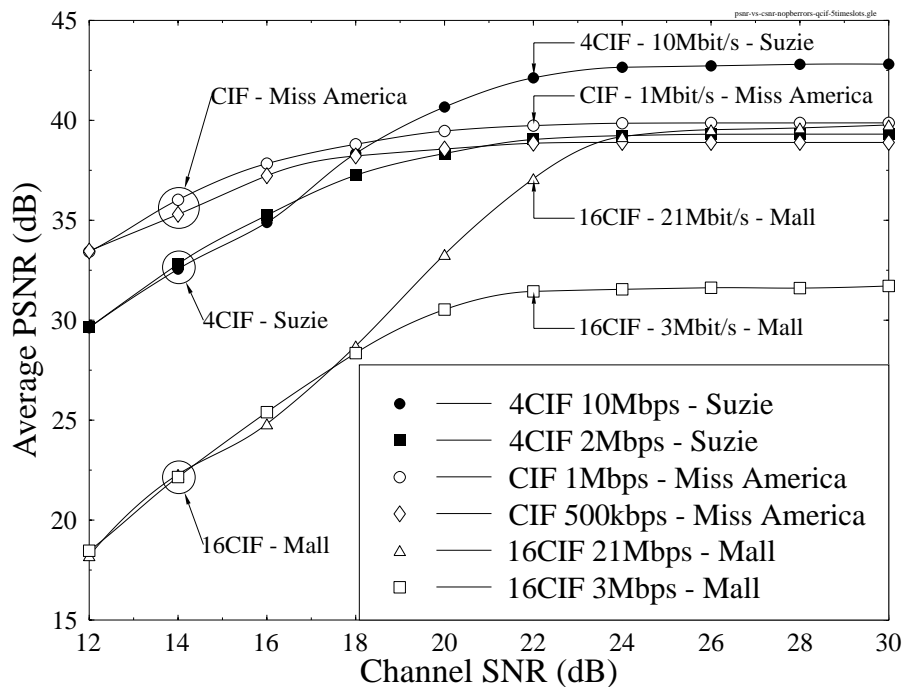


**Figure 21.43:** Video quality in PSNR versus channel SNR for CIF, 4CIF, and 16CIF resolution video at 30fps over the WATM system for various video sequences using the channel impulse response shown in Figure 21.37 ©IEEE, Cherriman, Keller, Hanzo, 1998, [595]

## 21.4 Subband-adaptive Turbo-coded OFDM-based Interactive Video Telephony<sup>9 10 11</sup>

### 21.4.1 Motivation and Background

In Sections 21.1 and 21.2 a wideband burst-by-burst adaptive QAM and a CDMA based video system was proposed, while the previous section considered the transmission of interactive video using OFDM transceivers in various propagation environments. In this section burst-by-burst adaptive OFDM is proposed and investigated

<sup>9</sup>This section is based on **P.J. Cherriman, T. Keller, L. Hanzo:** Subband-adaptive Turbo-coded OFDM-based Interactive Video Telephony, submitted to IEEE Tr. on CSVT, July 1999

<sup>10</sup>**Acknowledgement:** The financial support of the Mobile VCE, EPSRC, UK in the framework of the contract GR/K 74043 that of the European Commission is gratefully acknowledged.

<sup>11</sup>©1999 IEEE. Personal use of this material is permitted. However, permission to reprint/republish this material for advertising or promotional purposes or for creating new collective works for resale or redistribution to servers or lists, or to refuse any copyrighted component of this work in other works must be obtained from IEEE.

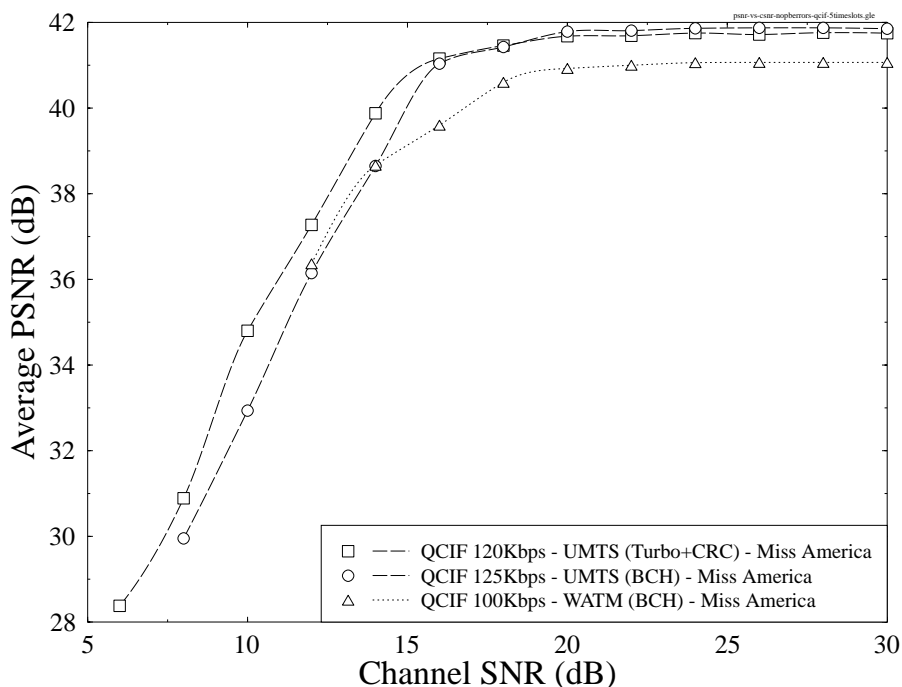


**Figure 21.44:** Video quality in PSNR versus channel SNR for the QCIF “Miss America” video sequence at 30fps, using both the WATM system, and the UMTS-type system with turbo-coding and CRC or BCH coding, using the impulse responses shown in Figures 21.37 and 21.39, respectively ©IEEE, Cherriman, Keller, Hanzo, 1998, [595]

in the context of interactive video telephony.

As mentioned, burst-by-burst adaptive quadrature amplitude modulation [10] (AQAM) was contrived by Steele and Webb [10, 125], in order for the transceiver to cope with the time-variant channel quality of narrowband fading channels. Further related research was conducted at the University of Osaka by Sampei and his colleagues, investigating variable coding rate concatenated coded schemes [585], at the University of Stanford by Goldsmith and her team, studying the effects of variable-rate, variable-power arrangements [129] and at Southampton University in the UK, investigating a variety of practical aspects of AQAM [592, 603]. The channel’s quality is estimated on a burst-by-burst basis and the most appropriate modulation mode is selected in order to maintain the required target bit error rate (BER) performance, whilst maximizing the system’s Bit Per Symbol (BPS) throughput. Using this re-configuration regime the distribution of channel errors becomes typically less bursty, than in conjunction with non-adaptive modems, which potentially increases the channel coding gains [604]. Furthermore, the soft-decision channel codec metrics can be

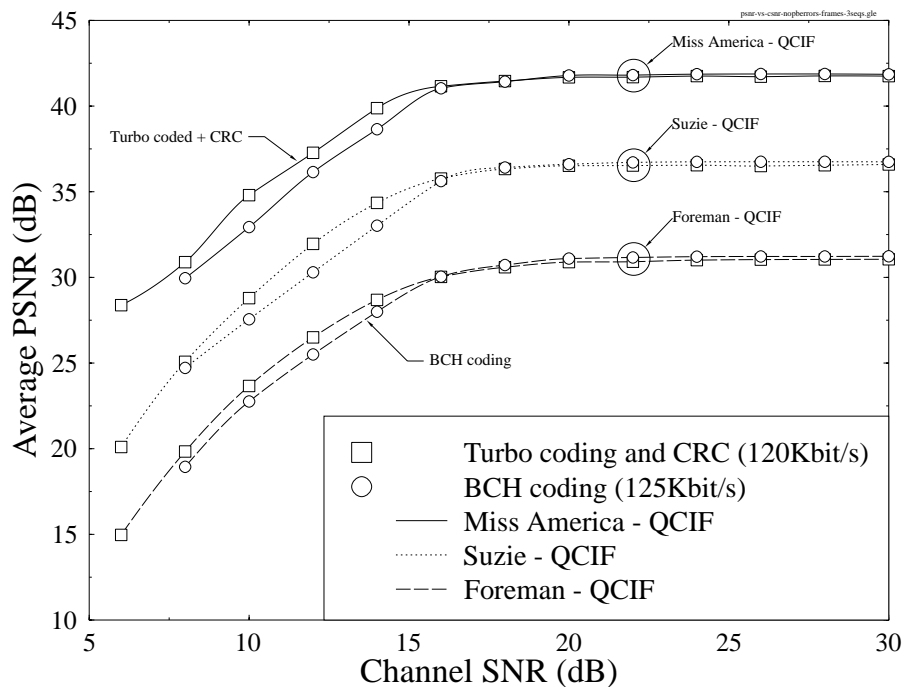


**Figure 21.45:** Video quality in PSNR versus channel SNR for a variety of QCIF resolution video sequences at 30fps over the UMTS-type system with turbo-coding and CRC or BCH coding using the COST 207 Bad Urban impulse response of Figure 21.39 ©IEEE, Cherriman, Keller, Hanzo, 1998, [595]

also invoked in estimating the instantaneous channel quality [604], irrespective of the type of channel impairments.

A range of coded AQAM schemes were analysed by Matsuoka *et al* [585], Lau *et al* [605] and Goldsmith *et al* [130]. For data transmission systems, which do not necessarily require a low transmission delay, variable-throughput adaptive schemes can be devised, which operate efficiently in conjunction with powerful error correction codecs, such as long block length turbo codes [28]. However, the acceptable turbo interleaving delay is rather low in the context of low-delay interactive speech. Video communications systems typically require a higher bitrate than speech systems and hence they can afford a higher interleaving delay.

The above principles - which were typically investigated in the context of narrow-band modems - were further advanced in conjunction with wideband modems, employing powerful block turbo coded wideband Decision Feedback Equaliser (DFE) assisted AQAM transceivers [143, 604]. A neural-network Radial Basis Function (RBF) DFE based AQAM modem design was proposed in [606], where the RBF DFE provided the channel quality estimates for the modem mode switching regime. This modem



was capable of removing the residual BER of conventional DFEs, when linearly non-separable received phasor constellations were encountered.

The above burst-by-burst adaptive principles can also be extended to Adaptive Orthogonal Frequency Division Multiplexing (AOFDM) schemes [607] and to adaptive joint-detection based Code Division Multiple Access (JD-ACDMA) arrangements [608]. The associated AQAM principles were invoked in the context of parallel AOFDM modems also by Czylwik et al [609], Fischer [610] and Chow et al [611]. Adaptive subcarrier selection has been advocated also by Rohling et al [612] in order to achieve BER performance improvements. Due to lack of space without completeness, further significant advances over benign, slowly varying dispersive Gaussian fixed links - rather than over hostile wireless links - are due to Chow, Cioffi and Bingham [611] from the USA, rendering OFDM the dominant solution for asymmetric digital subscriber loop (ADSL) applications, potentially up to bitrates of 54 Mbps. In Europe OFDM has been favoured for both Digital Audio Broadcasting (DAB) and Digital Video Broadcasting [613,614] (DVB) as well as for high-rate Wireless Asynchronous Transfer Mode (WATM) systems due to its ability to combat the effects of highly dispersive channels [615]. The idea of 'water-filling' - as allocating different modem modes to different subcarriers was referred to - was proposed for OFDM by Kalet [162] and later further advanced by Chow et al [611]. This approach was rendered later time-variant for duplex wireless links for example in [607]. Lastly, various OFDM-based speech and video systems were proposed in References [616,617], while the co-channel interference sensitivity of OFDM can be mitigated with the aid of adaptive beam-forming [618,619] in multi-user scenarios.

The remainder of this contribution is structured as follows. Section 21.4.2 outlines the architecture of the proposed video transceiver, while Section 21.4.6 quantifies the performance benefits of AOFDM transceivers in comparison to conventional fixed transceivers. Section 21.4.7 endeavours to highlight the effects of more 'aggressive' loading of the subcarriers in both BER and video quality terms, while Section 21.4.8 proposed time-variant, rather than constant rate AOFDM as a means of more accurately matching the transceiver to the time-variant channel quality fluctuations, before concluding in Section 21.4.9.

### 21.4.2 Burst-by-burst Adaptive Video Transceiver

### 21.4.3 AOFDM Modem Mode Adaptation and Signalling

The proposed duplex AOFDM scheme operates on the following basis:

- *Channel quality estimation* is invoked upon receiving an AOFDM symbol, in order select the modem mode allocation of the next AOFDM symbol.
- *The decision concerning the modem modes for the next AOFDM symbol* is based on the prediction of the expected channel conditions. Then the transmitter has to select the appropriate modem modes for the groups or subbands of OFDM subcarriers, where the subcarriers were grouped into subbands of identical modem modes, in order reduce the required number of signalling bits.

- *Explicit signalling or blind detection of the modem modes* is used to inform the receiver as to what type of demodulation to invoke.

More explicitly, if the channel is reciprocal, then the channel quality estimate for the uplink can be extracted from the downlink and vice versa. We refer to this regime as open-loop adaptation. In this case, the transmitter has to convey the modem modes to the receiver, or the receiver can attempt blind detection of the transmission parameters employed. By contrast, if the channel cannot be considered reciprocal, then the channel quality estimation has to be performed at the receiver and the receiver has to instruct the transmitter as to what modem modes have to be used at the transmitter, in order to satisfy the target integrity requirements of the receiver. We refer to this mode as closed-loop adaptation. Blind modem mode recognition was invoked for example in [607] - a technique, which results in bitrate savings due to refraining from dedicating bits to explicit modem mode signalling at the cost of increased complexity. Let us address the issues of channel quality estimation on a subband-by-subband basis in the next subsection.

#### 21.4.4 AOFDM Subband BER Estimation

A reliable channel quality metric can be devised by calculating the expected overall bit error probability for all available modulation schemes  $M_n$  in each sub-band, which is denoted by  $\bar{p}_e(n) = 1/N_s \sum_j p_e(\gamma_j, M_n)$ . For each AOFDM sub-band the modem mode having the highest throughput, while exhibiting an estimated BER below the target value is then chosen. While the adaptation granularity is limited to the sub-band width, the channel quality estimation is quite reliable, even in interference-impaired environments.

Against this background in our forthcoming discussions the design trade-offs of turbo-coded Adaptive Orthogonal Frequency Division Multiplex (AOFDM) wideband video transceivers are presented. We will demonstrate that AOFDM provides a convenient framework for adjusting the required target integrity and throughput both with and without turbo channel coding and lends itself to attractive video system construction, provided that a near-instantaneously programmable rate video codec - such as the H.263 scheme highlighted in the next section - can be invoked.

#### 21.4.5 Video Compression and Transmission Aspects

In this study we investigate the transmission of 704x576 pixel Four-times Common Intermediate Format (4CIF) high-resolution video sequences at 30 frames/s using subband-adaptive turbo-coded Orthogonal Frequency Division Multiplex (AOFDM) transceivers. The transceiver can modulate 1, 2 or 4 bits onto each AOFDM sub-carrier, or simply disable transmissions for sub-carriers which exhibit a high attenuation or phase distortion due to channel effects.

The H.263 video codec [593] exhibits an impressive compression ratio, although this is achieved at the cost of a high vulnerability to transmission errors, since a run-length coded bitstream is rendered undecodable by a single bit error. In order to mitigate this problem, when the channel codec protecting the video stream is overwhelmed by the transmission errors, we refrain from decoding the corrupted

video packet, in order to prevent error propagation through the reconstructed video frame buffer [189]. We found that it was more beneficial in video quality terms, if these corrupted video packets were dropped and the reconstructed frame buffer was not updated, until the next video packet replenishing the specific video frame area was received. The associated video performance degradation was found perceptually unobjectionable for packet dropping- or transmission frame error rates (FER) below about 5%. These packet dropping events were signalled to the remote video decoder by superimposing a strongly protected one-bit packet acknowledgement flag on the reverse-direction packet, as outlined in [189]. Turbo error correction codes [28] were used. The associated parameters will be discussed in more depth during our further discourse.

#### 21.4.6 Comparison of subband-adaptive OFDM and fixed mode OFDM transceivers

In order to show the benefits of the proposed subband-adaptive OFDM transceiver, we compare its performance to that of a fixed modulation mode transceiver under identical propagation conditions, while having the same transmission bitrate. The subband-adaptive modem is capable of achieving a low bit error ratio (BER), since it can disable transmissions over low quality sub-carriers and compensate for the lost throughput by invoking a higher modulation mode, than that of the fixed-mode transceiver over the high-quality sub-carriers.

Table 21.13 shows the system parameters for the fixed BPSK and QPSK transceivers, as well as for the corresponding subband-adaptive OFDM (AOFDM) transceivers. The system employs constraint length three, half-rate turbo coding, using octal generator polynomials of 5 and 7 as well as random turbo interleavers. Therefore the unprotected bitrate is approximately half the channel coded bitrate. The protected to unprotected video bitrate ratio is not exactly half, since two tailing bits are required to reset the convolutional encoders' memory to their default state in each transmission burst. In both modes a 16-bit Cyclic Redundancy Checking (CRC) is used for error detection and 9 bits are used to encode the reverse link feedback acknowledgement information by simple repetition coding. The feedback flag decoding ensues using majority logic decisions. The packetisation requires a small amount of header information added to each transmitted packet, which is 11 and 12 bits per packet for BPSK and QPSK, respectively. The effective or useful video bitrates for the BPSK and QPSK modes are then 3.4 and 7.0 Mbps.

The fixed mode BPSK and QPSK transceivers are limited to one and two bits per symbol, respectively. By contrast, the proposed AOFDM transceivers operate at the same bitrate, as their corresponding fixed modem mode counterparts, although they can vary their modulation mode on a sub-carrier by sub-carrier basis between 0, 1, 2 and 4 bits per symbol. Zero bits per symbol implies that transmissions are disabled for the sub-carrier concerned.

The "micro-adaptive" nature of the subband-adaptive modem is characterised by Figure 21.46, portraying at the top a contour plot of the channel Signal-to-Noise Ratio (SNR) for each subcarrier versus time. At the centre and bottom of the figure the modulation mode chosen for each 32-subcarrier subband is shown versus time for the

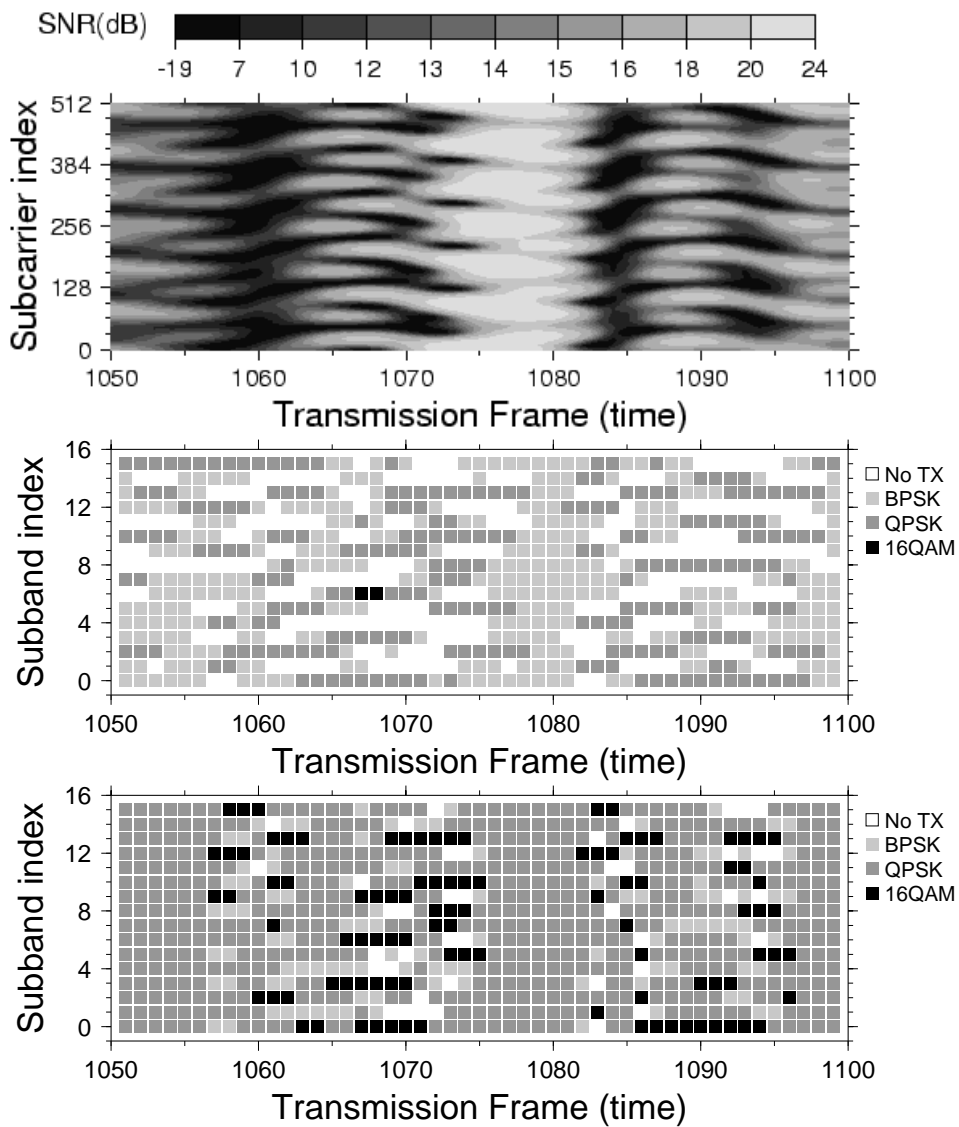


**Figure 21.46:** The micro-adaptive nature of the subband-adaptive OFDM modem. The top graph is a contour plot of the channel SNR for all 512 subcarriers versus time. The bottom two graphs show the modulation modes chosen for all 16 32-subcarrier subbands for the same period of time. The middle graph shows the performance of the 3.4Mbps subband-adaptive modem, which operates at the same bitrate as a fixed BPSK modem. The bottom graph represents the 7.0Mbps subband-adaptive modem, which operated at the same bitrate as a fixed QPSK modem. The average channel SNR was 16dB.

	BPSK mode	QPSK mode
Packet rate	4687.5 Packets/s	
FFT length	512	
OFDM symbols/packet	3	
OFDM symbol duration	2.6667 $\mu$ s	
OFDM time frame	80 Timeslots = 213 $\mu$ s	
Normalised Doppler frequency, $f'_d$	$1.235 \times 10^{-4}$	
OFDM symbol normalised Doppler frequency, $F_D$	$7.41 \times 10^{-2}$	
FEC coded bits/packet	1536	3072
FEC-coded video bitrate	7.2Mbps	14.4Mbps
Unprotected Bits/Package	766	1534
Unprotected bitrate	3.6Mbps	7.2Mbps
Error detection CRC (bits)	16	16
Feedback error flag bits	9	9
Packet header bits/packet	11	12
Effective video bits/packet	730	1497
Effective video bitrate	3.4Mbps	7.0Mbps

**Table 21.13:** System parameters for the fixed QPSK and BPSK transceivers, as well as for the corresponding subband-adaptive OFDM (AOFDM) transceivers for Wireless Local Area Networks (WLANs).

3.4 and 7.0 Mbps target-rate subband-adaptive modems, respectively. The channel SNR variation versus both time and frequency is also shown in a three-dimensional form in Figure 21.47, which maybe more convenient to visualise. This was recorded for the channel impulse response of Figure 21.48. It can be seen that when the channel is of high quality – like for example at about frame 1080 – the subband-adaptive modem used the same modulation mode, as the equivalent fixed rate modem in all subcarriers. When the channel is hostile – like around frame 1060 – the subband-adaptive modem used a lower-order modulation mode in some subbands, than the equivalent fixed mode scheme, or in extreme cases disabled transmission for that subband. In order to compensate for the loss of throughput in this subband a higher-order modulation mode was used in the higher quality subbands.

One video packet is transmitted per OFDM symbol, therefore the video packet loss ratio is the same, as the OFDM symbol error ratio. The video packet loss ratio is plotted versus the channel SNR in Figure 21.49. It is shown in the graph that the subband-adaptive transceivers – or synonymously termed as microscopic-adaptive ( $\mu$ AOFDM), in contrast to OFDM symbol-by-symbol adaptive transceivers – have a lower packet loss ratio (PLR) at the same SNR compared to the fixed modulation mode transceiver. Note in Figure 21.49 that the subband-adaptive transceivers can operate at lower channel SNRs, than the fixed modem mode transceivers, while maintaining the same required video packet loss ratio. Again, the figure labels the subband-adaptive OFDM transceivers as  $\mu$ AOFDM, implying that the adaption is not noticeable from the upper layers of the system. A macro-adaption could be ap-

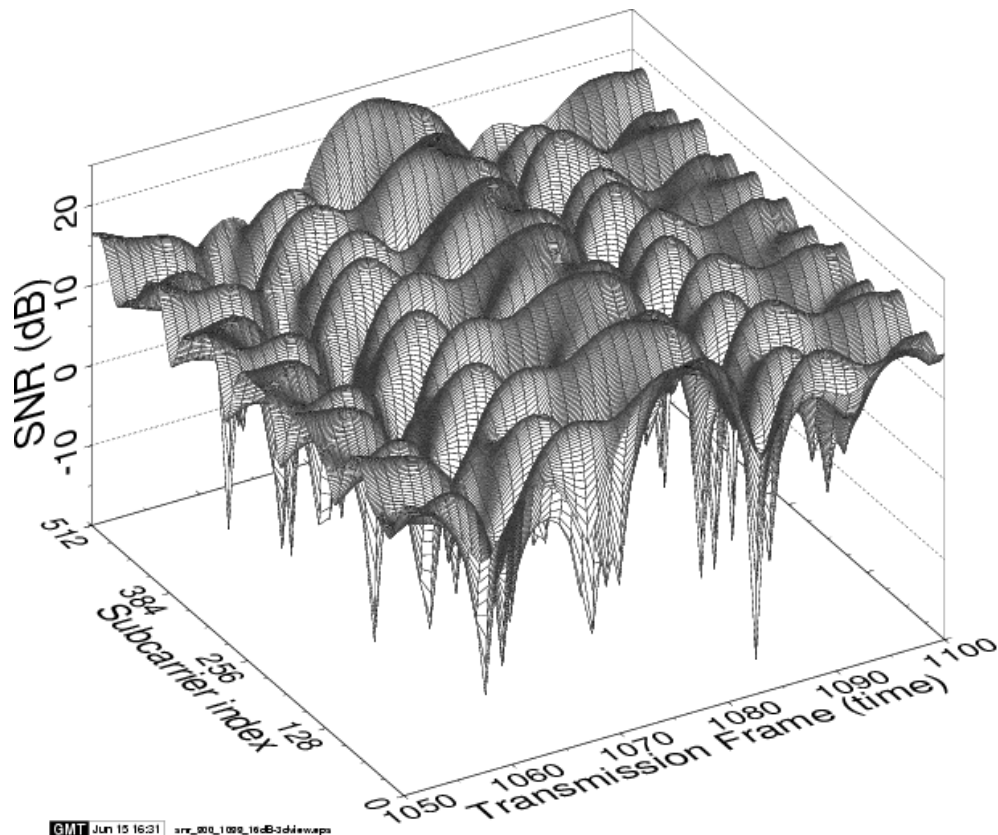
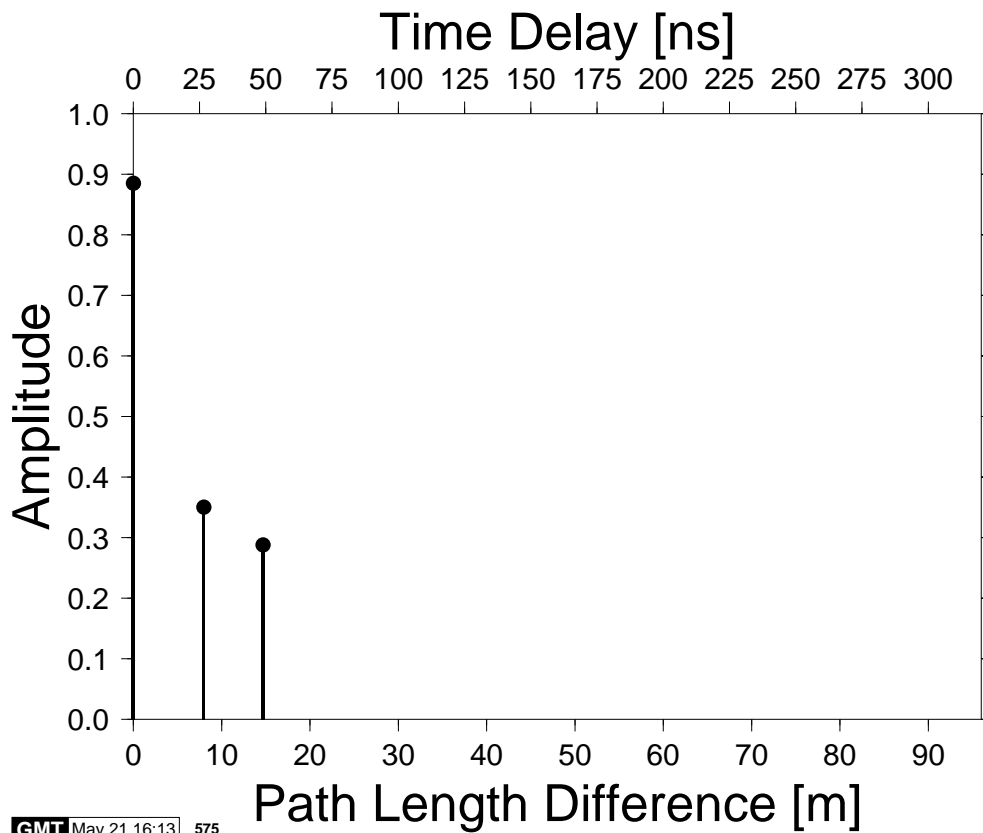


**Figure 21.47:** Instantaneous channel SNR for all 512 subcarriers versus time, for an average channel SNR of 16dB over the channel characterised by the channel impulse response (CIR) of Figure 21.48.

plied in addition to the microscopic adaption by switching between different target bitrates, as the longer-term channel quality improves and degrades. This issue is the subject of Section 21.4.8.

Having shown that the subband-adaptive OFDM transceiver achieved a reduced video packet loss, in comparison to fixed modulation mode transceivers under identical channel conditions, we now compare the effective throughput bitrate of the fixed and adaptive OFDM transceivers in Figure 21.50. The figure shows that when the channel quality is high, the throughput bitrate of the fixed and adaptive transceivers are identical. However, as the channel degrades, the loss of packets results in a lower throughput bitrate. The lower packet loss ratio of the subband-adaptive transceiver results in a higher throughput bitrate than that of the fixed modulation mode transceiver.

The throughput bitrate performance results translate to the decoded video quality performance results evaluated in terms of PSNR in Figure 21.51. Again, for high channel SNRs the performance of the fixed and adaptive OFDM transceivers is



GMT May 21 16:13 575

**Figure 21.48:** Indoor three-path WATM channel impulse response.

identical. However, as the channel quality degrades, the video quality of the subband-adaptive transceiver degrades less dramatically, than that of the corresponding fixed modulation mode transceiver.

### 21.4.7 Subband-adaptive OFDM transceivers having different target bitrates

As mentioned before, the subband-adaptive modems employ different modulation modes for different subcarriers, in order to meet the target bitrate requirement at the lowest possible channel SNR. This is achieved by using a more robust modulation mode or eventually by disabling transmissions over subcarriers having a low channel quality. By contrast, the adaptive system can invoke less robust, but higher throughput modulation modes over subcarriers exhibiting a high channel quality. In the examples we have previously considered we chose the AOFDM target bitrate to be identical to that of a fixed modulation mode transceiver. In this section we comparatively study the performance of various  $\mu$ AOFDM systems having different target

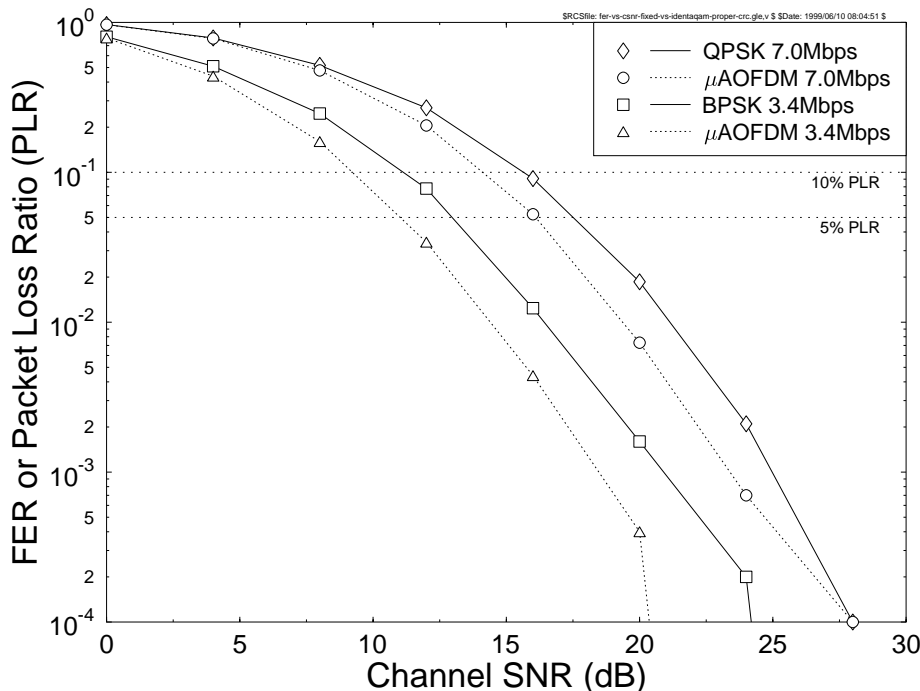


**Figure 21.49:** Frame Error Rate (FER) or video packet loss ratio (PLR) versus channel SNR for the BPSK and QPSK fixed modulation mode OFDM transceivers and for the corresponding subband-adaptive  $\mu$ AOFDm transceiver, operating at identical effective video bitrates, namely at 3.4 and 7.0 Mbps, over the channel model of Figure 21.48 at a normalised Doppler frequency of  $F_D = 7.41 \times 10^{-2}$ .

bitrates.

The previously described  $\mu$ AOFDm transceiver of Table 21.13 exhibited a FEC-coded bitrate of 7.2Mbps, which provided an effective video bitrate of 3.4Mbps. If the video target bitrate is lower than 3.4Mbps, then the system can disable transmission in more of the subcarriers, where the channel quality is low. Such a transceiver would have a lower bit error rate, than the previous BPSK-equivalent  $\mu$ AOFDm transceiver, and therefore could be used at lower average channel SNRs, while maintaining the same bit error ratio target. By contrast, as the target bitrate is increased, the system has to employ higher-order modulation modes in more subcarriers, at the cost of an increased bit-error ratio. Therefore high target bitrate  $\mu$ AOFDm transceivers can only perform within the required bit error ratio constraints at high channel SNRs, while low target bitrate  $\mu$ AOFDm systems can operate at low channel SNRs without inflicting excessive BERs. Therefore a system, which can adjust its target bitrate, as the channel SNR changes, would operate over a wide range of channel SNRs, providing the maximum possible average throughput bitrate, while maintaining the required bit



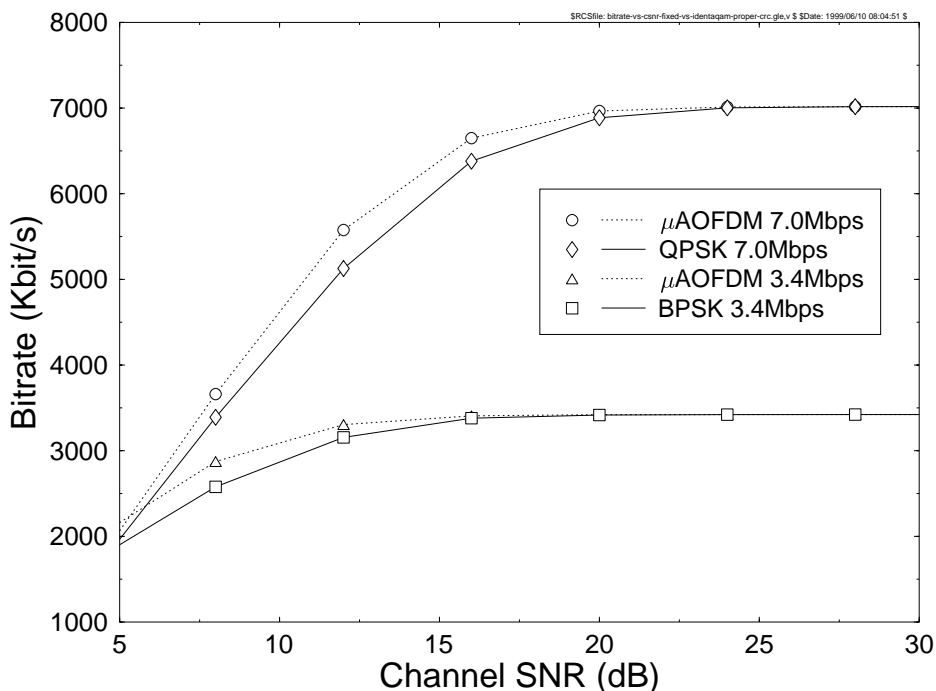


**Figure 21.50:** Effective throughput bitrate versus channel SNR for the BPSK and QPSK fixed modulation mode OFDM transceivers and that of the corresponding subband-adaptive or  $\mu$ AOFDM transceiver operating at identical effective video bitrates of 3.4 and 7.0 Mbps, over the channel of Figure 21.48 at a normalised Doppler frequency of  $F_D = 7.41 \times 10^{-2}$ .

error ratio.

Hence below we provide a performance comparison of various  $\mu$ AOFDM transceivers having four different target bitrates, of which two are equivalent to that of the BPSK and QPSK fixed modulation mode transceivers of Table 21.13. The system parameters for all four different bitrate modes are summarised in Table 21.14. The modes having effective video bitrates of 3.4 and 7.0Mbps are equivalent to the bitrates of a fixed BPSK and QPSK mode transceiver, respectively.

Figure 21.52 shows the Frame Error Rate (FER) or video packet loss ratio (PLR) performance versus channel SNR for the four different target bitrates of Table 21.14, demonstrating – as expected – that the higher target bitrate modes require higher channel SNRs in order to operate within given PLR constraints. For example, the mode having an effective video bitrate of 9.8Mbps can only operate for channel SNRs in excess of 19dB under the constraint of a maximum PLR of 5%. However, the mode having an effective video bitrate of 3.4Mbps can operate at channel SNRs of 11dB and above, whilst maintaining the same 5% PLR constraint, albeit at about half the throughput bitrate and hence at a lower video quality.

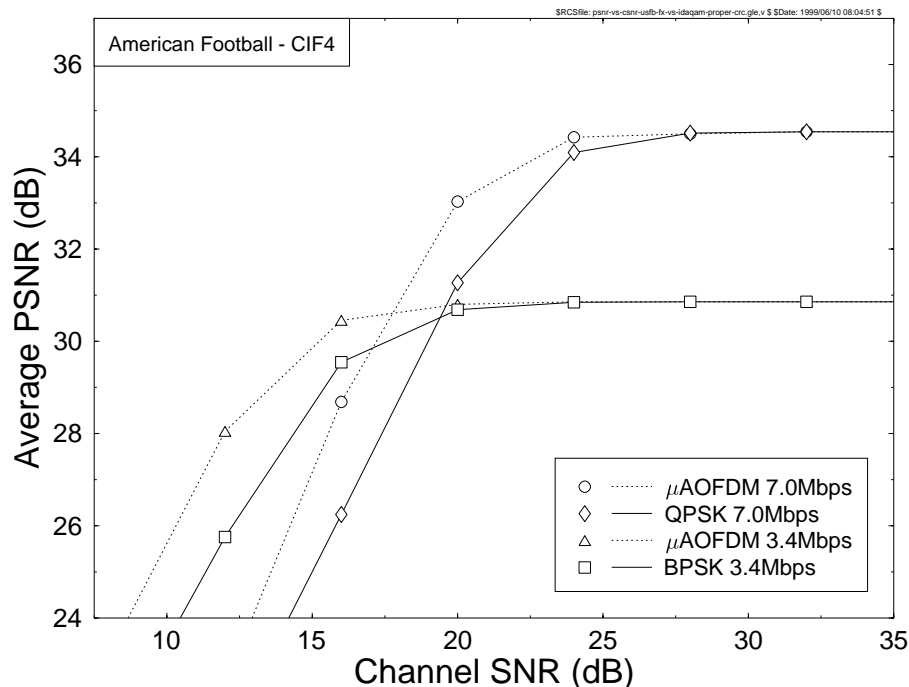


**Figure 21.51:** Average video quality expressed in PSNR versus channel SNR for the BPSK and QPSK fixed modulation mode OFDM transceivers and for the corresponding  $\mu$ AOFDM transceiver operating at identical channel SNRs over the channel model of Figure 21.48 at a normalised Doppler frequency of  $F_D = 7.41 \times 10^{-2}$ .

The tradeoffs between video quality and channel SNR for the various target bitrates can be judged from Figure 21.53, suggesting – as expected – that the higher target bitrates result in a higher video quality, provided that channel conditions are sufficiently favorable. However, as the channel quality degrades, the video packet loss ratio increases, thereby reducing the throughput bitrate, and hence the associated video quality. The lower target bitrate transceivers operate at an inherently lower video quality, but they are more robust to the prevailing channel conditions and hence can operate at lower channel SNRs, while guaranteeing a video quality, which is essentially unaffected by channel errors. It was found that the perceived video quality became impaired for packet loss ratios in excess of about 5%.

The tradeoffs between video-quality, packet loss ratio and the target bitrate are further augmented with reference to Figure 21.54. The figure shows the video quality measured in PSNR versus video frame index at a channel SNR of 16dB and also for an error free situation. At the bottom of each graph the packet loss ratio per video frame is shown. The three figures indicate the tradeoffs to be made in choosing the target bitrate for the specific channel conditions experienced – in this specific example

Packet rate	4687.5 Packets/s			
FFT length	512			
OFDM Symbols/Packet	3			
OFDM Symbol Duration	2.6667 $\mu$ s			
OFDM Time Frame	80 Timeslots = 213 $\mu$ s			
Normalised Doppler frequency, $f'_d$	$1.235 \times 10^{-4}$			
OFDM symbol normalised Doppler frequency, $F_D$	$7.41 \times 10^{-2}$			
FEC Coded Bits/Packet	858	1536	3072	4272
FEC-coded video bitrate	4.0Mbps	7.2Mbps	14.4Mbps	20.0Mbps
No. of unprotected bits/packet	427	766	1534	2134
Unprotected bitrate	2.0Mbps	3.6Mbps	7.2Mbps	10.0Mbps
No. of CRC bits	16	16	16	16
No. of feedback error flag bits	9	9	9	9
No. of packet header bits/packet	10	11	12	13
Effective video bits/packet	392	730	1497	2096
Effective video bitrate	1.8Mbps	3.4Mbps	7.0Mbps	9.8Mbps
Equivalent modulation mode		BPSK	QPSK	
Minimum channel SNR for 5% PLR (dB)	8.8	11.0	16.1	19.2
Minimum channel SNR for 10% PLR (dB)	7.1	9.2	14.1	17.3

**Table 21.14:** System parameters for the four different target bitrates of the various subband-adaptive OFDM ( $\mu$ AOFDM) transceivers

for a channel SNR of 16dB. Note that under error free conditions the video quality improved upon increasing the bitrate.

Specifically, video PSNRs of about 40, 41.5 and 43dB were observed for the effective video bitrates of 1.8, 3.4 and 7.0Mbps. The figure shows that for the target bitrate of 1.8Mbps, the system has a high grade of freedom in choosing, which sub-carriers to invoke and therefore it is capable of reducing the number of packets that are lost. The packet loss ratio remains low and the video quality remains similar to that of the error free situation. The two instances, where the PSNR is significantly different from the error free performance correspond to video frames, in which video packets were lost. However, the system recovers in both instances in the following video frame.

As the target bitrate of the subband-adaptive OFDM transceiver is increased to 3.4Mbps, the subband modulation mode selection process has to be more “aggressive”, resulting in increased video packet loss. Observe in the figure that the transceiver having an effective video bitrate of 3.4Mbps, exhibits increased packet loss, and in one frame as much as 5% of the packets transmitted for that video frame were lost, although the average PLR was only 0.4%. Due to the increased packet loss the video PSNR curve diverges from the error-free performance curve more often. However, in almost all cases the effects of the packet losses are masked in the next video frame,

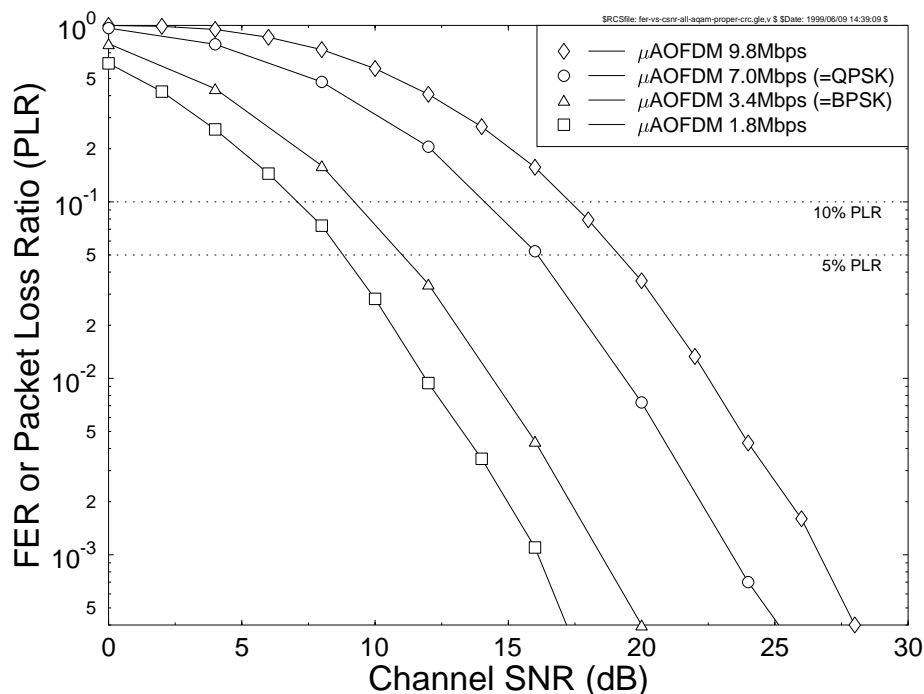


**Figure 21.52:** FER or video packet loss ratio (PLR) versus channel SNR for the subband-adaptive OFDM transceivers of Table 21.14 operating at four different target bitrates, over the channel model of Figure 21.48 at a normalised Doppler frequency of  $F_D = 7.41 \times 10^{-2}$ .

indicated by the re-merging PSNR curves in the figure, maintaining a close to error-free PSNR. The subjective effect of this level of packet loss is almost imperceivable.

When the target bitrate is further increased to 7.0Mbps, the average PLR is about 5% under the same channel conditions, and the effects of this packet loss ratio are becoming objectionable in perceived video quality terms. At this target bitrate, there are several video frames, where at least 10% of the video packets have been lost. The video quality measured in PSNR terms rarely reaches its error-free level, due to the fact that every video frame contains at least one lost packet. The perceived video quality remains virtually unimpaired, until the head movement in the “Suzie” video sequence around frames 40–50, where the effect of lost packets becomes obvious, and the PSNR drops to about 30dB.

#### 21.4.8 Time-variant target bitrate OFDM transceivers

By using a high target bitrate, when the channel quality is high, while a reduced target bitrate, when the channel quality is poor, an adaptive system is capable of maximising the average throughput bitrate over a wide range of channel SNRs, while

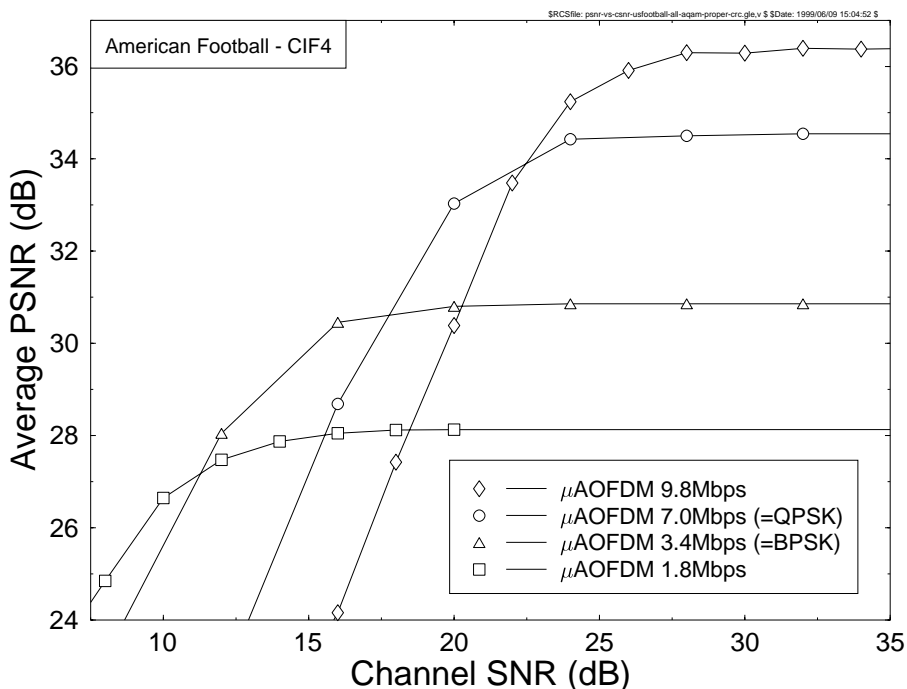


**Figure 21.53:** Average video quality expressed in PSNR versus channel SNR for the subband-adaptive OFDM transceivers of Table 21.14, operating at four different target bitrates, over the channel model of Figure 21.48 at a normalised Doppler frequency of  $F_D = 7.41 \times 10^{-2}$ .

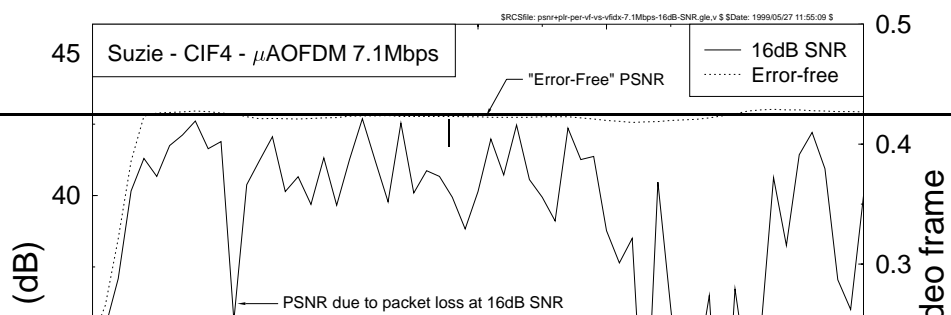
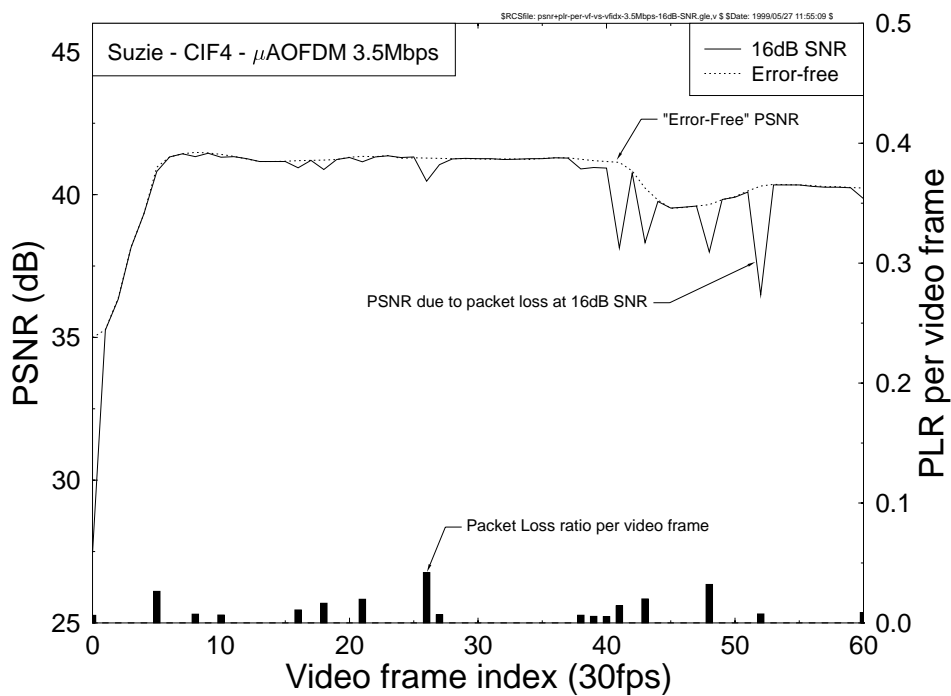
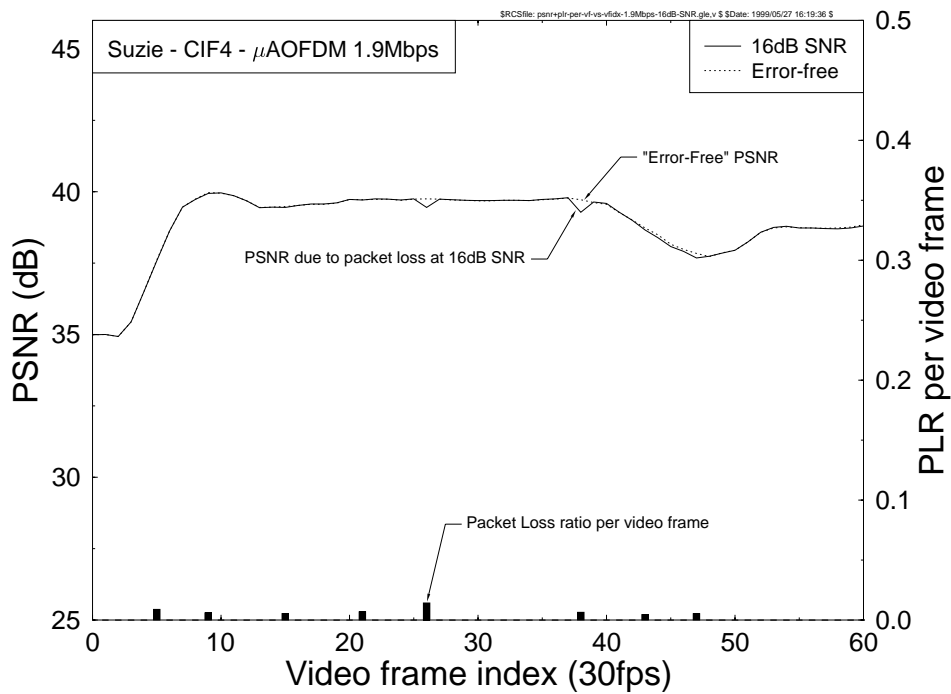
maintaining a given quality constraint. This quality constraint for our video system could be a maximum packet loss ratio.

However, there is a substantial processing delay associated with evaluating the packet loss information and therefore modem mode switching based on this metric would be less efficient due to this latency. Therefore we decided to invoke an estimate of the bit error ratio (BER) for mode switching, which can be estimated as follows. Since the noise energy in each subcarrier is independent of the channel's frequency domain transfer function  $H_n$ , the local Signal-to-Noise Ratio  $SNR$  in subcarrier  $n$  can be expressed as

$$\gamma_n = |H_n|^2 \cdot \gamma, \tag{21.3}$$

where  $\gamma$  is the overall SNR. If no signal degradation due to Inter-Subcarrier Interference (ISI) or interference from other sources appears, then the value of  $\gamma_n$  determines the bit error probability for the transmission of data symbols over the subcarrier  $n$ . Given  $\gamma_j$  across the  $N_s$  subcarriers in the  $j$ -th sub-band, the expected overall BER for all available modulation schemes  $M_n$  in each sub-band can be estimated, which is denoted by  $\bar{p}_e(n) = 1/N_s \sum_j p_e(\gamma_j, M_n)$ . For each sub-band, the scheme with the

21.4. ADAPTIVE TURBO-CODED OFDM-BASED VIDEO TELEPHONY 985



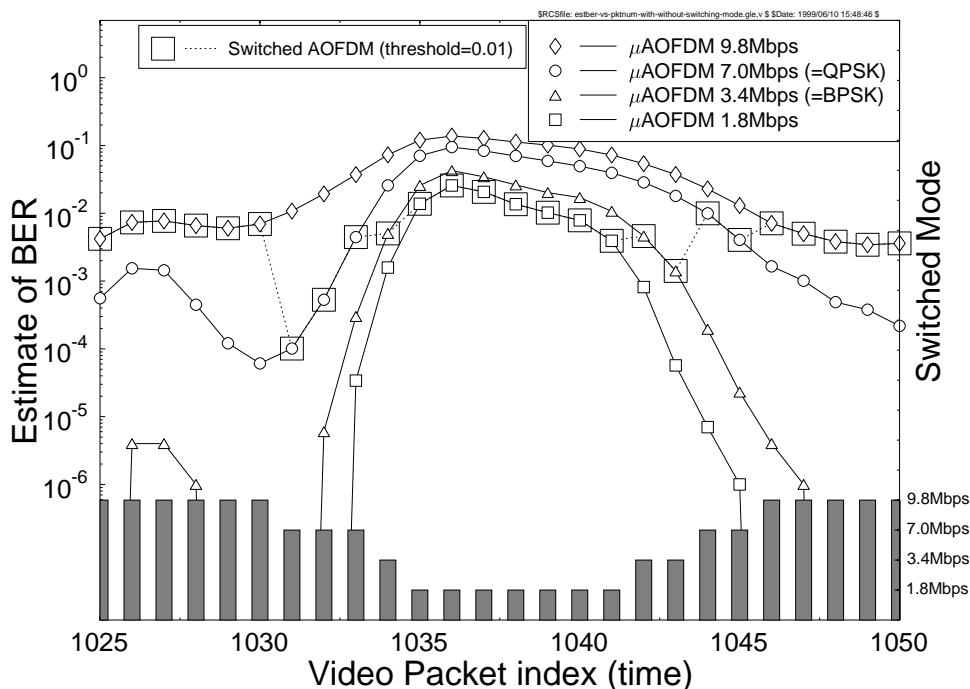


**Figure 21.55:** Illustration of mode switching for the switched subband adaptive modem. The figure shows the estimate of the bit error ratio for the four possible modes. The large square and the dotted line indicate the modem mode chosen for each time interval by the mode switching algorithm. At the bottom of the graph the bar chart specifies the bitrate of the switched subband adaptive modem on the right-hand axis versus time when using the channel model of Figure 21.48 at a normalised Doppler frequency of  $F_D = 7.41 \times 10^{-2}$ .

highest throughput, whose estimated BER is lower than a given threshold, is then chosen.

We decided to use a quadruple-mode switched subband-adaptive modem, using the four target bitrates of Table 21.14. The channel estimator can then estimate the expected bit error ratio of the four possible modem modes. Our switching scheme opted for the modem mode, whose estimated BER was below the required threshold. This threshold could be varied in order to tune the behaviour of the switched subband-adaptive modem for a high or a low throughput. The advantage of a higher throughput was a higher error-free video quality at the expense of increased video packet losses, which could reduce the perceived video quality.

Figure 21.55 demonstrates, how the switching algorithm operates for a 1% estimated BER threshold. Specifically, the figure portrays the estimate of the bit error ratio for the four possible modem modes versus time. The large square and the dotted line indicates the mode chosen for each time interval by the mode switching algorithm.

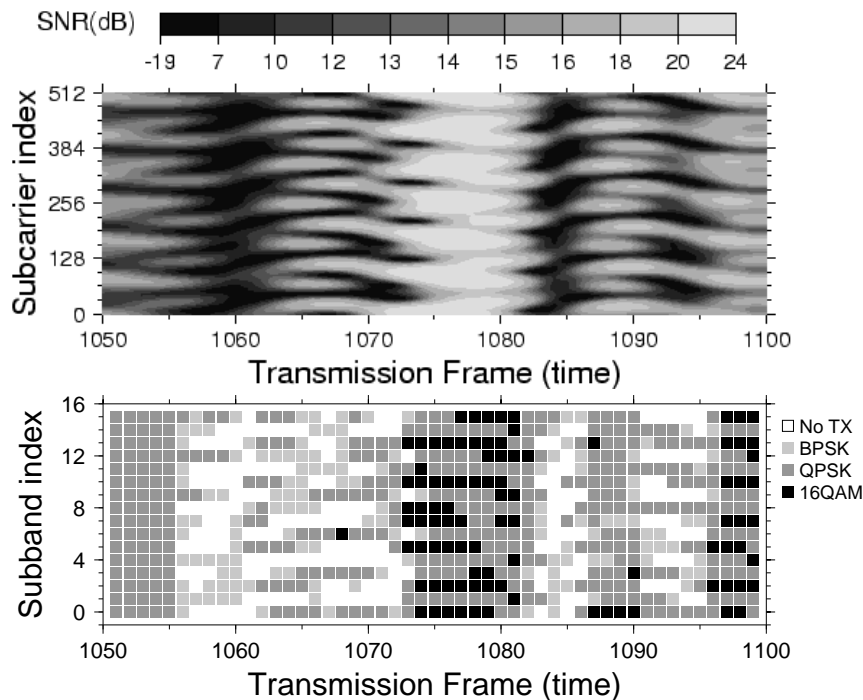


**Figure 21.56:** The micro-adaptive nature of the time-variant target bitrate subband-adaptive (TVTBR-AOFDM) modem. The top graph is a contour plot of the channel SNR for all 512 subcarriers versus time. The bottom graph shows the modulation mode chosen for all 16 subbands for the same period of time. Each subband is comprised of 32 subcarriers. The TVTBR AOFDM modem switches between target bitrates of 2, 3.4, 7 and 9.8Mbps, while attempting to maintain an estimated BER of 0.1% before channel coding. Average Channel SNR is 16dB over the channel of Figure 21.48 at a normalised Doppler frequency of  $F_D = 7.41 \times 10^{-2}$ .

The algorithm attempts to use the highest bitrate mode, whose BER estimate is less than the target threshold namely, 1% in this case. However, if all the four modes' estimate of the BER is above the 1% threshold, then the lowest bitrate mode is chosen, since this will be the most robust to channel errors. An example of this is shown around frames 1035–1040. At the bottom of the graph a bar chart specifies the bitrate of the switched subband adaptive modem versus time, in order to emphasise, when the switching occurs.

An example of the algorithm, when switching amongst the target bitrates of 1.8, 3.4, 7 and 9.8Mbps is shown in Figure 21.56. The upper part of the figure portrays the contour plot of the channel SNR for each subcarrier versus time. The lower part of the figure displays the modulation mode chosen for each 32-subcarrier subband versus time for the time-variant target bitrate (TVTBR) subband adaptive modem. It can be seen at frames 1051–1055 that all the subbands employ QPSK modulation,

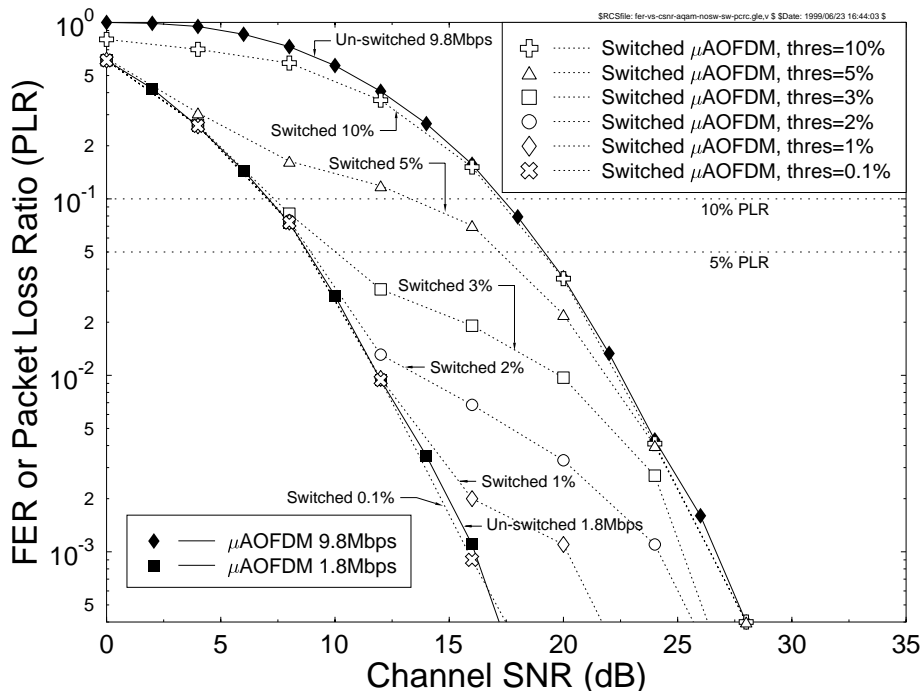


therefore the TVTBR-AOFDM modem has an instantaneous target bitrate of 7Mbps. As the channel degrades around frame 1060, the modem has switched to the more robust 1.8Mbps mode. When the channel quality is high around frames 1074-1081, the highest bitrate 9.8Mbps mode is used. This demonstrates that the TVTBR-AOFDM modem can reduce the number of lost video packets by using reduced bitrate but more robust modulation modes, when the channel quality is poor. However, this is at the expense of a slightly reduced average throughput bitrate. Usually a higher throughput bitrate results in a higher video quality, however a high bitrate is also associated with a high packet loss ratio, which is usually less attractive in terms of perceived video quality than a lower bitrate, lower packet loss ratio mode.

Having highlighted, how the time-domain mode switching algorithm operates, we will now characterise its performance for a range of different BER switching thresholds. A low BER switching threshold implies that the switching algorithm is cautious about switching to the higher bitrate modes, and therefore the system performance is characterised by a low video packet loss ratio and a low throughput bitrate. A high BER switching threshold results in the switching algorithm attempting to use the highest bitrate modes in all but the worst channel conditions. This results in a higher video packet loss ratio. However, if the packet loss ratio is not excessively high, a higher video throughput is achieved.

Figure 21.57 portrays the video packet loss ratio or FER performance of the TVTBR-AOFDM modem for a variety of BER thresholds, compared to the minimum and maximum rate un-switched modes. It can be seen that for a conservative BER switching threshold of 0.1% the time-variant target bitrate subband adaptive (TVTBR-AOFDM) modem has a similar packet loss ratio performance to that of the 1.8Mbps non-switched or constant target bitrate (CTBR) subband adaptive modem. However, as we will show, the throughput of the switched modem is always better or equal to that of the un-switched modem, and becomes far superior, as the channel quality improves. Observe in the figure that the “aggressive” switching threshold of 10% has a similar packet loss ratio performance to that of the 9.8Mbps CTBR-AOFDM modem. We found that in order to maintain a packet loss ratio of below 5%, the BER switching thresholds of 2 and 3% offered the best overall performance, since the packet loss ratio was fairly low, while the throughput bitrate was higher, than that of an un-switched CTBR-AOFDM modem.

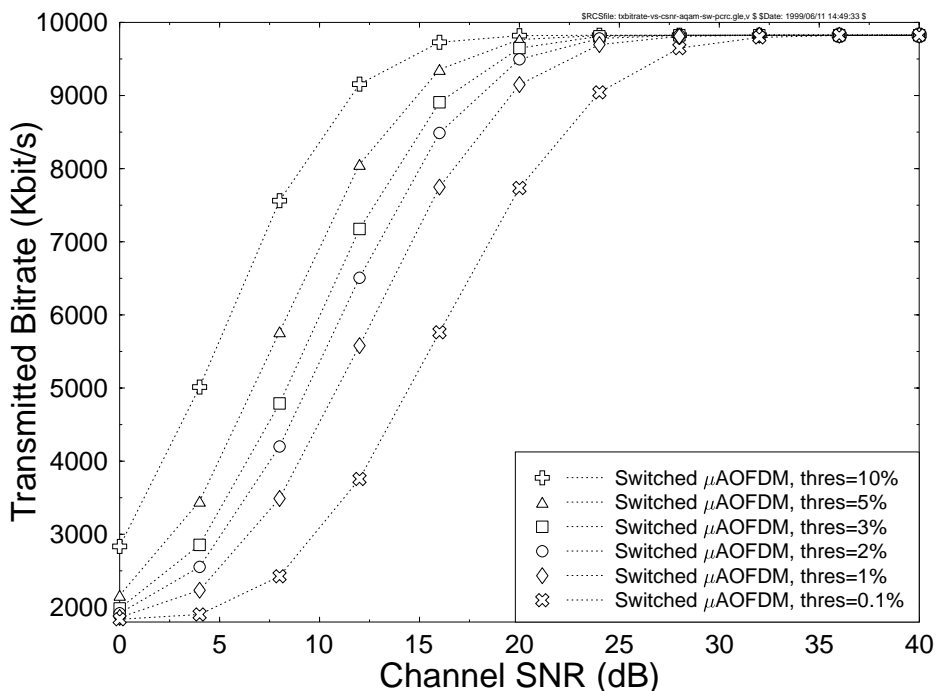
A high BER switching threshold results in the switched subband adaptive modem transmitting at a high average bitrate. However, we have shown in Figure 21.57 how the packet loss ratio increases, as the BER switching threshold is increased. Therefore the overall useful or effective throughput bitrate - ie. the bitrate excluding lost packets - may in fact be reduced in conjunction with high BER switching thresholds. Figure 21.58 demonstrates how the transmitted bitrate of the switched TVTBR-AOFDM modem increases with higher BER switching thresholds. However, when this is compared to the effective throughput bitrate, where the effects of packet loss are taken into account, the tradeoff between the BER switching threshold and the effective bitrate is less obvious. Figure 21.59 portrays the corresponding effective throughput bitrate versus channel SNR for a range of BER switching thresholds. The figure demonstrates that for a BER switching threshold of 10% the effective throughput bitrate performance was reduced in comparison to some of the lower BER switching



**Figure 21.57:** FER or video packet loss ratio versus channel SNR for the TVTBR-AOFDM modem for a variety of BER switching thresholds. The switched modem uses four modes, with target bitrates of 1.8, 3.4, 7 and 9.8Mbps. The un-switched 1.8 and 9.8Mbps results are also shown in the graph as solid markers using the channel model of Figure 21.48 at a normalised Doppler frequency of  $F_D = 7.41 \times 10^{-2}$ .

threshold scenarios. Therefore the BER=10% switching threshold is obviously too aggressive, resulting in a high packet loss ratio, and a reduced effective throughput bitrate. For the switching thresholds considered, the BER=5% threshold achieved the highest effective throughput bitrate. However, even though the BER=5% switching threshold produces the highest effective throughput bitrate, this is at the expense of a relatively high video packet loss ratio, which – as we will show – has a detrimental effect on the perceived video quality.

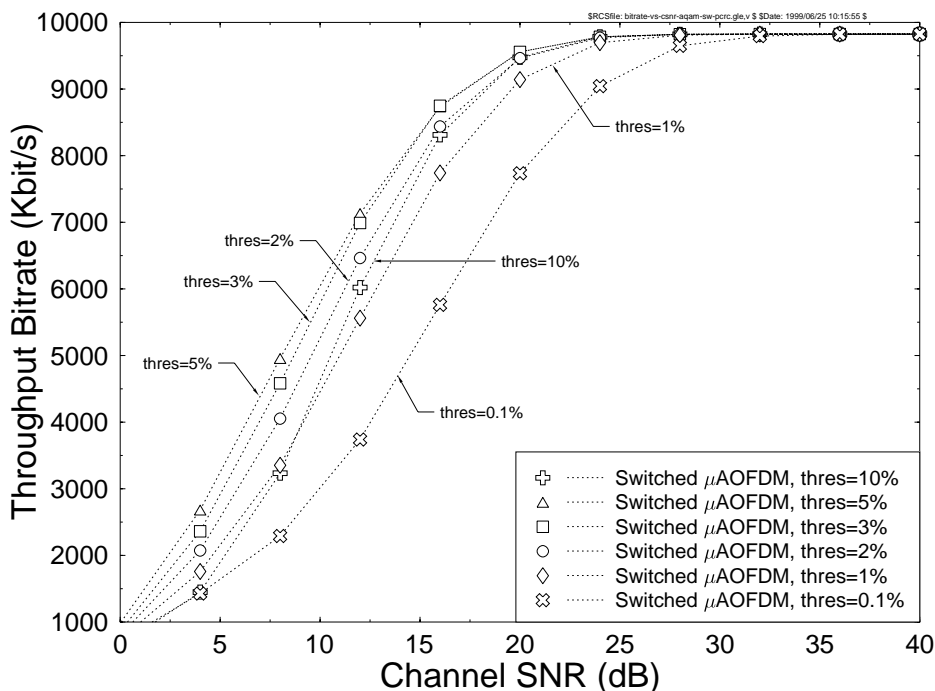
We will now demonstrate the effects associated with different BER switching thresholds on the video quality represented by the peak-signal-to-noise ratio (PSNR). Figure 21.60 portrays the PSNR and packet loss performance versus time for a range of BER switching thresholds. The top graph in the figure indicates that for a BER switching threshold of 1% the PSNR performance is very similar to the corresponding error-free video quality. However, the PSNR performance diverges from the error-free curve, when video packets are lost, although the highest PSNR degradation is limited to 2dB. Furthermore, the PSNR curve typically reverts to the error-free PSNR perfor-



**Figure 21.58:** Transmitted bitrate of the switched TVTBR-AOFDM modem for a variety of BER switching thresholds. The switched modem uses four modes, having target bitrates of 1.8, 3.4, 7 and 9.8Mbps, over the channel model of Figure 21.48 at a normalised Doppler frequency of  $F_D = 7.41 \times 10^{-2}$ .

mance curve in the next frame. In this example about 80% of the video frames have no video packet loss. When the BER switching threshold is increased to 2%, as shown in the center graph of Figure 21.60, the video packet loss ratio has increased, such that now only 41% of video frames have no packet loss. The result of the increased packet loss is a PSNR curve, which diverges from the error-free PSNR performance curve more regularly, with PSNR degradations of upto 7dB. It is worth noting that when there are video frames with no packet losses, the PSNR typically recovers, achieving a similar PSNR performance to the error-free case. When the BER switching threshold was further increased to 3% - which is not shown in the figure - the maximum PSNR degradation increased to 10.5dB, and the number of video frames without packet losses was reduced to 6%.

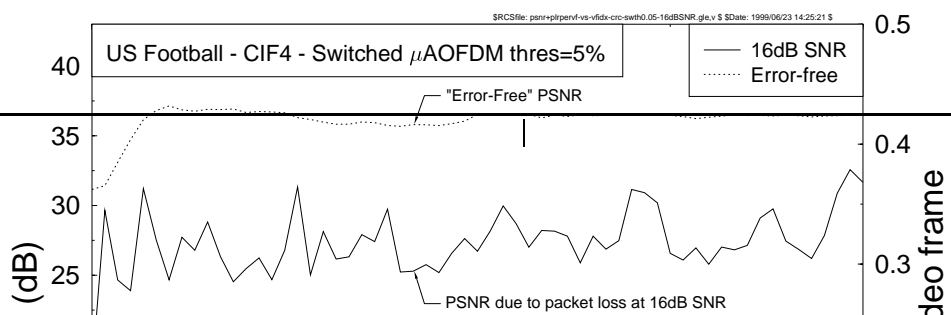
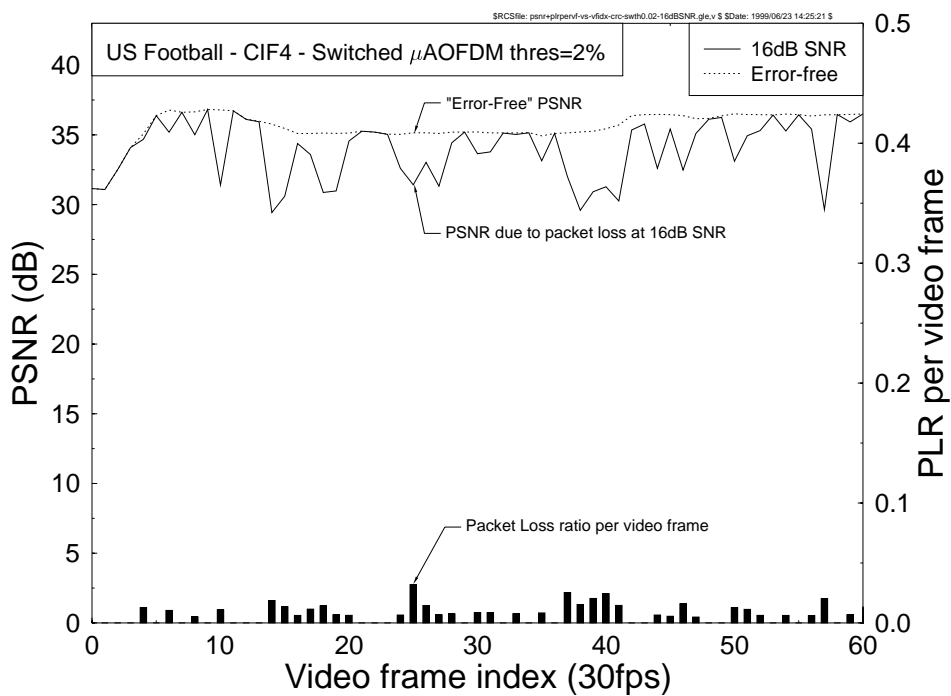
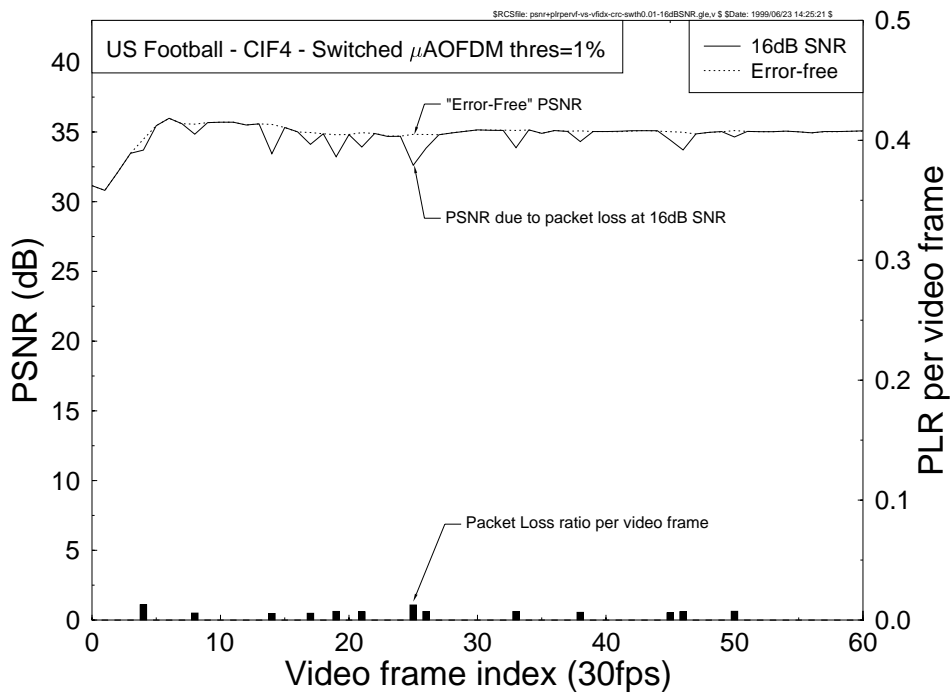
The bottom graph of Figure 21.60 portrays the PSNR and packet loss performance for a BER switching threshold of 5%. The PSNR degradation in this case ranges from 1.8 to 13dB and all video frames contain at least one lost video packet. Even though the BER=5% switching threshold provides the highest effective throughput bitrate, the associated video quality is poor. The PSNR degradation in most video frames is

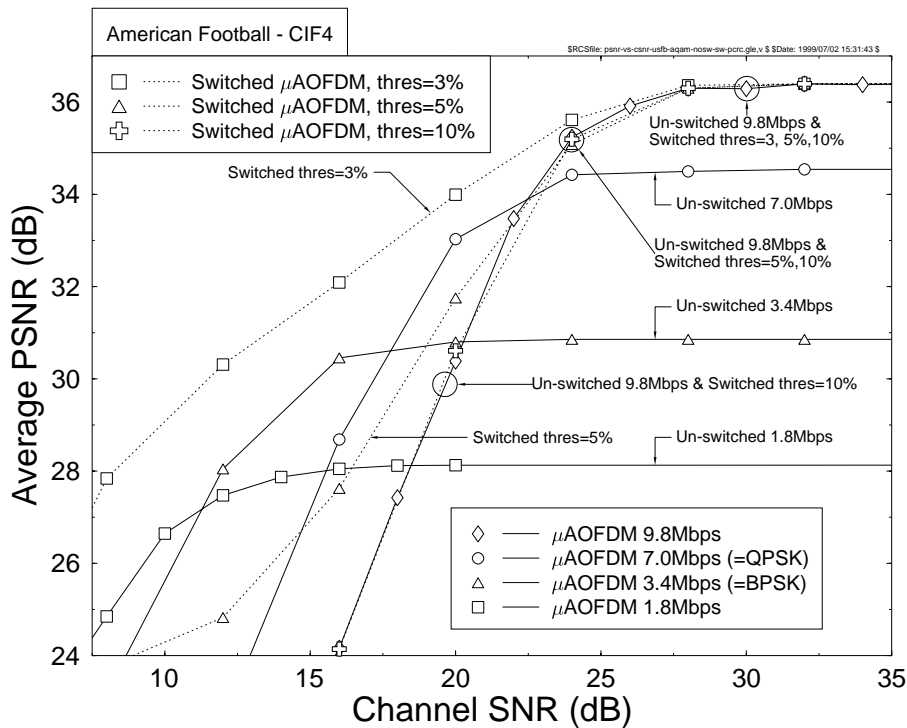


**Figure 21.59:** Effective throughput bitrate of the switched TVTBR-AOFDM modem for a variety of BER switching thresholds. The switched modem uses four modes, with target bitrates of 1.8, 3.4, 7 and 9.8Mbps. The channel model of Figure 21.48 is used at a normalised Doppler frequency of  $F_D = 7.41 \times 10^{-2}$ .

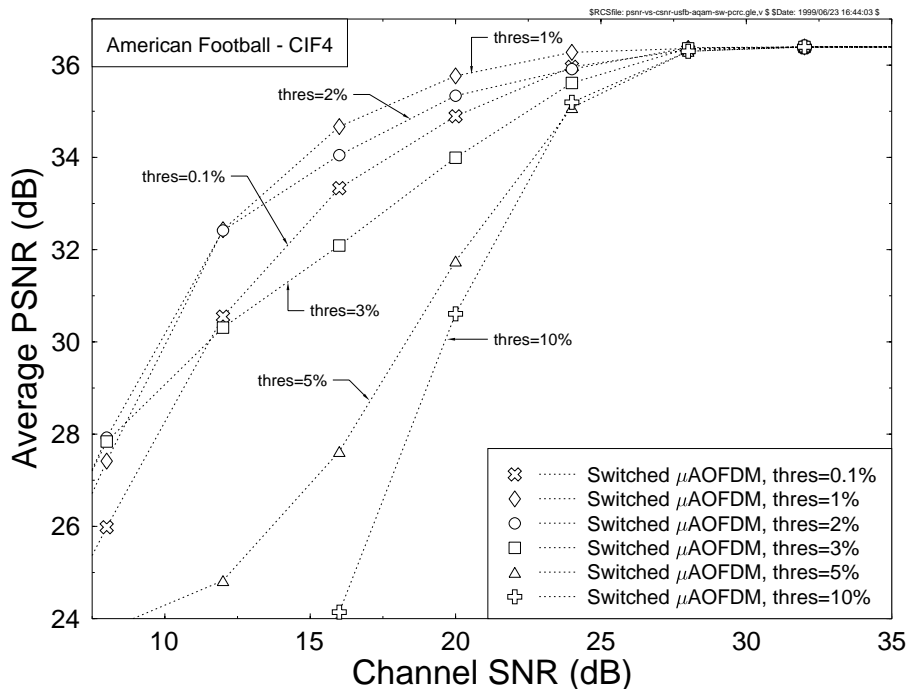
about 10dB. Clearly, the highest effective throughput bitrate does not guarantee the best video quality. We will now demonstrate that the switching threshold of BER=1% provides the best video quality, when using the average PSNR as our performance metric.

Figure 21.61(a) compares the average PSNR versus channel SNR performance for a range of switched (TVTBR) and un-switched (CTBR) AOFDM modems. The figure compares the four un-switched, ie. CTBR subband adaptive modems with switching, ie. TVTBR subband adaptive modems, which switch between the four fixed-rate modes, depending on the BER switching threshold. The figure indicates that the switched TVTBR subband adaptive modem having a switching threshold of BER=10% results in similar PSNR performance to the un-switched CTBR 9.8Mbps subband adaptive modem. When the switching threshold is reduced to BER=3%, the switched TVTBR AOFDM modem outperforms all of the un-switched CTBR AOFDM modems. A switching threshold of BER=5% achieves a PSNR performance, which is better than the un-switched 9.8Mbps CTBR AOFDM modem, but worse than that of the un-switched 7.0Mbps modem, at low and medium channel SNRs.





(a)



(b)

Figure 21.61: Average PSNR versus channel SNR performance for switched- and unswitched subband adaptive modems. Figure (a) compares the four unswitched CTBR subband adaptive modems with switched TVTBR subband

A comparison of the switched TVTBR AOFDM modem employing all six switching thresholds that we have used previously is shown in Figure 21.61(b). This figure suggests that switching thresholds of BER=0.1, 1 and 2% perform better than the BER=3% threshold, which outperformed all of the un-switched CTBR subband adaptive modems. The best average PSNR performance was achieved by a switching threshold of BER=1%. The more conservative BER=0.1% switching threshold results in a lower PSNR performance, since its throughput bitrate was significantly reduced. Therefore the best tradeoff in terms of PSNR, throughput bitrate and video packet loss ratio was achieved with a switching threshold of about BER=1%.

### 21.4.9 Summary and Conclusions

A range of AOFDM video transceivers have been proposed for robust, flexible and low-delay interactive video telephony. In order to minimize the amount of signalling required we divided the OFDM subcarriers into subbands and controlled the modulation modes on a subband-by-subband basis. The proposed constant target bitrate AOFDM modems provided a lower BER, than the corresponding conventional OFDM modems. The slightly more complex switched TVTBR-AOFDM modems can provide a balanced video quality performance, across a wider range of channel SNRs than the other schemes investigated.

## 21.5 MPEG2 / OFDM-based Turbo-Coded Digital Video Broadcasting to Mobile Receivers<sup>12 13</sup>

### 21.5.1 Background and Motivation

Commencing with a brief overview of the section, the MPEG-2 codec is subjected to a rigorous bit error sensitivity investigation, in order to assist in contriving various error protection schemes for wireless broadcast video transmission. Turbo-coded performance enhancement of the terrestrial Digital Video Broadcast (DVB) systems is proposed for transmission over mobile channels to receivers on the move. The turbo codec is shown to provide substantial performance advantages over conventional convolutional coding both in terms of bit error rate and video quality terms. Our experiments suggested that multi-class data partitioning did not result in error resilience improvements, since a high proportion of relatively sensitive video bits had to be relegated to the lower integrity subchannel, when invoking a powerful low-rate channel codec in the high-integrity protection class. We demonstrate that DVB transmission to mobile receivers is feasible, when using turbo-coded OFDM transceivers at realistic power-budget requirements under the investigated highly dispersive fading channel conditions.

<sup>12</sup>This section is based on C. S. Lee, T. Keller and L. Hanzo: Turbo-coded Hierarchical and Non-hierarchical Mobile Digital Video Broadcasting, submitted to IEEE Tr. on Broadcasting, 1999

<sup>13</sup>©1999 IEEE. Personal use of this material is permitted. However, permission to reprint/republish this material for advertising or promotional purposes or for creating new collective works for resale or redistribution to servers or lists, or to refuse any copyrighted component of this work in other works must be obtained from IEEE.

Following the standardization of the Pan-European Digital Video Broadcasting (DVB) systems, we have begun to witness the arrival of digital television services to the home. However, for a high proportion of business and leisure travellers it is desirable to have access to DVB services, while on the move. Although it is feasible to receive these services with the aid of dedicated DVB receivers, these receivers may also find their way into the laptop computers of the near future. These intelligent laptops may also become the portable DVB receivers of wireless in-home networks.

In recent years three DVB standards have emerged in Europe for terrestrial [620], cable-based [621] and satellite-oriented [622] delivery of DVB signals. The more hostile propagation environment of the terrestrial system requires concatenated Reed-Solomon [4,9] (RS) and rate compatible punctured convolutional coding [4,9] (RCPCC) combined with Orthogonal Frequency Division Multiplexing (OFDM) based modulation [10]. By contrast, the more benign cable and satellite based media facilitates the employment of blind-equalised multi-level modems using upto 256 quadrature amplitude modulation (QAM) levels [10]. These schemes are capable of delivering high-definition video at bitrates of upto 20 Mbits/s in stationary broadcast-mode distributive wireless scenarios.

Recently, there has been a range of DVB system performance studies in the literature [623–626]. Against this background in this section we have proposed turbo-coding based improvements to the terrestrial DVB system [620] and investigated its performance under hostile mobile channel conditions. We have also studied various partitioning and channel coding schemes both in the so-called hierarchical and non-hierarchical transceiver modes and compared their performance.

The rest of this section is divided into the following subsections. In Section 21.5.2 the bit error sensitivity of the MPEG-2 coding parameters [627] is characterised. A brief overview of the turbo-coded and standard DVB terrestrial scheme is presented in Section 21.5.3, while the channel model is described in Section 21.5.4. Following this, in Section 21.5.5 the reader is introduced to the MPEG-2 data partitioning scheme [628] used to split the input MPEG-2 video bitstream into two error protection classes, which can then be protected either equally or unequally. These two protection classes of data can then be communicated to the receiver using the so-called DVB terrestrial hierarchical transmission format. The performance of the data partitioning scheme was investigated by corrupting either the high or low priority data using randomly distributed errors for a range of system configurations in Section 21.5.6 and their effects on the overall reconstructed video quality was evaluated. Following this, the performance of the improved DVB terrestrial system employing the so-called non-hierarchical and hierarchical format was examined in a mobile environment in Sections 21.5.7 and 21.5.7, before our conclusions and future work areas were presented in Section 21.5.9. Let us now commence our discourse by quantifying the sensitivity of the MPEG-2 video parameters in the next section.

### 21.5.2 MPEG-2 Bit Error Sensitivity

In this section, we assume familiarity with the MPEG-2 standard [627]. The aim of our MPEG-2 error resilience study was to quantify the average PSNR degradation inflicted by each video codec parameter in the bitstream, so that appropriate protection can



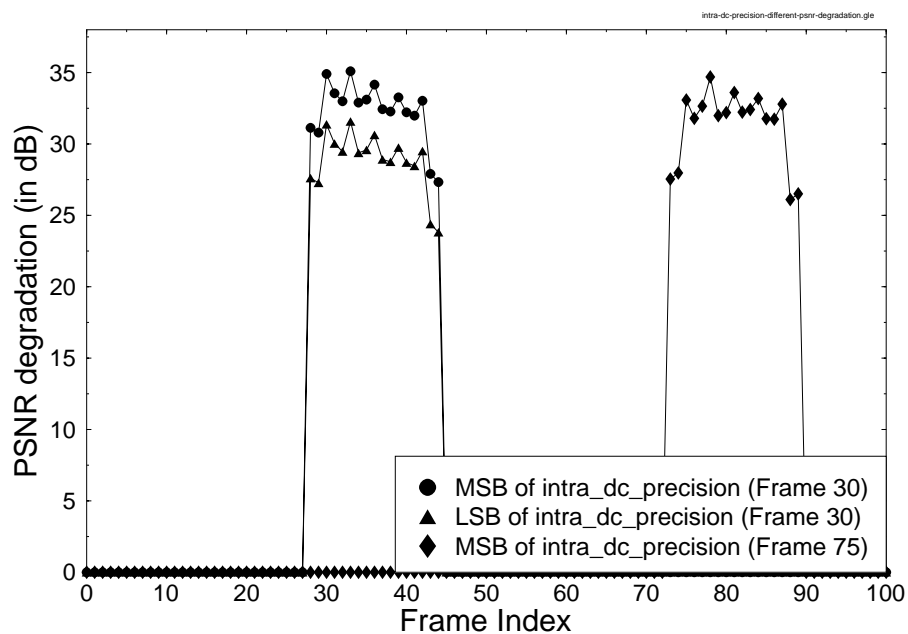


**Figure 21.62:** PSNR degradation profile for different bits encoding the so-called `intra_dc_precision` parameter in different corrupted video frames.

be assigned to them.

Most MPEG-2 parameters are encoded by several bits and they may occur in different positions in the video sequence. Furthermore, different encoded bits of the same parameter may exhibit different sensitivity to channel errors. Figure 21.62 shows such an example for the parameter known as `intra_dc_precision` [627], which is coded under the so-called Picture Coding Extension. In this example, the PSNR degradation profiles due to bit errors at Frame 28 showed that the degradation is dependent on the significance of the bit, where errors in the most significant bit (MSB) inflicted approximately 3 dB higher PSNR degradation, than the least significant bit (LSB) errors. Furthermore, the PSNR degradation due to MSB errors in Frame 75 is similar to the PSNR degradation profile for the MSB of the `intra_dc_precision` parameter around Frame 30. Due to the variation of the PSNR degradation profile for the different significance bits of a particular parameter, as well as for the same parameter at its different occurrences in the bitstream, it is necessary to determine the *average* PSNR degradation for each parameter in the MPEG-2 bitstream.

Our approach in obtaining the average PSNR degradation was similar to that suggested in References [32] and [473]. The average measure used here takes into

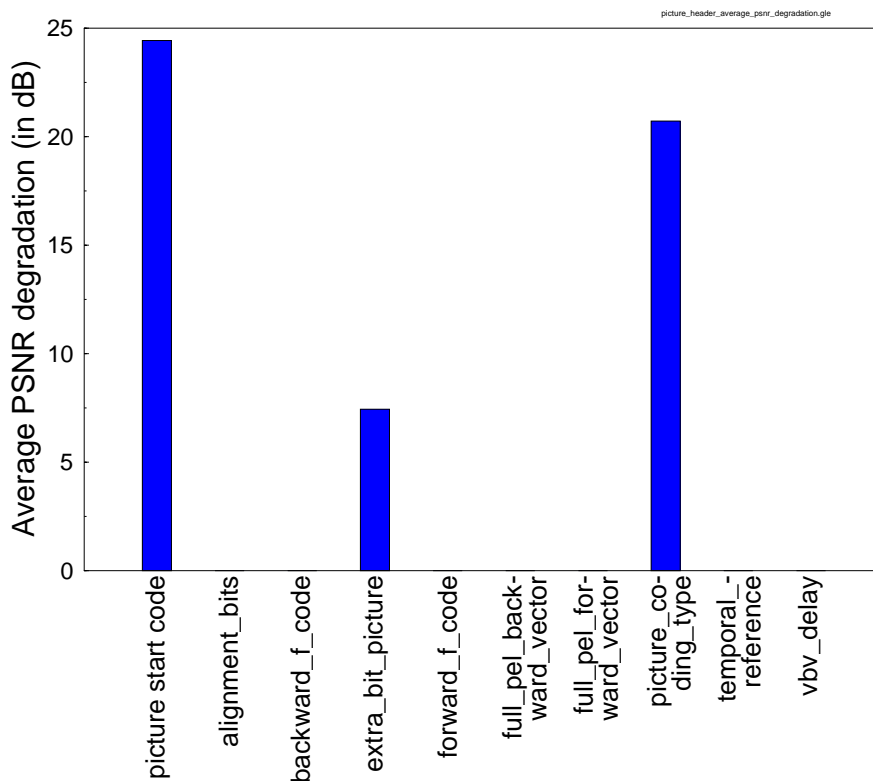


**Figure 21.63:** Average PSNR degradation for the various MPEG-2 parameters in the Picture Header Information

account the significance of the bits corresponding to the parameter concerned, as well as the occurrence of the same parameter at different locations in the encoded video bitstream. In order to acquire the average PSNR degradation for each MPEG-2 bitstream parameter, the different bits encoding the parameter, as well as the bits of the same parameter but occurring at different locations in the bitstream were corrupted and the associated PSNR degradation profile versus frame index was registered. The observed PSNR degradation profile for each case was then used to compute the average PSNR degradation. As an example, we shall use the PSNR degradation profile shown in Figure 21.62. In the figure there are three degradation profiles. The average PSNR degradation for each profile is first computed in order to produce three average PSNR degradation values. The mean of these three averages will then form the final average PSNR degradation for the `intra_dc_precision` parameter. The same process is repeated for all parameters from the Picture Layer up to the Block Layer. The difference with respect to the approach adopted in [32, 473] was that whilst in [32, 473] the average PSNR degradation was acquired for each bit of the output bitstream, due to the large

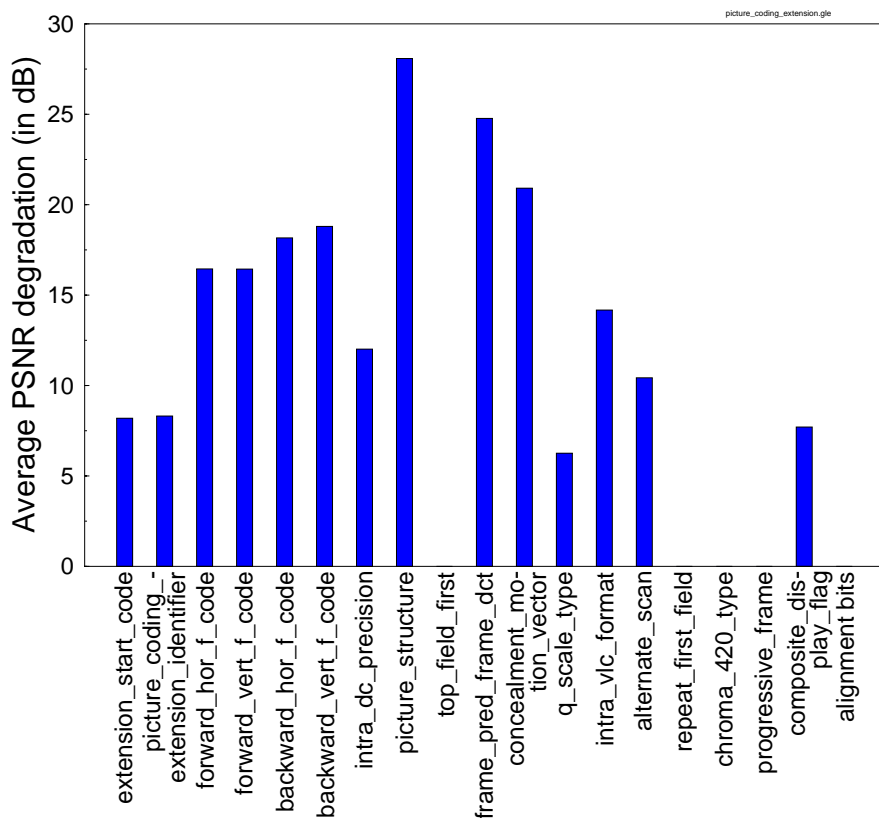


**Figure 21.64:** Average PSNR degradation for the various MPEG-2 parameters in the Picture Coding Extension

number of different parameters within the MPEG-2 bitstream in this contribution a simpler approach was adopted. Figures 21.63 - 21.65 show the typical average PSNR degradation of the various parameters of the Picture Header Information, Picture Coding Extension, Slice Layer, Macroblock Layer and Block Layer, respectively, which was obtained using the QCIF Miss America video sequence at 30 frames/s and an average bitrate of 1.15 Mbits/s.

However, the different MPEG2 codewords occur with different probability and they are allocated different number of bits. Therefore, the average PSNR degradation registered in Figures 21.63 - 21.65 for each parameter was multiplied with the long-term probability of this parameter occurring in the bitstream and with the relative probability of bits being allocated to that parameter. Figure 21.66 and Figure 21.67 show the probability of occurrence of the various MPEG-2 parameters characterised in Figures 21.63 - 21.65 and the probability of bits allocated to the parameters in Picture Header Information, Picture Coding Extension, Slice-, Macroblock- and Block-Layers, respectively.

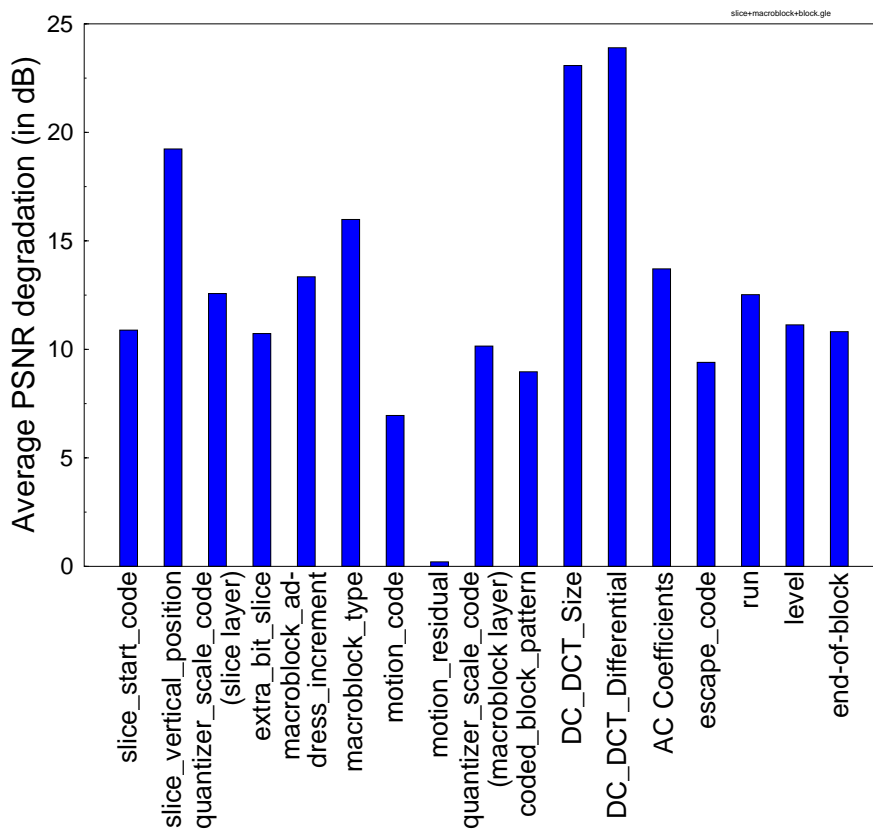
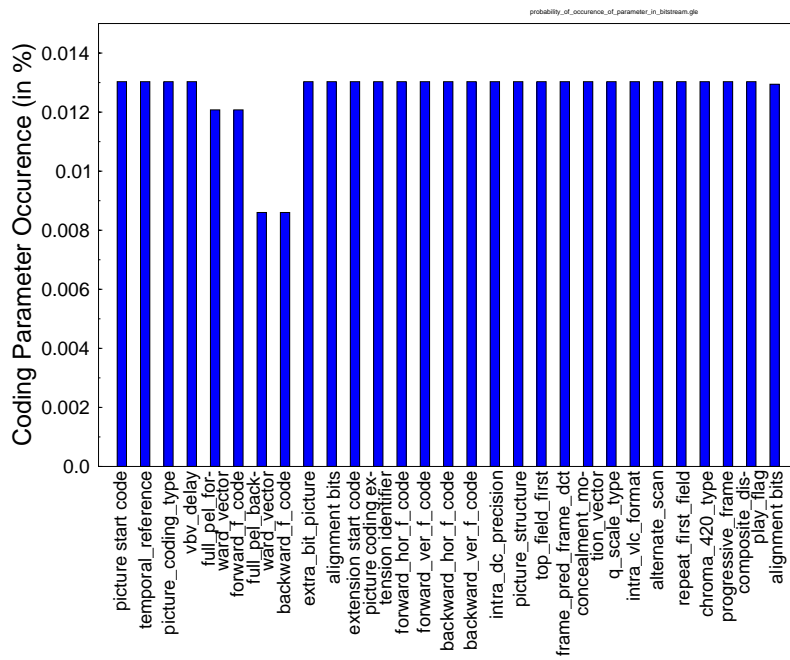


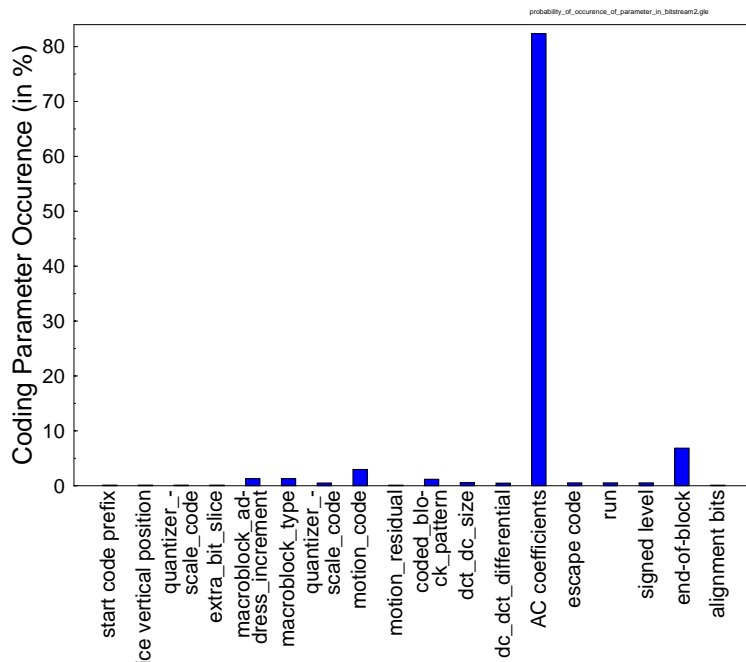
**Figure 21.65:** Average PSNR degradation for the various MPEG-2 parameters in the Slice-, Macroblock- and Block-Layers.

We shall concentrate first on Figure 21.66(a). It is observed that all parameters - except for `full_pel_forward_vector`, `forward_f_code`, `full_pel_backward_vector` and `backward_f_code` - have the same probability of occurrence, since they appear once for every coded video frame. The parameters `full_pel_forward_vector` and `forward_f_code` have a higher probability of occurrence than `full_pel_backward_vector` and `backward_f_code`, since the former two appear in both P-frames and B-frames, while the latter two only occur in B-frames and for every P-frame, there are two B-frames. However, when compared with the parameters from the Slice-Layer, Macroblock-Layer and Block-Layer, which is portrayed by the bar chart of Figure 21.66(b), the parameters of the Picture Header Information and Picture Coding Extension appeared less often.

If we compare the frequency of occurrence of the parameters in the Slice-Layer with those in the Macroblock- and Block-Layers, the former appeared less often since there were 11 macroblocks and 44 blocks per slice. The parameter having the highest probability of occurrence was constituted by the AC coefficients, having a probability of occurrence exceeding eighty percent.

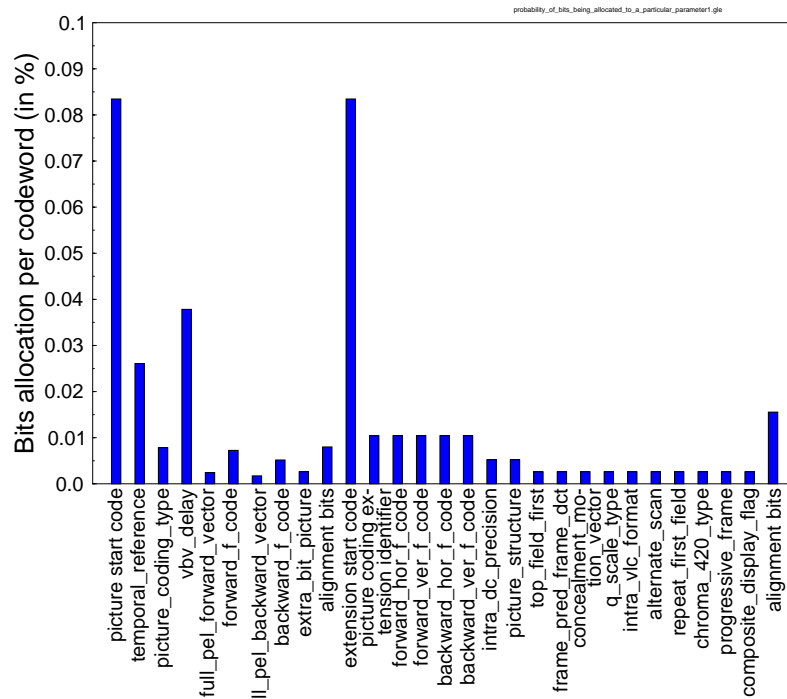


(a) Picture Header Information and Picture Coding Extension

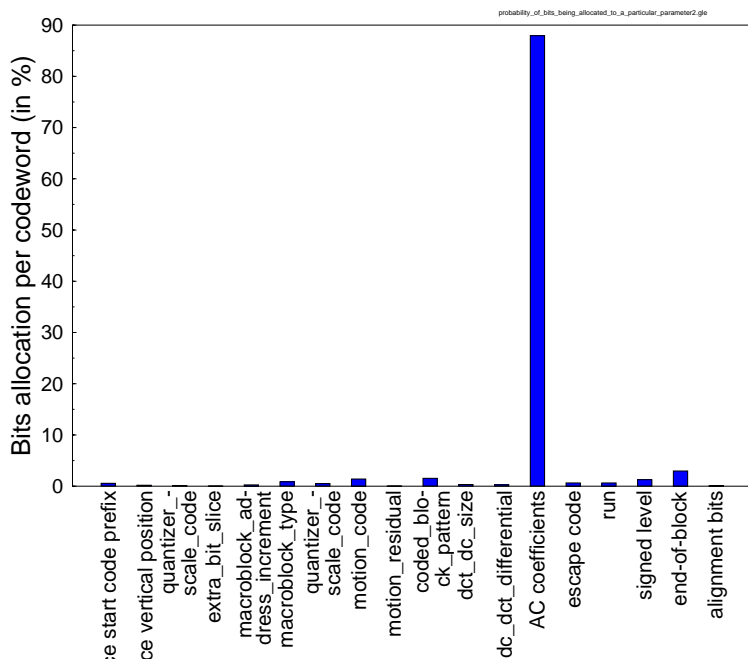


(b) Slice, Macroblock and Block Layers

**Figure 21.66:** Probability of occurrence of the various MPEG-2 parameters characterised in Figures 21.63 - 21.65 (a) Picture Header Information and Picture Coding Extension (b) Slice-, Macroblock- and Block-Layers.



(a) Picture Header Information and Picture Coding Extension



(b) Slice-, Macroblock- and Block-Layers

**Figure 21.67:** Probability of bits being allocated to parameters in (a) Picture Header Information and Picture Coding Extension (b) Slice-, Macroblock- and Block-Layers.

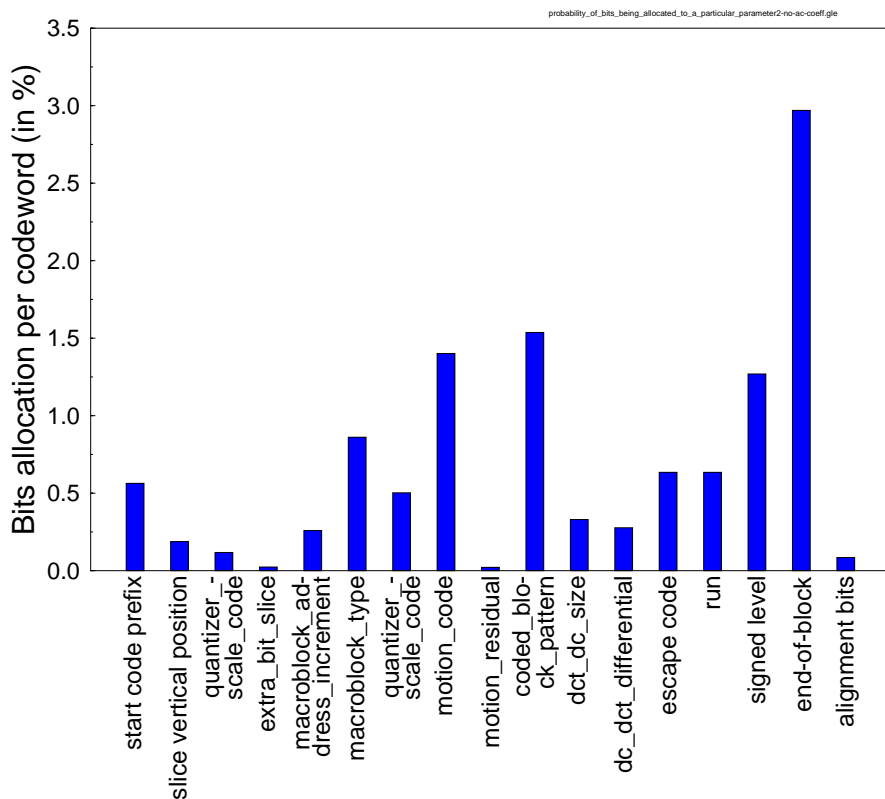


**Figure 21.68:** Probability of bits being allocated to the various MPEG-2 Slice-, Macroblock- and Block-Layer parameters, as seen in Figure 21.67(b), where the probability of bits allocated to the AC coefficients was omitted, in order to show the allocation of bits to the other parameters more clearly.

Figure 21.67 shows the probability of bits being allocated to the various parameters in the Picture Header Information, Picture Coding Extension, Slice-, Macroblock- and Block-Layers. Figure 21.68 was invoked in order to better illustrate the probability of bit allocation seen in Figure 21.67(b), with the probability of allocation of bits to the AC coefficients being omitted from the bar-chart. Considering Figure 21.67(a), the two dominant parameters which require the most encoding bits are the picture start code (PSC) and the picture coding extension start code (PCESC). However, comparing these probabilities with the probability of bits being allocated to the various parameters in the Slice-, Macroblock- and Block-Layers, the percentage of bits allocated can still be considered minimal. In the Block-Layer, the AC coefficients require in excess of 85 percent of the bits available for the whole video sequence. However, at lower bitrates the proportion of AC-coefficient encoding bits was significantly reduced, as illustrated by Figure 21.69. At 30 frames/s and 1.15 Mbits/s the average number of bits per video frame is about 38 000 and a given proportion of

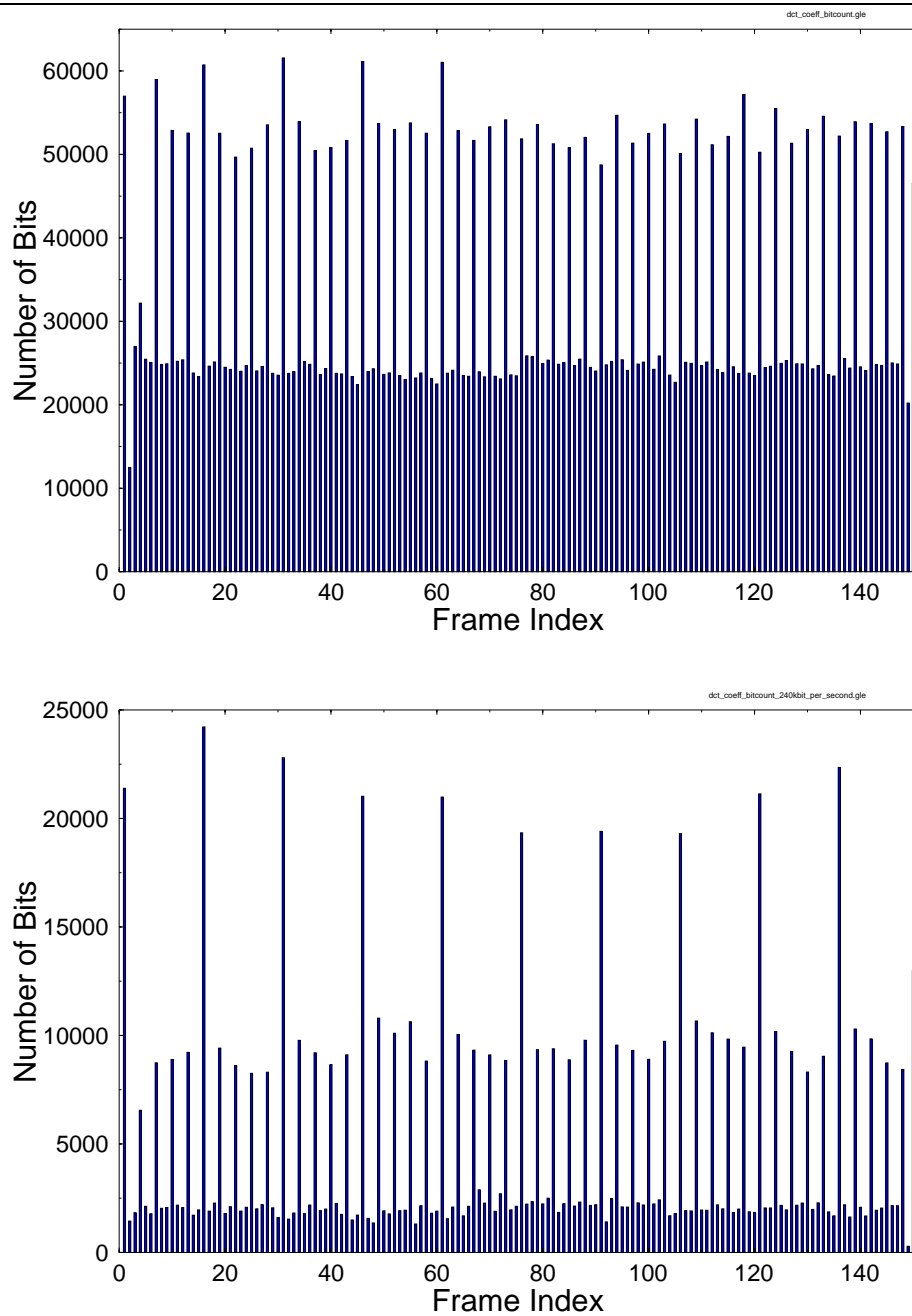


**Figure 21.69:** Profile of bits allocated to the DCT coefficients, when the Miss America video sequence is coded at (a) 1.15 Mbits/s (top) and (b) 240 kbits/s (bottom).



these bits is allocated to the control header information, motion information and to the DCT coefficients. Upon reducing the total bitrate budget - since the number of control header bits is more or less independent of the target bitrate - the proportion of bits allocated to the DCT coefficients is substantially reduced.

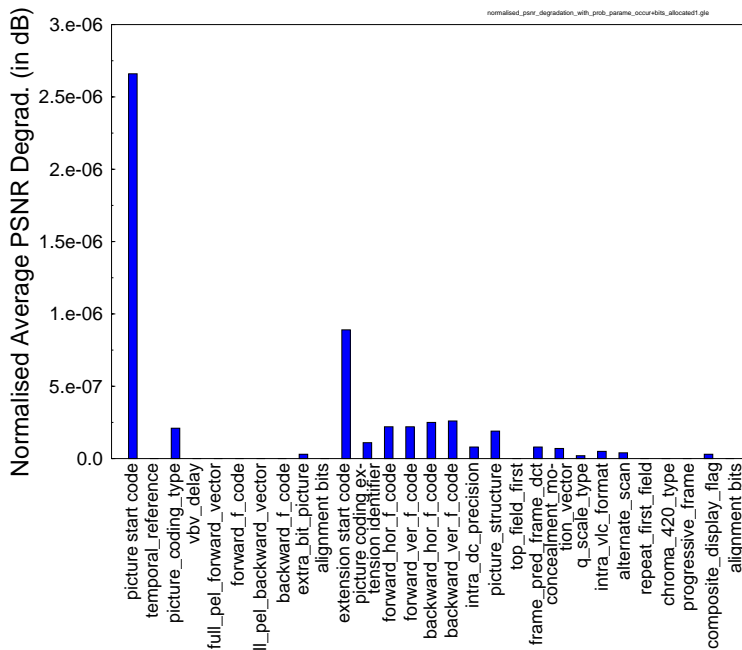
The next process, as discussed earlier, was to normalise the measured average PSNR degradation according to the probability of occurrence of the respective parameters in the bitstream and the probability of bits being allocated to this parameter. The normalised average PSNR degradation inflicted by corrupting the parameters of the Picture Header Information and Picture Coding Extension is portrayed in Figure 21.70(a). Similarly, the normalised average PSNR degradation for the parameters of the Slice-, Macroblock- and Block-Layers is shown in Figure 21.70(b). In order to visually enhance Figure 21.70(b), the normalised average PSNR degradation for the AC coefficients was omitted in the bar-chart shown in Figure 21.71.

The highest PSNR degradation was inflicted by the AC coefficients, since these parameters occur most frequently and are allocated the highest number of bits. When a bit error occurs in the bitstream, the AC coefficients have a high probability of being corrupted. The other parameters, such as the DC\_DCT\_size and DC\_DCT\_differential, though exhibited high average PSNR degradations when corrupted, registered low normalised average PSNR degradations since their occurrence in the bitstream is confined to intra-coded frames.

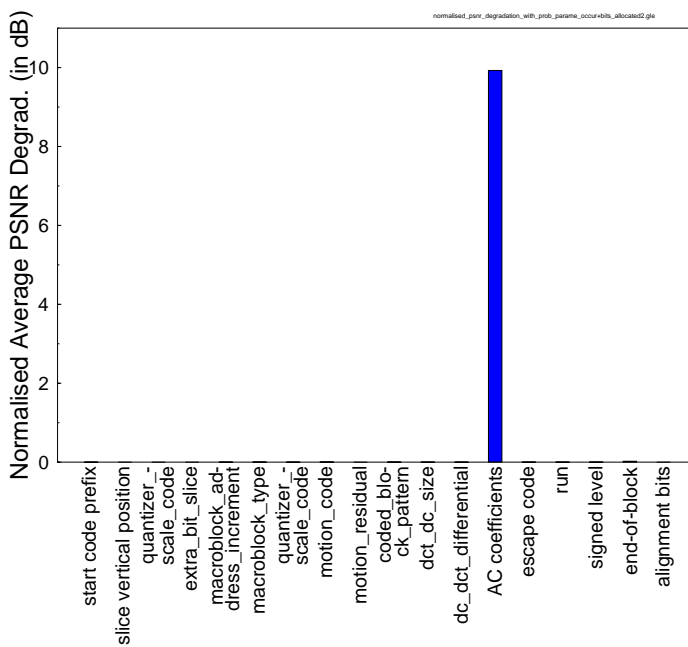
The end-of-block parameter exhibited the second highest normalised average PSNR degradation in this study. Although the average number of bits used for the end-of-block is approximately 2.17 bits, the probability of occurrence and the probability of bits being allocated to it is higher than those of other parameters, with the exception of the AC coefficients. Furthermore, in general, the parameters of the Slice-, Macroblock- and Block-Layers exhibit higher average normalised PSNR degradations due to their more frequent occurrence in the bitstream than that due to the Picture Header Information and Picture Coding Extension. This also implies that the percentage of bits allocated to these parameters is higher.

If the comparison of the normalised average PSNR degradations is conducted in the context of the parameters in the Picture Header Information and Picture Coding Extension, the picture start code exhibits the highest normalised average PSNR degradation. Although most of the parameters here occur with equal probability as seen in Figure 21.66(b), the picture start code requires a higher portion of the bits compared to the other parameters here, with the exception of the extension start code. Despite having the same probability of occurrence and the same allocation of bits, the extension start code exhibits a lower normalised PSNR degradation than the picture start code, since its average un-normalised degradation is lower, as it was shown in Figures 21.63 - 21.65.

From Figures 21.70 and 21.71, we observed that the video PSNR degradation was dominated by the erroneous decoding of the AC DCT coefficients, which appeared in the MPEG-2 video bitstream in the form of variable length codewords. This suggested invoking unequal error protection techniques for protecting the MPEG-2 parameters during transmission. In a low complexity implementation, two protection classes may be envisaged. The higher priority class would contain all the important header information and some of the more important low-frequency variable-length coded



(a) Picture Header Information and Picture Coding Extension



(b) Slice, Macroblock and Block Layers

**Figure 21.70:** Normalised average PSNR degradation for the various parameters in (a) Picture Header Information and Picture Coding Extension (b) Slice-, Macroblock- and Block-Layers, normalised to the probability of occurrence of the respective parameters in the bitstream and the probability of bits being allocated to the parameter.

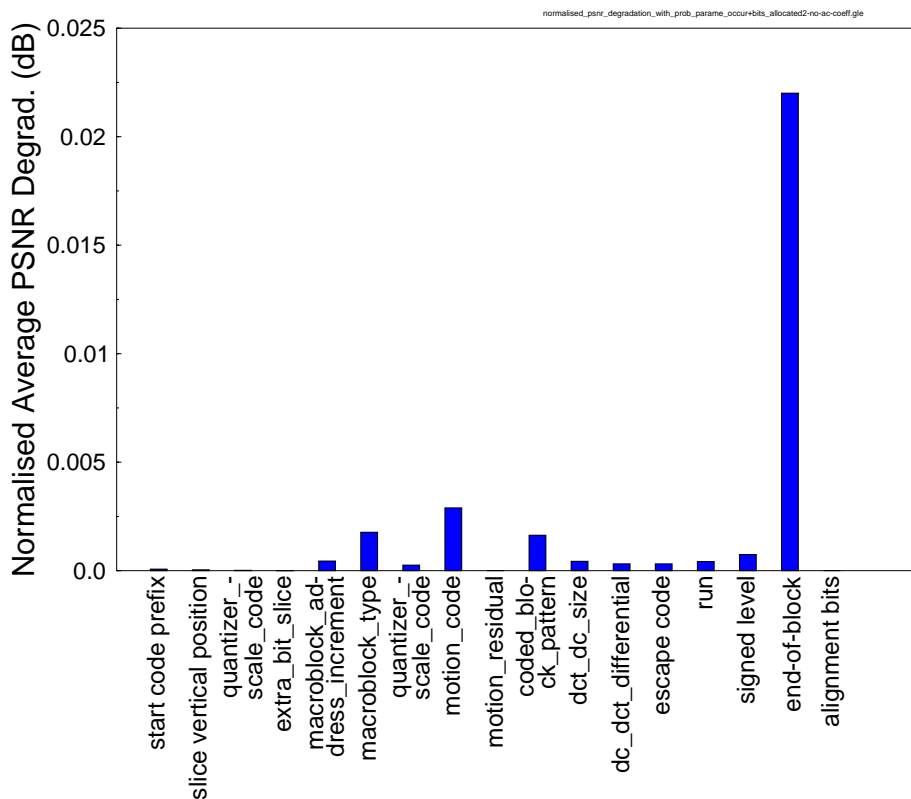


**Figure 21.71:** This bar chart is the same as Figure 21.70(b), although the normalised average PSNR degradation for the AC coefficients was omitted in order to show the average PSNR degradation of the other parameters.

DCT coefficients. The lower priority class would then contain the remaining less important, higher frequency variable length coded DCT coefficients. This partitioning process will be detailed in Section 21.5.5 together with its associated performance in the context of the hierarchical digital video broadcasting (DVB) [620] transmission scheme in Section 21.5.8.

### 21.5.3 DVB Terrestrial Scheme

The block diagram of the DVB terrestrial (DVB-T) transmitter [620] is shown in Figure 21.72, which is constituted by an MPEG-2 video encoder, channel coding modules and an Orthogonal Frequency Division Multiplex (OFDM) modem [10, 629]. Due to the poor error resilience of the MPEG-2 video codec, strong concatenated channel coding is employed, consisting of a shortened Reed-Solomon RS(204,188) outer code [9], which corrects up to eight erroneous bytes in a block of 204 bytes, and a half-rate inner convolutional encoder with a constraint length of 7 [4, 9]. The

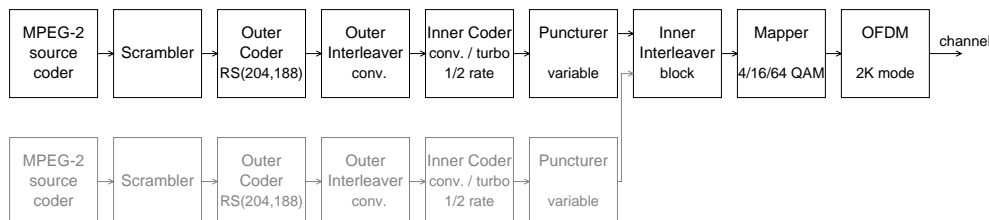


**Figure 21.72:** Schematic of the DVB terrestrial transmitter functions.

overall code rate can be adapted by the variable puncturer, which supports code rates of 1/2 (no puncturing) as well as 2/3, 3/4, 5/6, and 7/8. The parameters of the convolutional encoder are summarised in Table 21.15. If only one of the two branches of the transmitter in Figure 21.72 is utilised, the DVB-T modem is said to be operating in its non-hierarchical mode. In this mode, the modem can have a choice of QPSK, 16-QAM or 64-QAM modulation constellations.

Rate	1/2
Constraint Length	7
$k$	1
$n$	2
Polynomials (octal)	171,133

**Table 21.15:** Parameters of the CC(n,k,K) convolutional inner encoder in the DVB-T modem.

A second video bitstream can also be multiplexed with the first one by the inner interleaver, when the DVB modem is in its so-called hierarchical mode [620]. The choice of modulation constellations in this mode is between 16-QAM and 64-QAM. We shall be employing this transmission mode, when the so-called data partitioning scheme is used to split the incoming MPEG-2 video bitstream into two classes of data, as proposed in Section 21.5.5, with one class having a higher priority than the other one. The higher priority data will be multiplexed to the most significant bits (MSBs) of the modulation constellation points and the lower priority data to the least significant bits [10] (LSBs). For 16-QAM and 64-QAM, the upper 2 bits of each 4- or 6-bit symbol will contain the more important video data. The lower priority data will then be multiplexed to the lower significance 2 bits and 4 bits of 16-QAM and 64-QAM, respectively.

Beside implementing the standard DVB-T system as a benchmarker, we have improved the system by replacing the convolutional coder by a turbo codec [28]. The turbo codec's parameters used in the experiment are displayed by Table 21.16.

In this section, we have given an overview of the DVB-T system which we have used in our experiments. Readers interested in the details of the DVB-T system are referred to the DVB-T standard [620]. The performance of the standard DVB-T system and the turbo coded system is characterised in Section 21.5.7 and 21.5.8

Rate	1/2
Input block length	17952 bits
Interleaver	random
Number of iterations	8
Constraint Length	3
$k$	1
$n$	2
Polynomials	7,5

**Table 21.16:** Parameters of the inner turbo encoder used to replace the DVB-T system's convolutional coder.

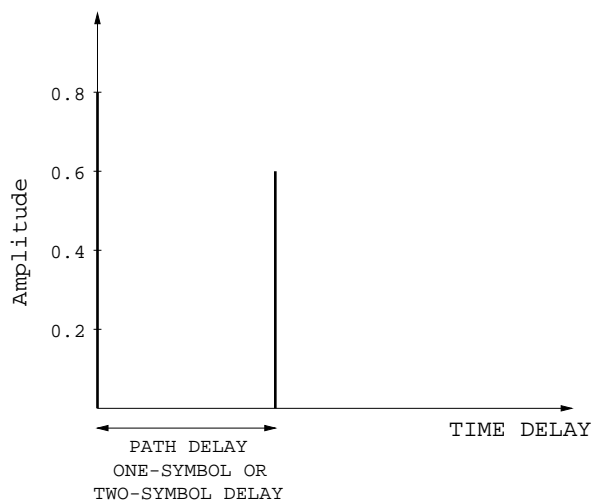


**Figure 21.73:** COST 207 hilly terrain (HT) type impulse response.

for non-hierarchical and hierarchical transmissions, respectively. Let us now briefly consider the multipath channel model used in our experiments.

### 21.5.4 Channel Model

In the system characterised here, we have used a carrier frequency of 500MHz and a sampling rate of  $7/64\mu s$ . The channel model employed in this study was the twelve-path COST 207 [630] hilly terrain (HT) type impulse response, with a maximal relative path delay of  $19.9 \mu s$ . Each of the paths was faded independently obeying a Rayleigh fading distribution, according to a normalised Doppler frequency of  $10^{-5}$ . This corresponds to a worst-case vehicular velocity of about 200 km/h. The unfaded impulse response is depicted in Figure 21.73. In order to facilitate un-equal error protection, let us now consider, how to partition the video data stream.

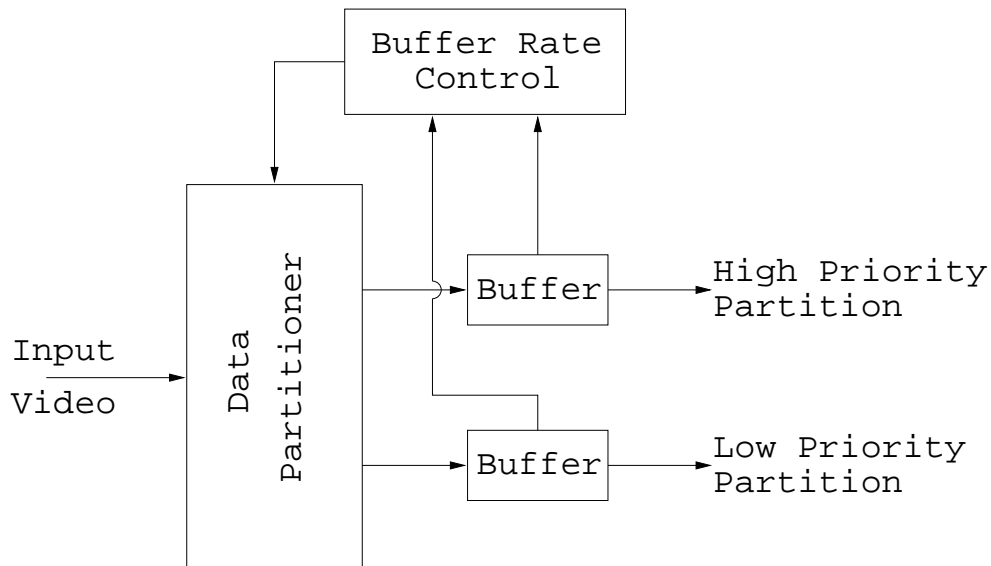


Figure 21.74: Block diagram of the data partitioner and rate controller.

### 21.5.5 Data Partitioning Scheme

As portrayed in Figures 21.70 and 21.71, the corrupted variable-length coded DCT coefficients inflict a high video PSNR degradation. Assuming that all header information is received correctly, the fidelity of the reconstructed images at the receiver side is dependent on the number of correctly decoded DCT coefficients. However, the effect of the loss of higher spatial frequency DCT coefficients are less dramatic compared to lower spatial frequency DCT coefficients. The splitting of the video bitstream into two different integrity bitstreams is termed as data partitioning [628]. Recall from Section 21.5.3 that the hierarchical DVB-T transmission scheme can enable us to multiplex two un-equal protected input bitstreams for transmission. This section describes the details of our proposed data partitioning scheme.

Figure 21.74 shows the block diagram of the data partitioning scheme, which splits a constant bitrate video bitstream into two resultant bitstreams. The position in which the input is split is based on a variable referred to here as the priority breakpoint (PBP). The PBP can be adjusted at the beginning of the encoding of every image slice, based on the buffer occupancy or 'fullness' of the two output buffers. For example, if the high priority buffer is 80 % full and the low priority buffer is only 40 % full, the rate control module would have to adjust the PBP such that more data is directed to the low priority partition. This measure is taken in order to avoid high priority buffer overflow and low priority buffer underflow events. The valid values for the PBP are summarized in Table 21.17 [628].

There are two main stages in updating the PBP. The first stage involves the rate control module in order to decide on the preferred new PBP value for each partition

PBP	Syntax elements in high priority partition
0	Low priority partition always has its PBP set to 0.
1	Sequence, GOP, Picture and Slice layer information upto extra bit slice.
2	Same as above and upto macroblock address increment.
3	Same as above plus including macroblock syntax elements but excluding coded block pattern.
4 ... 63	Reserved for future use.
64	Same as above plus including DC coefficient and the first runlength coded DCT coefficient.
65	Same as above and up to the second runlength coded DCT coefficient.
64 + x	Same as above and up to x runlength coded DCT coefficient.
127	Same as above and up to 64 runlength coded DCT coefficient.

**Table 21.17:** Priority breakpoint values and the associated syntax elements that will be directed to the high priority partition [628].

based on their individual buffer fullness and on the current value of the PBP. The second stage then combines the two desired PBPs based on the buffer occupancy of both buffers in order to produce a new PBP.

The updating of the PBP in the first stage of the rate control module is based on a heuristic approach, similar to that suggested by Aravind *et.al.* [631]. The update procedure is detailed in Algorithm 1, which is discussed below and augmented by a numerical example at the end of this section.

The variable ‘sign’ is used in Algorithm 1, in order to indicate how the PBP has to be adjusted in the high- and low-priority partitions, so as to arrive at the required target buffer fullness. More explicitly, the variable ‘sign’ in Algorithm 1 is necessary, because the PBP values shown in Table 21.17 indicate the amount of information, which should be directed to the high priority partition. Therefore, if the low priority partition requires more data, then the new PBP must be lower than the current PBP, which is contrary to the requirements of the high priority partition, where a higher PBP implies obtaining more data.

Once the desired PBPs for both partitions have been acquired with the aid of Algorithm 1, Algorithm 2 is invoked, in order to compute the final PBP for the current image slice. The inner working of these algorithms will be augmented by a numerical example at the end of this section. There are two main cases to consider. The first one occurs, when both partitions have a buffer occupancy of less than 50%. By using the reciprocal of the buffer occupancy in Algorithm 2 as a weighting factor, the algorithm will favour the new PBP decision of the less occupied buffer, in order to fill the buffer with more data in the current image slice. This assists in preventing the particular buffer from under-flowing. On the other hand, when both buffers

---

**Algorithm 1** Computes the desired PBP update for the high- and low-priority partitions which is then passed to Algorithm 2, in order to determine the PBP to be set for the current image slice.

---

**Step 1:** Initialize parameters

```
if High Priority Partition then
    sign := +1
else
    sign := -1
end if
```

**Step 2:**

```
if buffer occupancy ≥ 80% then
    diff := 64 - PBP
end if
```

```
if buffer occupancy ≥ 70% and buffer occupancy < 80% then
```

```
    if PBP ≥ 100 then
```

```
        diff := -9
```

```
    end if
```

```
    if PBP ≥ 80 and PBP < 100 then
```

```
        diff := -5
```

```
    end if
```

```
    if PBP ≥ 64 and PBP < 80 then
```

```
        diff := -2
```

```
    end if
```

```
end if
```

```
if buffer occupancy ≥ 50% and buffer occupancy < 70% then
```

```
    diff := +1
```

```
end if
```

```
if buffer occupancy < 50% then
```

```
    if PBP ≥ 80 then
```

```
        diff := +1
```

```
    end if
```

```
    if PBP ≥ 70 and PBP < 80 then
```

```
        diff := +2
```

```
    end if
```

```
    if PBP ≥ 2 and PBP < 70 then
```

```
        diff := +3
```

```
    end if
```

```
end if
```

**Step 3:**

```
diff := sign × diff
```

```
Return diff
```

---



---

**Algorithm 2** Compute new PBP for the current image slice based on current buffer occupancy of both partitions

---

**Step 1:**

```

if      OccupancyHighPriority < 50%    and    OccupancyLowPriority < 50%
or      OccupancyHighPriority = 50%    and    OccupancyLowPriority < 50%
or      OccupancyHighPriority < 50%    and    OccupancyLowPriority = 50%
or      OccupancyHighPriority < 25%    and    50% < OccupancyLowPriority < 70%
or      50% < OccupancyHighPriority < 70% and    OccupancyLowPriority < 25%

```

**then**

$$\text{delta} := \frac{\text{Occupancy}_{HighPriority}^{-1} \times \text{diff}_{HighPriority} + \text{Occupancy}_{LowPriority}^{-1} \times \text{diff}_{LowPriority}}{\text{Occupancy}_{HighPriority}^{-1} + \text{Occupancy}_{LowPriority}^{-1}}$$

**else**

$$\text{delta} := \frac{\text{Occupancy}_{HighPriority} \times \text{diff}_{HighPriority} + \text{Occupancy}_{LowPriority} \times \text{diff}_{LowPriority}}{\text{Occupancy}_{HighPriority} + \text{Occupancy}_{LowPriority}}$$

**end if**

**Step 2:**

New\_PBP := Previous\_PBP + [delta] where [ ] means rounding up to the nearest integer

**Return** New\_PBP

---

experience a buffer fullness of more than 50%, the buffer occupancy itself is used as a weighting factor instead. Now, the algorithm will instruct the buffer having a higher fullness to have its desired PBP adjusted such that less data is inserted into it in the current image slice. Hence, the buffer overflow problems are prevented.

The new PBP value is then compared to its legitimate range tabulated in Table 21.17. Furthermore, we restricted the minimum PBP value such that I-, P- and B-pictures have minimum PBP values of 64, 3 and 2, respectively. Since B-pictures are not used for future predictions, it was decided that its data need not be protected as strongly as that of the I- and P-pictures. As for P-pictures, Ghanbari and Seferidis [566] showed that correctly decoded motion vectors can still provide a subjectively pleasing reconstruction of the image, even if the DCT coefficients were discarded. Hence, the minimum splitting location or PBP for P-pictures has been set to be just before the coded block pattern parameter, which would then ensure that the motion vectors would be mapped to the high priority partition. For I-pictures, the fidelity of the reconstructed image is dependent on the number of DCT coefficients that can be decoded successfully. Therefore, the minimum splitting location or PBP was set to include at least the first runlength coded DCT coefficient. The MPEG-2 syntax does not allow the split to be made after the first DC coefficient alone, which could lead to start code emulation, should decoding errors occur.

Below we demonstrate the operation of Algorithm 1 and Algorithm 2 with the aid of a simple numerical example. We shall assume that the PBP prior to the update is 75 and the buffer fullness for the high- and low-priority partition buffers is 40% and 10%, respectively. Considering the high priority partition, Algorithm 1 will set the

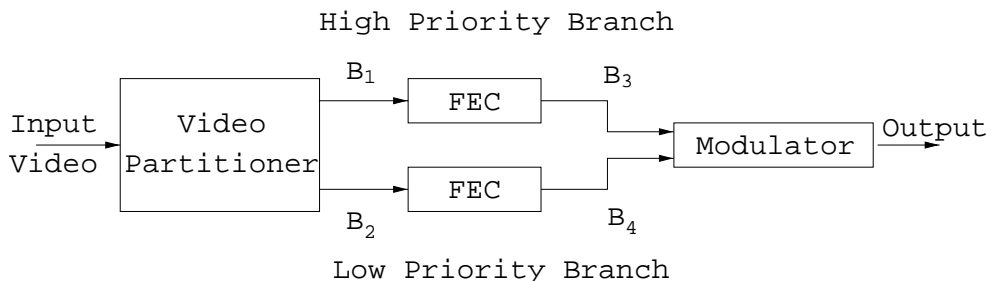


**Figure 21.75:** Video partitioning scheme for the DVB-T system operating in hierarchical mode.

desired update for PBP to +2 and this desired update is referred to as  $\text{diff}_{HighPriority}$  in Algorithm 2. For the low priority partition, Algorithm 1 will set the desired update for PBP to -2. The desired PBP update for the low priority partition is referred to as  $\text{diff}_{LowPriority}$  in Algorithm 2. Since both partition buffers' occupancy is less than 50%, Algorithm 2 will use the reciprocal of the buffer occupancy as the weighting factor, which will then favour the desired update of the low priority partition due to its 10 % occupancy. The final update value - which is denoted by  $\delta$  in Algorithm 2 - is equal to -2 (after being rounded up). Hence, the new PBP is 73. This means that for the current image slice, more data will be directed into the low priority partition in order to prevent buffer underflow.

Apart from adjusting the PBP values from one image slice to another, in order to avoid buffer underflow or overflow, the output bitrate of each partition buffer has to be adjusted, such that the input bitrate of the inner interleaver and modulator in Figure 21.72 is properly matched between the two partitions. Hence, it is imperative to take into account the redundancy added by forward error correction (FEC), especially when the two partition's FECs operate at different code rate. Figure 21.75 shows a stylised block diagram of the DVB-T system operating in the hierarchical mode and receiving its input from the video partitioner. The FEC module represents the concatenated coding system, constituted by a Reed-Solomon codec and a convolutional codec. The modulator can invoke both 16-QAM and 64-QAM. We shall now use an example to illustrate the choice of the various partitioning ratios tabulated in Table 21.18.

We shall assume that 64-QAM is selected and the high- and low-priority partitions employ rate 1/2 and 3/4 convolutional codes, respectively. We do not have to take the Reed-Solomon code rate into account, since both partitions invoke the same Reed-Solomon codec. Based on these facts and upon referring to Figure 21.75, the input bitrates  $B_3$  and  $B_4$  of the modulator will have to obey the ratio 1:2 since the two MSBs of the 64-QAM constellation are assigned to the high priority partition and the remaining four bits to the low priority partition.

At the same time, the ratio of  $B_3$  to  $B_4$  is related to the ratio of  $B_1$  to  $B_2$  with the FEC redundancy taken into account, requiring:

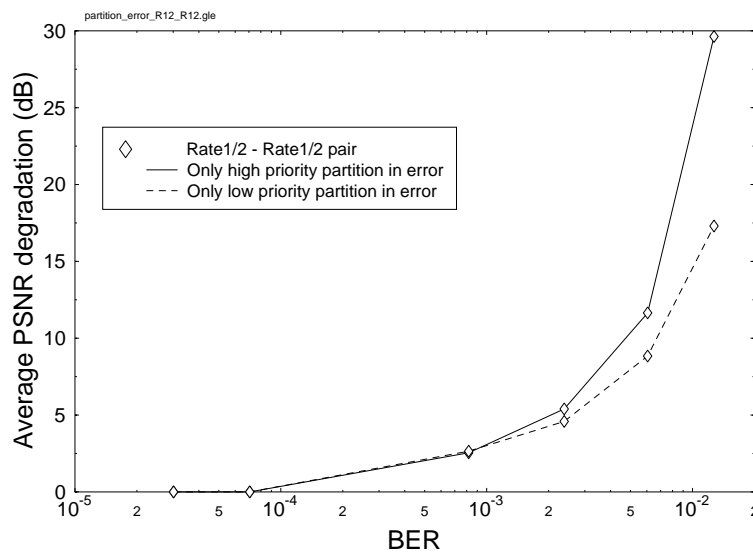
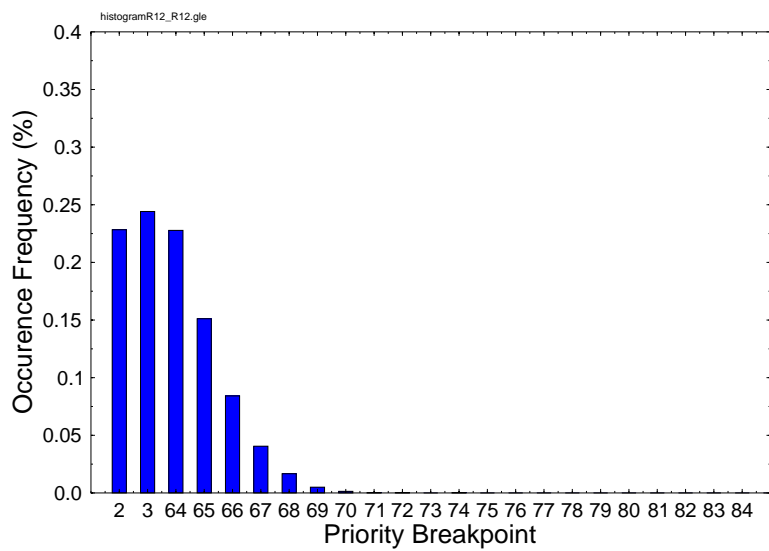


**Figure 21.76:** (a) Histogram of the probability of occurrence for various priority breakpoints and (b) average PSNR degradation versus BER for rate-1/2 convolutional coded high and low priority data in Scheme 1.

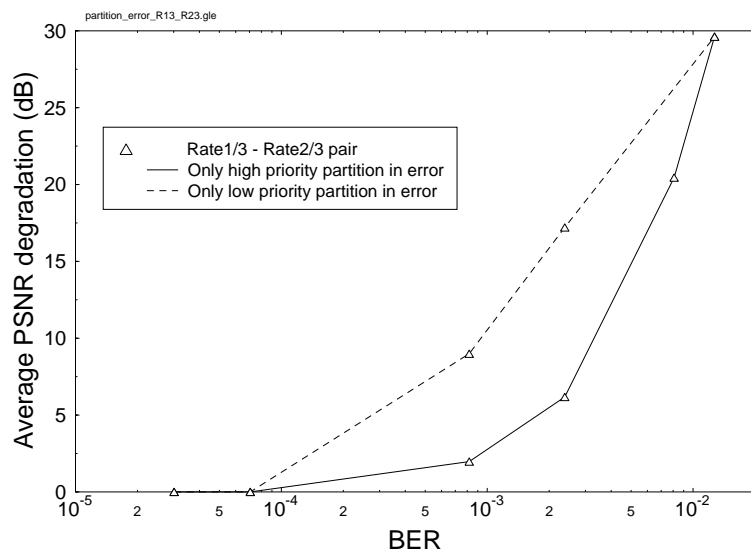
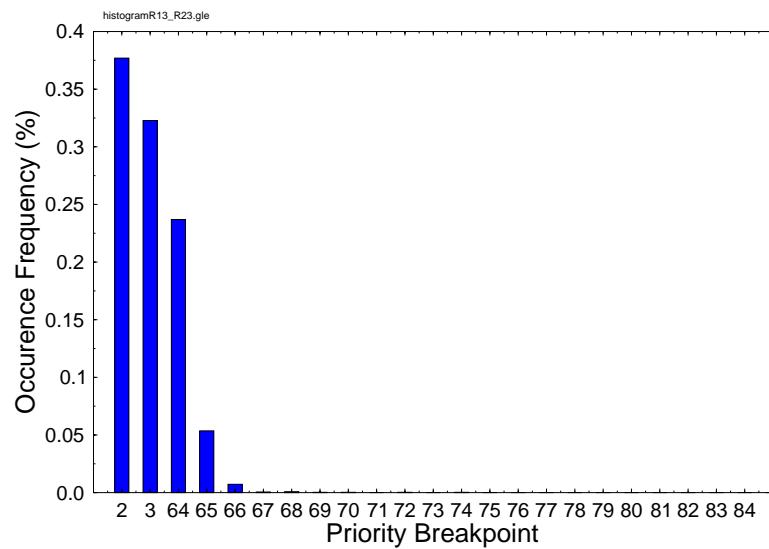
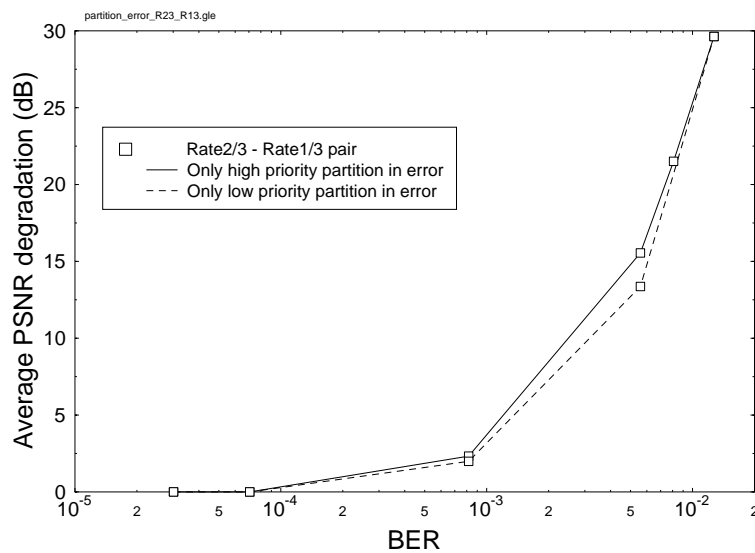
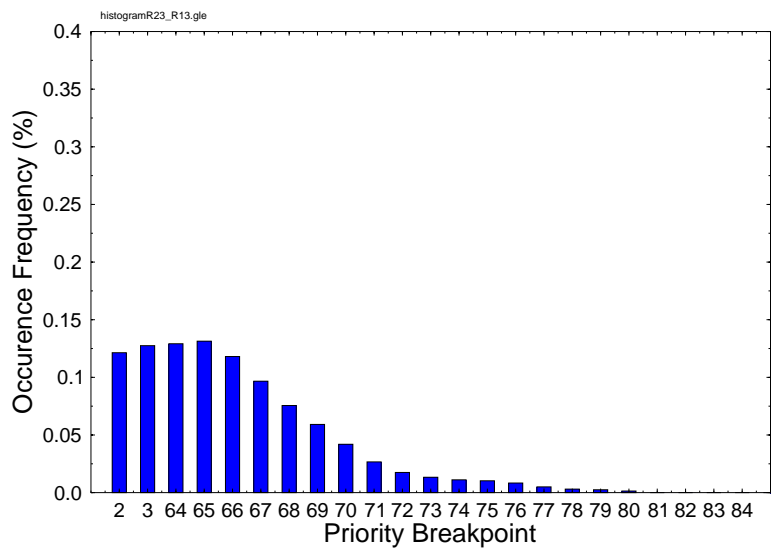


Figure 21.77: (a) Histogram of the probability of occurrence for various priority breakpoints and (b) average PSNR degradation versus BER for the rate-1/3 convolutional coded high priority data and rate-2/3 convolutional coded low priority data in Scheme 2.



**Figure 21.78:** (a) Histogram of the probability of occurrence for various priority breakpoints and (b) average PSNR degradation versus BER for the rate-2/3 convolutional coded high priority data and rate-1/3 convolutional coded low priority data in Scheme 3.

Modulation	Conv. Code Rate (High Priority)	Conv. Code Rate (Low Priority)	Bitrate Ratio (High Priority): Low Priority)
16-QAM	1/2	1/2	1 : 1
	1/2	2/3	3 : 4
	1/2	3/4	2 : 3
	1/2	5/6	3 : 5
	1/2	7/8	4 : 7
	2/3	1/2	4 : 3
64-QAM	1/2	2/3	1 : 2
	1/2	2/3	3 : 8
	1/2	3/4	1 : 3
	1/2	5/6	3 : 10
	1/2	7/8	2 : 7
	2/3	1/2	2 : 3

**Table 21.18:** The partitioning ratios for the high- and low-priority partition's output bitrate based on the modulation mode and code rates selected for the DVB-T hierarchical mode.

$$\begin{aligned}
 \frac{B_3}{B_4} &= \frac{2 \times B_1}{\frac{4}{3} \times B_2} = \frac{1}{2} \\
 &= \frac{3}{2} \cdot \frac{B_1}{B_2} = \frac{1}{2} \times \frac{2}{3} \\
 &= \frac{B_1}{B_2} = \frac{1}{3}
 \end{aligned}
 \tag{21.4}$$

If, for example, the input video bitrate to the data partitioner module is 1 Mbit/s, the output bitrate of the high- and low-priority partition would be  $B_1 = 250$  kbit/s and  $B_2 = 750$  kbit/s respectively, according to the ratio indicated by Equation 21.4.

In this section, we have outlined the data partitioning scheme, which we used in the DVB-T hierarchical transmission scheme. Its performance in the overall system will be characterised in Section 21.5.8. Let us however first evaluate the BER-sensitivity of the partitioned MPEG-2 bitstream to randomly distributed bit errors using various partitioning ratios.

### 21.5.6 Performance of Data Partitioning Scheme

Let us refer to the equally split rate-1/2 convolutional coded high and low priority scenario as Scheme 1. Furthermore, the rate-1/3 convolutional coded high priority data and rate-2/3 convolutional coded low priority data based scenario is referred to here as Scheme 2. Lastly, the rate-2/3 convolutional coded high priority data and rate-1/3 coded low priority data based partitioning scheme is termed as Scheme 3. We then programmed the partitioning scheme of Figure 21.75 for maintaining the required splitting ratio. This was achieved by continuously adjusting the PBP using Algorithm 1 and Algorithm 2. The associated PBP histograms are

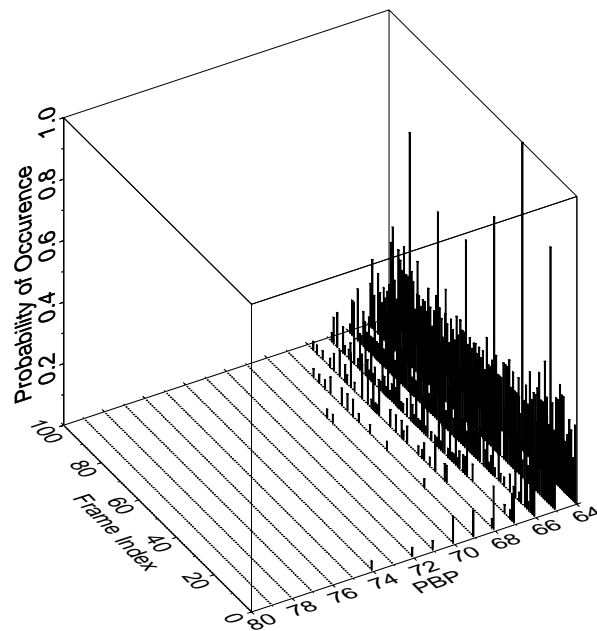
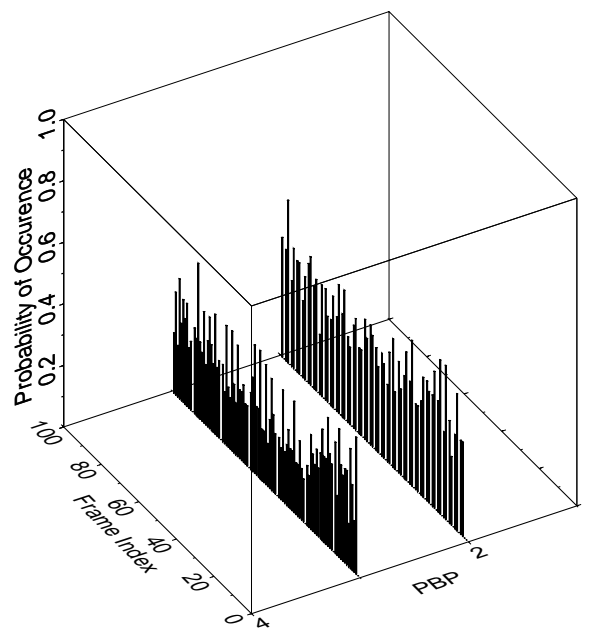
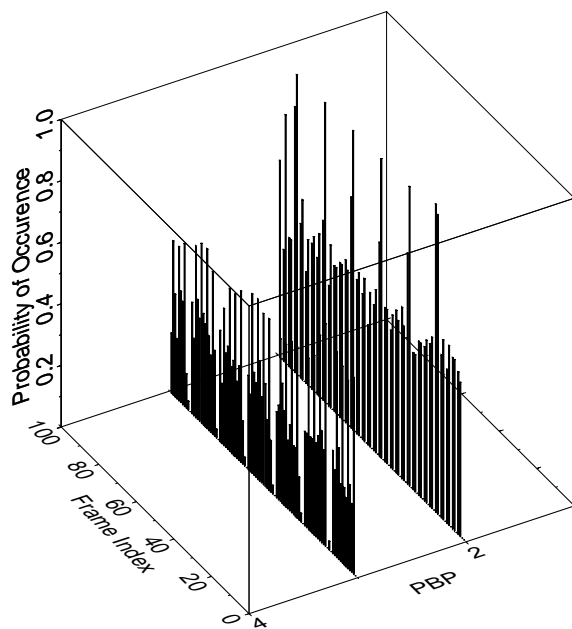
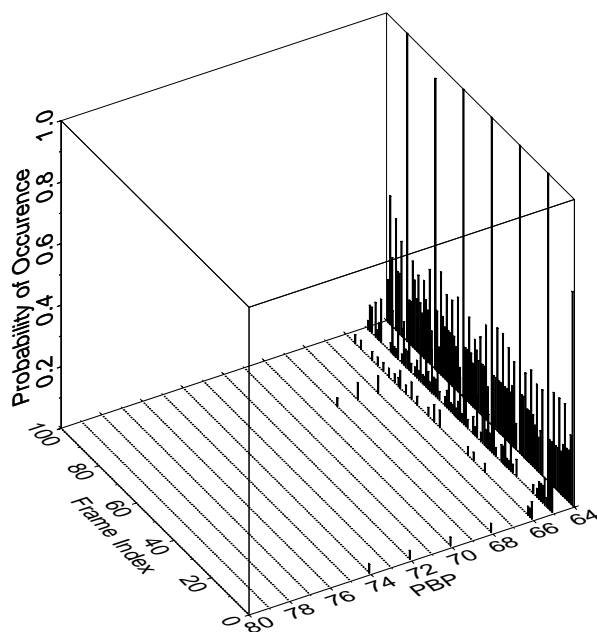


**Figure 21.79:** Evolution of the probability of occurrence of PBP values from one picture to another for Scheme 1.



GMT Jun 1 11:29



GMT Jun 1 11:29

**Figure 21.80:** Evolution of the probability of occurrence of PBP values from one picture to another for Scheme 2.



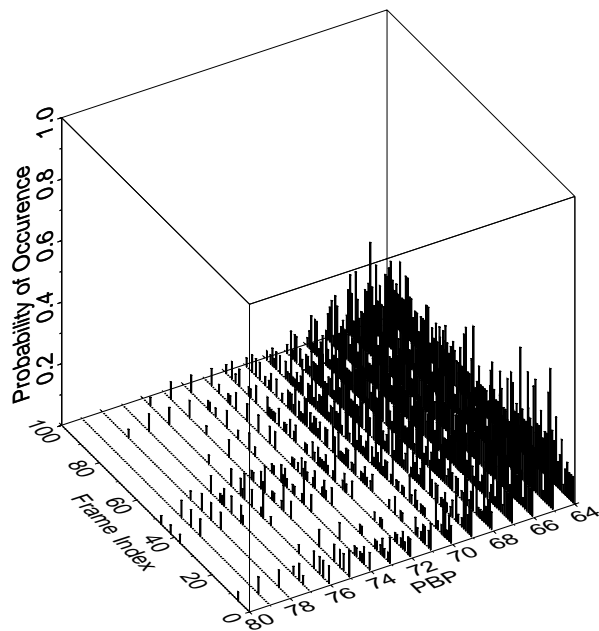
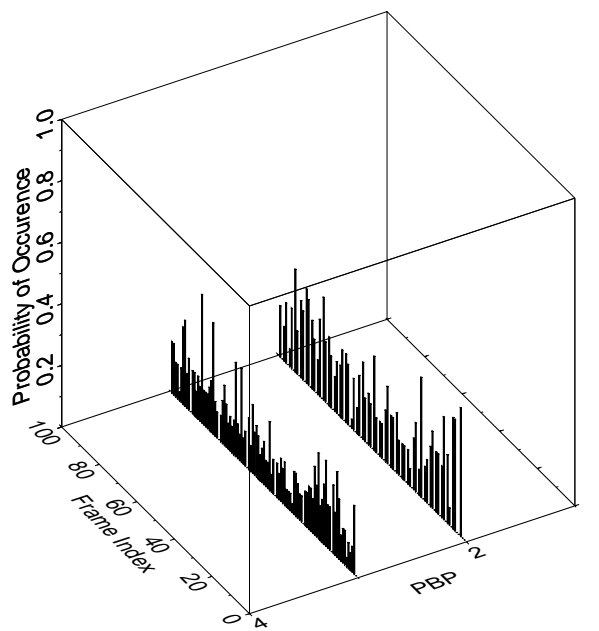


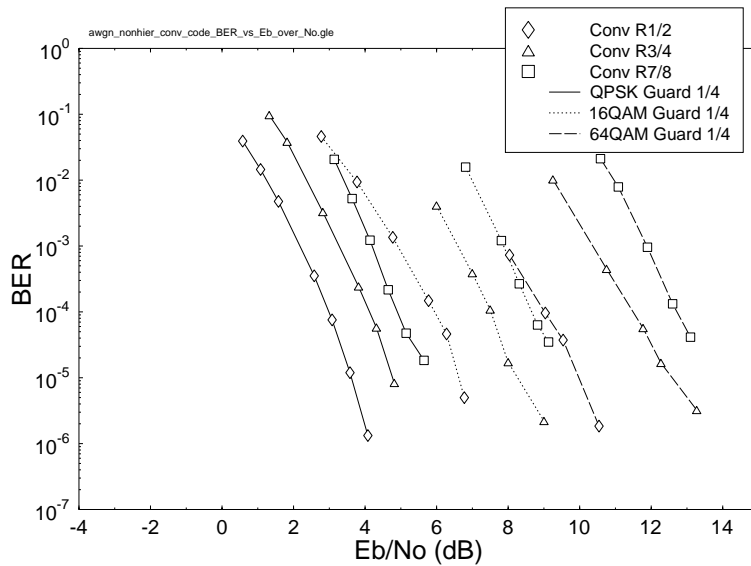
**Figure 21.81:** Evolution of the probability of occurrence of PBP values from one picture to another for Scheme 3.

shown in Figures 21.76(a), 21.77(a) and 21.78(a). Comparing the histograms in Figure 21.76(a), 21.77(a) and Figure 21.78(a), we observed that as expected, Scheme 3 had the most data in the high priority partition, followed by Schemes 1 and 2.

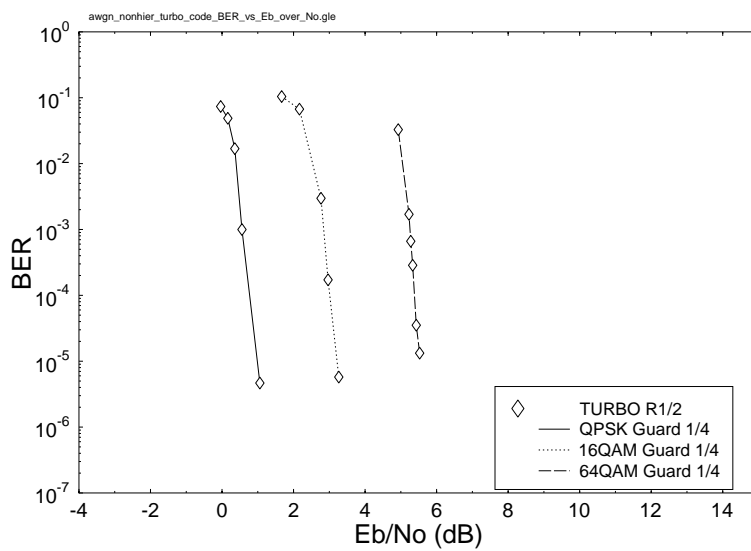
We then embarked on quantifying the error sensitivity of the partitioning Schemes 1 to 3, when subjected to randomly distributed bit errors. Specifically, the previously defined average PSNR degradation was evaluated for given error probabilities inflicting random errors imposed on one of the partitions, while keeping the other partition error-free. These results are portrayed in Figures 21.76(b), 21.77(b) and 21.78(b), for Schemes 1 to 3. More explicitly, when aiming for  $B_3 = B_4$  in Figure 21.75, the coding rate of the partitions predetermines the proportion of unprotected video data in the two partitions, i.e. the bitrates  $B_1$  and  $B_2$ , as quantified by Equation 21.4. If instead of a 1/2-rate code we assume a strong 1/3-rate code for the high-sensitivity video partition, which we refer to as C1, more video data is directed to the lower sensitivity C2 subchannel, as in Scheme 2. Therefore the most error-sensitive 1/3 of the video data is expected to result in a higher PSNR degradation at a given BER, than the most sensitive rate-1/2 case. Furthermore, when assigning 2/3 of the bits to the less sensitive partition - again, as in Scheme 2 - the overall sensitivity is expected to increase in comparison to allocating only 1/2 of the bits to this class, since now a larger proportion of the higher-sensitivity bits belongs to this partition. We note however that the expected trends are strongly ameliorated by the fact that bit errors of any of the sensitivity classes influence the PSNR degradation of the reconstructed video through the reconstructed frame buffer of the remote decoder, while the encoder's local reconstructed frame buffer contains the error-free reconstructed video frames. Schemes 1 and 3 exhibited a higher PSNR degradation, when the high priority partitions were corrupted compared to corruption of the low priority partition only. The opposite was observed for Scheme 2. This showed that the average PSNR degradation was dependent on the amount of data in the partitions. In Scheme 2, there was more data in the low priority partition, inevitably increasing its sensitivity. Hence, when the low priority stream was corrupted, the amount of data left in the high priority partition was insufficient for concealing the effect of errors. Hence in Scheme 2 the dominant contributor to the average PSNR degradation was the low priority partition containing a large fraction of sensitive bits.

Furthermore, for Schemes 1 and 3 at BERs less than  $10^{-3}$ , the PSNR degradation experienced by corrupting either the high or low priority partition was similar. These findings will assist us in explaining our observations in the context of the hierarchical transmission scheme of Section 21.5.8, suggesting that the data partitioning scheme did not provide overall gain in terms of error resilience over the non-partitioned case.

Figures 21.79, 21.80 and 21.81 show the evolution of the probability of occurrence of the PBP values, as the video encoder progressed in encoding one picture after another for the "Football" HDTV video sequence. These figures again illustrate that Scheme 3 had the most data in the high priority partition, followed by Scheme 1 and Scheme 2.

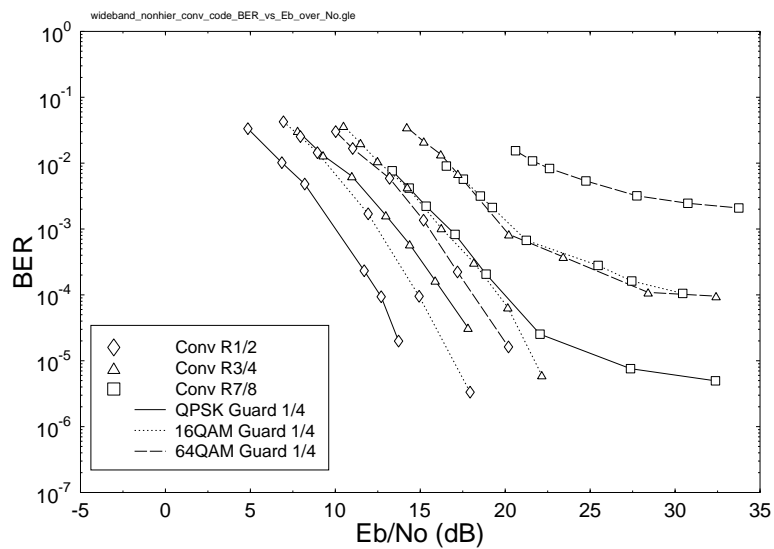


(a) Convolutional Code



(b) Turbo Code

**Figure 21.82:** BER after (a) convolutional decoding and (b) turbo decoding for the DVB-T scheme over stationary, non-dispersive AWGN channels for non-hierarchical transmission.



(a) Convolutional Code

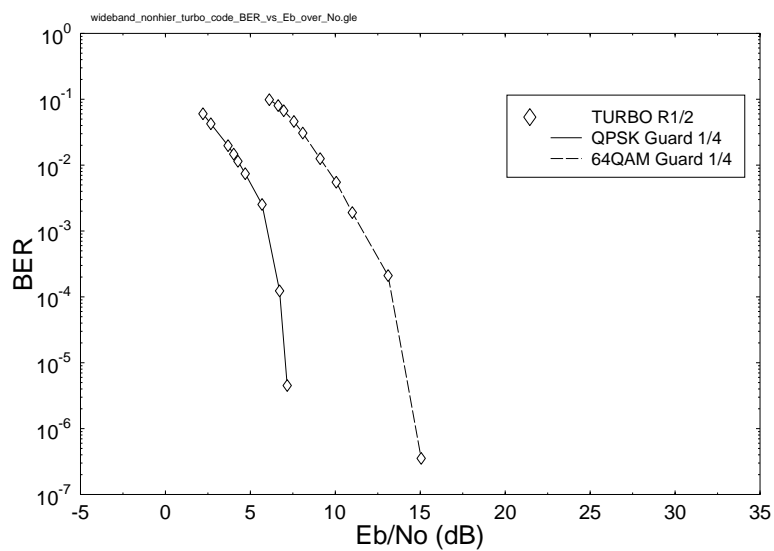
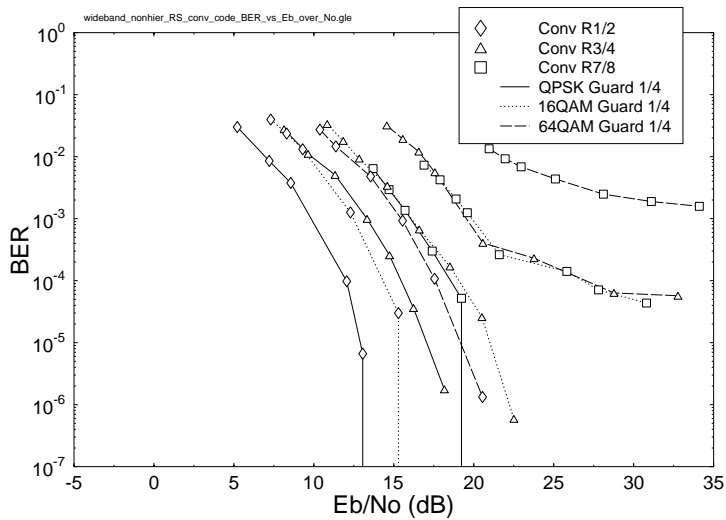
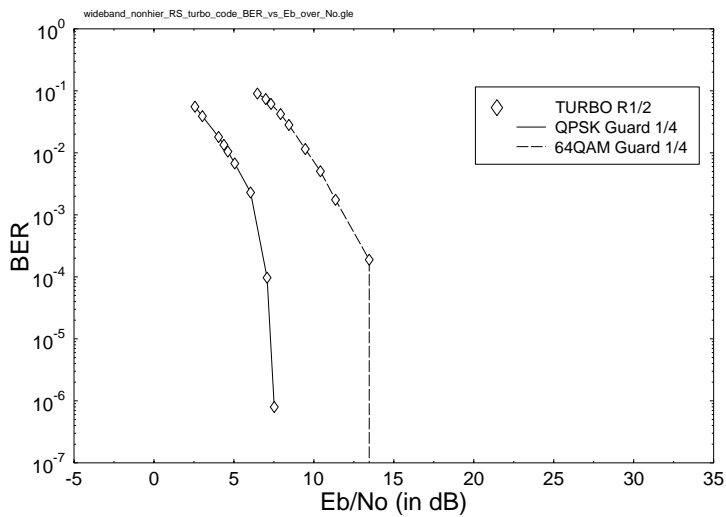


**Figure 21.83:** BER after (a) convolutional decoding and (b) turbo decoding for the DVB-T scheme over the wideband channel of Figure 21.73 for non-hierarchical transmission.



(a) RS and Convolutional Code



(b) RS and Turbo Code

**Figure 21.84:** BER after (a) RS and convolutional decoding and (b) RS and turbo decoding for the DVB-T scheme over the wideband channel of Figure 21.73 for non-hierarchical transmission.

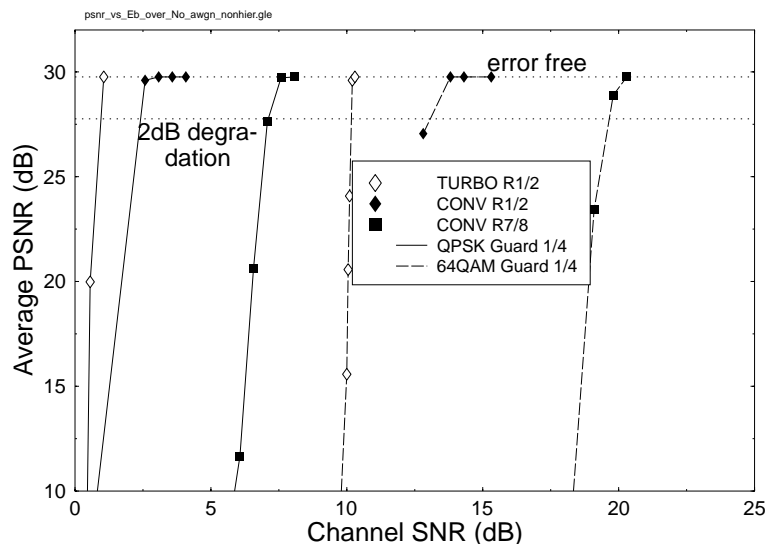


**Figure 21.85:** Average PSNR versus channel SNR of the DVB scheme [620] over non-dispersive AWGN channels for non-hierarchical transmission.

### 21.5.7 Performance of the DVB Terrestrial Scheme Employing Non-hierarchical Transmission

In this section we shall elaborate on our findings, when replacing the convolutional code used in the standard DVB scheme [620] with a turbo code. We will invoke a range of standard-compliant schemes as benchmarks. The "Football" HDTV video sequence was used in our experiments. In Figures 21.82(a) and 21.82(b) the bit error rate (BER) performance of the various modem modes in conjunction with the diverse channel coding schemes are portrayed over stationary, narrowband Additive White Gaussian Noise (AWGN) channels, where the turbo codec exhibits a significantly steeper BER reduction in comparison to the convolutionally coded arrangements.

Specifically, comparing the performance of the various turbo and convolutional codes for QPSK and 64-QAM at a BER of  $10^{-4}$ , the turbo code exhibited an additional coding gain of about 2.24 dB and 3.7 dB respectively, when using half-rate codes in Figures 21.82(a) and 21.82(b). Hence the Peak Signal to Noise Ratio (PSNR) versus channel Signal to Noise Ratio (SNR) graphs in Figure 21.85 demonstrate that approximately 2 dB and 3.5 dB lower channel SNRs are required in conjunction with the rate 1/2 turbo codec for QPSK and 64-QAM, respectively, than for convolutional coding, in order to maintain error free video performance.

Comparing the BER performance of the 1/2-rate convolutional decoder in Figure 21.83(a) and the so-called Log-Map turbo decoder using eight iterations in Fig-

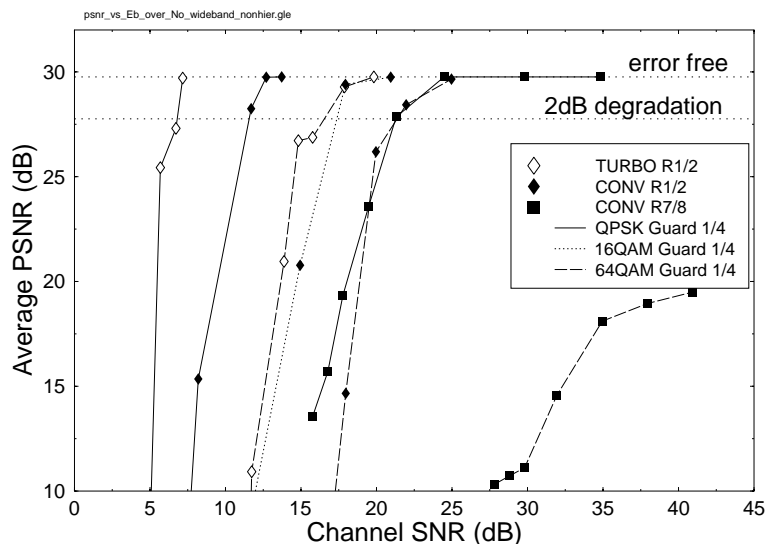


**Figure 21.86:** Average PSNR versus channel SNR of the DVB scheme [620] over the wideband fading channel of Figure 21.73 for non-hierarchical mobile transmission.

ure 21.83(b) for QPSK modulation over the worst-case fading mobile channel of Figure 21.73 we observe that the turbo code provided an additional coding gain of 6 dB in comparison to the convolutional code at a BER of about  $10^{-4}$ . By contrast, for 64QAM using similar codes, a 5 dB coding gain was observed at this BER.

Similar observations were also made with respect to the average Peak Signal to Noise Ratio (PSNR) versus channel Signal to Noise Ratio (SNR) plots of Figure 21.86. For example, for the QPSK modulation mode and a 1/2 coding rate, the turbo code required an approximately 5.5 dB lower channel SNR, than the convolutional code for maintaining error free video transmission.

In conclusion, Tables 21.19 and 21.20 summarize the system performance in terms of the required channel SNR (CSNR) in order to maintain less than 2 dB PSNR video degradation. It was observed that at this PSNR degradation decoding errors were still perceptually unnoticeable to the viewer due to the 30 frames/s refresh-rate, although the still-frame shown in Figure 21.87 exhibits some degradation. In the next section, we shall present the results of our experiments employing the DVB-T system [620] in a hierarchical transmission scenario.



**Figure 21.87:** Frame 79 of "Football" sequence, which illustrates the visual effects of minor decoding errors at a BER of  $2 \cdot 10^{-4}$  after convolutional decoding. The PSNR degradation observed is approximately 2 dB. The sequence was coded using a rate-7/8 convolutional code and transmitted employing QPSK modulation.

Mod.	Code	CSNR (dB)	$E_b/N_0$	BER
QPSK	Turbo (1/2)	1.02	-1.99	$6 \cdot 10^{-6}$
64QAM	Turbo (1/2)	9.94	2.16	$2 \cdot 10^{-3}$
QPSK	Turbo (7/8)	8.58	5.57	$1.5 \cdot 10^{-4}$
64QAM	Turbo (7/8)	21.14	13.36	$4.3 \cdot 10^{-4}$
QPSK	Conv (1/2)	2.16	-0.85	$1.1 \cdot 10^{-3}$
64QAM	Conv (1/2)	12.84	5.06	$6 \cdot 10^{-4}$
QPSK	Conv (7/8)	6.99	3.98	$2 \cdot 10^{-4}$
64QAM	Conv (7/8)	19.43	11.65	$3 \cdot 10^{-4}$

**Table 21.19:** Summary of performance results over non-dispersive AWGN channels tolerating a PSNR degradation of 2dB.



Mod.	Code	CSNR (dB)	$E_b/N_0$	BER
QPSK	Turbo (1/2)	6.63	3.62	$2.5 \cdot 10^{-4}$
64QAM	Turbo (1/2)	15.82	8.03	$2 \cdot 10^{-3}$
QPSK	Turbo (7/8)	28.47	25.46	$10^{-6}$
QPSK	Conv (1/2)	10.82	7.81	$6 \cdot 10^{-4}$
64QAM	Conv (1/2)	20.92	13.14	$7 \cdot 10^{-4}$
QPSK	Conv (7/8)	20.92	17.91	$3 \cdot 10^{-4}$

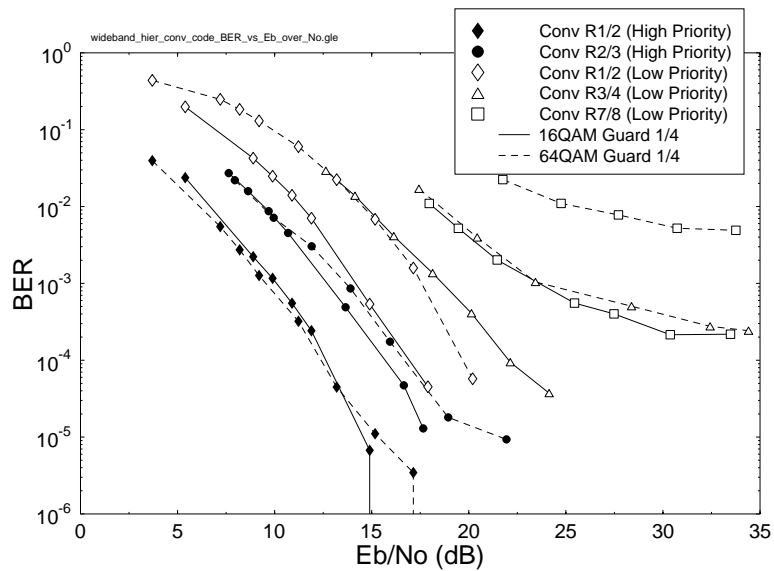
**Table 21.20:** Summary of performance results over fading wideband channels tolerating a PSNR degradation of 2dB.

### 21.5.8 Performance of the DVB Terrestrial Scheme Employing Hierarchical Transmission

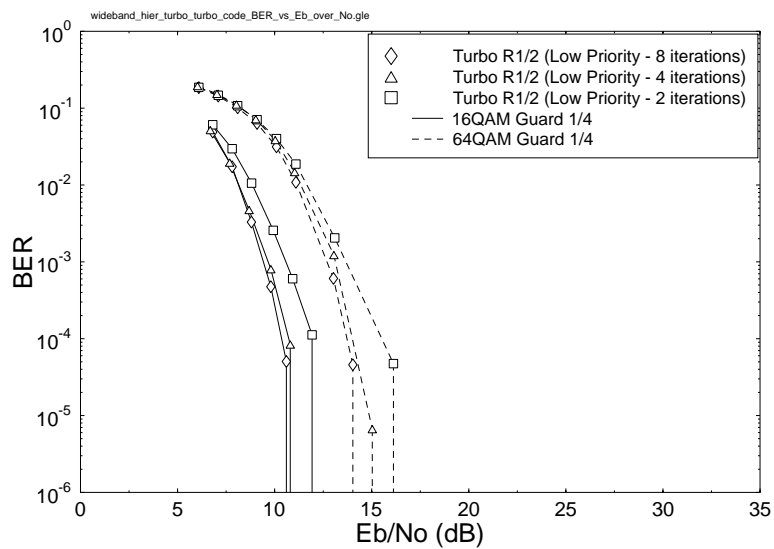
Below we will invoke the DVB-T hierarchical scheme in a mobile broadcasting scenario. We shall also show the improvements which turbo codes offer, when replacing the convolutional code in the standard scheme. Hence, the convolutional codec in both the high and low priority partitions was replaced by the turbo codec. We have also investigated replacing only the high priority convolutional codec with the turbo codec, pairing the 1/2-rate turbo codec in the high priority partition with the convolutional codec in the low priority partition. Such a hybrid arrangement would constitute a reduced-complexity compromise scheme. Again, the "Football" sequence was used in these experiments. Partitioning was carried out using the schematic of Figure 21.75 as well as Algorithms 1 and 2.

Referring to Figure 21.88 and comparing the performance of the 1/2-rate convolutional code and turbo code at a BER of  $10^{-4}$  for the low priority partition, the turbo code, employing 8 iterations, exhibited a coding gain of about 6.6 dB and 5.97 dB for 16-QAM and 64-QAM, respectively. When the number of iterations was reduced to 4, the coding gains offered by the turbo code over that of the convolutional code were 6.23 dB and 5.7 dB for 16-QAM and 64-QAM respectively. We observed that by reducing the number of iterations to 4 halved the associated complexity but the turbo code exhibited a coding loss of only about 0.37 dB and 0.27 dB in comparison to the 8-iteration scenario for 16-QAM and 64-QAM, respectively. Hence, the computational complexity of the turbo codec can be halved by sacrificing only a small amount of coding gain. The substantial coding gain provided by turbo coding is also reflected in the PSNR versus channel SNR graphs of Figure 21.90. In order to achieve error free transmission, Figure 21.90 demonstrated that approximately 5.72 dB and 4.56 dB higher channel SNRs are required by the standard scheme compared to the scheme employing turbo coding, using 4 iterations in both partitions. We have only shown the performance of turbo coding for the low priority partition in Figures 21.88(b) and 21.89(b), since the high priority partition experienced error-free reception after Reed-Solomon decoding for the range of SNRs used.

We also observed that the rates 3/4 and 7/8 convolutional codes in the low priority partition were unable to provide sufficient protection to the transmitted data, as it

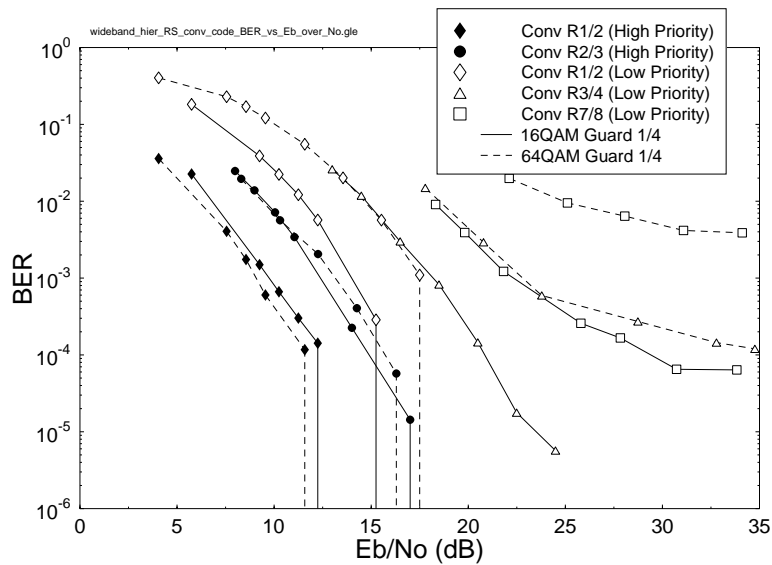


(a) Convolutional Code

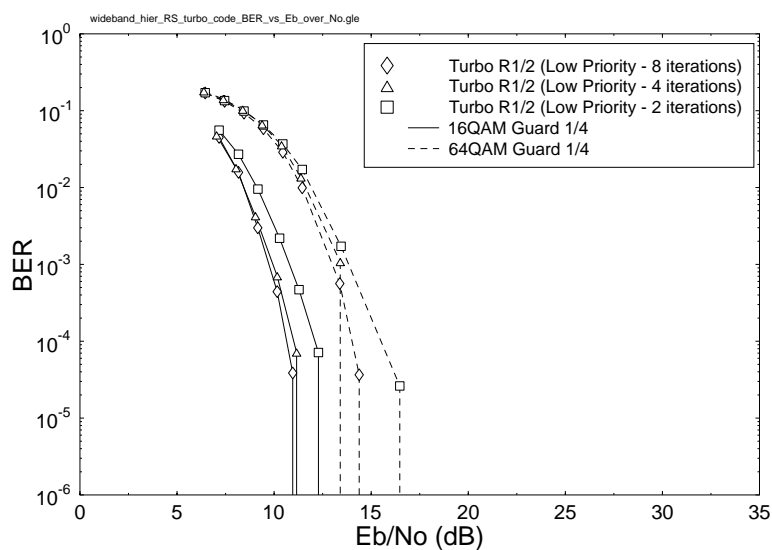


(b) Turbo Code

**Figure 21.88:** BER after (a) convolutional decoding and (b) turbo decoding for the DVB-T hierarchical scheme over the wideband fading channel of Figure 21.73 using the schematic of Figure 21.75 as well as Algorithms 1 and 2.

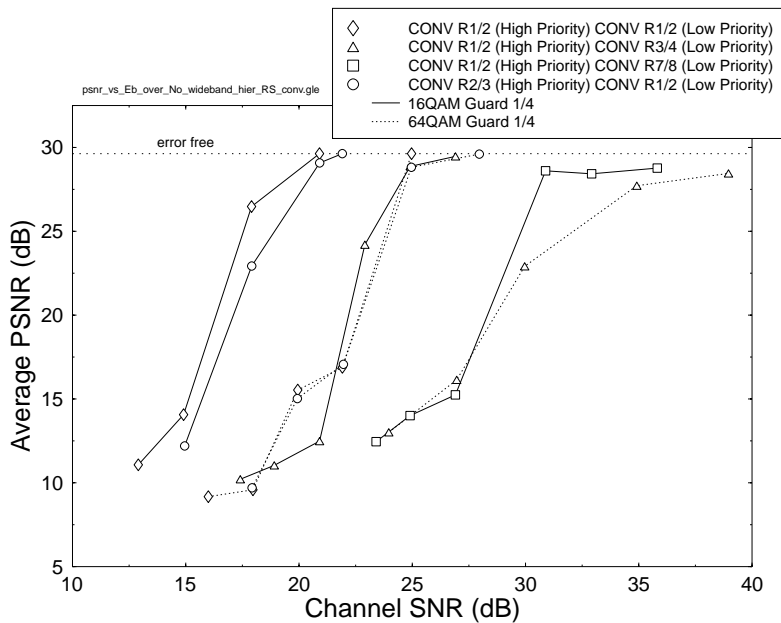


(a) RS and Convolutional Code

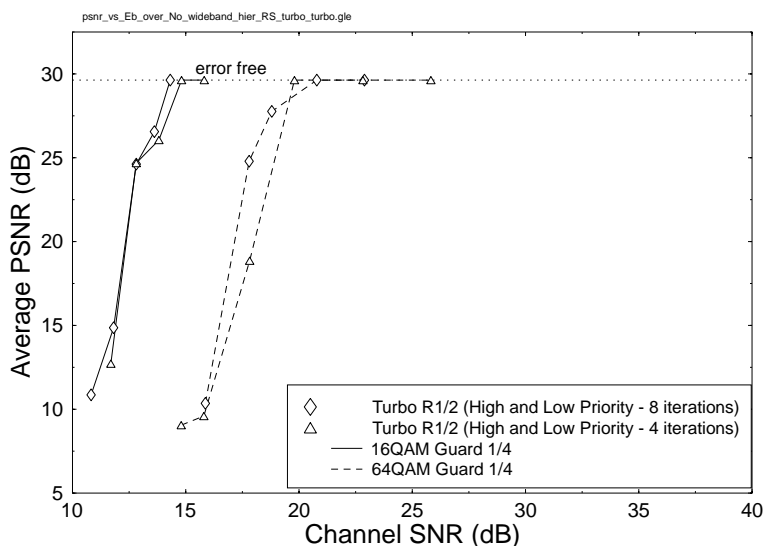


(b) RS and Turbo Code

**Figure 21.89:** BER after (a) RS and convolutional decoding and (b) RS and turbo decoding for the DVB-T hierarchical scheme over the wideband fading channel of Figure 21.73 using the schematic of Figure 21.75 as well as Algorithms 1 and 2.



(a) Standard Scheme



(b) Turbo Code in both partitions

**Figure 21.90:** Average PSNR versus channel SNR for (a) standard DVB scheme [620] and (b) system with turbo coding employed in both partitions, for transmission over the wideband fading channel of Figure 21.73 for hierarchical transmission using the schematic of Figure 21.75 as well as Algorithms 1 and 2.

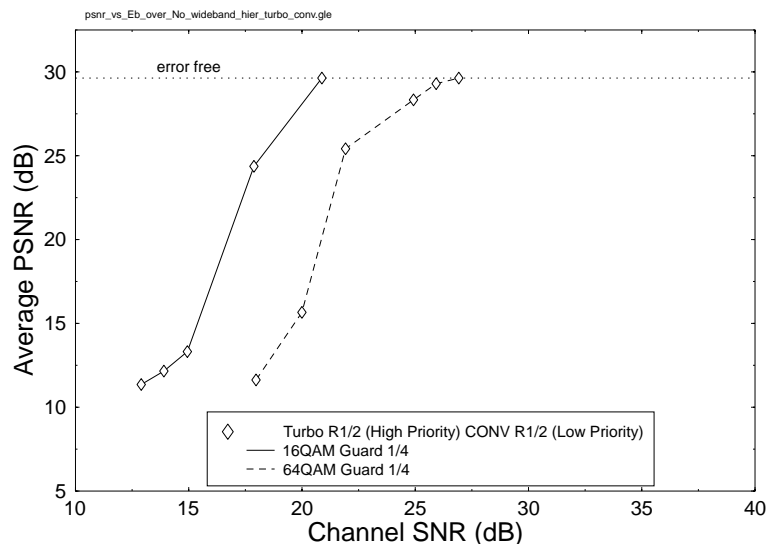


**Figure 21.91:** Average PSNR versus channel SNR of the DVB scheme, employing turbo coding in the high priority partition and convolutional coding in the low priority partition, over the wideband fading channel of Figure 21.73 for hierarchical transmission using the schematic of Figure 21.75 as well as Algorithms 1 and 2.

becomes evident in Figures 21.88(a) and 21.89(a). Due to the presence of residual errors even after the Reed-Solomon decoder, the decoded video always exhibited some decoding errors, which is shown by the flattening of the PSNR versus channel SNR curves in Figure 21.90(a), before reaching the error free PSNR.

A specific problem faced, when using the data partitioning scheme in conjunction with the high priority partition being protected by the rate 1/2 code and the low priority partition protected by the rate 3/4 and 7/8 codes was that when the low priority partition data was corrupted, the error-free high priority data available was insufficient for concealing the errors. We have also experimented with the combination of rate 2/3 convolutional coding and rate 1/2 convolutional coding, in order to protect the high and low priority data, respectively. From Figure 21.90(a) we observed that the performance of this combination approached that of the rate 1/2 convolutional code in both partitions. This was expected, since now more data can be inserted into the high priority partition. Hence, in the event of decoding errors in the low priority data we had more error-free high priority data that can be used to reconstruct the received image.

Our last combination investigated involved using rate 1/2 turbo coding and convolutional coding for the high- and low-priority partitions, respectively. Comparing

Figures 21.91 and 21.90(a), the channel SNR required for achieving error free transmission in both cases were similar. This was expected, since the turbo-convolutional combination's performance is dependent on the convolutional code's performance in the low priority partition.

Lastly, comparing Figures 21.90 and 21.86, we found that the error-free condition was achieved at similar channel SNRs suggesting that the data partitioning scheme had not provided sufficient performance improvements in the context of the mobile DVB scheme, in order to justify its added complexity.

### 21.5.9 Conclusions and Future Work

In this section we have investigated the performance of a turbo-coded DVB system in a mobile environment. A range of system performance results was presented based on the standard scheme as well as on a turbo-coded scheme. The convolutional code specified in the standard system was substituted with turbo coding, which resulted in a substantial coding gain of around 5 dB. We have also applied data partitioning to the MPEG-2 video stream in order to gauge its effectiveness in increasing the error resilience of the video codec. However, from these experiments we found that the data partitioning scheme did not provide substantial improvements compared to the non-partitioned video transmitted over the non-hierarchical DVB-T system. Our future work in this field will be focused on improving the system's robustness by invoking a range of so-called maximum-minimum distance Redundant Residue Number System (RRNS) codes and turbo BCH codes. Let us now in the next section consider a variety of satellite-based turbo-coded blind-equalised multi-level modulation assisted video broadcasting schemes.

## 21.6 Satellite Based Turbo-coded, Blind-equalised 4-QAM and 16-QAM Digital Video Broadcasting<sup>14 15</sup>

### 21.6.1 Background and Motivation

In recent years three harmonised Digital Video Broadcasting (DVB) standards have emerged in Europe for terrestrial [620], cable-based [621] and satellite-oriented [622] delivery of video signals. The dispersive wireless propagation environment of the terrestrial system requires concatenated Reed-Solomon [4, 305] (RS) and rate compatible punctured convolutional coding [4, 305] (RCPCC) combined with Orthogonal Frequency Division Multiplexing (OFDM) based modulation. The satellite-based system employs the same concatenated channel coding arrangement, as the terrestrial schem,

<sup>14</sup>This section is based on C. S. Lee, S. Vlahoyiannatos and L. Hanzo: Satellite Based Turbo-coded, Blind-equalised 4-QAM and 16-QAM Digital Video Broadcasting, submitted to IEEE Tr. on Broadcasting, 1999

<sup>15</sup>©1999 IEEE. Personal use of this material is permitted. However, permission to reprint/republish this material for advertising or promotional purposes or for creating new collective works for resale or redistribution to servers or lists, or to refuse any copyrighted component of this work in other works must be obtained from the IEEE.

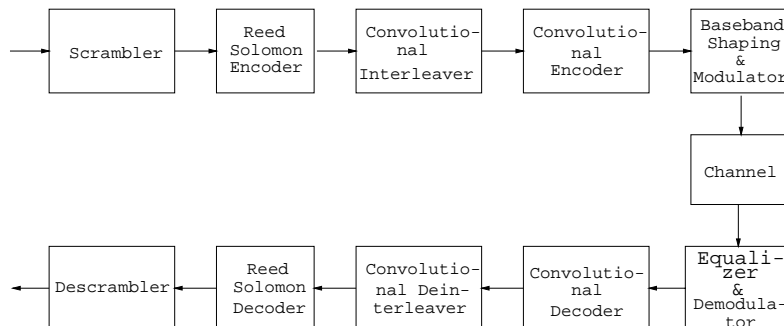


Figure 21.92: Schematic of the DVB satellite transmitter functions.

while the cable-based system refrains from using concatenated channel coding, opting for RS coding only. Both of the latter schemes employ furthermore blind-equalised multi-level modems. Lastly, the video codec in all three systems is the Motion Pictures Expert Group's MPEG-2 codec. These standardisation activities were followed by a variety of system performance studies in the open literature [632–635]. Against this backdrop, in this treatise we suggested turbo-coding based improvements to the satellite-based DVB system [622] and studied the performance of the proposed system under dispersive channel conditions in conjunction with a variety of blind channel equalisation algorithms. The transmitted power requirements of the standard convolutional codecs can be reduced upon invoking the more complex turbo codec. Alternatively, the standard system's bit error rate (BER) versus signal-to-noise-ratio (SNR) performance can be almost matched by a turbo-coded 16-level quadrature amplitude modulation (16QAM) based scheme, whilst doubling the achievable bit rate within the same bandwidth and hence improving the associated video quality. This is achieved at the cost of an increased system complexity.

The remainder of this section is organised as follows. A terse overview of the turbo-coded and standard DVB satellite scheme is presented in Subsection 21.6.2, while our channel model is described in Section 21.6.3. A brief digest of the blind equaliser algorithms employed is presented in Subsection 21.6.4. Following this, the performance of the improved DVB satellite system was examined over a dispersive two-path channel in Subsection 21.6.5, before our conclusions and future work areas were presented in Subsection 21.6.6.

### 21.6.2 DVB Satellite Scheme

The block diagram of the DVB satellite (DVB-S) transmitter [622] is shown in Figure 21.92, which is constituted by an MPEG-2 video encoder, channel coding modules and a QPSK modem. Due to the poor error resilience of the MPEG-2 video codec, strong concatenated channel coding is employed, consisting of a shortened Reed-Solomon RS(204,188) outer code [305], which corrects up to eight erroneous bytes in a block of 204 bytes, and a half-rate inner convolutional encoder with a constraint length of 7 [4, 305]. The overall code rate can be adapted by a variable puncturer,

not shown in the figure, which supports code rates of  $1/2$  (no puncturing) as well as  $2/3$ ,  $3/4$ ,  $5/6$  and  $7/8$ . The parameters of the convolutional encoder are summarised in Table 21.21.

Rate	$1/2$
Constraint Length	7
$k$	1
$n$	2
Polynomials (octal)	171,133

**Table 21.21:** Parameters of the  $CC(n,k,K)$  convolutional inner encoder in the DVB-S modem.

Rate	$1/2$
Input block length	17952 bits
Interleaver	random
Number of iterations	8
Constraint Length	3
$k$	1
$n$	2
Polynomials (octal)	7,5

**Table 21.22:** Parameters of the inner turbo encoder used to replace the DVB-S system's convolutional coder.

In addition to implementing the standard DVB-S system as a benchmarker, we have improved the system upon replacing the convolutional codec by a turbo codec [28]. The turbo codec's [636] parameters used in our studies are displayed in Table 21.22.

Readers interested in further details of the DVB-S system are referred to the DVB-S standard [622]. The performance of the standard DVB-S system and that of the turbo coded 16QAM system is characterised in Section 21.6.5. Let us now briefly consider the multipath channel model used in our investigations.

### 21.6.3 Channel Model

The properties of the satellite channel have been characterised for example by Vogel and his colleagues [637–640]. The channel model employed in this study was the two-path ( $nT$ )-symbol spaced impulse response, where  $T$  is the symbol-duration and in our studies we used  $n = 1$  and  $n = 2$ . This corresponds to a stationary dispersive transmission channel. Our channel model assumed that the receiver had a direct line-of-sight with the satellite as well as a second path caused by a single reflector. In our work, we studied the ability of a range of 4QAM/16QAM blind equaliser algorithms to converge under various path delay conditions. In the next section we provide a brief overview of the various blind equalisers employed in our experiments, noting



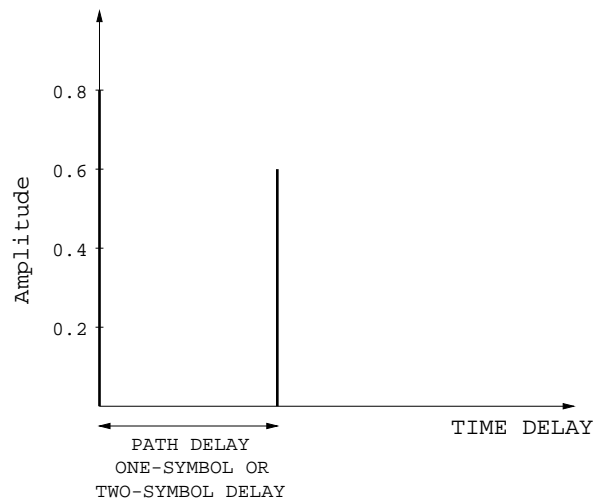


**Figure 21.93:** Two-path satellite channel model with either a one-symbol or two-symbol delay.

that readers mainly interested in the system's performance may proceed directly to our performance analysis section, namely to Section 21.6.5.

In the following section, we will present the performance results of our satellite-based DVB system.

### 21.6.4 The blind equalisers

In this section the blind equalisers used in the system are presented. The following blind equalisers have been studied:

- The Modified Constant Modulus Algorithm (or Modified CMA) [641]
- The Benveniste-Goursat Algorithm (or B-G) [642]
- The Stop-and-Go algorithm [643]
- The Per-Survivor Processing (PSP) Algorithm [644]

We will now briefly introduce these algorithms.

The **Modified CMA** (MCMA) is an improved version of Godard's well-known constant modulus algorithm [645] which was proposed by Wesolowsky [641]. This algorithm, unlike the CMA, equalises both the real and imaginary parts of the complex signal, according to the equaliser tap update equation of [641]:

$$\mathbf{c}^{(n+1)} = \mathbf{c}^{(n)} - \lambda \cdot \mathbf{y}^*(n) \cdot (Re[z(n)] \cdot ((Re[z(n)])^2 - R_{2,R}) + j \cdot Im\{z(n)\} \cdot ((Im\{z(n)\})^2 - R_{2,I}))$$

where  $\mathbf{c}^{(n)}$  is the equaliser tap vector at the  $n$ th iteration,  $\mathbf{y}(n)$  is the received signal vector at time  $n$ ,  $z(n)$  is the equalised signal at time  $n$ ,  $\lambda$  is the step-size parameter and  $R_{2,R}$ ,  $R_{2,I}$  are constant parameters of the algorithm, the values of which depend on the QAM signal constellation.

The **Benveniste-Goursat** (B-G) algorithm [642] is an amalgam of Sato's algorithm [646] and the decision-directed algorithm. The decision-directed algorithm is not a blind equalisation technique, since its convergence is highly dependent on the channel. The B-G algorithm combines the above two algorithms into one using the following equaliser coefficient update equations:

$$\mathbf{c}^{(n+1)} = \mathbf{c}^{(n)} - \lambda \cdot \mathbf{y}^*(n) \cdot \epsilon^G(n) \quad (21.5)$$

where

$$\epsilon^G(n) = k_1 \cdot \epsilon(n) + k_2 \cdot |\epsilon(n)| \cdot \epsilon^S(n) \quad (21.6)$$

is the B-G error term, which consists of the combination of the decision-directed error

$$\epsilon(n) = z(n) - \hat{z}(n), \quad (21.7)$$

( $\hat{z}(n)$  is the estimated symbol) and the Sato-type error

$$\epsilon^S(n) = z(n) - \gamma \cdot \text{csgn}(z(n)), \quad (21.8)$$

$\gamma$  being a constant Sato-algorithm parameter and  $\text{csgn}(x) = \text{sign}(\text{Re}\{x\}) + j \cdot \text{sign}(\text{Im}\{x\})$  is the complex sign function. The two error terms are suitably weighted by the constant parameters  $k_1$  and  $k_2$  in Equation (21.6).

The **Stop-and-Go** (S-a-G) algorithm [643] is a variant of the decision-directed algorithm, where at each equaliser coefficient adjustment iteration the update is enabled or disabled, depending on whether the update is likely to be correct. The update equations of this algorithm are given by:

$$\mathbf{c}^{(n+1)} = \mathbf{c}^{(n)} - \lambda \mathbf{y}^*(n) (f_{n,R} \text{Re}\{\epsilon(n)\} + j f_{n,I} \text{Im}\{\epsilon(n)\}) \quad (21.9)$$

where  $\epsilon(n)$  is the decision-directed error as in Equation (21.7) and the functions  $f_{n,R}$ ,  $f_{n,I}$  enable or disable the update of the equaliser according to the following rule: if the sign of the Sato-error (the real or the imaginary part independently) is the same as the sign of the decision-directed error, then the update takes place, otherwise it does not. In a blind equaliser, this condition provides us with a measure of the probability of the coefficient update being correct.

The **PSP algorithm** [644] is a sequence estimation technique, in which the channel is not known "a priori". Hence, an iterative channel estimation technique is employed in order to estimate the channel jointly with the symbol estimation. In this sense, an initial channel estimation is used and the estimation is updated at each new symbol's arrival. Each of the surviving paths in the trellis carries not only its own signal estimation, but also its own channel estimation. Moreover, convolutional decoding can take place jointly with this procedure, leading to an improved Bit Error Rate (BER) performance.

The summary of the equalisers' parameters is given in Table 21.23.

Following the above brief overview of the blind equaliser algorithms studied, let us now consider the overall system performance.

	Step-size $\lambda$	No. of Equal. Taps	Initial Tap- Vector
Benveniste-Goursat	$5 \cdot 10^{-4}$	10	$(1.2, 0, \dots, 0)$
Modified-CMA	$5 \cdot 10^{-4}$	10	$(1.2, 0, \dots, 0)$
Stop-and-Go	$5 \cdot 10^{-4}$	10	$(1.2, 0, \dots, 0)$
PSP (1 sym delay)	$10^{-2}$	2	$(1.2, 0)$
PSP (2 sym delay)	$10^{-2}$	3	$(1.2, 0, 0)$

**Table 21.23:** Summary of the equaliser parameters used in the simulations. The tap-vector  $(1.2, 0, \dots, 0)$  indicates that the first equaliser coefficient is initialised to the value of 1.2, while the others to 0.

### 21.6.5 Performance of the DVB Satellite Scheme

In this section, the performance of the DVB-S system was evaluated by means of simulations. Two modulation types were used, i.e. QPSK and 16-QAM, and the channel model of Figure 21.93 was employed. The first channel model had a one-symbol second-path delay, while in the second one the path-delay corresponded to the period of two symbols. The average BER versus SNR per bit performance is presented after the equalisation and demodulation process, as well as after Viterbi [305] or turbo decoding [636]. The SNR per bit is defined as follows:

$$\text{SNR per bit} = 10 \log_{10} \frac{\bar{S}}{\bar{N}} + \delta, \quad (21.10)$$

where  $\bar{S}$  is the average received signal amplitude,  $\bar{N}$  is the average received noise amplitude and  $\delta$  is the adjustment required to transform average signal-to-noise ratio into bit energy or SNR per bit. The adjustment is dependent on the type of modulation and channel code rate used in the system. In Figure 21.94, the linear equalisers' performance was quantified and compared for QPSK modulation over the one-symbol delay two-path channel model of Figure 21.93. Since all the equalisers' BER performance is similar, only the Modified CMA results are shown in the figure.

The equalised performance was inferior to that over the non-dispersive AWGN channel. However, as expected, it was better than without any equalisation. Another observation for Figure 21.94 was that the different punctured channel coding rates appeared to give slightly different bit error rates after equalisation. This is because the linear blind equalisers require uncorrelated input bits in order to converge. However, the input bits were not entirely random, when convolutional coding was used. The consequences of violating the zero-correlation constraint are not generally known. Nevertheless, two potential problems are apparent. Firstly, the equaliser may diverge from the desired equaliser equilibrium [647].

Secondly, the performance of the equaliser is expected to degrade, owing to the violation of the randomness requirement, which is imposed on the input bits in order to ensure that the blind equalisers will converge.

Since the channel used in our investigations was static, the first problem was

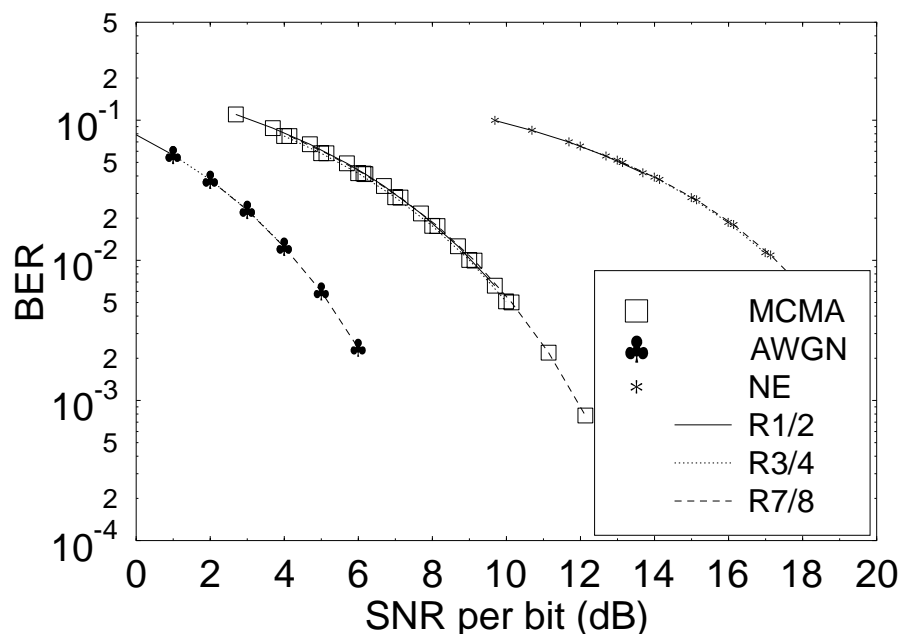


**Figure 21.94:** Average BER versus SNR per bit performance after equalisation and demodulation but before channel decoding employing QPSK modulation and one-symbol delay channel (NE:Non-Equalised).

not encountered. Instead, the second problem was what we actually observed. Figure 21.95 quantifies the equalisers' performance degradation due to the correlation introduced by convolutional coding. We can observe a 0.1 dB SNR degradation, when the convolutional codec creates correlation among the bits for this specific case.

The average BER curves after equalisation and demodulation are shown in Figure 21.96(a). In this figure, the average BER over the non-dispersive AWGN channel after turbo decoding constitutes the best performance, while the average BER of the one-symbol delay two-path unequalised channel after turbo decoding exhibits the worst performance. Again, in this figure only the Modified-CMA was featured for simplicity. The performance of the remaining equalisers was characterised in Figure 21.96(b). Clearly, the performance of the linear equalisers is similar.

It is observed in Figure 21.96(a) that the combination of the MCMA-based blind equaliser with turbo decoding exhibited the best SNR performance. The only comparable alternative was the PSP algorithm. Although the performance of the PSP algorithm is better at low SNRs, the associated curves cross over and the PSP algo-

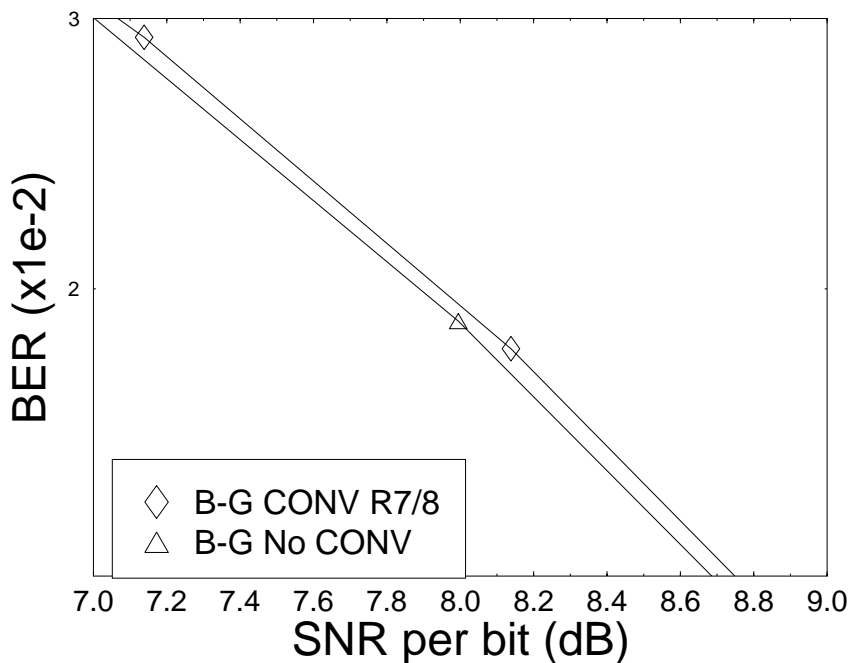
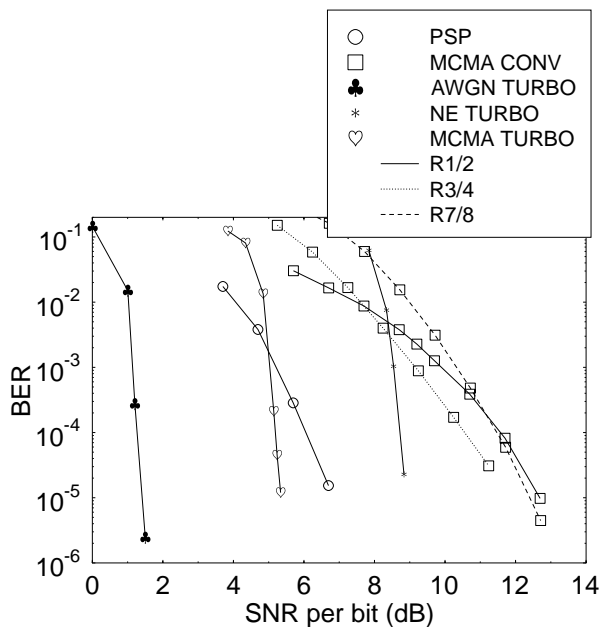


**Figure 21.95:** Average BER versus SNR per bit performance after equalisation and demodulation but before channel decoding employing QPSK modulation and the one-symbol delay two-path channel of Figure 21.93, for the Benveniste-Goursat algorithm, where the input bits are random (No CONV) or correlated (CONV 7/8) as a result of convolutional coding having a coding rate of 7/8.

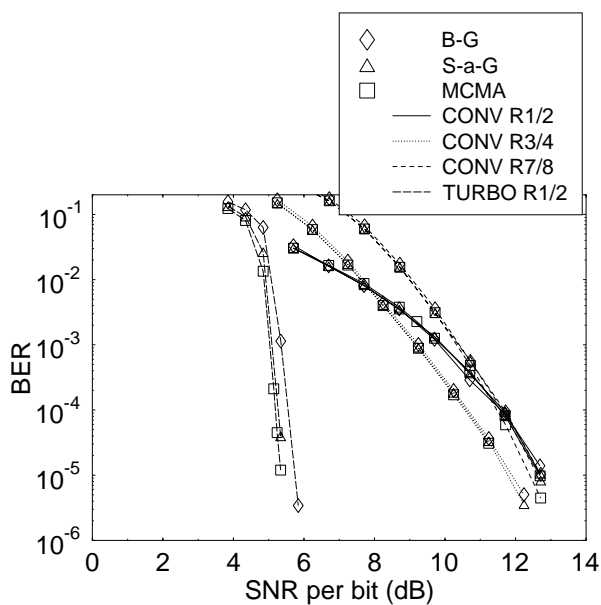
rithm's performance becomes inferior after the average BER becomes approximately  $10^{-3}$ . Although not shown in Figure 21.96, the Reed-Solomon decoder, which was concatenated to either the convolutional or the turbo decoder, gave an error-free output after the average BER of its input reached approximately  $10^{-4}$ . In this case, the PSP algorithm's performed worse by at least 1 dB in the area of interest, which is at an average BER of  $10^{-4}$ .

A final observation in the context of Figure 21.96(a) is that when convolutional decoding was used, the associated  $E_b/N_0$  performance of rate 1/2 convolutional coding appears inferior to that of the rate 3/4 and the rate 7/8 scenarios beyond certain  $E_b/N_0$  values.

In Figure 21.97, the corresponding BER curves are given for 16-QAM, under the same channel and equaliser conditions. Again, for simplicity, only the Modified CMA results are given. In this case the ranking order of the different coding rates follows our expectations more closely in the sense that the lowest coding rate of 1/2 is the

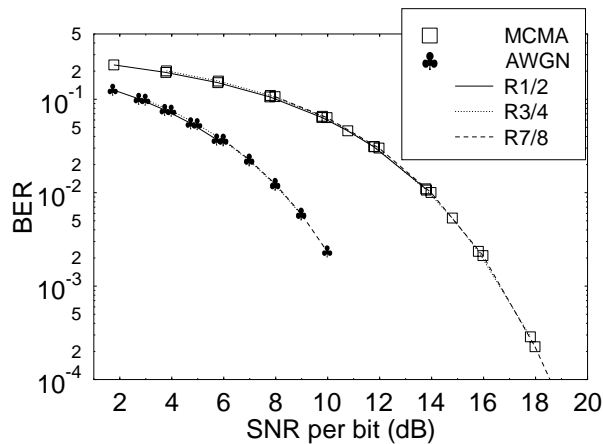


(a) PSP and linear equalisers

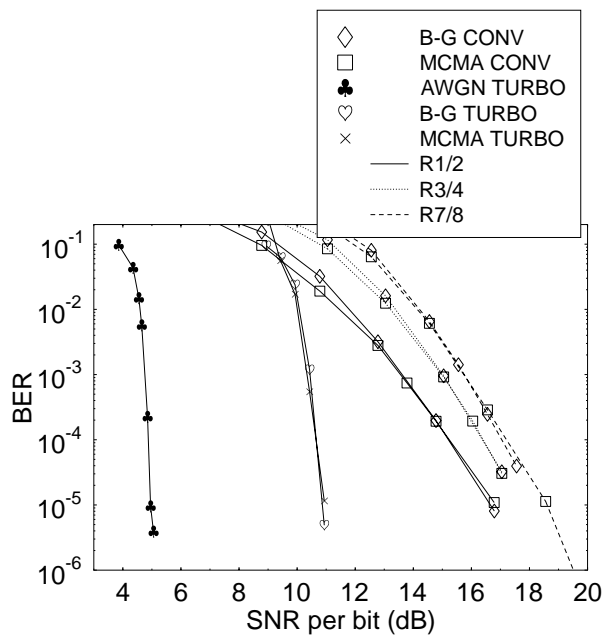


(b) Linear equalisers only

**Figure 21.96:** Average BER versus SNR per bit performance after convolutional or turbo decoding but before RS(204,188) decoding for QPSK modulation over the one-symbol delay channel (NE:Non-Equalised B-G:Benveniste-Goursat S-a-G:Stop-and-Go MCMA:Modified Constant Modulus Algorithm PSP:Per-Survivor-Processing).



(a) After equalisation and demodulation



(b) After viterbi or turbo decoding

**Figure 21.97:** Average BER versus SNR per bit (a) after equalisation and demodulation but before channel decoding and (b) after Viterbi or turbo decoding but before RS(204,188) decoding for 16-QAM modulation over the one-symbol delay two-path channel of Figure 21.93.

best performer, followed by the rate 3/4 codec, in turn followed by the weakest rate 7/8 codec.

The Stop-and-Go algorithm has not been included in these results. The reason is that this algorithm does not converge for high SNR values. This happens because this procedure is only activated when there is a high probability of correct update. In our case, the equaliser is initialised far from its convergence point and hence the decision-directed updates are unlikely to provide correct updates. In the absence of noise this leads to the algorithm being permanently de-activated. If noise is present though, then some random perturbations from the point of the equaliser's initialization can activate the algorithm and can lead to convergence. This is what we observe at medium SNR values. For high SNR values though, the algorithm does not converge.

It is also interesting to compare the performance of the system for the QPSK and 16-QAM schemes. When the one-symbol delay two-path channel model of Figure 21.93 was considered, the system was capable of supporting the use of 16-QAM with the provision of an additional SNR per bit of 5 dB. Although the original DVB-Satellite system only employs QPSK modulation, our simulations had shown that 16-QAM can be employed equally well for the range of blind equalisers that we have used in our work. This allows us to double the video bitrate and hence to substantially improve the video quality. The comparison of Figures 21.96 and 21.97 also reveals that the extra SNR requirement of 5 dB of 16QAM over 4QAM can be eliminated by employing turbo coding at the cost of a higher implementational complexity. This allowed us to accommodate a doubled bitrate within a given bandwidth, which improved the video quality.

In Figures 21.98 (only for Benveniste-Goursat for simplicity) and 21.99 the corresponding BER results for the two-symbol delay two-path channel of Figure 21.93 are given for QPSK. They are similar to Figures 21.94 and 21.96 in terms of their trends, although we observed some differences:

- The “cross-over point”, beyond which the performance of the PSP algorithm becomes worse than that of the Modified CMA in conjunction with turbo decoding is now at  $10^{-4}$ , which is in the area where the RS decoder provides an error-free output.
- The rate 1/2 convolutional decoding is now the best performer, while the rate 3/4 scheme exhibited the worst performance.

Finally, in Figure 21.100, the associated 16-QAM results are presented. Notice that the Stop-and-Go algorithm was again excluded from the results. We can observe a high performance difference between the B-G and the Modified CMA.

In the previous cases we did not observe such a significant difference. The difference in this case is that the channel exhibits an increased delay spread. In fact, what we observe here is the capability of the equalisers to cope with more wide-spread multipaths, while keeping their length constant. The Benveniste-Goursat equaliser is more efficient, than the Modified CMA in this case.

It is interesting to note that in this case, the performance of the different coding rates is again in the expected order, the rate 1/2 being the best, followed by the rate 3/4 and then the rate 7/8 scheme.



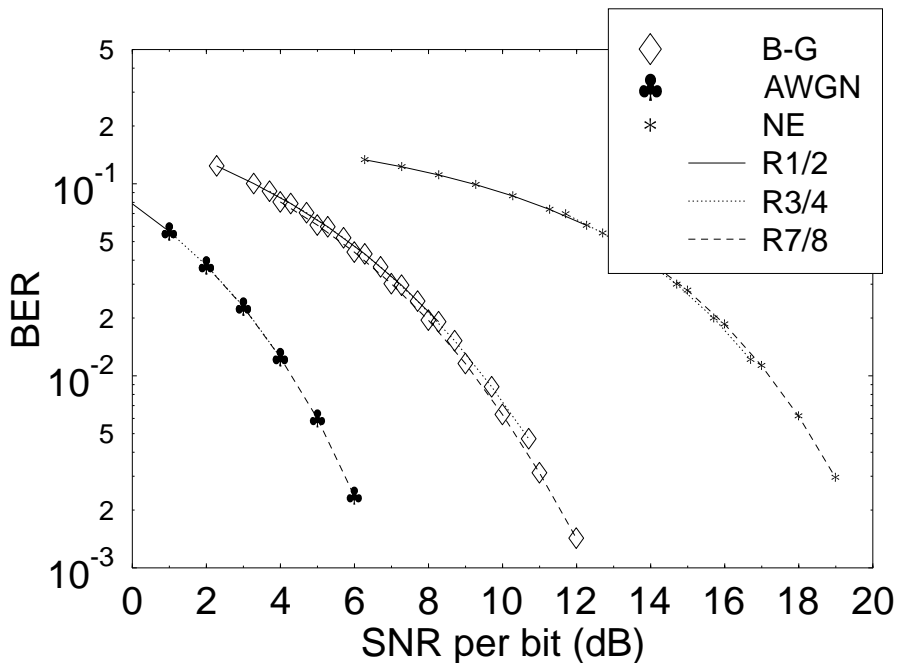


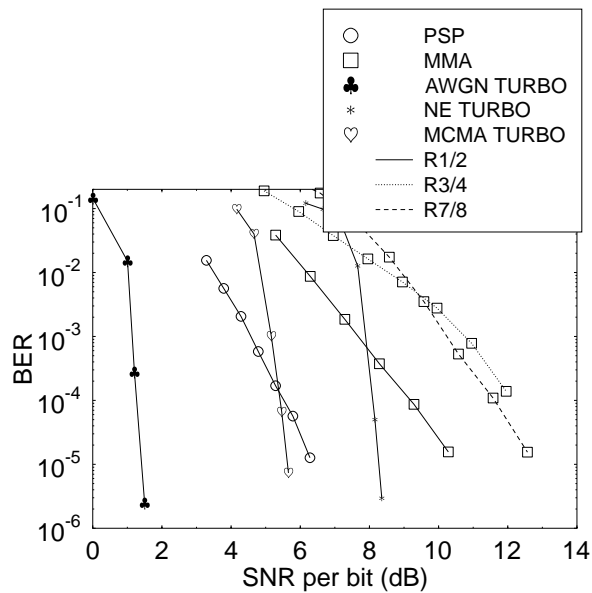
**Figure 21.98:** Average BER versus SNR per bit performance after equalisation and demodulation but before channel decoding for QPSK modulation over the two-symbol delay two-path channel of Figure 21.93.

If we compare the performance of the system employing QPSK and 16-QAM under the two-symbol delay two-path channel model of Figure 21.93, we again observe that 16-QAM can be incorporated into the DVB system if an extra 5 dB of SNR per bit is affordable in power budget terms. However, only the B-G algorithm is worthwhile considering here out of the three linear equalisers used in our work.

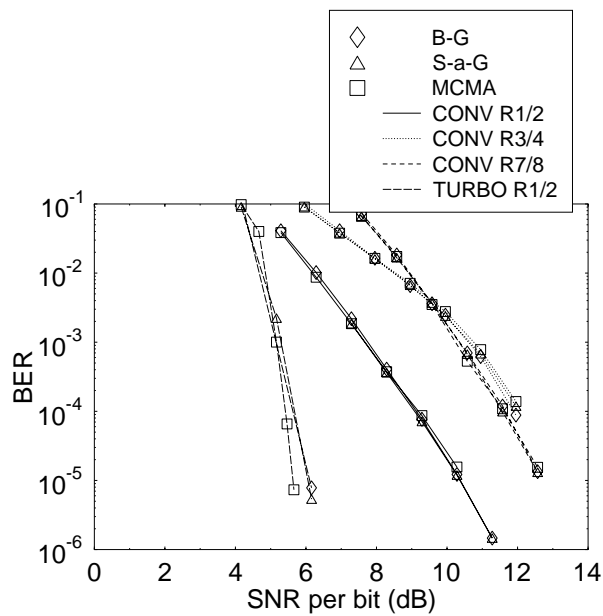
Figure 21.101 portrays the corresponding reconstructed video performance in terms of the average PSNR versus channel SNR for the one-symbol delay and two-symbol delay two-path channel model of Figure 21.93.

Tables 21.24 and 21.25 provide a summary of the DVB-Satellite system's performance tolerating a PSNR degradation of 2 dB, which was deemed to be imperceptible in terms of subjective video degradations. The average BER values quoted in the tables refer to the average BER achieved after Viterbi or turbo decoding. The channel SNR (CSNR) is quoted in association with the 2 dB average PSNR degradation since the viewer will begin to perceive video degradations due to erroneous decoding of the received video at this threshold, as noted in [648].

Table 21.28 provides an approximation of the convergence speed of each blind equalisation algorithm for each case. It is clear that PSP converges significantly faster than any of the other techniques. On the other hand, the Benveniste-Goursat algorithm is the fastest of the other techniques. In our simulations the convergence

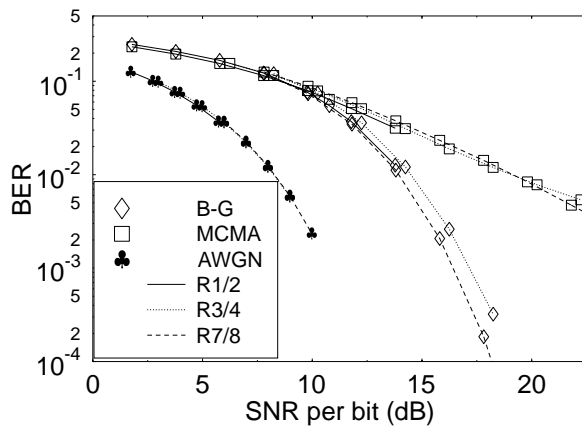


(a) PSP and linear equalisers

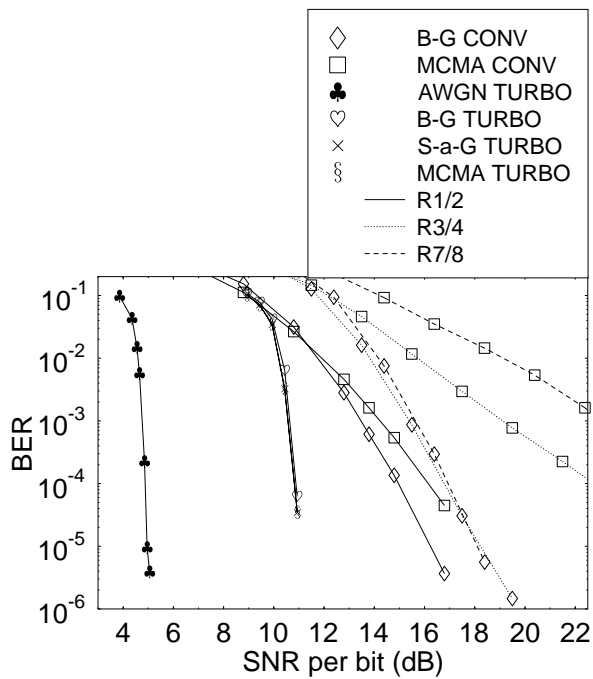


(b) Linear equalisers only

**Figure 21.99:** Average BER versus SNR per bit performance after convolutional or turbo decoding but before RS(204,188) decoding for QPSK modulation over the two-symbol delay two-path channel of Figure 21.93.

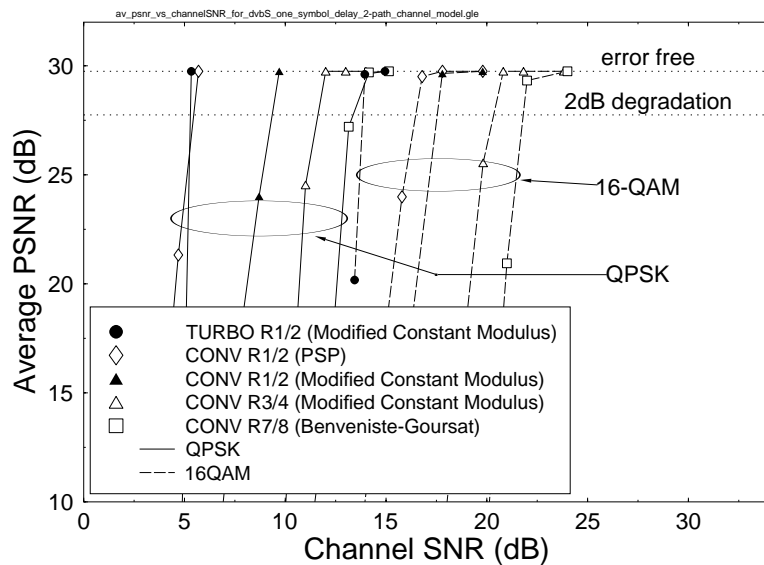


(a) After equalisation and demodulation

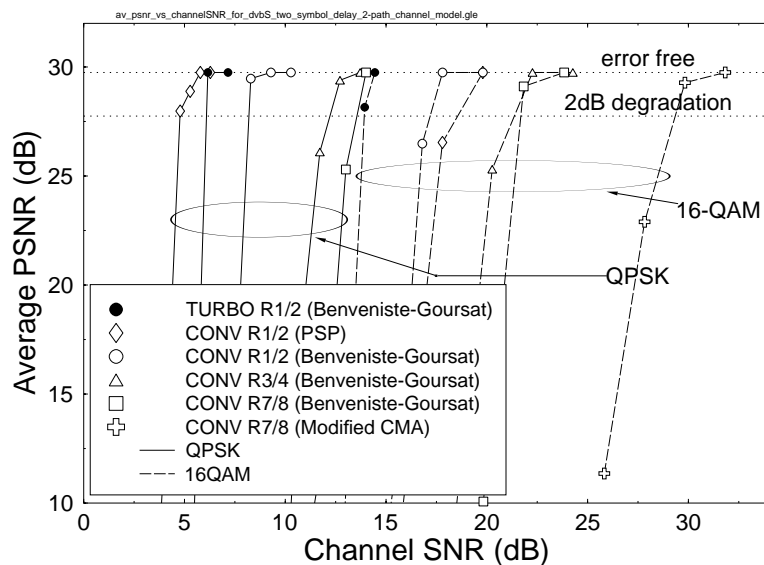


(b) After viterbi or turbo decoding

**Figure 21.100:** Average BER versus SNR per bit performance (a) after equalisation and demodulation but before channel decoding and (b) after Viterbi or turbo decoding but before RS(204,188) decoding for 16-QAM over the two-symbol delay two-path channel of Figure 21.93.



(a) One-symbol delay two-path channel model



(b) Two-symbol delay two-path channel model

**Figure 21.101:** Average PSNR versus channel SNR for (a) one-symbol delay two-path channel model after concatenated channel decoding and (b) two-symbol delay two-path channel model of Figure 21.93 after concatenated channel decoding.

Mod.	Equaliser	Code	CSNR (dB)	$E_b/N_0$
QPSK	PSP( $R=1/2$ )		5.3	5.3
QPSK	MCMA	Turbo (1/2)	5.2	5.2
16QAM	MCMA	Turbo (1/2)	13.6	10.6
QPSK	MCMA	Conv (1/2)	9.1	9.1
16QAM	MCMA	Conv (1/2)	17.2	14.2
QPSK	MCMA	Conv (3/4)	11.5	9.7
16QAM	MCMA	Conv (3/4)	20.2	15.4
QPSK	B-G	Conv (7/8)	13.2	10.8
16QAM	B-G	Conv (7/8)	21.6	16.2

**Table 21.24:** Summary of performance results over the dispersive one-symbol delay two-path AWGN channel of Figure 21.93 tolerating a PSNR degradation of 2 dB. The average BER was evaluated after Viterbi or turbo decoding and concatenated RS(204,188) decoding.

Mod.	Equaliser	Code	CSNR (dB)	$E_b/N_0$
QPSK	PSP( $R=1/2$ )		4.7	4.7
QPSK	B-G	Turbo (1/2)	5.9	5.9
16QAM	B-G	Turbo (1/2)	13.7	10.7
QPSK	B-G	Conv (1/2)	8.0	8.0
16QAM	B-G	Conv (1/2)	17.0	14.0
QPSK	B-G	Conv (3/4)	12.1	10.3
16QAM	B-G	Conv (3/4)	21.1	16.3
QPSK	B-G	Conv (7/8)	13.4	11.0
16QAM	MCMA	Conv (7/8)	29.2	23.8

**Table 21.25:** Summary of performance results over the dispersive two-symbol delay two-path AWGN channel of Figure 21.93 tolerating a PSNR degradation of 2 dB. The average BER was evaluated after Viterbi or turbo decoding and concatenated RS(204,188) decoding.

Mod.	Equaliser	Code	$E_b/N_0$
QPSK	PSP( $R=1/2$ )		6.1
QPSK	MCMA	Turbo (1/2)	5.2
16QAM	MCMA	Turbo (1/2)	10.7
QPSK	MCMA	Conv (1/2)	11.6
16QAM	MCMA	Conv (1/2)	15.3
QPSK	MCMA	Conv (3/4)	10.5
16QAM	MCMA	Conv (3/4)	16.4
QPSK	B-G	Conv (7/8)	11.8
16QAM	B-G	Conv (7/8)	17.2

**Table 21.26:** Summary of system performance results over the dispersive one-symbol delay two-path AWGN channel of Figure 21.93 tolerating an average BER of  $10^{-4}$ . The average BER was evaluated after Viterbi or turbo decoding but before RS(204,188) decoding.

Mod.	Equaliser	Code	$E_b/N_0$
QPSK	PSP( $R=1/2$ )		5.6
QPSK	B-G	Turbo (1/2)	5.7
16QAM	B-G	Turbo (1/2)	10.7
QPSK	B-G	Conv (1/2)	9.2
16QAM	B-G	Conv (1/2)	15.0
QPSK	B-G	Conv (3/4)	12.0
16QAM	B-G	Conv (3/4)	16.8
QPSK	B-G	Conv (7/8)	11.7
16QAM	MCMA	Conv (7/8)	26.0

**Table 21.27:** Summary of system performance results over the dispersive two-symbol delay two-path AWGN channel of Figure 21.93 tolerating an average BER of  $10^{-4}$ . The average BER was evaluated after Viterbi or turbo decoding but before RS(204,188) decoding.

	B-G	MCMA	S-a-G	PSP
QPSK 1-sym	$2 \cdot 10^5$	$4.4 \cdot 10^5$	$2.6 \cdot 10^5$	380
QPSK 2-sym	$2 \cdot 10^5$	$3.9 \cdot 10^5$	$2.1 \cdot 10^5$	380
16-QAM 1-sym	$5.6 \cdot 10^5$	$8.8 \cdot 10^5$	$19 \cdot 10^5$	
16-QAM 2-sym	$4.9 \cdot 10^5$	$5.6 \cdot 10^5$	$18 \cdot 10^5$	

**Table 21.28:** Equaliser convergence speed measured in the simulations, given as the number of bits required for convergence (x-sym: x-symbol delay two-path channel).

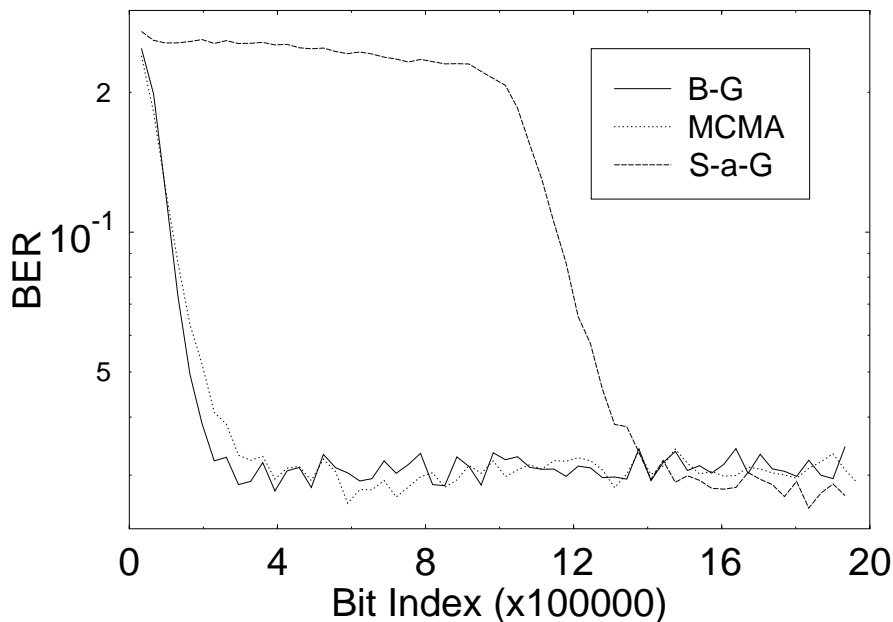


**Figure 21.102:** Learning curves for 16-QAM, one-symbol delay two-path channel at SNR=18dB.

was quantified by measuring the slope of the BER curve, as this curve was reaching the associated residual BER. Convergence was established, when this slope gradient became smaller than a threshold value, implying that the BER has reached its steady-state. Figure 21.102 gives an illustrative example of the equaliser convergence for the case of 16-QAM. It is observed that the Stop-and-Go algorithm converges significantly slower than the other algorithms, which can also be seen from Table 21.28. This happens because, during the startup, the algorithm is de-activated most of the time, an effect which becomes more severe with an increasing QAM order.

Tables 21.26 and 21.27 provide a summary of the SNR per bit required for the various system configurations. The threshold of  $10^{-4}$  is selected here, since at this average BER after Viterbi or turbo decoding the RS decoder becomes effective. This means that the output bits have a high probability of being error free. This also translates into error-free video decoding.

### 21.6.6 Conclusions and Future Work

In this section, we have investigated the performance of a turbo-coded DVB system in a satellite broadcast environment. A range of system performance results was presented based on the standard DVB-S scheme, as well as on a turbo-coded scheme in

conjunction with blind equalised 4QAM/16QAM. The convolutional code specified in the standard system was substituted by turbo coding, which resulted in a substantial coding gain of around 4-5 dB. We have also shown that 16-QAM can be utilised instead of QPSK, if an extra 5 dB SNR per bit gain is added to the link budget. This extra transmitted power requirement can be eliminated upon invoking the more complex turbo codec, which requires lower transmitted power for attaining the same performance as the standard convolutional codecs. Our future work will be focused on extending the DVB-Satellite system to supporting mobile users for the reception of satellite broadcast video signals. The use of turbo equalisers will also be investigated in comparison to blind equalisers. Further work will also be dedicated to trellis coded modulation (TCM) and turbo trellis coded modulation (TTCM) based OFDM and single-carrier equalised modems.





# Glossary

<b>16CIF</b>	Sixteen Common Intermediate Format Frames are sixteen times as big as CIF frames, and contain 1408 pixels vertically and 1152 pixels horizontally
<b>4CIF</b>	Four Common Intermediate Format Frames are four times as big as CIF frames, and contain 704 pixels vertically and 576 pixels horizontally
<b>ACO</b>	Augmented Channel Occupancy matrix, which contains the channel occupancy for the local and surrounding basestations. Often used by locally distributed DCA algorithms to aid allocation decisions.
<b>ACTS</b>	Advanced Communications Technologies and Services. The 4th framework for European research (1994-98). A series of consortia consisting of universities and industrialists considering future communications systems.
<b>ADPCM</b>	Adaptive Differential Pulse Coded Modulation.
<b>ARQ</b>	Automatic Repeat Request, Automatic request for retransmission of corrupted data
<b>AV.26M</b>	A draft recommendation for transmitting compressed video over error-prone channels, based on the H.263 [182] video codec.
<b>AWGN</b>	Additive White Gaussian Noise
<b>BCH</b>	Bose-Chaudhuri-Hocquenghem, A class of forward error correcting codes (FEC)
<b>BER</b>	Bit error rate, the fraction of the bits received incorrectly
<b>BS</b>	A common abbreviation for Base Station

<b>CBER</b>	Channel bit error rate, the bit error rate before FEC correction
<b>CBP</b>	Coded block pattern, a H.261 video codec symbol that indicates which of the blocks in the macroblock are active
<b>CBPB</b>	A fixed length codeword used by the H.263 video codec to convey the coded block pattern for bi-directionally predicted (B) blocks
<b>CBPY</b>	A variable length codeword used by the H.263 video codec to indicate the coded block pattern for luminance blocks
<b>CCITT</b>	Now ITU, standardisation group
<b>CD</b>	Code Division, a multiplexing technique where signals are coded and then combined, in such a way that they can be separated using the assigned user signature codes at a later stage.
<b>CDF</b>	Cumulative density function, the integral of the probability density function (PDF)
<b>CDMA</b>	Code Division Multiple Access
<b>CIF</b>	Common Intermediate Format Frames containing 352 pixels vertically and 288 pixels horizontally
<b>CIR</b>	Carrier to Interference Ratio, same as SIR.
<b>COD</b>	A one bit codeword used by the H.263 video codec, that indicates whether the current macroblock is empty or non-empty.
<b>DC</b>	Direct Current, normally used in electronic circuits to describe a power source that has a constant voltage, as opposed to AC power in which the voltage is a sine-wave. It is also used to describe things which are constant, and hence have no frequency component.
<b>DCA</b>	Dynamic Channel Allocation
<b>DCS1800</b>	A digital mobile radio system standard, based on GSM, but operates at 1.8GHz at a lower power.
<b>DCT</b>	A discrete cosine transform, transforms data into the frequency domain. Commonly used for video compression by removing high frequency components of the video frames
<b>DECT</b>	A Pan-European digital cordless telephone standard.

<b>DQUANT</b>	A fixed length coding parameter used to differential change the current quantiser used by the H.263 video codec.
<b>EOB</b>	An end of block variable-length symbol used to indicate the end of the current block in the H.261 video codec
<b>EREC</b>	Error Resilient Entropy Coding. A coding technique improving the robustness of variable length coding, by allowing easier re-synchronisation after errors.
<b>FA</b>	First Available, a simple centralised DCA scheme, which allocates the first channel found that is not reused within a given preset reuse distance.
<b>FBER</b>	Feedback error ratio, the ratio of feedback acknowledgement messages that are received in error.
<b>FCA</b>	Fixed Channel Allocation
<b>FD</b>	Frequency Division, a multiplexing technique, where different frequencies are used for each communications link.
<b>FDD</b>	Frequency-Division Duplex, a multiplexing technique, where the forward and reverse links use a different carrier frequency.
<b>FDMA</b>	Frequency Division multiple access, a multiple access technique, where frequency division (FD) is used to provide a set of access channels.
<b>FEC</b>	Forward Error Correction
<b>FEF</b>	Frame Error Flag
<b>FER</b>	Frame error rate
<b>FIFO</b>	First-In First-Out, a queuing strategy in which elements that have been in the queue longest are served first.
<b>fps</b>	Frames per second
<b>GBSC</b>	Group of blocks (GOB) start code, used by the H.261 and H.263 video codecs to regain synchronisation, playing a similar role to PSC
<b>GEI</b>	Functions similar to PEI, but in the GOB layer of the H.261 video codec
<b>GFID</b>	A fixed length codeword used by H.263 video codec to aid correct re-synchronisation after an error

<b>GMSK</b>	Gaussian Mean Shift Keying, a modulation scheme used by the Pan-European GSM standard by virtue of its spectral compactness.
<b>GN</b>	Group of block number, an index number for a GOB used by the H.261 and H.263 video codecs
<b>GOB</b>	Group of blocks, a term used by the H.261 and H.263 video codecs, consisting of a number of macroblocks.
<b>GOS</b>	Grade of Service, a performance metric to describe the quality of a mobile radio network.
<b>GQUANT</b>	Group of blocks quantiser, a symbol used by the H.261 and H.263 video codecs to modify the quantiser used for the GOB
<b>GSM</b>	A Pan-European digital mobile radio standard, operating at 900MHz.
<b>GSPARE</b>	Functions similar to PSPARE, but in the GOB layer of the H.261 video codec
<b>H.261</b>	A video coding standard [505], published by the ITU in 1990
<b>H.263</b>	A video coding standard [182], published by the ITU in 1996
<b>HCA</b>	Hybrid Channel Allocation, a hybrid of FCA and DCA.
<b>HTA</b>	Highest interference below Threshold Algorithm, a distributed DCA algorithm also known as MTA. The algorithm allocates the most interfered channel, whose interference is below the maximum tolerable interference threshold.
<b>IS-95</b>	North American mobile radio standard, that uses CDMA technology.
<b>ISDN</b>	Integrated Services Digital Network, digital replacement of the analogue telephone network
<b>ITU</b>	International Telecommunications Union, formerly the CCITT, standardisation group
<b>LFA</b>	Lowest Frequency below threshold Algorithm, a distributed DCA algorithm which is a derivative of the LTA algorithm, the difference being that the algorithm attempts to reduce the number of carrier frequencies being used concurrently.

<b>LIA</b>	Least Interference Algorithm, a distributed DCA algorithm that assigns the channel with the lowest measured interference that is available.
<b>LODA</b>	Locally Optimised Dynamic Assignment, a centralised DCA scheme, which bases its allocation decisions upon the future blocking probability in the vicinity of the cell.
<b>LOLIA</b>	Locally Optimised Least Interference Algorithm, a locally distributed DCA algorithm, that allocates channels using a hybrid of the LIA and an ACO matrix.
<b>LOMIA</b>	Locally Optimised Most Interference Algorithm, a locally distributed DCA algorithm, that allocates channels using a hybrid of the MTA and an ACO matrix.
<b>LP-DDCA</b>	Local Packing Dynamic Distributed Channel Assignment, a locally distributed DCA algorithm that assigns the first channel available that is not used by the surrounding base stations, whose information is contained in an ACO matrix.
<b>LTA</b>	Least interference below Threshold Algorithm, a distributed DCA algorithm, which allocates the least interfered channel, whose interference is below a preset maximum tolerable interference level.
<b>MA</b>	Abbreviation for Miss America, a commonly used head and shoulders video sequence referred to as Miss America
<b>Macroblock</b>	A grouping of 8 by 8 pixel blocks used by the H.261 and H.263 video codecs. Consists of four luminance blocks and two chrominance blocks.
<b>MB</b>	Macroblock.
<b>MBA</b>	Macroblock address symbol used by the H.261 video codec, indicating the position of the macroblock in the current GOB
<b>MBS</b>	Mobile Broadband System
<b>MCBPC</b>	A variable length codeword used by the H.263 video codec to convey the macroblock type and the coded block pattern for the chrominance blocks
<b>MODB</b>	A variable length coding parameter used by the H.263 video codec to indicate the macroblock mode for bi-directionally predicted (B) blocks
<b>MPEG</b>	Motion Picture Expert Group, also a video coding standard designed by this group that is widely used

<b>MQUANT</b>	A H.261 video codec symbol that changes the quantiser used by current and future macroblocks in the current GOB
<b>MS</b>	A common abbreviation for Mobile Station
<b>MSQ</b>	Mean Square centralised DCA algorithm, which attempts to minimize the mean square distance between cells using the same channel.
<b>MTA</b>	Most interference below Threshold Algorithm, a distributed DCA algorithm also known as HTA. The algorithm allocates the most interfered channel, whose interference is below the maximum tolerable interference level.
<b>MTYPE</b>	H.261 video codec symbol that contains information about the macroblock, such as coding mode, and flags to indicate whether optional modes are used, like motion vectors, and loop filtering
<b>MV</b>	Motion Vector, a vector to estimate the motion in a frame
<b>MVD</b>	Motion vector data symbol used by H.261 and H.263 video codecs
<b>MVDB</b>	A variable length codeword used by the H.263 video codec to convey the motion vector data for bi-directionally predicted (B) blocks
<b>NCC</b>	Normalised Channel Capacity
<b>NN</b>	Nearest-Neighbour centralised DCA algorithm, allocates a channel used by the nearest cell, which is at least the reuse distance away.
<b>NN+1</b>	Nearest-Neighbour-plus-one centralised DCA algorithm, allocates a channel used by the nearest cell, which is at least the reuse distance plus one cell radius away.
<b>OFDM</b>	Orthogonal Frequency Division Multiplexing is a technique splitting a highly dispersive high-rate channel into a high number of low-rate non-dispersive subchannels using Fast Fourier Transform (FFT) based modulation [10].
<b>PCN</b>	Personal Communications Network
<b>PCS</b>	Personal Communications System, a term used to describe third generation mobile radio systems in North America
<b>PDF</b>	Probability Density Function
<b>PEI</b>	Picture layer extra insertion bit, used by the H.261 video codec, indicating that extra information is to be expected

<b>PQUANT</b>	A fixed length codeword used by the H.263 video codec to indicate the quantiser to use for the next frame
<b>PRMA</b>	Packet Reservation Multiple Access, a statistical multiplexing arrangement contrived to improve the efficiency of conventional TDMA systems, by detecting inactive speech segments using a voice activity detector, surrendering them and allocating them to subscribers contending to transmit an active speech packet.
<b>PSAM</b>	Pilot symbol assisted modulation, a technique where known symbols (pilots) are transmitted regularly. The effect of channel fading on all symbols can then be estimated by interpolating between the pilots
<b>PSC</b>	Picture start code, a preset sequence used by the H.261 and H.263 video codec, that can be searched for to regain synchronisation after an error
<b>PSNR</b>	Peak Signal to Noise Ratio, noise energy compared to the maximum possible signal energy. Commonly used to measure video image quality
<b>PSPARE</b>	Picture layer extra information bits, indicated by a PEI symbol in H.261 video codec
<b>PTYPE</b>	Picture layer information, used by H.261 and H.263 video codec to transmit information about the picture, e.g. Resolution, etc
<b>QAM</b>	Quadrature Amplitude Modulation
<b>QCIF</b>	Quarter Common Intermediate Format Frames containing 176 pixels vertically and 144 pixels horizontally
<b>RACE</b>	Research in Advanced Communications Equipment Programme in Europe, from June 1987 to December 1995.
<b>RING</b>	A centralised DCA algorithm, which attempts to allocate channels in one of the cells, which is at least the reuse distance away that forms a "ring" of cells.
<b>RSSI</b>	Received Signal Strength Indicator, commonly used as an indicator of channel quality in a mobile radio network.
<b>SAC</b>	Syntax based arithmetic coding is an alternative to variable length coding. It is a variant of arithmetic coding
<b>SCS</b>	Sequential Channel Search distributed DCA algorithm, searches the available channels in a pre-determined order, picking the first channel found, which meets the interference constraints.



<b>SINR</b>	Signal to Interference plus Noise ratio, same as signal to noise ratio (SNR), when there is no interference.
<b>SIR</b>	Signal to Interference ratio
<b>SNR</b>	Signal to Noise Ratio, noise energy compared to the signal energy
<b>SQCIF</b>	Sub-Quarter Common Intermediate Format Frames containing 128 pixels vertically and 96 pixels horizontally
<b>TCOEFF</b>	An H.261 and H.263 video codec symbol, that contains the transform coefficients for the current block
<b>TD</b>	Time Division, a multiplexing technique where several communications links are multiplexed onto a single carrier, by dividing the channel into time-periods, and assigning a time-period to each communications link.
<b>TDD</b>	Time-Division Duplex, a technique where the forward and reverse links are multiplexed in time.
<b>TDMA</b>	Time Division Multiple Access
<b>TR</b>	Temporal reference, a symbol used by H.261 and H.263 video codecs to indicate the real time difference between transmitted frames
<b>UMTS</b>	Universal Mobile Telecommunications System, a future Pan-European third generation mobile radio standard.
<b>VAF</b>	Voice activity factor, the fraction of time the voice activity detector of a speech codec is active
<b>WLAN</b>	Wireless Local Area Network
<b>WWW</b>	World Wide Web is the name given to computers that can be accessed via the Internet using the HTTP protocol. These computers can provide information in a easy to digest multimedia format using hyper-links.

## Bibliography

- [1] E. Berlekamp, *Algebraic Coding Theory*. McGraw-Hill, New York, 1968.
- [2] J. Massey, "Shift-register synthesis and BCH decoding," *IEEE Tr. on Inf. Theory*, vol. IT-15, pp. 122–127, January 1969.
- [3] R. Blahut, *Theory and practice of error control codes*. Addison-Wesley, 1983. ISBN 0-201-10102-5.
- [4] A. Michelson and A. Levesque, *Error control techniques for digital communication*. J. Wiley and Sons, 1985.
- [5] S. Lin and D. J. Costello Jr, *Error Control Coding: Fundamentals and Applications*. New Jersey, USA: Prentice-Hall, October 1982. ISBN: 013283796X.
- [6] W. Peterson and E. Weldon, Jr, *Error correcting codes*. MIT. Press, 2nd ed., August 1972. ISBN: 0262160390.
- [7] G. C. Clark, Jr and J. B. Cain, *Error correction coding for digital communications*. New York: Plenum Press, May 1981. ISBN: 0306406152.
- [8] K. Wong, *Transmission of channel coded speech and data over mobile channels*. PhD thesis, University of Southampton, 1989.
- [9] R. Steele, ed., *Mobile Radio Communications*. IEEE Press-Pentech Press, 1992.
- [10] W. T. Webb and L. Hanzo, *Modern Quadrature Amplitude Modulation: Principles and Applications for Wireless Communications*. IEEE Press-Pentech Press, 1994. ISBN 0-7273-1701-6.
- [11] J. M. Torrance and L. Hanzo, "Comparative study of pilot symbol assisted modem schemes," in *Proceedings of IEE Conference on Radio Receivers and Associated Systems (RRAS'95)*, (Bath, UK), pp. 36–41, IEE, 26–28 September 1995.
- [12] P. G. Howard and J. S. Vitter, "Arithmetic coding for data compression," *Proceedings of the IEEE*, vol. 82, pp. 857–865, June 1994.
- [13] H. Nyquist, "Certain factors affecting telegraph speed," *Bell System Tech Jrnal*, p. 617, April 1928.

- [14] C. Shannon, *Mathematical Theory of Communication*. University of Illinois Press, 1963.
- [15] C. Shannon, "A mathematical theory of communication - part I," *Bell Systems Technical Journal*, pp. 379–405, 1948.
- [16] C. Shannon, "A mathematical theory of communication - part II," *Bell Systems Technical Journal*, pp. 405–423, 1948.
- [17] C. Shannon, "A mathematical theory of communication - part III," *Bell Systems Technical Journal*, pp. 623–656, 1948.
- [18] R. V. L. Hartley, "Transmission of information," *BSTJ*, p. 535, 1928.
- [19] N. Abramson, *Information Theory and Coding*. McGraw-Hill, 1975.
- [20] A. B. Carlson, *Communication Systems*. McGraw-Hill, 1975.
- [21] H. R. Raemer, *Statistical communication theory and applications*. Englewood Cliffs, New Jersey: Prentice Hall, Inc., 1969.
- [22] P. Ferenczy, *Telecommunications Theory*. Budapest, Hungary: Tankonyvkiado, 1972.
- [23] K. S. Shanmugam, *Digital and Analog Communications Systems*. New York, USA: John Wiley, 1979.
- [24] C. Shannon, "Communication in the presence of noise," *Proc IRE*, vol. 37, pp. 10–21, 1949.
- [25] C. Shannon, "Probability of error for optimal codes in a gaussian channel," *Bell Systems Technical Journal*, vol. 38, pp. 611–656, 1959.
- [26] A. K. Jain, *Fundamentals of Digital Image Processing*. Prentice-Hall, 1989.
- [27] A. Hey and R. Allen, eds., *R.P. Feynman: Feynman lectures on computation*. Addison-Wesley, 1996.
- [28] C. Berrou, A. Glavieux, and P. Thitimajshima, "Near shannon limit error-correcting coding and decoding: Turbo codes," in *Proceedings of the International Conference on Communications*, pp. 1064–1070, May 1993.
- [29] J. Hagenauer, "Quellengesteuerte kanalcodierung fuer sprach- und tonuebertragung im mobilfunk," *Aachener Kolloquium Signaltheorie*, pp. 67–76, 23-25 March 1994.
- [30] A. J. Viterbi, "Wireless digital communications: A view based on three lessons learned," *IEEE Communications Magazine*, pp. 33–36, September 1991.
- [31] D. Greenwood and L. Hanzo, "Characterisation of mobile radio channels," in Steele [9], ch. 2, pp. 92–185.
- [32] L. Hanzo and J. P. Woodard, "An intelligent multimode voice communications system for indoor communications," *IEEE Transactions on Vehicular Technology*, vol. 44, pp. 735–748, Nov 1995. ISSN 0018-9545.
- [33] L. Hanzo, R. A. Salami, R. Steele, and P. Fortune, "Transmission of digitally encoded speech at 1.2 kbaud for PCN," *IEE Proceedings, Part I*, vol. 139, pp. 437–447, August 1992.

- [34] K. H. H. Wong and L. Hanzo, "Channel coding," in Steele [9], ch. 4, pp. 347–488.
- [35] W. C. Jakes, ed., *Microwave Mobile Communications*. John Wiley and Sons, 1974. ISBN 0-471-43720-4.
- [36] W. Lee, *Mobile cellular communications*. New York: McGraw Hill, 1989.
- [37] R. Steele, "Towards a high capacity digital cellular mobile radio system," *Proc. of the IEE*, vol. 132, Part F, pp. 405–415, August 1985.
- [38] R. Steele and V. Prabhu, "High-user density digital cellular mobile radio system," *IEE Proc.*, vol. 132, Part F, pp. 396–404, August 1985.
- [39] R. Steele, "The cellular environment of lightweight hand-held portables," *IEEE Communications Magazine*, pp. 20–29, July 1989.
- [40] L. Hanzo and J. Stefanov, "The Pan-European Digital Cellular Mobile Radio System – known as GSM," in Steele [9], ch. 8, pp. 677–765.
- [41] P. Mermelstein, "The IS-54 digital cellular standard," in Gibson [283], ch. 26, pp. 419–429.
- [42] K. Kinoshita and M. Nakagawa, "Japanese cellular standard," in Gibson [283], ch. 28, pp. 449–461.
- [43] L. Hanzo, "The British cordless telephone system: CT2," in Gibson [283], ch. 29, pp. 462–477.
- [44] S. Asghar, "Digital European Cordless Telephone," in Gibson [283], ch. 30, pp. 478–499.
- [45] J. Parsons and J. Gardiner, *Mobile communication systems*. London: Blackie, 1989.
- [46] D. Parsons, *The mobile radio propagation channel*. London: Pentech Press, 1992.
- [47] I. J. Wassell and R. Steele, "Wideband systems," in Steele [9], ch. 6, pp. 523–600.
- [48] R. Edwards and J. Durkin, "Computer prediction of service area for VHF mobile radio networks," *Proc IRE 116 (9)*, pp. 1493–1500, 1969.
- [49] M. Hata, "Empirical formula for propagation loss in land mobile radio," *IEEE Trans. on Vehicular Technology*, vol. 29, pp. 317–325, August 1980.
- [50] Y. Okumura, E. Ohmori, T. Kawano, and K. Fukuda, "Field strength and its variability in VHF and UHF land mobile service," *Review of the Electrical Communication Laboratory*, vol. 16, pp. 825–873, September-October 1968.
- [51] J. G. Proakis, *Digital Communications*. McGraw Hill, 3rd ed., 1995.
- [52] M. J. Gans, "A power-spectral theory of propagation in the mobile-radio environment," *IEEE Trans. on Vehicular Technology*, vol. 21, pp. 27–38, Feb. 1972.
- [53] W. H. Press, S. A. Teukolsky, W. T. Vetterling, and B. P. Flannery, "Random numbers," in *Numerical Recipes in C* [140], ch. 7, pp. 289–290.

- [54] R. Hamming, "Error detecting and error correcting codes," *Bell Sys. Tech. J.*, 29, pp. 147–160, 1950.
- [55] P. Elias, "Coding for noisy channels," *IRE Conv. Rec. pt.4*, pp. 37–47, 1955.
- [56] J. Wozencraft, "Sequential decoding for reliable communication," *IRE Natl. Conv. Rec.*, vol. 5, pt.2, pp. 11–25, 1957.
- [57] J. Wozencraft and B. Reiffen, *Sequential decoding*. MIT Press, Cambridge, Mass., 1961.
- [58] R. Fano, "A heuristic discussion of probabilistic coding," *IEEE Trans. Info. Theory*, vol. IT-9, pp. 64–74, April 1963.
- [59] J. Massey, *Threshold decoding*. MIT Press, Cambridge, Mass., 1963.
- [60] A. Viterbi, "Error bounds for convolutional codes and an asymptotically optimum decoding algorithm," *IEEE Trans. Info. Theory*, vol. IT-13, pp. 260–269, April 1967.
- [61] G. D. Forney, "The Viterbi algorithm," *Proceedings of the IEEE*, vol. 61, pp. 268–278, March 1973.
- [62] J. Heller and I. Jacobs, "Viterbi decoding for satellite and space communication," *IEEE Trans. Commun. Technol.*, vol. COM-19, pp. 835–848, October 1971.
- [63] L. Bahl, J. Cocke, F. Jelinek, and J. Raviv, "Optimal decoding of linear codes for minimising symbol error rate," *IEEE Transactions on Information Theory*, vol. 20, pp. 284–287, March 1974.
- [64] A. Hocquenghem, "Codes correcteurs d'erreurs," *Chiffres (Paris)*, vol. 2, pp. 147–156, September 1959.
- [65] R. Bose and D. Ray-Chaudhuri, "On a class of error correcting binary group codes," *Information and Control*, vol. 3, pp. 68–79, March 1960.
- [66] R. Bose and D. Ray-Chaudhuri, "Further results on error correcting binary group codes," *Information and Control*, vol. 3, pp. 279–290, September 1960.
- [67] W. Peterson, "Encoding and error correction procedures for the Bose-Chaudhuri codes," *IRE Trans. Inform. Theory*, vol. IT-6, pp. 459–470, September 1960.
- [68] D. Gorenstein and N. Zierler, "A class of cyclic linear error-correcting codes in  $p^m$  symbols," *J. Soc. Ind. Appl. Math.*, 9, pp. 107–214, June 1961.
- [69] I. Reed and G. Solomon, "Polynomial codes over certain finite fields," *J. Soc. Ind. Appl. Math.*, vol. 8, pp. 300–304, June 1960.
- [70] E. Berlekamp, "On decoding binary Bose-Chaudhuri-Hocquenghem codes," *IEEE Trans. Info. Theory*, vol. 11, pp. 577–579, 1965.
- [71] J. Massey, "Step-by-step decoding of the Bose-Chaudhuri-Hocquenghem codes," *IEEE Trans. Info. Theory*, vol. 11, pp. 580–585, 1965.
- [72] Consultative Committee for Space Data Systems, "Blue book," *Recommendations for Space Data System Standards: Telemetry Channel Coding*, May 1984.
- [73] W. Peterson, *Error correcting codes*. Cambridge, Mass, USA: MIT. Press, 1st ed., 1961.

- [74] V. Pless, *Introduction to the theory of error-correcting codes*. John Wiley and Sons, 1982. ISBN: 0471813044.
- [75] I. Blake, ed., *Algebraic coding theory: History and development*. Dowden, Hutchinson and Ross Inc., 1973.
- [76] R. Lidl and H. Niederreiter, *Finite Fields*. Cambridge University Press, October 1996.
- [77] D. Gorenstein and N. Zierler, "A class of error-correcting codes in  $p^m$  symbols," *J.Soc.Ind.Appl.Math.*, no. 9, pp. 207–214, 1961.
- [78] J. Makhoul, "Linear prediction: A tutorial review," *Proceedings of the IEEE*, vol. 63, pp. 561–580, April 1975.
- [79] R. Blahut, *Fast algorithms for digital signal processing*. Addison-Wesley Publishing Company, 1985. ISBN 0-201-10155-6.
- [80] J. Schur, "Ueber Potenzreihen, die im Innern des Einheitskreises beschränkt sind," *Journal fuer Mathematik*, pp. 205–232. Bd. 147, Heft 4.
- [81] R. Chien, "Cyclic decoding procedure for the Bose-Chaudhuri-Hocquenghem codes," *IEEE Trans. on Info. Theory*, vol. 10, pp. 357–363, October 1964.
- [82] A. Jennings, *Matrix computation for engineers and scientists*. J. Wiley and Sons Ltd., 1977.
- [83] G. Forney, Jr, "On decoding BCH codes," *IEEE Tr. on Inf. Theory*, vol. IT-11, pp. 549–557, 1965.
- [84] Y. Sugiyama, M. Kasahara, S. Hirasawa, and T. Namekawa, "A method for solving key equation for decoding goppa codes," *Inf. Control*, no. 27, pp. 87–99, 1975.
- [85] S. Golomb, *Shift register sequences*. Laugana Hills, CA: Aegean Park Press, 1982.
- [86] A. Urie, M. Streeton, and C. Mourot, "An advanced TDMA mobile access system for UMTS," *IEEE Comms. Mag.*, pp. 38–47, February 1995.
- [87] "European RACE D731 public deliverable," September 1995. Mobile communication networks, general aspects and evolution.
- [88] Telcomm. Industry Association (TIA), Washington, DC, *Dual-mode subscriber equipment - Network equipment compatibility specification, Interim Standard IS-54*, 1989.
- [89] Research and Development Centre for Radio Systems, Japan, *Public Digital Cellular (PDC) Standard, RCR STD-27*.
- [90] "Feature topic: Software Radios," *IEEE Communications Magazine*, vol. 33, pp. 24–68, May 1995.
- [91] G. D. Forney Jr, R. G. Gallager, G. R. Lang, F. M. Longstaff, and S. U. Qureshi, "Efficient modulation for band-limited channels," *IEEE Journal on Selected Areas in Communications*, vol. 2, pp. 632–647, Sept 1984.
- [92] K. Feher, "Modems for emerging digital cellular mobile systems," *IEEE Tr. on VT*, vol. 40, pp. 355–365, May 1991.

- [93] W. Webb, L. Hanzo, and R. Steele, "Bandwidth-efficient QAM schemes for rayleigh-fading channels," *IEE Proceedings*, vol. 138, pp. 169–175, June 1991.
- [94] A. Wright and W. Durtler, "Experimental performance of an adaptive digital linearized power amplifier," *IEEE Tr. on VT*, vol. 41, pp. 395–400, November 1992.
- [95] M. Faulkner and T. Mattson, "Spectral sensitivity of power amplifiers to quadrature modulator misalignment," *IEEE Tr. on VT*, vol. 41, pp. 516–525, November 1992.
- [96] P. Kenington, R. Wilkinson, and J. Marvill, "Broadband linear amplifier design for a PCN base-station," in *Proceedings of IEEE Vehicular Technology Conference (VTC'91)*, (St. Louis, MO, USA), pp. 155–160, IEEE, 19–22 May 1991.
- [97] R. Wilkinson et al, "Linear transmitter design for MSAT terminals," in *Proc. of 2nd Int. Mobile Satellite Conference*, June 1990.
- [98] S. Stapleton and F. Costescu, "An adaptive predistorter for a power amplifier based on adjacent channel emissions," *IEEE Tr. on VT*, vol. 41, pp. 49–57, February 1992.
- [99] S. Stapleton, G. Kandola, and J. Cavers, "Simulation and analysis of an adaptive predistorter utilizing a complex spectral convolution," *IEEE Tr. on VT*, vol. 41, pp. 387–394, November 1992.
- [100] Y. Kamio, S. Sampei, H. Sasaoka, and N. Morinaga, "Performance of modulation-level-control adaptive-modulation under limited transmission delay time for land mobile communications," in *Proceedings of IEEE Vehicular Technology Conference (VTC'95)*, (Chicago, USA), pp. 221–225, IEEE, July 15–28 1995.
- [101] J. M. Torrance and L. Hanzo, "Upper bound performance of adaptive modulation in a slow Rayleigh fading channel," *Electronics Letters*, vol. 32, pp. 718–719, 11 April 1996.
- [102] J. M. Torrance and L. Hanzo, "Optimisation of switching levels for adaptive modulation in a slow Rayleigh fading channel," *Electronics Letters*, vol. 32, pp. 1167–1169, 20 June 1996.
- [103] J. M. Torrance and L. Hanzo, "Demodulation level selection in adaptive modulation," *Electronics Letters*, vol. 32, pp. 1751–1752, 12 September 1996.
- [104] J. Torrance and L. Hanzo, "Performance upper bound of adaptive QAM in slow Rayleigh-fading environments," in *Proc. of IEEE ICCS'96 / ISPACS'96* [662], pp. 1653–1657.
- [105] J. Torrance and L. Hanzo, "Adaptive modulation in a slow Rayleigh fading channel," in *Proc. of IEEE International Symposium on Personal, Indoor, and Mobile Radio Communications (PIMRC'96)* [666], pp. 497–501.
- [106] J. M. Torrance and L. Hanzo, "Latency considerations for adaptive modulation in a slow Rayleigh fading channel," in *Proceedings of IEEE VTC '97* [665], pp. 1204–1209.

## BIBLIOGRAPHY

1067

- [107] K. Feher, ed., *Digital communications - satellite/earth station engineering*. Prentice Hall, 1983.
- [108] Y. C. Chow, A. R. Nix, and J. P. McGeehan, "Analysis of 16-APSK modulation in AWGN and rayleigh fading channel," *Electronic Letters*, vol. 28, pp. 1608–1610, November 1992.
- [109] B. Sklar, *Digital communications - Fundamentals and Applications*. Prentice Hall, 1988.
- [110] J. Torrance, "Digital modulation," phd mini-thesis, Dept. of Electronics and Computer Science, Univ. of Southampton, UK, 1996.
- [111] J. Cavers, "An analysis of pilot symbol assisted modulation for rayleigh fading channels," *IEEE Transactions on Vehicular Technology*, vol. 40, pp. 686–693, Nov 1991.
- [112] F. Adachi, "Error rate analysis of differentially encoded and detected 16APSK under rician fading," *IEEE Tr. on Veh. Techn.*, vol. 45, pp. 1–12, February 1996.
- [113] J. McGeehan and A. Bateman, "Phase-locked transparent tone in band (TTIB): A new spectrum configuration particularly suited to the transmission of data over SSB mobile radio networks," *IEEE Transactions on Communications*, vol. COM-32, no. 1, pp. 81–87, 1984.
- [114] A. Bateman and J. McGeehan, "Feedforward transparent tone in band for rapid fading protection in multipath fading," in *IEE Int. Conf. Comms.*, vol. 68, pp. 9–13, 1986.
- [115] A. Bateman and J. McGeehan, "The use of transparent tone in band for coherent data schemes," in *IEEE Int. Conf. Comms.*, (Boston, Mass, USA), 1983.
- [116] A. Bateman, G. Lightfoot, A. Lymer, and J. McGeehan, "Speech and data transmissions over a 942MHz TAB and TTIB single sideband mobile radio system," *IEEE Transactions on Vehicular Technology*, vol. VT-34, pp. 13–21, Feb 1985.
- [117] A. Bateman and J. McGeehan, "Data transmissions over UHF fading mobile radio channels," *Proc IEE Pt.F*, vol. 131, pp. 364–374, 1984.
- [118] J. McGeehan and A. Bateman, "A simple simultaneous carrier and bit synchronisation system for narrowband data transmissions," *Proc. IEE, Pt.F*, vol. 132, pp. 69–72, 1985.
- [119] J. McGeehan and A. Bateman, "Theoretical and experimental investigation of feedforward signal regeneration," *IEEE Trans. Veh. Tech.*, vol. VT-32, pp. 106–120, 1983.
- [120] A. Bateman, "Feedforward transparent tone in band: Its implementation and applications," *IEEE Trans. Veh. Tech.*, vol. 39, pp. 235–243, August 1990.
- [121] M. L. Moher and J. H. Lodge, "TCMP – a modulation and coding strategy for rician fading channels," *IEEE Journal on Selected Areas in Communications*, vol. 7, pp. 1347–1355, December 1989.



- [122] S. Sampei and T. Sunaga, "Rayleigh fading compensation method for 16-QAM in digital land mobile radio channels," in *Proceedings of IEEE Vehicular Technology Conference (VTC'89)*, (San Francisco, CA, USA), pp. 640–646, IEEE, 1–3 May 1989.
- [123] S. Haykin, *Adaptive Filter Theory*. Prentice Hall, 1991.
- [124] J. Cavers, "The performance of phase locked transparent tone in band with symmetric phase detection," *IEEE Trans. on Comms.*, vol. 39, pp. 1389–1399, September 1991.
- [125] R. Steele and W. Webb, "Variable rate QAM for data transmission over Rayleigh fading channels," in *Proceedings of Wireless '91*, (Calgary, Alberta), pp. 1–14, IEEE, 1991.
- [126] W. Webb and R. Steele, "Variable rate QAM for mobile radio," *IEEE Transactions on Communications*, vol. 43, no. 7, pp. 2223–2230, 1995.
- [127] K. Arimochi, S. Sampei, and N. Morinaga, "Adaptive modulation system with discrete power control and predistortion-type non-linear compensation for high spectral efficient and high power efficient wireless communication systems," in *Proceedings of IEEE International Symposium on Personal, Indoor and Mobile Radio Communications, PIMRC'97* [649], pp. 472–477.
- [128] M. Najjoh, S. Sampei, N. Morinaga, and Y. Kamio, "ARQ schemes with adaptive modulation/TDMA/TDD systems for wireless multimedia communication systems," in *Proceedings of IEEE International Symposium on Personal, Indoor and Mobile Radio Communications, PIMRC'97* [649], pp. 709–713.
- [129] S. Chua and A. Goldsmith, "Variable-rate variable-power mQAM for fading channels," in *Proceedings of IEEE VTC '96* [664], pp. 815–819.
- [130] A. Goldsmith and S. Chua, "Variable-rate variable-power MQAM for fading channels," *IEEE Trans. on Communications*, vol. 45, pp. 1218–1230, Oct. 1997.
- [131] A. Goldsmith, "The capacity of downlink fading channels with variable rate and power," *IEEE Tr. on Veh. Techn.*, vol. 46, pp. 569–580, Aug. 1997.
- [132] A. Goldsmith and P. P. Varaiya, "Capacity of fading channels with channel side information," *IEEE Tr. on Inf. Theory*, vol. 43, pp. 1986–1992, Nov. 1997.
- [133] M.-S. Alouini and A. Goldsmith, "Capacity of rayleigh fading channels under different adaptive transmission and diversity-combining techniques," *to appear in IEEE Tr. on Veh. Techn.*, 1999. <http://www.systems.caltech.edu>.
- [134] M.-S. Alouini and A. Goldsmith, "Area spectral efficiency of cellular mobile radio systems," *to appear IEEE Tr. on Veh. Techn.*, 1999. <http://www.systems.caltech.edu>.
- [135] A. Goldsmith and S. Chua, "Adaptive coded modulation for fading channels," *IEEE Tr. on Communications*, vol. 46, pp. 595–602, May 1998.
- [136] D. A. Pearce, A. G. Burr, and T. C. Tozer, "Comparison of counter-measures against slow Rayleigh fading for TDMA systems," in *IEE Colloquium on Advanced TDMA Techniques and Applications*, (London, UK), pp. 9/1–9/6, IEE, 28 October 1996. digest 1996/234.

## BIBLIOGRAPHY

1069

- [137] W. C. Y. Lee, "Estimate of channel capacity in Rayleigh fading environment," *IEEE Trans. on Vehicular Technology*, vol. 39, pp. 187–189, Aug 1990.
- [138] N. Morinaga, "Advanced wireless communication technologies for achieving high-speed mobile radios," *IEICE Transactions on Communications*, vol. 78, no. 8, pp. 1089–1094, 1995.
- [139] J. Woodard and L. Hanzo, "A low delay multimode speech terminal," in *Proceedings of IEEE VTC '96* [664], pp. 213–217.
- [140] W. H. Press, S. A. Teukolsky, W. T. Vetterling, and B. P. Flannery, *Numerical Recipes in C*. Cambridge University Press, 1992.
- [141] J. Torrance and L. Hanzo, "Statistical multiplexing for mitigating latency in adaptive modems," in *Proceedings of IEEE International Symposium on Personal, Indoor and Mobile Radio Communications, PIMRC'97* [649], pp. 938–942.
- [142] J. Torrance, L. Hanzo, and T. Keller, "Interference resilience of burst-by-burst adaptive modems," in *Proceeding of ACTS Mobile Communication Summit '97* [661], pp. 489–494.
- [143] C. Wong, T. Liew, and L. Hanzo, "Blind modem mode detection aided block turbo coded burst-by-burst wideband adaptive modulation," in *Proceeding of ACTS Mobile Communication Summit '99* [658].
- [144] C. Wong and L. Hanzo, "Channel capacity upper-bound of a wideband burst-by-burst adaptive modem," in *Proceeding of VTC'99 (Spring)* [657].
- [145] K. Narayanan and L. Cimini, "Equalizer adaptation algorithms for high speed wireless communications," in *Proceedings of IEEE VTC '96* [664], pp. 681–685.
- [146] J. Wu and A. H. Aghvami, "A new adaptive equalizer with channel estimator for mobile radio communications," *IEEE Transactions on Vehicular Technology*, vol. 45, pp. 467–474, August 1996.
- [147] Y. Gu and T. Le-Ngoc, "Adaptive combined DFE/MLSE techniques for ISI channels," *IEEE Transactions on Communications*, vol. 44, pp. 847–857, July 1996.
- [148] A. Clark and R. Harun, "Assessment of kalman-filter channel estimators for an HF radio link," *IEE Proceedings*, vol. 133, pp. 513–521, Oct 1986.
- [149] M. Zimmermann and A. Kirsch, "The AN/GSC-10/KATHRYN/ variable rate data modem for HF radio," *IEEE Trans. Commun. Techn.*, vol. CCM-15, pp. 197–205, April 1967.
- [150] E. Powers and M. Zimmermann, "A digital implementation of a multichannel data modem," in *Proc. of the IEEE Int. Conf. on Commun.*, (Philadelphia, USA), 1968.
- [151] B. Saltzberg, "Performance of an efficient parallel data transmission system," *IEEE Trans. Commun. Techn.*, pp. 805–813, December 1967.
- [152] R. Chang and R. Gibby, "A theoretical study of performance of an orthogonal multiplexing data transmission scheme," *IEEE Trans. Commun. Techn.*, vol. COM-16, pp. 529–540, August 1968.

- [153] S. Weinstein and P. Ebert, "Data transmission by frequency division multiplexing using the discrete fourier transform," *IEEE Trans. Commun. Techn.*, vol. COM-19, pp. 628-634, October 1971.
- [154] Peled and A. Ruiz, "Frequency domain data transmission using reduced computational complexity algorithms," in *Proceedings of International Conference on Acoustics, Speech, and Signal Processing, ICASSP'80* [650], pp. 964-967.
- [155] B. Hirosaki, "An orthogonally multiplexed QAM system using the discrete fourier transform," *IEEE Trans. Commun.*, vol. COM-29, pp. 983-989, July 1981.
- [156] L. J. Cimini, "Analysis and simulation of a digital mobile channel using orthogonal frequency division multiplexing," *IEEE Transactions on Communications*, vol. 33, pp. 665-675, July 1985.
- [157] K. Kammeyer, U. Tuisel, H. Schulze, and H. Bochmann, "Digital multicarrier transmission of audio signals over mobile radio channels," *European Transactions on Telecommunications*, vol. 3, pp. 243-253, May-Jun 1992.
- [158] F. Mueller-Roemer, "Directions in audio broadcasting," *Jnl Audio Eng. Soc.*, vol. 41, pp. 158-173, March 1993.
- [159] G. Plenge, "DAB - a new radio broadcasting system - state of development and ways for its introduction," *Rundfunktech. Mitt.*, vol. 35, no. 2, 1991.
- [160] M. Alard and R. Lassalle, "Principles of modulation and channel coding for digital broadcasting for mobile receivers," *EBU Review, Technical No. 224*, pp. 47-69, August 1987.
- [161] *Proc. 1st Int. Symp., DAB*, (Montreux, Switzerland), June 1992.
- [162] I. Kalet, "The multitone channel," *IEEE Tran. on Comms*, vol. 37, pp. 119-124, February 1989.
- [163] H. Kolb, "Untersuchungen über ein digitales mehrfrequenzverfahren zur datenübertragung," in *Ausgewählte Arbeiten über Nachrichtensysteme*, no. 50, Universität Erlangen-Nürnberg, 1982.
- [164] H. Schüssler, "Ein digitales Mehrfrequenzverfahren zur Datenübertragung," in *Professoren-Konferenz, Stand und Entwicklungsaussichten der Daten und Telekommunikation*, (Darmstadt, Germany), pp. 179-196, 1983.
- [165] K. Preuss, "Ein Parallelverfahren zur schnellen Datenübertragung Im Ortsnetz," in *Ausgewählte Arbeiten über Nachrichtensysteme*, no. 56, Universität Erlangen-Nürnberg, 1984.
- [166] R. Rückriem, "Realisierung und messtechnische Untersuchung an einem digitalen Parallelverfahren zur Datenübertragung im Fernsprechkanal," in *Ausgewählte Arbeiten über Nachrichtensysteme*, no. 59, Universität Erlangen-Nürnberg, 1985.
- [167] ETSI, *Digital Audio Broadcasting (DAB)*, 2nd ed., May 1997. ETS 300 401.
- [168] ETSI, *Digital Video Broadcasting (DVB)*, 1.1.2 ed., August 1997. EN 300 744.

- [169] J. Lindner et al, "OCDM – Ein Übertragungsverfahren für lokale Funknetze," in *Codierung fuer Quelle, Kanal und Uebertragung*, no. 130 in ITG Fachbericht, pp. pp 401–409, VDE Verlag, 26-28 Oct. 1994.
- [170] K. Fazel and G. Fettweis, eds., *Multi-carrier spread-spectrum*. Kluwer, 1997. p260, ISBN 0-7923-9973-0.
- [171] T. Keller, "Orthogonal frequency division multiplex techniques for wireless local area networks," 1996. Internal Report.
- [172] S. Nanda, D. J. Goodman, and U. Timor, "Performance of PRMA: A packet voice protocol for cellular systems," *IEEE Tr. on VT*, vol. 40, pp. 584–598, August 1991.
- [173] W. Webb, R. Steele, J. Cheung, and L. Hanzo, "A packet reservation multiple access assisted cordless telecommunications scheme," *IEEE Transactions on Veh. Technology*, vol. 43, pp. 234–245, May 1994.
- [174] R. A. Salami, C. Laflamme, J.-P. Adoul, and D. Massaloux, "A toll quality 8 kb/s speech codec for the personal communications system (PCS)," *IEEE Transactions on Vehicular Technology*, pp. 808–816, August 1994.
- [175] M. Frullone, G. Riva, P. Grazioso, and C. Carciofy, "Investigation on dynamic channel allocation strategies suitable for PRMA schemes," *1993 IEEE Int. Symp. on Circuits and Systems, Chicago*, pp. 2216–2219, May 1993.
- [176] M. Frullone, G. Falciasacca, P. Grazioso, G. Riva, and A. M. Serra, "On the performance of packet reservation multiple access with fixed and dynamic channel allocation," *IEEE Tr. on Veh. Techn.*, vol. 42, pp. 78–86, Feb. 1993.
- [177] J. Leduc and P. Delogne, "Statistic for variable bit-rate digital television sources," *Signal Processing: Image Communication*, vol. 8, pp. 443–464, July 1996.
- [178] S. S. Lam, S. Chow, and D. K.Y.Yau, "A lossless smoothing algorithm for compressed video," *IEEE/ACM Transactions on networking*, vol. 4, pp. 697–708, Oct 1996.
- [179] J. Cosmas, G. Petit, R. Lehenert, C. Blondia, K. Kontovassilis, O. Casals, and T.Theimer, "A review of voice, data and video traffic models for ATM," *European Transactions on Telecommunications*, vol. 5, pp. 139–154, Mar-Apr 1994.
- [180] O. Rose and M. R. Frater, "A comparison of models for VBR traffic sources in B-ISDN," in *Proceedings of the IFIP TC6 Second International Conference on Broadband Communications*, (Paris, France), pp. 275–287, Chapman and Hall Ltd, London, Mar 2–4 1994.
- [181] D. P. Heymann and T. Lakshman, "Source models for VBR broadcast-video traffic," *IEEE/ACM Transactions on networking*, vol. 4, pp. 40–48, Feb 1996.
- [182] ITU-T, *Recommendation H.263: Video coding for low bitrate communication*, March 1996.
- [183] M. W. Whybray and W. Ellis, "H.263 - video coding recommendation for PSTN videophone and multimedia," in *IEE Colloquium (Digest)*, pp. 6/1–6/9, IEE, England, Jun 1995.

- [184] M. Khansari, A. Jalali, E. Dubois, and P. Mermelstein, "Low bit-rate video transmission over fading channels for wireless microcellular systems," *IEEE Transactions on Circuits and Systems for Video Technology*, vol. 6, pp. 1–11, February 1996.
- [185] N. Färber, E. Steinbach, and B. Girod, "Robust H.263 video transmission over wireless channels," in *Proc. of International Picture Coding Symposium (PCS)*, (Melbourne, Australia), pp. 575–578, March 1996.
- [186] P. Cherriman and L. Hanzo, "Programmable H.263-based wireless video transceivers for interference-limited environments," in *Proc. of IEEE ICCS'96 / ISPACS'96* [662], pp. 1369–1373.
- [187] P. Cherriman and L. Hanzo, "Robust H.263 video transmission over mobile channels in interference-limited environments," in *Proc of First International Workshop on Wireless Image/Video Communications*, (Loughborough, UK), pp. 1–7, 4-5 September 1996.
- [188] P. Cherriman and L. Hanzo, "Power-controlled H.263-based wireless videophone performance in interference-limited scenarios," in *Proc. of IEEE International Symposium on Personal, Indoor, and Mobile Radio Communications (PIMRC'96)* [666], pp. 158–162.
- [189] P. Cherriman and L. Hanzo, "Programmable H.263-based wireless video transceivers for interference-limited environments," *IEEE Trans. on Circuits and Systems for Video Technology*, vol. 8, pp. 275–286, June 1998.
- [190] P. Cherriman, T. Keller, and L. Hanzo, "Orthogonal frequency division multiplex transmission of H.263 encoded video over wireless ATM networks," in *Proceeding of ACTS Mobile Communication Summit '97* [661], pp. 276–281.
- [191] A. S. Tanenbaum, "Introduction to queueing theory," in *Computer Networks*, pp. 631–641, Prentice-Hall, 2nd ed., 1989. ISBN 0131668366.
- [192] P. Skelly, M. Schwartz, and S. Dixit, "A histogram-based model for video traffic behavior in a ATM multiplexer," *IEEE/ACM Trans. Networking*, vol. 1, pp. 446–459, August 1993.
- [193] D. Habibi, S. Gabrielsson, and Z. Man, "A multiplexed four layers markov model for queueing studies of MPEG traffic," in *Proc. of IEEE ICCS'96 / ISPACS'96* [662], pp. 1180–1184.
- [194] F. J. Panken, "Multiple-access protocols over the years: a taxonomy and survey," in *1996 IEEE International Conference on Communication Systems (ICCS)*, pp. 2.1.1–2.1.5, Nov. 1996.
- [195] V. Li and X. Qiu, "Personal communications systems," *Proc. of the IEEE*, vol. 83, pp. 1210–1243, September 1995.
- [196] D. J. Goodman and S. X. Wei, "Efficiency of packet reservation multiple access," *IEEE Transactions. on Vehicular Technology*, vol. 40, pp. 170–176, Feb. 1991.
- [197] J. Dunlop, D. Robertson, P. Cosimi, and J. D. Vile, "Development and optimisation of a statistical multiplexing mechanism for ATDMA," in *Proceedings of IEEE VTC '94* [663], pp. 1040–1044.

## BIBLIOGRAPHY

1073

- [198] F. D. Priscoli, "Adaptive parameter computation in a PRMA, TDD based medium access control for ATM wireless networks," in *Proceeding of IEEE Global Telecommunications Conference, Globecom 96* [651], pp. 1779–1783.
- [199] A. S. Acampora, "Wireless ATM: a perspective on issues and prospects," *IEEE Personal Communications*, vol. 3, pp. 8–17, Aug 1996.
- [200] J. Brecht, M. del Buono, and L. Hanzo, "Multiframe packet reservation multiple access using oscillation-scaled histogram-based markov modelling of video codecs," *Signal Processing: Image Communications*, vol. 12, pp. 167–182, 1998.
- [201] "Group speciale mobile (GSM) recommendation," April 1988.
- [202] V. Claus, ed., *Duden zur Informatik*. Mannheim: Dudenverlag, 1993.
- [203] M. Schwartz, *Broadband Integrated Networks*. Prentice Hall Press, March 1996. ISBN: 0135192404.
- [204] A. Safak, "Optimal channel reuse in cellular radio systems with multiple correlated log-normal interferers," *IEEE Tr. on Vech. Tech*, vol. 43, pp. 304–312, May 1994.
- [205] L.-C. Wang and C.-T. Lea, "Incoherent estimation on co-channel interference probability for microcellular systems," *IEEE Tr. on Vech. Tech*, vol. 45, pp. 164–173, Feb 1996.
- [206] C. C. Lee and R. Steele, "Signal-to-interference calculations for modern TDMA cellular communication systems," *IEE Proc. Communication*, vol. 142, pp. 21–30, Feb 1995.
- [207] P. T. Brady, "A technique for investigating on-off patterns of speech," *Bell Systems Technical Journal*, vol. 44, pp. 1–22, Jan 1965.
- [208] P. T. Brady, "A model for generating on-off speech patterns in two-way conversation," *Bell Systems Technical Journal*, vol. 48, pp. 2445–2472, Sept 1969.
- [209] D. G. Appleby and Y. F. Ko, "Frequency hopping," in Steele [9], ch. 7, pp. 601–676.
- [210] C. C. Lee, *CDMA for Cellular Mobile Radio Systems*. PhD thesis, Department of Electronics and Computer Science, University of Southampton, UK, November 1994.
- [211] W. C. Y. Lee, "Spectrum efficiency in cellular," *IEEE Tr. on Vech. Tech*, vol. 38, pp. 69–75, May 1989.
- [212] R. R. Gejji, "Channel efficiency in digital cellular capacity," in *Proceedings of IEEE VTC '92*, vol. 2, (Denver, USA), pp. 1005–1007, May 10-13 1992.
- [213] M. Chiani, V. Tralli, and R. Verdone, "Outage and spectrum efficiency analysis in microcellular systems," in *Proceedings of IEEE VTC '93* [669], pp. 598–601.
- [214] R. Haas and J.-C. Belfiore, "Spectrum efficiency limits in mobile cellular systems," *IEEE Tr. on Vech. Tech*, vol. 45, pp. 33–40, Feb 1996.
- [215] M. Zorzi and S. Pupolin, "Outage probability in multiple access packet radio networks in the presence of fading," *IEEE Tr. on Vech. Tech*, vol. 43, pp. 604–610, Aug 1994.

- [216] N. G. Senarath and D. Everitt, "Combined analysis of transmission and traffic characteristics in micro-cellular mobile communications systems," in *Proceedings of IEEE VTC '93* [669], pp. 577–580.
- [217] A. A. Abu-Dayya and N. C. Beaulieu, "Outage probability in the presence of correlated lognormal interferers," *IEEE Tr. on Vehicular Technology*, vol. 43, pp. 33–39, Feb 1994.
- [218] Q. T. Zhang, "Outage probability in cellular mobile radio due to nakagami signal and interferers with arbitrary parameters," *IEEE Tr. on Vehicular Technology*, vol. 45, pp. 364–372, May 1996.
- [219] P. Cherriman, F. Romiti, and L. Hanzo, "Channel allocation for third-generation mobile radio systems," in *Proceeding of ACTS Mobile Communication Summit '98* [659], pp. 255–261.
- [220] P. Cherriman, F. Romiti, and L. Hanzo, "Comparative study of dynamic channel allocation algorithms." Submitted for publication in *IEEE Trans. on Vehicular Technology*, 1999.
- [221] S. W. Wales, "Technique for cochannel interference suppression in TDMA mobile radio systems," *IEE Proc. Communication*, vol. 142, no. 2, pp. 106–114, 1995.
- [222] J. Litva and T. Lo, *Digital Beamforming in Wireless Communications*. Artech House, London, 1996.
- [223] L. Godara, "Applications of antenna arrays to mobile communications, part I: Performance improvement, feasibility, and system considerations," *Proceedings of the IEEE*, vol. 85, pp. 1029–1060, July 1997.
- [224] L. Godara, "Applications of antenna arrays to mobile communications, part II: Beam-forming and direction-of-arrival considerations," *Proceedings of the IEEE*, vol. 85, pp. 1193–1245, Aug 1997.
- [225] E. Sourour, "Time slot assignment techniques for TDMA digital cellular systems," *IEEE Trans. Vech. Tech.*, vol. 43, pp. 121–127, Feb 1994.
- [226] D. Wong and T. J. Lim, "Soft handoffs in CDMA mobile systems," *IEEE Personal Comms.*, vol. 4, pp. 6–17, December 1997.
- [227] S. Tekinay and B. Jabbari, "A measurement-based prioritisation scheme for handovers in mobile cellular networks," *IEEE JSAC*, vol. 10, no. 8, pp. 1343–1350, 1992.
- [228] G. P. Pollini, "Trends in handover design," *IEEE Comms. Mag.*, vol. 34, pp. 82–90, March 1996.
- [229] R. C. Bernhardt, "Timeslot re-assignment in a frequency reuse TDMA portable radio system," *IEEE Tr. on Vech. Tech.*, vol. 41, pp. 296–304, August 1992.
- [230] A. J. Viterbi, *CDMA: Principles of Spread Spectrum Communication*. Addison-Wesley, June 1995. ISBN 0201633744.
- [231] R. Prasad, *CDMA for Wireless Personal Communications*. Artech House, May 1996. ISBN 0890065713.

## BIBLIOGRAPHY

1075

- [232] S. Glisic and B. Vucetic, *Spread Spectrum CDMA Systems for Wireless Communications*. Artech House, April 1997. ISBN 0890068585.
- [233] S. Glisic and P. A. Leppanen, eds., *Wireless Communications : TDMA versus CDMA*. Kluwer Academic Publishers, June 1997. ISBN 0792380053.
- [234] A. H. M. Ross and K. S. Gilhousen, "CDMA technology and the IS-95 north american standard," in Gibson [283], ch. 27, pp. 430–448.
- [235] ETSI, *Universal Mobile Telecommunications Systems (UMTS); UMTS Terrestrial Radio Access (UTRA); Concept evaluation*, Dec 1997. TR 101 146 V3.0.0.
- [236] I. Katzela and M. Naghshineh, "Channel assignment schemes for cellular mobile telecommunication systems: A comprehensive survey," *IEEE Personal Comms.*, pp. 10–31, June 1996.
- [237] S. Tekinay and B. Jabbari, "Handover and channel assignment in mobile cellular networks," *IEEE Comms. Mag.*, pp. 42–46, November 1991.
- [238] B. Jabbari, "Fixed and dynamic channel assignment," in Gibson [283], ch. 83, pp. 1175–1181.
- [239] J. Zander, "Radio resource management in future wireless networks: Requirements and limitations," *IEEE Comms. Magazine*, pp. 30–36, Aug 1997.
- [240] D. E. Everitt, "Traffic engineering of the radio interface for cellular mobile networks," *Proc. of the IEEE*, vol. 82, pp. 1371–1382, Sept 1994.
- [241] J. Dahlin, "Ericsson's multiple reuse pattern for DCS1800," *Mobile Communications International*, November 1996.
- [242] M. Madfors, K. Wallstedt, S. Magnusson, H. Olofsson, P.-O. Backman, and S. Engström, "High capacity with limited spectrum in cellular systems," *IEEE Comms. Mag.*, vol. 35, pp. 38–45, August 1997.
- [243] H. Jiang and S. S. Rappaport, "Prioritized channel borrowing without locking: a channel sharing strategy for cellular communications," *IEEE/ACM Transactions on Networking*, vol. 43, pp. 163–171, April 1996.
- [244] L. G. Anderson, "A simulation study of some dynamic channel assignment algorithms in a high capacity mobile telecommunications system," *IEEE Trans. on Communication*, vol. 21, pp. 1294–1301, November 1973.
- [245] J. S. Engel and M. M. Peritsky, "Statistically optimum dynamic server assignment in systems with interfering servers," *IEEE Trans. on Vehicular Tech.*, vol. 22, pp. 203–209, Nov 1973.
- [246] M. Zhang and T.-S. P. Yum, "Comparisons of channel assignment strategies in cellular mobile telephone systems," *IEEE Trans. on Vehicular Tech.*, vol. 38, pp. 211–215, Nov 1989.
- [247] S. M. Elnoubi, R. Singh, and S. C. Gupta, "A new frequency channel assignment algorithm in high capacity mobile communications systems," *IEEE Trans. on Vehicular Tech.*, vol. 31, pp. 125–131, Aug 1982.
- [248] M. Zhang and T.-S. P. Yum, "The non-uniform compact pattern allocation algorithm for cellular mobile systems," *IEEE Trans. on Vehicular Tech.*, vol. 40, pp. 387–391, May 1991.



- [249] S. S. Kuek and W. C. Wong, "Ordered dynamic channel assignment scheme with reassignment in highway microcell," *IEEE Trans. on Vehicular Tech.*, vol. 41, pp. 271–277, Aug 1992.
- [250] T.-S. P. Yum and W.-S. Wong, "Hot spot traffic relief in cellular systems," *IEEE Journal on selected areas in Comms.*, vol. 11, pp. 934–940, Aug 1993.
- [251] J. Tajima and K. Imamura, "A strategy for flexible channel assignment in mobile communication systems," *IEEE Trans. on Vehicular Tech.*, vol. 37, pp. 92–103, May 1988.
- [252] ETSI, *Digital European Cordless Telecommunications (DECT)*, 1st ed., October 1992. ETS 300 175-1 – ETS 300 175-9.
- [253] R. Steele, "Digital European Cordless Telecommunications (DECT) systems," in *Mobile Radio Communications* [9], ch. 1.7.2, pp. 79–83.
- [254] H. Ochsner, "The digital european cordless telecommunications specification, DECT," in Tuttlebee [255], pp. 273–285. ISBN 3540196331.
- [255] W. H. Tuttlebee, ed., *Cordless telecommunications in Europe : the evolution of personal communications*. London: Springer-Verlag, 1990. ISBN 3540196331.
- [256] A. Law and L. B. Lopes, "Performance comparison of DCA call assignment algorithms within DECT," in *Proceedings of IEEE VTC '96* [664], pp. 726–730.
- [257] H. Salgado-Galicia, M. Sirbu, and J. M. Peha, "A narrowband approach to efficient PCS spectrum sharing through decentralized DCA access policies," *IEEE Personal Communications*, pp. 24–34, Feb 1997.
- [258] R. Steele, J. Whitehead, and W. C. Wong, "System aspects of cellular radio," *IEEE Communications Magazine*, vol. 33, pp. 80–86, Jan 1995.
- [259] J. C. I. Chuang, "Performance issues and algorithms for dynamic channel assignment," *IEEE JSAC*, vol. 11, pp. 955–963, August 1993.
- [260] D. C. Cox and D. O. Reudink, "The behavior of dynamic channel-assignment mobile communications systems as a function of number of radio channels," *IEEE Trans. on Communications*, vol. 20, pp. 471–479, June 1972.
- [261] D. D. Dimitrijević and J. Vučerić, "Design and performance analysis of the algorithms for channel allocation in cellular networks," *IEEE Trans. on Vehicular Tech.*, vol. 42, pp. 526–534, Nov 1993.
- [262] D. C. Cox and D. O. Reudink, "Increasing channel occupancy in large scale mobile radio systems: Dynamic channel reassignment," *IEEE Trans. on Vehicular Tech.*, vol. 22, pp. 218–222, Nov 1973.
- [263] D. C. Cox and D. O. Reudink, "A comparison of some channel assignment strategies in large-scale mobile communications systems," *IEEE Trans. on Communications*, vol. 20, pp. 190–195, April 1972.
- [264] M. M. L. Cheng and J. C. I. Chuang, "Performance evaluation of distributed measurement-based dynamic channel assignment in local wireless communications," *IEEE JSAC*, vol. 14, pp. 698–710, May 1996.

## BIBLIOGRAPHY

1077

- [265] S. A. Grandhi, R. D. Yates, and D. J. Goodman, "Resource allocation for cellular radio systems," *IEEE Trans. Veh. Tech.*, vol. 46, pp. 581–587, Aug 1997.
- [266] J. C. I. Chuang and N. R. Sollenberger, "Performance of autonomous dynamic channel assignment and power control for TDMA/FDMA wireless access," *IEEE JSAC*, vol. 12, pp. 1314–1323, October 1994.
- [267] M. Serizawa and D. J. Goodman, "Instability and deadlock of distributed dynamic channel allocation," in *Proceedings of IEEE VTC '93*, (Secaucus, New Jersey, USA), pp. 528–531, May 18–20 1993.
- [268] Y. Akaiwa and H. Andoh, "Channel segregation - a self-organized dynamic channel allocation method: Application to tdma/fdma microcellular system," *IEEE Journal on Selected Areas in Comms.*, vol. 11, pp. 949–954, Aug 1993.
- [269] A. Baiocchi, F. D. Priscoli, F. Grilli, and F. Sestini, "The geometric dynamic channel allocation as a practical strategy in mobile networks with bursty user mobility," *IEEE Trans. on Veh. Tech.*, vol. 44, pp. 14–23, Feb 1995.
- [270] F. D. Priscoli, N. P. Magnani, V. Palestini, and F. Sestini, "Application of dynamic channel allocation strategies to the GSM cellular network," *IEEE Journal on Selected Areas in Comms.*, vol. 15, pp. 1558–1567, Oct 1997.
- [271] I. ChihLin and C. PiHui, "Local packing - distributed dynamic channel allocation at cellular base station," in *Proceedings of IEEE Globecom '93*, vol. 1, (Houston, TX, USA), pp. 293–301, Nov 29–Dec 2 1993.
- [272] E. D. Re, R. Fantacci, and G. Giambene, "Handover and dynamic channel allocation techniques in mobile cellular networks," *IEEE Trans. on Veh. Tech.*, vol. 44, pp. 229–237, May 1995.
- [273] T. J. Kahwa and N. D. Georganas, "A hybrid channel assignment scheme in large-scale, cellular-structured mobile communication systems," *IEEE Trans. on Communications*, vol. 26, pp. 432–438, April 1978.
- [274] J. K. S. Sin and N. D. Georganas, "A simulation study of a hybrid channel assignment scheme for cellular land-mobile radio systems with erlang-c service," *IEEE Trans. on Communications*, vol. 29, pp. 143–147, Feb 1981.
- [275] S.-H. Oh and D.-W. Tcha, "Prioritized channel assignment in a cellular radio network," *IEEE Trans. on Communications*, vol. 40, pp. 1259–1269, July 1992.
- [276] D. Hong and S. S. Rappaport, "Traffic model and performance analysis for cellular mobile radio telephone systems with prioritized and nonprioritized handoff procedures," *IEEE Trans. on Vehicular Technology*, vol. 35, pp. 77–92, Aug 1986.
- [277] R. Guérin, "Queueing-blocking system with two arrival streams and guard channels," *IEEE Trans. on Communications*, vol. 36, pp. 153–163, Feb 1988.
- [278] S. A. Grandhi, R. Vijayan, D. J. Goodman, and J. Zander, "Centralized power control in cellular radio systems," *IEEE Trans. Veh. Tech.*, vol. 42, pp. 466–468, Nov 1993.

- [279] J. Zander, "Performance of optimum transmitter power control in cellular radio systems," *IEEE Tr. on Vehicular Technology*, vol. 41, pp. 57–62, Feb 1992.
- [280] J. Zander, "Distributed cochannel interference control in cellular radio systems," *IEEE Tr. on Vehicular Technology*, vol. 41, pp. 305–311, Aug 1992.
- [281] D. C. Cox and D. O. Reudink, "Effects of some nonuniform spatial demand profiles on mobile radio system performance," *IEEE Trans. on Vehicular Tech.*, vol. 21, pp. 62–67, May 1972.
- [282] M. Sonka, V. Hlavac, and R. Boyle, "Image pre-processing," in *Image Processing, Analysis and Machine Vision*, ch. 4, pp. 59–61, London: Chapman and Hall, 1st ed., 1993.
- [283] J. D. Gibson, ed., *The Mobile Communications Handbook*. CRC Press and IEEE Press, 1996.
- [284] "Special issue: The European Path Toward UMTS," *IEEE Personal Communications: The magazine of nomadic communications and computing*, vol. 2, Feb 1995.
- [285] European Commission, *Advanced Communications Technologies and Services (ACTS)*, Aug 1994. Workplan DGXIII-B-RA946043-WP.
- [286] Telcomm. Industry Association (TIA), Washington, DC, *Mobile station - Base station compatibility standard for dual-mode wideband spread spectrum cellular system, EIA/TIA Interim Standard IS-95*, 1993.
- [287] P. Baier, P. Jung, and A. Klein, "Taking the challenge of multiple access for third-generation cellular mobile radio systems - a european view," *IEEE Comms. Mag.*, vol. 34, pp. 82–89, February 1996.
- [288] F. Adachi, M. Sawahashi, and K. Okawa, "Tree-structured Generation of Orthogonal Spreading Codes with Different Lengths for Forward Link of DS-CDMA Mobile Radio," *Electronic Letters*, vol. 33, pp. 27–28, January 1997.
- [289] F. Adachi, K. Ohno, A. Higashi, T. Dohi, and Y. Okumura, "Coherent multicode DS-CDMA mobile Radio Access," *IEICE Transactions on Communications*, vol. E79-B, pp. 1316–1324, September 1996.
- [290] F. Adachi and M. Sawahashi, "Wideband Wireless Access Based on DS-CDMA," *IEICE Transactions on Communications*, vol. E81-B, pp. 1305–1316, July 1998.
- [291] F. Adachi, M. Sawahashi, and H. Suda, "Wideband DS-CDMA for Next-generation Mobile Communications Systems," *IEEE Communications Magazine*, vol. 36, pp. 56–69, September 1998.
- [292] D. N. Knisely, S. Kumar, S. Laha, and S. Nanda, "Evolution of Wireless Data Services : IS-95 to cdma2000," *IEEE Communications Magazine*, vol. 36, pp. 140–149, October 1998.
- [293] TIA, "The cdma2000 ITU-R RTT Candidate Submission," tech. rep., Telecommunications Industry Association, 1998.
- [294] D. N. Knisely, Q. Li, and N. S. Rames, "cdma2000 : A Third Generation Radio Transmission Technology," *Bell Labs Technical Journal*, vol. 3, pp. 63–78, July-September 1998.

- [295] "Feature topic: Wireless Personal Communications," *IEEE Personal Communications*, vol. 2, April 1995.
- [296] "Feature topic: Universal Telecommunications at the beginning of the 21st century," *IEEE Communications Magazine*, vol. 33, November 1995.
- [297] "Feature topic: Wireless Personal Communications," *IEEE Communications Magazine*, vol. 33, January 1995.
- [298] "Feature topic: European research in mobile communications," *IEEE Communications Magazine*, vol. 34, February 1996.
- [299] R. V. Cox and P. Kroon, "Low bit-rate speech coders for multimedia communications," *IEEE Comms. Mag.*, pp. 34–41, December 1996.
- [300] A. D. Kucar, "Mobile radio: An overview," in Gibson [283], ch. 15, pp. 242–262.
- [301] C. Li, C. Zheng, and C. Tai, "Detection of ECG characteristic points using wavelet transforms," *IEEE Transactions in Biomedical Engineering*, vol. 42, pp. 21–28, January 1995.
- [302] "Personal handy phone (PHP) system." RCR Standard, STD-28, Japan.
- [303] P. Vary and R. Sluyter, "MATS-D speech codec: Regular-pulse excitation LPC," in *Proc. of the Nordic Seminar on Digital Land Mobile Radio Communications (DMR11)*, (Stockholm, Sweden), pp. 257–261, October 1986.
- [304] R. A. Salami, L. Hanzo, R. Steele, K. H. J. Wong, and I. Wassell, "Speech coding," in Steele [9], ch. 3, pp. 186–346.
- [305] R. Steele and L. Hanzo, eds., *Mobile Radio Communications*. IEEE Press-John Wiley, 2 ed., 1999.
- [306] J. Rapeli, "UMTS:targets, system concept, and standardization in a global framework," *IEEE Personal Communications*, vol. 2, pp. 20–28, February 1995.
- [307] P.-G. Andermo and L.-M. Ewerbring, "A CDMA-based radio access design for UMTS," *IEEE Personal Communications*, vol. 2, pp. 48–53, February 1995.
- [308] E. Nikula, A. Toskala, E. Dahlman, L. Girard, and A. Klein, "FRAMES multiple access for UMTS and IMT-2000," *IEEE Personal Communications*, vol. 5, pp. 16–24, April 1998.
- [309] T. Ojanperä and R. Prasad, "An overview of air interface multiple access for IMT-2000/UMTS," *IEEE Communications Magazine*, vol. 36, pp. 82–95, September 1998.
- [310] A. Toskala, J. P. Castro, E. Dahlman, M. Latva-aho, and T. Ojanperä, "FRAMES FMA2 wideband-CDMA for UMTS," *European Transactions on Telecommunications*, vol. 9, pp. 325–336, July-August 1998.
- [311] E. Berruto, M. Gudmundson, R. Menolascino, W. Mohr, and M. Pizarroso, "Research activities on UMTS radio interface, network architectures, and planning," *IEEE Communications Magazine*, vol. 36, pp. 82–95, February 1998.
- [312] M. H. Callendar, "Future public land mobile telecommunication systems," *IEEE Personal Communications*, vol. 12, no. 4, pp. 18–22, 1994.

- [313] W. C. Y. Lee, "Overview of cellular CDMA," *IEEE Transactions on Vehicular Technology*, vol. 40, pp. 291–302, May 1991.
- [314] K. S. Gilhousen, I. M. Jacobs, R. Padovani, A. J. Viterbi, L. A. Weaver Jr, and C. E. Wheatley III, "On the capacity of a cellular CDMA system," *IEEE Transactions on Vehicular Technology*, vol. 40, pp. 303–312, May 1991.
- [315] R. L. Pickholtz, L. B. Milstein, and D. L. Schilling, "Spread spectrum for mobile communications," *IEEE Transactions on Vehicular Technology*, vol. 40, pp. 312–322, May 1991.
- [316] R. Kohno, R. Meidan, and L. B. Milstein, "Spread spectrum access methods for wireless communication," *IEEE Communications Magazine*, vol. 33, pp. 58–67, January 1995.
- [317] V. K. Garg, K. F. Smolik, J. E. Wilkes, and K. Smolik, *Applications of CDMA in Wireless/Personal Communications*. Prentice-Hall, 1996.
- [318] R. Price and E. P. Green, Jr., "A communication technique for multipath channels," *Proceedings of the IRE*, vol. 46, pp. 555–570, March 1958.
- [319] B. Sklar, "Rayleigh fading channels in mobile digital communication systems part I : Characterization," *IEEE Communications Magazine*, vol. 35, pp. 90–100, July 1997.
- [320] B. Sklar, "Rayleigh fading channels in mobile digital communication systems part II : Mitigation," *IEEE Communications Magazine*, vol. 35, pp. 148–155, July 1997.
- [321] F. Amoroso, "Use of DS/SS signaling to mitigate rayleigh fading in a dense scatterer environment," *IEEE Personal Communications*, vol. 3, pp. 52–61, April 1996.
- [322] M. Nakagami, "The  $m$ -distribution—a general formula of intensity distribution of fading," *Statistical Methods in Radio Wave Propagation*. W.C. Hoffman, Ed. New York:Pergamon, 1960.
- [323] H. Suzuki, "A statistical model for urban multipath propagation," *IEEE Transactions on Communications*, vol. COM-25, pp. 673–680, July 1977.
- [324] "COST 207: Digital land mobile radio communications, final report." Office for Official Publications of the European Communities, 1989. Luxembourg.
- [325] M. Whitmann, J. Marti, and T. Kürner, "Impact of the power delay profile shape on the bit error rate in mobile radio systems," *IEEE Transactions on Vehicular Technology*, vol. 46, pp. 329–339, May 1997.
- [326] T. Eng, N. Kong, and L. B. Milstein, "Comparison of diversity combining techniques for Rayleigh-fading channels," *IEEE Transactions on Communications*, vol. 44, pp. 1117–1129, September 1996.
- [327] M. Kavehrad and P. J. McLane, "Performance of low-complexity channel coding and diversity for spread spectrum in indoor, wireless communications," *AT&T Technical Journal*, vol. 64, pp. 1927–1965, October 1985.
- [328] K.-T. Wu and S.-A. Tsaur, "Selection diversity for DS-SSMA communications on nakagami fading channels," *IEEE Transactions on Vehicular Technology*, vol. 43, pp. 428–438, August 1994.

- [329] L.-L. Yang and L. Hanzo, "Serial acquisition techniques for DS-CDMA signals in frequency-selective multi-user mobile channels," in *Proceeding of VTC'99 (Spring)* [657].
- [330] L.-L. Yang and L. Hanzo, "Serial acquisition of DS-CDMA signals in multipath fading mobile channels." submitted to *IEEE Transactions on Vehicular Technology*, 1998.
- [331] R. E. Ziemer and R. L. Peterson, *Digital Communications and Spread Spectrum System*. New York: Macmillan Publishing Company, 1985.
- [332] R. L. Pickholtz, D. L. Schilling, and L. B. Milstein, "Theory of spread-spectrum communications - a tutorial," *IEEE Transactions on Communications*, vol. COM-30, pp. 855–884, May 1982.
- [333] S. S. Rappaport and D. M. Grieco, "Spread-spectrum signal acquisition: Methods and technology," *IEEE Communications Magazine*, vol. 22, pp. 6–21, June 1984.
- [334] E. G. Ström, S. Parkvall, S. L. Miller, and B. E. Ottersten, "Propagation delay estimation in asynchronous direct-sequence code division multiple access systems," *IEEE Transactions on Communications*, vol. 44, pp. 84–93, January 1996.
- [335] R. R. Rick and L. B. Milstein, "Optimal decision strategies for acquisition of spread-spectrum signals in frequency-selective fading channels," *IEEE Transactions on Communications*, vol. 46, pp. 686–694, May 1998.
- [336] J. S. Lee, *CDMA Systems Engineering Handbook*. Artech House Publishers, 1998.
- [337] M. K. Varanasi and B. Aazhang, "Multistage detection in asynchronous code-division multiple-access communications," *IEEE Transactions on Communications*, vol. 38, pp. 509–519, April 1990.
- [338] S. Moshavi, "Multi-user detection for DS-CDMA communications," *IEEE Communications Magazine*, vol. 34, pp. 124–136, October 1996.
- [339] S. Verdu, "Minimum probability of error for asynchronous gaussian multiple-access channel," *IEEE Transactions on Communications*, vol. 32, pp. 85–96, January 1986.
- [340] E. L. Kuan and L. Hanzo, "Joint detection CDMA techniques for third-generation transceivers," in *Proceeding of ACTS Mobile Communication Summit '98* [659], pp. 727–732.
- [341] E. L. Kuan, C. H. Wong, and L. Hanzo, "Burst-by-burst adaptive joint detection CDMA," in *Proceeding of VTC'99 (Spring)* [657].
- [342] E. L. Kuan, C. H. Wong, and L. Hanzo, "Upper-bound performance of burst-by-burst adaptive joint detection CDMA." submitted to *IEEE Communications Letters*, 1998.
- [343] S. Verdu, *Multiuser Detection*. Cambridge University Press, 1998.
- [344] F. Simpson and J. M. Holtzman, "Direct sequence CDMA power control, interleaving, and coding," *IEEE Journal on Selected Areas in Communications*, vol. 11, pp. 1085–1095, September 1993.

- [345] M. B. Pursley, "Performance evaluation for phase-coded spread-spectrum multiple-access communication-part I: System analysis," *IEEE Transactions on Communications*, vol. COM-25, pp. 795–799, August 1977.
- [346] R. K. Morrow Jr, "Bit-to-bit error dependence in slotted DS/SSMA packet systems with random signature sequences," *IEEE Transactions on Communications*, vol. 37, pp. 1052–1061, October 1989.
- [347] J. M. Holtzman, "A simple, accurate method to calculate spread-spectrum multiple-access error probabilities," *IEEE Transactions on Communications*, vol. 40, pp. 461–464, March 1992.
- [348] U.-C. G. Fiebig and M. Schnell, "Correlation properties of extended m-sequences," *Electronic Letters*, vol. 29, pp. 1753–1755, September 1993.
- [349] F. Davarian, "Mobile digital communications via tone calibration," *IEEE Transactions on Vehicular Technology*, vol. VT-36, pp. 55–62, May 1987.
- [350] G. T. Irvine and P. J. McLane, "Symbol-aided plus decision-directed reception for PSK/TCM modulation on shadowed mobile satellite fading channels," *IEEE Journal on Selected Areas in Communications*, vol. 10, pp. 1289–1299, October 1992.
- [351] A. Baier, U.-C. Fiebig, W. Granzow, W. Koch, P. Teder, and J. Thielecke, "Design study for a CDMA-based third-generation mobile system," *IEEE Journal on Selected Areas in Communications*, vol. 12, pp. 733–743, May 1994.
- [352] P. B. Rapajic and B. S. Vucetic, "Adaptive receiver structures for asynchronous CDMA systems," *IEEE Journal on Selected Areas in Communications*, vol. 12, pp. 685–697, May 1994.
- [353] M. Benthin and K.-D. Kammeyer, "Influence of channel estimation on the performance of a coherent DS-CDMA system," *IEEE Transactions on Vehicular Technology*, vol. 46, pp. 262–268, May 1997.
- [354] M. Sawahashi, Y. Miki, H. Andoh, and K. Higuchi, "Pilot symbol-assisted coherent multistage interference canceller using recursive channel estimation for DS-CDMA mobile radio," *IEICE Transactions on Communications*, vol. E79-B, pp. 1262–1269, September 1996.
- [355] S. Sampei and T. Sunaga, "Rayleigh fading compensation for QAM in land mobile radio communications," *IEEE Transactions on Vehicular Technology*, vol. 42, pp. 137–147, May 1993.
- [356] T. Ojanperä and R. Prasad, *Wideband CDMA for Third Generation Mobile Communications*. Artech House, 1998.
- [357] E. Dahlman, B. Gudmundson, M. Nilsson, and J. Sköld, "UMTS/IMT-2000 based on wideband CDMA," *IEEE Communications Magazine*, vol. 36, pp. 70–80, September 1998.
- [358] T. Ojanpera, "Overview of research activities for third generation mobile communications," in Glisic and Leppanen [233], ch. 2 (Part 4), pp. 415–446. ISBN 0792380053.

- [359] European Telecommunications Standards Institute, *The ETSI UMTS Terrestrial Radio Access (UTRA) ITU-R RTT Candidate Submission*, June 1998. ETSI/SMG/SMG2.
- [360] Association of Radio Industries and Businesses, *Japan's Proposal for Candidate Radio Transmission Technology on IMT-2000 : W-CDMA*, June 1998.
- [361] A. Sasaki, "Current situation of IMT-2000 radio transmission technology study in japan," *IEICE Transactions on Communications*, vol. E81-B, pp. 1299–1304, July 1998.
- [362] J. S. da Silva, B. Barani, and B. Arroyo-Fernández, "European mobile communications on the move," *IEEE Communications Magazine*, vol. 34, pp. 60–69, February 1996.
- [363] F. Ovesjö, E. Dahlman, T. Ojanperä, A. Toskala, and A. Klein, "FRAMES multiple access mode 2 - wideband CDMA," in *Proceedings of IEEE International Symposium on Personal, Indoor and Mobile Radio Communications, PIMRC'97* [649].
- [364] M. O. Sunay, Z.-C. Honkasalo, A. Hottinen, H. Honkasalo, and L. Ma, "A dynamic channel allocation based TDD DS CDMA residential indoor system," in *IEEE 6th International Conference on Universal Personal Communications, ICUPC'97*, (San Diego), pp. 228–234, October 1997.
- [365] L. Hanzo, "Wireless qam-based multi-media systems: Components and architecture," in Steele and Hanzo [305], ch. 9, pp. 777–896.
- [366] A. Fujiwara, H. Suda, and F. Adachi, "Turbo codes application to DS-CDMA mobile radio," *IEICE Transactions on Communications*, vol. E81A, pp. 2269–2273, November 1998.
- [367] M. J. Juntti, "System concept comparison for multirate CDMA with multiuser detection," in *Proceedings of IEEE Vehicular Technology Conference (VTC'98)* [652], pp. 18–21.
- [368] S. Ramakrishna and J. M. Holtzman, "A comparison between single code and multiple code transmission schemes in a CDMA system," in *Proceedings of IEEE Vehicular Technology Conference (VTC'98)* [652], pp. 791–795.
- [369] R. F. Ormondroyd and J. J. Maxey, "Performance of low rate orthogonal convolutional codes in DS-CDMA," *IEEE Transactions on Vehicular Technology*, vol. 46, pp. 320–328, May 1997.
- [370] M. K. Simon, J. K. Omura, R. A. Scholtz, and B. K. Levitt, *Spread Spectrum Communications Handbook*. McGraw-Hill, 1994.
- [371] T. Kasami, *Combinational Mathematics and its Applications*. University of North Carolina Press, 1969.
- [372] A. Chockalingam, P. Dietrich, L. B. Milstein, and R. R. Rao, "Performance of closed-loop power control in DS-CDMA cellular systems," *IEEE Transactions on Vehicular Technology*, vol. 47, pp. 774–789, August 1998.
- [373] R. R. Gejji, "Forward-link-power control in CDMA cellular-systems," *IEEE Transactions on Vehicular Technology*, vol. 41, pp. 532–536, November 1992.



- [374] K. Higuchi, M. Sawahashi, and F. Adachi, "Fast cell search algorithm in DS-CDMA mobile radio using long spreading codes," in *Proceedings of IEEE VTC '97* [665], pp. 1430–1434.
- [375] C. C. Lee and R. Steele, "Effects of Soft and Softer Handoffs on CDMA System Capacity," *IEEE Transactions on Vehicular Technology*, vol. 47, pp. 830–841, August 1998.
- [376] M. Gustafsson, K. Jamal, and E. Dahlman, "Compressed mode techniques for inter-frequency measurements in a wide-band DS-CDMA system," in *Proceedings of IEEE International Symposium on Personal, Indoor and Mobile Radio Communications, PIMRC'97* [649], pp. 231–235.
- [377] Y. Okumura and F. Adachi, "Variable-rate data transmission with blind rate detection for coherent DS-CDMA mobile radio," *IEICE Transactions on Communications*, vol. E81B, pp. 1365–1373, July 1998.
- [378] J. C. Liberti Jr and T. S. Rappaport, "Analytical results for capacity improvements in CDMA," *IEEE Transactions on Vehicular Technology*, vol. 43, pp. 680–690, August 1994.
- [379] J. H. Winters, "Smart antennas for wireless systems," *IEEE Personal Communications*, vol. 5, pp. 23–27, February 1998.
- [380] T. J. Lim and L. K. Rasmussen, "Adaptive symbol and parameter estimation in asynchronous multiuser CDMA detectors," *IEEE Transactions on Communications*, vol. 45, pp. 213–220, February 1997.
- [381] T. J. Lim and S. Roy, "Adaptive filters in multiuser (MU) CDMA detection," *Wireless Networks*, vol. 4, pp. 307–318, June 1998.
- [382] L. Wei, L. K. Rasmussen, and R. Wyrwas, "Near optimum tree-search detection schemes for bit-synchronous multiuser CDMA systems over Gaussian and two-path Rayleigh fading channels," *IEEE Transactions on Communications*, vol. 45, pp. 691–700, June 1997.
- [383] T. J. Lim and M. H. Ho, "LMS-based simplifications to the kalman filter multiuser CDMA detector," in *Proceedings of IEEE Asia-Pacific Conference on Communications/International Conference on Communication Systems*, (Singapore), November 1998.
- [384] D. You and T. J. Lim, "A modified blind adaptive multiuser CDMA detector," in *Proceedings of IEEE International Symposium on Spread Spectrum Techniques and Application (ISSSTA '98)* [653], pp. 878–882.
- [385] S. M. Sun, L. K. Rasmussen, T. J. Lim, and H. Sugimoto, "Impact of estimation errors on multiuser detection in CDMA," in *Proceedings of IEEE Vehicular Technology Conference (VTC'98)* [652], pp. 1844–1848.
- [386] Y. Sanada and Q. Wang, "A co-channel interference cancellation technique using orthogonal convolutional codes on multipath rayleigh fading channel," *IEEE Transactions on Vehicular Technology*, vol. 46, pp. 114–128, February 1997.
- [387] P. Patel and J. Holtzman, "Analysis of a simple successive interference cancellation scheme in a DS/CDMA system," *IEEE Journal on Selected Areas in Communications*, vol. 12, pp. 796–807, June 1994.

- [388] P. H. Tan and L. K. Rasmussen, "Subtractive interference cancellation for DS-CDMA systems," in *Proceedings of IEEE Asia-Pacific Conference on Communications/International Conference on Communication Systems*, (Singapore), November 1998.
- [389] K. L. Cheah, H. Sugimoto, T. J. Lim, L. K. Rasmussen, and S. M. Sun, "Performance of hybrid interference canceller with zero-delay channel estimation for CDMA," in *Proceeding of Globecom'98* [660], pp. 265–270.
- [390] S. M. Sun, L. K. Rasmussen, and T. J. Lim, "A matrix-algebraic approach to hybrid interference cancellation in CDMA," in *Proceedings of IEEE International Conference on Universal Personal Communications '98*, (Florence, Italy), pp. 1319–1323, October 1998.
- [391] A. L. Johansson and L. K. Rasmussen, "Linear group-wise successive interference cancellation in CDMA," in *Proceedings of IEEE International Symposium on Spread Spectrum Techniques and Application (ISSSTA'98)* [653], pp. 121–126.
- [392] S. M. Sun, L. K. Rasmussen, H. Sugimoto, and T. J. Lim, "A hybrid interference canceller in CDMA," in *Proceedings of IEEE International Symposium on Spread Spectrum Techniques and Application (ISSSTA'98)* [653], pp. 150–154.
- [393] D. Guo, L. K. Rasmussen, S. M. Sun, T. J. Lim, and C. Cheah, "MMSE-based linear parallel interference cancellation in CDMA," in *Proceedings of IEEE International Symposium on Spread Spectrum Techniques and Application (ISSSTA'98)* [653], pp. 917–921.
- [394] L. K. Rasmussen, D. Guo, Y. Ma, and T. J. Lim, "Aspects on linear parallel interference cancellation in CDMA," in *Proceedings of IEEE International Symposium on Information Theory*, (Cambridge, US), p. 37, August 1998.
- [395] L. K. Rasmussen, T. J. Lim, H. Sugimoto, and T. Oyama, "Mapping functions for successive interference cancellation in CDMA," in *Proceedings of IEEE Vehicular Technology Conference (VTC'98)* [652], pp. 2301–2305.
- [396] S. M. Sun, T. J. Lim, L. K. Rasmussen, , T. Oyama, H. Sugimoto, and Y. Matsumoto, "Performance comparison of multi-stage SIC and limited tree-search detection in CDMA," in *Proceedings of IEEE Vehicular Technology Conference (VTC'98)* [652], pp. 1854–1858.
- [397] A. Wittneben and T. Kaltenschnee, "TX selection diversity with prediction: Systematic nonadaptive predictor design," in *Proceedings of IEEE VTC '94* [663], pp. 1246–1250.
- [398] A. Hottinen and R. Wichman, "Transmit diversity by antenna selection in CDMA downlink," in *Proceedings of IEEE International Symposium on Spread Spectrum Techniques and Application (ISSSTA'98)* [653].
- [399] G. Turin, "The effects of multipath and fading on the performance of direct-sequence CDMA systems," *IEEE Journal on Selected Areas in Communications*, vol. SAC-2, pp. 597–603, July 1984.
- [400] M. Kavehrad and B. Ramamurthi, "Direct-sequence spread spectrum with DPSK modulation and diversity for indoor wireless communications," *IEEE Transactions on Communications*, vol. COM-35, pp. 224–236, February 1987.

- [401] P. K. Enge and D. V. Sarwate, "Spread spectrum multiple access performance of orthogonal code:linear receivers," *IEEE Transactions on Communications*, vol. COM-35, pp. 1309–1319, December 1987.
- [402] K. Pahlavan and M. Chase, "Spread-spectrum multiple-access performance of orthogonal codes for indoor radio communications," *IEEE Transactions on Communications*, vol. 38, pp. 574–577, May 1990.
- [403] L. M. A. Jalloul and J. M. Holtzman, "Performance analysis of DS/CDMA with noncoherent  $M$ -ary orthogonal modulation in multipath fading channels," *IEEE Journal on Selected Areas in Communications*, vol. 12, pp. 862–870, June 1994.
- [404] E. K. Hong, K. J. Kim, and K. C. Whang, "Performance evaluation of DS-CDMA system with  $M$ -ary orthogonal signalling," *IEEE Transactions on Vehicular Technology*, vol. 45, pp. 57–63, February 1996.
- [405] V. Aalo, O. Ugweje, and R. Sudhakar, "Performance analysis of a DS/CDMA system with noncoherent  $M$ -ary orthogonal modulation in nakagami fading," *IEEE Transactions on Vehicular Technology*, vol. 47, pp. 20–29, February 1998.
- [406] A. F. Naguib and A. Paulraj, "Performance of wireless CDMA with  $m$ -ary orthogonal modulation and cell site antenna arrays," *IEEE Journal on Selected Areas in Communications*, vol. 14, pp. 1770–1783, December 1996.
- [407] Q. Bi, "Performance analysis of a CDMA cellular system," in *Proceedings of the IEEE Vehicular Technology Conference*, (Denver, CO), pp. 43–46, May 1992.
- [408] Q. Bi, "Performance analysis of a CDMA cellular system in the multipath fading environment," in *Proceedings of the IEEE International Conference on Personal, Indoor and Mobile Radio Communications*, (Boston, MA), pp. 108–111, October 1992.
- [409] K. Cheun, "Performance of direct-sequence spread-spectrum RAKE receivers with random spreading sequences," *IEEE Transactions on Communications*, vol. 45, pp. 1130–1143, September 1997.
- [410] R. S. Lunayach, "Performance of a direct sequence spread-spectrum system with long period and short period code sequences," *IEEE Transactions on Communications*, vol. COM-31, pp. 412–419, March 1983.
- [411] L.-L. Yang and L. Hanzo, "Performance of a residue number system based orthogonal signalling scheme in AWGN channels." Yet to be published.
- [412] L.-L. Yang and L. Hanzo, "Performace of a residue number system based orthogonal signalling scheme over frequency-nonselective , slowly fading channel." Yet to be published.
- [413] L. L. Yang and L. Hanzo, "Performance of Residue Number System Based DS-CDMA over Multipath Fading Channels Using Orthogonal Sequences," *European Transactions on Telecommunications*, vol. 9, pp. 525–535, November/December 1998.
- [414] L.-L. Yang and L. Hanzo, "Residue number system arithmetic assisted  $m$ -ary modulation," *IEEE Communications Letters*, vol. 3, pp. 28–30, February 1999.

- [415] L. L. Yang and L. Hanzo, "Residue number system based multiple code ds-cdma systems," in *Proceeding of VTC'99 (Spring)* [657].
- [416] L. Hanzo and L. L. Yang, "Ratio statistic test assisted residue number system based parallel communication systems," in *Proceeding of VTC'99 (Spring)* [657].
- [417] K. Yen, L. L. Yang, and L. Hanzo, "Residual number system assisted cdma – a new system concept," in *Proceeding of ACTS Mobile Communication Summit '99* [658].
- [418] S. Haykin, *Digital Communications*. John Wiley and Sons, 1988.
- [419] R. D. Gaudenzi, T. Garde, F. Giannetti, and M. Luise, "A performance comparison of orthogonal code division multiple-access techniques for mobile satellite communications," *IEEE Journal on Selected Areas in Communications*, vol. 13, pp. 325–332, February 1995.
- [420] M. Chase and K. Pahlavan, "Performance of DS-CDMA over measured indoor radio channels using random orthogonal codes," *IEEE Transactions on Vehicular Technology*, vol. 42, pp. 617–624, November 1993.
- [421] D. Radhakrishnan and Y. Yuan, "Novel Approachs to the Design of VLSI RNS Multiplier," *IEEE Transactions on Circuits and Systems-II*, vol. 39, pp. 52–57, January 1992.
- [422] E. D. D. Claudio, G. Orlandi, and F. Piazza, "A Systolic Redundant Residue Arithmetic Error Correction Circuit," *IEEE Transactions on Computers*, vol. 42, pp. 427–432, April 1993.
- [423] F. J. Taylor, "Residue arithmetic: A tutorial with examples," *IEEE Computer Magazine*, vol. 17, pp. 50–62, May 1984.
- [424] F. Barsi and P. Maestrini, "Error correction properties of redundant residue number systems," *IEEE Transactions on Computers*, vol. 22, pp. 307–315, March 1973.
- [425] A. J. Viterbi, "A Robust Ratio-Threshold Technique to Mitigate Tone and Partial Band Jamming in Coded MFSK Systems," in *Proceedings of the IEEE Military Communications Conference*, pp. 22.4–1–5, October 1982.
- [426] M. F. Barnsley, "A better way to compress images," *BYTE*, pp. 215–222, January 1988.
- [427] J. M. Beaumont, "Image data compression using fractal techniques," *BT Technology*, vol. 9, pp. 93–109, October 1991.
- [428] A. E. Jacquin, "Image coding based on a fractal theory of iterated contractive image transformations," *IEEE Trans. Image Processing*, vol. 1, pp. 18–30, January 1992.
- [429] D. Monro and F. Dudbridge, "Fractal block coding of images," *Electronic Letters*, vol. 28, pp. 1053–1055, May 1992.
- [430] D. Monroe, D. Wilson, and J. Nicholls, "High speed image coding with the bath fractal transform," in *Damper et al.* [654], pp. 23–30.

- [431] B. Ramamurthi and A. Gersho, "Classified vector quantization of images," *IEEE Transactions on communications*, vol. COM-34, pp. 1105–1115, November 1986.
- [432] J. Streit and L. Hanzo, "A fractal video communicator," in *Proceedings of IEEE VTC '94* [663], pp. 1030–1034.
- [433] W. Welsh, "Model based coding of videophone images," *Electronic and Communication Engineering Journal*, pp. 29–36, February 1991.
- [434] J. Ostermann, "Object-based analysis-synthesis coding based on the source model of moving rigid 3D objects," *Signal Processing: Image Communication*, vol. 6, pp. 143–161, 1994.
- [435] M. Chowdhury, "A switched model-based coder for video signals," *IEEE Transactions on Circuits and Systems*, vol. 4, pp. 216–227, June 1994.
- [436] G. Bozdagi, A. Tekalp, and L. Onural, "3-d motion estimation and wireframe adaptation including photometric effects for model-based coding of facial image sequences," *IEEE Transactions on circuits and Systems for Video Technology*, vol. 4, pp. 246–256, June 1994.
- [437] Q. Wang and R. Clarke, "Motion estimation and compensation for image sequence coding," *Signal Processing: Image Communications*, vol. 4, pp. 161–174, 1992.
- [438] H. Gharavi and M. Mills, "Blockmatching motion estimation algorithms - new results," *IEEE Transactions on Circuits and Systems*, vol. 37, pp. 649–651, May 1990.
- [439] J. Jain and A. Jain, "Displacement measurement and its applications in inter frame image coding," *IEEE Transactions on Communications*, vol. 29, December 1981.
- [440] B. Wang, J. Yen, and S. Chang, "Zero waiting-cycle hierarchical block matching algorithm and its array architectures," *IEEE Transactions on Circuits and Systems for Video Technology*, vol. 4, pp. 18–27, February 1994.
- [441] P. Strobach, "Tree-structured scene adaptive coder," *IEEE Transactions on Communications*, vol. 38, pp. 477–486, April 1990.
- [442] B. Liu and A. Zaccarin, "New fast algorithms for the estimation of block motion vectors," *IEEE Transactions on Circuits and Systems*, vol. 3, pp. 148–157, April 1993.
- [443] R. Li, B. Zeng, and N. Liou, "A new three step search algorithm for motion estimation," *IEEE Transactions on Circuits and Systems*, vol. 4, pp. 439–442, August 1994.
- [444] L. Lee, J. Wang, J. Lee, and J. Shie, "Dynamic search-window adjustment and interlaced search for block-matching algorithm," *IEEE Transactions on Circuits and Systems for Video Technology*, vol. 3, pp. 85–87, February 1993.
- [445] B. Girod, "Motion-compensating prediction with fractional-pel accuracy," *IEEE Transactions on Communications*, vol. 41, pp. 604–611, April 1993.

- [446] J. Huang et al, "A multi-frame pel-recursive algorithm for varying frame-to-frame displacement estimation," in *Proceedings of International Conference on Acoustics, Speech, and Signal Processing, ICASSP'92* [655], pp. 241–244.
- [447] N. Efstratiadis and A. Katsaggelos, "Adaptive multiple-input pel-recursive displacement estimation," in *Proceedings of International Conference on Acoustics, Speech, and Signal Processing, ICASSP'92* [655], pp. 245–248.
- [448] C. Huang and C. Hsu, "A new motion compensation method for image sequence coding using hierarchical grid interpolation," *IEEE Transactions on Circuits and Systems for Video Technology*, vol. 4, pp. 42–51, February 1994.
- [449] J. Nieweglowski, T. Moisala, and P. Haavisto, "Motion compensated video sequence interpolation using digital image warping," in *Proceedings of the IEEE International Conference on Acoustics, Speech and Signal Processing (ICASSP'94)* [656], pp. 205–208.
- [450] C. Papadopoulos and T. Clarkson, "Motion compensation using second-order geometric transformations," *IEEE Transactions on Circuits and Systems for Video Technology*, vol. 5, pp. 319–331, August 1995.
- [451] C. Papadopoulos, *The use of geometric transformations for motion compensation in video data compression*. PhD thesis, University of London, 1994.
- [452] M. Hoetter, "Differential estimation based on object oriented mapping parameter estimation," *Signal Processing*, vol. 16, pp. 249–265, March 1989.
- [453] S. A. Karunaserker and N. G. Kingsbury, "A distortion measure for blocking artifacts in images based on human visual sensitivity," *IEEE Transactions on Image Processing*, vol. 6, pp. 713–724, June 1995.
- [454] D. Pearson and M. Whybray, "Transform coding of images using interleaved blocks," *IEE Proceedings*, vol. 131, pp. 466–472, August 1984.
- [455] J. Magarey and N. G. Kingsbury, "Motion estimation using complex wavelets," in *Proceedings of the IEEE International Conference on Acoustics, Speech and Signal Processing (ICASSP'96)* [667], pp. 2371–2374.
- [456] R. W. Young and N. G. Kingsbury, "Frequency-domain motion estimation using a complex lapped transform," *IEEE Transactions on Image Processing*, vol. 2, pp. 2–17, January 1993.
- [457] R. W. Young and N. G. Kingsbury, "Video compression using lapped transforms for motion estimation / compensation and coding," in *Proceedings of the SPIE Communication and Image Processing Conference*, (Boston), pp. 1451–1463, SPIE, November 1992.
- [458] K. Rao and P. Yip, *Discrete Cosine Transform*. Academic Press, New York, 1990.
- [459] A. Sharaf, *Video coding at very low bit rates using spatial transformations*. PhD thesis, Dept. of Electronic and Electrical Engineering, Kings College, London, UK, 1997.
- [460] R. J. Clarke, *Transform Coding of Images*. Academic Press, 1985.

- [461] A. Palau and G. Mirchandani, "Image coding with discrete cosine transforms using efficient energy-based adaptive zonal filtering," in *Proceedings of the IEEE International Conference on Acoustics, Speech and Signal Processing (ICASSP'94)* [656], pp. 337–340.
- [462] H. Yamaguchi, "Adaptive DCT coding of video signals," *IEEE Transactions on Communications*, vol. 41, pp. 1534–1543, October 1993.
- [463] K. Ngan, "Adaptive transform coding of video signals," *IEE Proceedings*, vol. 129, pp. 28–40, February 1982.
- [464] R. Clarke, "Hybrid intra-frame transform coding of image data," *IEE Proceedings*, vol. 131, pp. 2–6, February 1984.
- [465] F.-M. Wang and S. Liu, "Hybrid video coding for low bit-rate applications," in *Proceedings of the IEEE International Conference on Acoustics, Speech and Signal Processing (ICASSP'94)* [656], pp. 481–484.
- [466] M. Ghanbari and J. Azari, "Effect of bit rate variation of the base layer on the performance of two-layer video codecs," *IEEE Transactions on Communications for Video Technology*, vol. 4, pp. 8–17, February 1994.
- [467] N. Jayant and P. Noll, *Digital coding of waveforms, Principles and applications to speech and video*. Prentice-Hall, 1984.
- [468] N. T. Cheng and N. G. Kingsbury, "The ERPC: an efficient error-resilient technique for encoding positional information of sparse data," *IEEE Transactions on Communications*, vol. 40, pp. 140–148, January 1992.
- [469] M. Narasimha and A. Peterson, "On the computation of the discrete cosine transform," *IEEE Transactions on Communications*, vol. 26, pp. 934–936, June 1978.
- [470] R. M. Pelz, "An un-equal error protected px8 kbit/s video transmission for DECT," in *Proceedings of IEEE VTC '94* [663], pp. 1020–1024.
- [471] L. Hanzo, R. Stedman, R. Steele, and J. Cheung, "A portable multimedia communicator scheme," in Damper *et al.* [654], pp. 31–54.
- [472] R. Stedman, H. Gharavi, L. Hanzo, and R. Steele, "Transmission of subband-coded images via mobile channels," *IEEE Tr. on Circuits and Systems for Video Technology*, vol. 3, pp. 15–27, Feb 1993.
- [473] L. Hanzo and J. Streit, "Adaptive low-rate wireless videophone systems," *IEEE Tr. on CS for Video Technology*, vol. 5, pp. 305–319, Aug 1995.
- [474] ETSI, *GSM Recommendation 05.05, Annex 3*, Nov 1988.
- [475] G. Djuknic and D. Schilling, "Performance analysis of an ARQ transmission scheme for meteor burst communications," *IEEE Tr. on Comms.*, vol. 42, pp. 268–271, Feb/Mar/Apr 1994.
- [476] L. de Alfaro and A. Meo, "Codes for second and third order GH-ARQ schemes," *IEEE Transactions on Communications*, vol. 42, pp. 899–910, Feb-Apr 1994.
- [477] T.-H. Lee, "Throughput performance of a class of continuous ARQ strategies for burst-error channels," *IEEE Tr. on Veh. Tech.*, vol. 41, pp. 380–386, Nov 1992.

- [478] S. Lin, D. J. Costello Jr, and M. J. Miller, "Automatic-repeat-request error-control schemes," *IEEE Communications Magazine*, vol. 22, pp. 5–17, December 1984.
- [479] A. Gersho and R. Gray, *Vector Quantization and Signal Compression*. Kluwer Academic Publishers, 1992.
- [480] L. Torres, J. R. Casas, and S. deDiego, "Segmentation based coding of textures using stochastic vector quantization," in *Proceedings of the IEEE International Conference on Acoustics, Speech and Signal Processing (ICASSP'94)* [656], pp. 597–600.
- [481] M. Y. Jaisimha, J. R. Goldschneider, A. E. Mohr, E. A. Riskin, and R. M. Haralick, "On vector quantization for fast facet edge detection," in *Proceedings of the IEEE International Conference on Acoustics, Speech and Signal Processing (ICASSP'94)* [656], pp. 37–40.
- [482] P. Yu and A. Venetsanopoulos, "Hierarchical finite-state vector quantisation for image coding," *IEEE Transactions on Communications*, vol. 42, pp. 3020–3026, November 1994.
- [483] C.-H. Hsieh, K.-C. Chuang, and J.-S. Shue, "Image compression using finite-state vector quantization with derailment compensation," *IEEE Transactions on Circuits and Systems for Video Technology*, vol. 3, pp. 341–349, October 1993.
- [484] N. Nasrabadi, C. Choo, and Y. Feng, "Dynamic finite-state vector quantisation of digital images," *IEEE Transactions on Communications*, vol. 42, pp. 2145–2154, May 1994.
- [485] V. Sitaram, C. Huang, and P. Israelsen, "Efficient codebooks for vector quantisation image compression with an adaptive tree search algorithm," *IEEE Transactions on Communications*, vol. 42, pp. 3027–3033, November 1994.
- [486] W. Yip, S. Gupta, and A. Gersho, "Enhanced multistage vector quantisation by joint codebook design," *IEEE Transactions on Communications*, vol. 40, pp. 1693–1697, November 1992.
- [487] L. Po and C. Chan, "Adaptive dimensionality reduction techniques for tree-structured vector quantisation," *IEEE Transactions on Communications*, vol. 42, pp. 2246–2257, June 1994.
- [488] L. Lu and W. Pearlman, "Multi-rate video coding using pruned tree-structured vector quantization," in *Proceedings of the IEEE International Conference on Acoustics, Speech and Signal Processing (ICASSP'93)*, vol. 5, (Minneapolis, MN, USA), pp. 253–256, IEEE, 27–30 Apr 1993.
- [489] F. Bellifemine and R. Picco, "Video signal coding with DCT and vector quantisation," *IEEE Transactions on Communications*, vol. 42, pp. 200–207, February 1994.
- [490] K. Ngan and K. Sin, "HDTV coding using hybrid MRVQ / DCT," *IEEE Transactions on Circuits and Systems for Video Technology*, vol. 3, pp. 320–323, August 1993.



- [491] D. Kim and S. Lee, "Image vector quantiser based on a classification in the DCT domain," *IEEE Transactions on Communications*, pp. 549–556, April 1991.
- [492] L. Torres and J. Huguet, "An improvement on codebook search for vector quantisation," *IEEE Transactions on Communications*, vol. 42, pp. 208–210, February 1994.
- [493] J. Streit and L. Hanzo, "Dual-mode vector-quantised low-rate cordless videophone systems for indoors and outdoors applications," *IEEE Tr. on Vehicular Technology*, vol. 46, pp. 340–357, May 1997.
- [494] X. Zhang, M. Cavenor, and J. Arnold, "Adaptive quadtree coding of motion-compensated image sequences for use on the broadband ISDN," *IEEE Transactions on Circuits and Systems for Video Technology*, vol. 3, pp. 222–229, June 1993.
- [495] J. Vaisey and A. Gersho, "Image compression with variable block size segmentation," *IEEE Transactions on Signal Processing*, vol. 40, pp. 2040–2060, August 1992.
- [496] M. Lee and G. Crebbin, "Classified vector quantisation with variable block-size DCT models," *IEE Proceedings. Vision, Image and Signal Processing*, pp. 39–48, February 1994.
- [497] E. Shustermann and M. Feder, "Image compression via improved quadtree decomposition algorithms," *IEEE Transactions on Image Processing*, vol. 3, pp. 207–215, March 1994.
- [498] F. DeNatale, G. Desoli, and D. Giusto, "A novel tree-structured video codec," in *Proceedings of the IEEE International Conference on Acoustics, Speech and Signal Processing (ICASSP'94)* [656], pp. 485–488.
- [499] M. Hennecke, K. Prasad, and D. Stork, "Using deformable templates to infer visual speech dynamics," in *Proceedings of the 28th Asilomar Conference on Signals, Systems and Computers*, vol. 1, (Pacific Grove, CA, USA), pp. 578–582, 30 Oct. – 2 Nov. 1994.
- [500] G. J. Wolf et al, "Lipreading by neural networks: Visual preprocessing, learning and sensory integration," *Proceedings of the neural information processing systems*, vol. 6, pp. 1027–1034, 1994.
- [501] J. Streit and L. Hanzo, "Quad-tree based parametric wireless videophone systems," *IEEE Transactions Video Technology*, vol. 6, pp. 225–237, April 1996.
- [502] E. Biglieri and M. Luise, "Coded modulation and bandwidth-efficient transmission," in *Proc. of the Fifth Tirrenia Intern. Workshop*, (Elsevier, Netherlands), 8–12 Sept 1991.
- [503] L. Wei, "Rotationally-invariant convolutional channel coding with expanded signal space, part i and ii," *IEEE Tr. on Selected Areas in Comms*, vol. SAC-2, pp. 659–686, September 1984.
- [504] ITU-T, *ISO/IEC-CD-11172 - Coding of moving pictures and associated audio for digital storage*.

- [505] ITU-T, *Recommendation H.261: Video codec for audiovisual services at px64 Kbit/s*, March 1993.
- [506] D. W. Redmill and N. G. Kingsbury, "Improving the error resilience of entropy encoded video signals," in *Proceedings of the Conference on Image Processing: Theory and Applications (IPTA)*, pp. 67–70, Elsevier, 1993.
- [507] S. Emani and S. Miller, "DPCM picture transmission over noisy channels with the aid of a markov model," *IEEE Transactions on Image Processing*, vol. 4, pp. 1473–1481, November 1995.
- [508] M. Chan, "The performance of DPCM operating on lossy channels with memory," *IEEE Transactions on Communications*, vol. 43, pp. 1686–1696, April 1995.
- [509] N. Jayant, "Adaptive quantization with a one-word memory," *Bell System Technical Journal*, vol. 52, pp. 1119–1144, September 1973.
- [510] L. Zetterberg, A. Ericsson, and C. Couturier, "DPCM picture coding with two-dimensional control of adaptive quantisation," *IEEE Transactions on Communications*, vol. 32, no. 4, pp. 457–642, 1984.
- [511] C. Hsieh, P. Lu, and W. Liou, "Adaptive predictive image coding using local characteristics," *IEE Proceedings*, vol. 136, pp. 385–389, December 1989.
- [512] P. Wellstead, G. Wagner, and J. Caldas-Pinto, "Two-dimensional adaptive prediction, smoothing and filtering," *Proceedings of the IEE*, vol. 134, pp. 253–266, June 1987.
- [513] O. Mitchell, E. Delp, and S. Carlton, "Block truncation coding: A new approach to image compression," in *IEEE International Conference on Communications (ICC)*, pp. 12B.1.1–12B.1.4, 1978.
- [514] E. Delp and O. Mitchell, "Image compression using block truncation coding," *IEEE Transactions on Communications*, vol. 27, pp. 1335–1342, September 1979.
- [515] D. R. Halverson, N. C. Griswold, and G. L. Wiese, "A generalized block truncation coding algorithm for image compression," *IEEE Transactions Acoustics, Speech and Signal Processing*, vol. 32, pp. 664–668, June 1984.
- [516] G. Arce and N. Gallanger, "BTC image coding using median filter roots," *IEEE Transactions on Communications*, vol. 31, pp. 784–793, June 1983.
- [517] M. Noah, "Optimal Lloyd-Max quantization of LPC speech parameters," in *Proceedings of International Conference on Acoustics, Speech, and Signal Processing, ICASSP'84*, (San Diego, California, USA), pp. 1.8.1 – 1.8.4, IEEE, 19–21 March 1984.
- [518] R. Crochiere, S. Webber, and J. Flangan, "Digital coding of speech in subbands," *Bell System Technology Journal*, vol. 52, pp. 1105–1118, 1973.
- [519] R. Crochiere, "On the design of sub-band coders for low bit rate speech communication," *Bell System Technology Journal*, vol. 56, pp. 747–770, 1977.
- [520] J. Woods and S. O'Neil, "Subband coding of images," *IEEE Trans. ASSP*, vol. 34, pp. 1278–1288, October 1986.

- [521] J. W. Woods, ed., *Subband Image Coding*. Kluwer Academic Publishers, March 1991. ISBN: 0792390938.
- [522] H. Gharavi and A. Tabatabai, "Subband coding of digital images using two-dimensional quadrature mirror filtering," in *Proc. SPIE*, 1986.
- [523] H. Gharavi and A. Tabatabai, "Subband coding of monochrome and color images," *IEEE Trans. on Circuits and Systems*, vol. 35, pp. 207–214, February 1988.
- [524] H. Gharavi, "Subband coding algorithms for video applications: Videophone to HDTV-conferencing," *IEEE Transactions on Circuits and Systems for Video Technology*, vol. 1, pp. 174–183, February 1991.
- [525] A. Alasmari, "An adaptive hybrid coding scheme for HDTV and digital video sequences," *IEEE Transactions on consumer electronics*, vol. 41, no. 3, pp. 926–936, 1995.
- [526] K. Irie et al, "High-quality subband coded for hdtv transmission," *IEEE Transactions on Circuits and Systems for Video Technology*, vol. 4, pp. 195–199, April 1994.
- [527] E. Simoncelli and E. Adelson, "Subband transforms," in Woods [521], pp. 143–192. ISBN: 0792390938.
- [528] K. Irie and R. Kishimoto, "A study on perfect reconstructive subband coding," *IEEE Transactions on Circuits and Systems for Video Technology*, vol. 1, pp. 42–48, January 1991.
- [529] J. Woods and T. Naveen, "A filter based bit allocation scheme for subband compression of HDTV," *IEEE Transactions on Image Processing*, vol. 1, pp. 436–440, July 1992.
- [530] D. Esteban and C. Galand, "Application of quadrature mirror filters to split band voice coding scheme," in *Proceedings of International Conference on Acoustics, Speech, and Signal Processing, ICASSP'77*, (Hartford, Conn, USA), pp. 191–195, IEEE, 9–11 May 1977.
- [531] J. Johnston, "A filter family designed for use in quadrature mirror filter banks," in *Proceedings of International Conference on Acoustics, Speech, and Signal Processing, ICASSP'80* [650], pp. 291–294.
- [532] H. Nussbaumer, "Complex quadrature mirror filters," in *Proceedings of International Conference on Acoustics, Speech, and Signal Processing, ICASSP'83*, (Boston, Mass, USA), pp. 221–223, IEEE, 14–16 April 1983.
- [533] C. Galand and H. Nussbaumer, "New quadrature mirror filter structures," *IEEE Trans. on ASSP*, vol. ASSP-32, pp. 522–531, June 1984.
- [534] R. Crochiere and L. Rabiner, *Multirate digital Processing*. Prentice Hall, 1993.
- [535] S. Aase and T. Ramstad, "On the optimality of nonunitary filter banks in subband coders," *IEEE Transactions on Image Processing*, vol. 4, pp. 1585–1591, December 1995.
- [536] V. Nuri and R. H. Bamberger, "Size limited filter banks for subband image compression," *IEEE Transactions on Image Processin*, vol. 4, pp. 1317–1323, September 1995.

## BIBLIOGRAPHY

1095

- [537] H. Gharavi, "Subband coding of video signals," in Woods [521], pp. 229–271. ISBN: 0792390938.
- [538] O. Egger, W. Li, and M. Kunt, "High compression image coding using an adaptive morphological subband decomposition," *Proceedings of the IEEE*, vol. 83, pp. 272–287, February 1995.
- [539] P. H. Westerink and D. E. Boekee, "Subband coding of color images," in Woods [521], pp. 193–228. ISBN: 0792390938.
- [540] Q. T. Nguyen, "Near-perfect-reconstruction pseudo-QMF banks," *IEEE Transactions on signal processing*, vol. 42, pp. 65–76, January 1994.
- [541] S.-M. Phoong, C. W. Kim, P. P. Vaidyanathan, and R. Ansari, "A new class of two-channel biorthogonal filter banks and wavelet bases," *IEEE Transactions on Signal Processing*, vol. 43, pp. 649–665, March 1995.
- [542] E. Jang and N. Nasrabadi, "Subband coding with multistage VQ for wireless image communication," *IEEE Transactions in Circuit and Systems for Video Technology*, vol. 5, pp. 347–253, June 1995.
- [543] P. C. Cosman, R. M. Gray, and M. Vetterli, "Vector quantisation of image subbands: A survey," *IEEE Transactions on Image Processing*, vol. 5, pp. 202–225, February 1996.
- [544] ITU, *Joint Photographic Experts Group ISO/IEC, JTC/SC/WG8, CCITT SGVIII. JPEG technical specifications, revision 5. Report JPEG-8-R5*, January 1990.
- [545] P. Franti and O. Nevalainen, "Block truncation coding with entropy coding," *IEEE Transactions on Communications*, vol. 43, no. 4, pp. 1677–1685, 1995.
- [546] V. Udpikar and J. Raina, "BTC image coding using vector quantisation," *IEEE Transactions on Communications*, vol. 35, pp. 353–359, March 1987.
- [547] International Standards Organization, *ISO/IEC 11172 MPEG 1 International Standard, Coding of moving pictures and associated audio for digital storage media up to about 1.5 Mbit/s, Parts 1-3*.
- [548] International Standards Organization, *ISO/IEC CD 13818 MPEG 2 International Standard, Information Technology, Generic coding of moving video and associated audio information, Parts 1-3*.
- [549] Telenor Research and Development, P.O.Box 83, N-2007 Kjeller, Norway, *Video Codec Test Model 'TMN 5', ITU Study Group 15, Working Party 15/1*.
- [550] D. W. Choi, "Frame alignment in a digital carrier system – a tutorial," *IEEE Communications Magazin*, vol. 28, pp. 46–54, February 1990.
- [551] ITU (formerly CCITT), *ITU Recommendation X25*, 1993.
- [552] M. Al-Subbagh and E. V. Jones, "Optimum patterns for frame alignment," *IEE Proceedings*, vol. 135, pp. 594–603, December 1988.
- [553] T. Turletti, "A H.261 software codec for videoconferencing over the internet," Tech. Rep. 1834, INRIA, 06902 Sophia-Antipolis, France, Jan 1993.

- [554] N. D. Kenyon and C. Nightingale, eds., *Audiovisual Telecommunications*. London, UK: Chapman and Hall, 1992.
- [555] N. MacDonald, "Transmission of compressed video over radio links," *BT technology Journal*, vol. 11, pp. 182–185, April 1993.
- [556] M. Khansari, A. Jalali, E. Dubois, and P. Mermelstein, "Robust low bit-rate video transmission over wireless access systems," in *Proc. of International Comms. Conf. (ICC)*, pp. 571–575, 1994.
- [557] N. T. Cheng, *Error resilient video coding for Noisy Channels*. PhD thesis, Department of Engineering, University of Cambridge, UK, 1991.
- [558] D. W. Redmill, *Image and Video Coding for Noisy Channels*. PhD thesis, Signal Processing and Communication Laboratory, Department of Engineering, University of Cambridge, UK, November 1994.
- [559] Y. Matsumura, S. Nakagawa, and T. Nakai, "Very low bit rate video coding with error resilience," in VLBV'95 [668], pp. L–1.
- [560] K. N. Ngan and D. Chai, "Enhancement of image quality in VLBR coding," in VLBV'95 [668], pp. L–3.
- [561] K. N. Ngan and D. Chai, "Very low bit rate video coding using H.263 coder," *IEEE Tr. on Circuits and Systems for Video Technology*, vol. 6, pp. 308–312, June 1996.
- [562] W. Webb and L. Hanzo, "Square QAM," in *Modern Quadrature Amplitude Modulation: Principles and Applications for Wireless Communications* [10], ch. 5, pp. 156–169. ISBN 0-7273-1701-6.
- [563] IBM Corp., White Plains, NY, *General Information: Binary Synchronous Communication, IBM Publication GA27-3004*, 1969.
- [564] S. Sampei, S. Komaki, and N. Morinaga, "Adaptive modulation / TDMA scheme for large capacity personal multi-media communication systems," *IE-ICE Trans. Communications (Japan)*, vol. E77-B, pp. 1096–1103, September 1994.
- [565] W. Webb and L. Hanzo, "Variable rate QAM," in *Modern Quadrature Amplitude Modulation: Principles and Applications for Wireless Communications* [10], ch. 13, pp. 384–406. ISBN 0-7273-1701-6.
- [566] M. Ghanbari and V. Seferidis, "Cell-loss concealment in ATM video codecs," *IEEE Tr. on Circuits and Systems for Video Technology*, vol. 3, pp. 238–247, June 1993.
- [567] W. C. Chung, F. Kossentini, and M. J. T. Smith, "An efficient motion estimation technique based on a rate-distortion criterion," in *Proceedings of the IEEE International Conference on Acoustics, Speech and Signal Processing (ICASSP'96)* [667], pp. 1977–1980.
- [568] Telenor Research and Development, P.O.Box 83, N-2007 Kjeller, Norway, *H.263 Software Codec*. <http://www.nta.no/brukere/DVC>.
- [569] W. Ding and B. Liu, "Rate control of MPEG video coding and recording by rate-quantization modeling," *IEEE Tr. on Circuits and Systems for Video Technology*, vol. 6, pp. 12–20, Feb 1996.

- [570] G. M. Schuster and A. K. Katsaggelos, "A video compression scheme with optimal bit allocation between displacement vector field and displaced frame difference," in *Proceedings of the IEEE International Conference on Acoustics, Speech and Signal Processing (ICASSP'96)* [667], pp. 1967–1970.
- [571] F. C. M. Martins, W. Ding, and E. Feig, "Joint control of spatial quantization and temporal sampling for very low bitrate video," in *Proceedings of the IEEE International Conference on Acoustics, Speech and Signal Processing (ICASSP'96)* [667], pp. 2074–2077.
- [572] T. Wiegand, M. Lightstone, and D. Mukherjee, "Rate-distortion optimized mode selection for very low bit rate video coding and the emerging H.263 standard," *IEEE Tr. on Circuits and Systems for Video Technology*, vol. 6, pp. 182–190, Apr 1996.
- [573] A. Paulraj, "Diversity techniques," in Gibson [283], ch. 12, pp. 166–176.
- [574] A. Mämmelä, *Diversity receivers in a fast fading multipath channel*. PhD thesis, Department of Electrical Engineering, University of Oulu, Finland, 1995.
- [575] P. Crespo, R. M. Pelz, and J. Cosmas, "Channel error profile for DECT," *IEE Proc. Communications*, vol. 141, pp. 413–420, Dec 1994.
- [576] M. Zorzi, "Power control and diversity in mobile radio cellular systems in the presence of rician fading and log-normal shadowing," *IEEE Tr. on Vehicular Technology*, vol. 45, pp. 373–382, May 1996.
- [577] Y.-W. Leung, "Power control in cellular networks subject to measurement error," *IEEE Tr. on Communications*, vol. 44, pp. 772–775, July 1996.
- [578] S. Ariyavisitakul and L. F. Chang, "Signal and interference statistics of a CDMA system with feedback power control," *IEEE Tr. on Communications*, vol. 41, pp. 1626–1634, Nov 1993.
- [579] R. Pichna and Q. Wang, "Power control," in Gibson [283], ch. 23, pp. 370–380.
- [580] T.-H. Lee, J.-C. Lin, and Y. T. Su, "Downlink power control algorithms for cellular radio systems," *IEEE Tr. on Vehicular Technology*, vol. 44, pp. 89–94, Feb 1995.
- [581] M. D. Austin and G. L. Stüber, "In-service signal quality estimation for TDMA cellular systems," *Wireless Personal Communications*, vol. 2, pp. 245–254, 1995. Kluwer Academic Publishers.
- [582] J. C. I. Chuang and N. R. Sollenberger, "Uplink power control for TDMA portable radio channels," *IEEE Tr. on Vehicular Technology*, vol. 43, pp. 33–39, Feb 1994.
- [583] P. S. Kumar, R. D. Yates, and J. Holtzman, "Power control based on bit error rate (BER) measurements," in *Proceedings of the Military Communications Conference (MILCOM)*, (San Diego, CA, USA), Nov 5–8 1995.
- [584] W. H. Press, S. A. Teukolsky, W. T. Vetterling, and B. P. Flannery, "Minimization or maximization of functions," in *Numerical Recipes in C* [140], ch. 10, pp. 394–455.

- [585] H. Matsuoka, S. Sampei, N. Morinaga, and Y. Kamio, "Adaptive modulation system with variable coding rate concatenated code for high quality multi-media communications systems," in *Proceedings of IEEE VTC '96* [664], pp. 487–491.
- [586] A. Goldsmith and S. Chua, "Adaptive coded modulation for fading channels," in *Proceedings of IEEE International Conference on Communications*, vol. 3, (Montreal, Canada), pp. 1488–1492, Jun 8–12 1997.
- [587] J. Torrance, *Adaptive Full Response Digital Modulation for Wireless Communications Systems*. PhD thesis, Dept. of Electronics and Computer Science, Univ. of Southampton, UK, 1997.
- [588] J. C. Cheung, *Adaptive Equalisers for Wideband TDMA Mobile Radio*. PhD thesis, Dept. of Electronics and Computer Science, Univ. of Southampton, UK, 1991.
- [589] N. Färber, E. Steinbach, and B. Girod, "Robust h.263 compatible transmission for mobile video server access," in *Proc of First International Workshop on Wireless Image/Video Communications*, (Loughborough, UK), pp. 122–124, 4–5 September 1996.
- [590] A. Sadka, F. Eryurtlu, and A. Kondo, "Improved performance H.263 under erroneous transmission conditions," *Electronics Letters*, vol. 33, pp. 122–124, Jan 16 1997.
- [591] A. Klein, R. Pirhonen, J. Skoeld, and R. Suoranta, "FRAMES multiple access mode 1 - wideband TDMA with and without spreading," in *Proceedings of IEEE International Symposium on Personal, Indoor and Mobile Radio Communications, PIMRC'97* [649], pp. 37–41.
- [592] J. M. Torrance and L. Hanzo, "Latency and networking aspects of adaptive modems over slow indoors rayleigh fading channels," *IEEE Tr. on Veh. Techn.*, vol. 48, no. 4, pp. 1237–1251, 1998.
- [593] L. Hanzo, P. Cherriman, and J. Streit, "Video compression and communications over wireless channels: From second to third generation systems, WLANs and beyond." Book in preparation<sup>16</sup>.
- [594] P. Cherriman, C. Wong, and L. Hanzo, "Multi-mode H.263-assisted video telephony using wideband adaptive burst-by-burst modems," Core programme deliverable - terminals work area, Mobile VCE, UK, 1998.
- [595] P. Cherriman, T. Keller, and L. Hanzo, "Orthogonal frequency division multiplex transmission of H.263 encoded video over highly frequency-selective wireless networks." Accepted for publication in *IEEE Trans. on Circuits and Systems for Video Technology*, 1998.
- [596] M. Sandell, J.-J. van de Beek, and P. O. Börjesson, "Timing and frequency synchronisation in OFDM systems using the cyclic prefix," in *Proceedings of International Symposium on Synchronisation*, (Essen, Germany), pp. 16–19, 14–15 Dec 1995.

<sup>16</sup>For detailed contents please refer to <http://www-mobile.ecs.soton.ac.uk>

- [597] J. D. Marca and N. Jayant, "An algorithm for assigning binary indices to the codevectors of a multi-dimensional quantizer," in *Proceedings of IEEE International Conference on Communications 1987*, (Seattle, WA, USA), pp. 1128–1132, IEEE, 7–10 June 1987.
- [598] T. Keller and L. Hanzo, "Orthogonal frequency division multiplex synchronisation techniques for wireless local area networks," in *Proc. of IEEE International Symposium on Personal, Indoor, and Mobile Radio Communications (PIMRC'96)* [666], pp. 963–967.
- [599] J. Brecht and L. Hanzo, "Statistical packet assignment multiple access for wireless asynchronous transfer mode systems," in *Proceeding of ACTS Mobile Communication Summit '97* [661].
- [600] K. Pehkonen, H. Holma, I. Keskitalo, E. Nikula, and T. Westman, "Performance analysis of TDMA and CDMA based air interface solutions for UMTS high bit rate services," in *Proceedings of IEEE International Symposium on Personal, Indoor and Mobile Radio Communications, PIMRC'97* [649], pp. 22–26.
- [601] K. Pajukoski and J. Savusalo, "Wideband CDMA test system," in *Proceedings of IEEE International Symposium on Personal, Indoor and Mobile Radio Communications, PIMRC'97* [649], pp. 669–673.
- [602] R. Blahut, "Transform techniques for error control codes," *IBM J. Res. Dev.*, vol. 23, pp. 299–315, May 1979.
- [603] J. M. Torrance, L. Hanzo, and T. Keller, "Interference aspects of adaptive modems over slow rayleigh fading channels," *IEEE Tr. on Veh. Techn.*, vol. 48, pp. 1527–1545, Sept 1999.
- [604] T. Liew, C. Wong, and L. Hanzo, "Block turbo coded burst-by-burst adaptive modems," in *Proceeding of Microcoll'99, Budapest, Hungary*, pp. 59–62, 21-24 March 1999.
- [605] V. K. N. Lau and M. D. Macleod, "Variable rate adaptive trellis coded QAM for high bandwidth efficiency applications in rayleigh fading channels," in *Proceedings of IEEE Vehicular Technology Conference (VTC'98)* [652], pp. 348–352.
- [606] M. Yee and L. Hanzo, "Upper-bound performance of radial basis function decision feedback equalised burst-by-burst adaptive modulation," in *Proceedings of ECMCS'99*, (Krakow, Poland), 24-26 June 1999.
- [607] T. Keller and L. Hanzo, "Adaptive orthogonal frequency division multiplexing schemes," in *Proceeding of ACTS Mobile Communication Summit '98* [659], pp. 794–799.
- [608] E. L. Kuan, C. H. Wong, and L. Hanzo, "Burst-by-burst adaptive joint detection CDMA," in *Proceeding of VTC'99 (Spring)* [657].
- [609] A. Czylik, "Adaptive OFDM for wideband radio channels," in *Proceeding of IEEE Global Telecommunications Conference, Globecom 96* [651], pp. 713–718.
- [610] R. F. H. Fischer and J. B. Huber, "A new loading algorithm for discrete multi-tone transmission," in *Proceeding of IEEE Global Telecommunications Conference, Globecom 96* [651].



- [611] P. S. Chow, J. M. Cioffi, and J. A. C. Bingham, "A practical discrete multi-tone transceiver loading algorithm for data transmission over spectrally shaped channels," *IEEE Trans. on Communications*, vol. 48, pp. 772–775, 1995.
- [612] H. Rohling and R. Grünheid, "Performance of an OFDM-TDMA mobile communication system," in *Proceeding of IEEE Global Telecommunications Conference, Globecom 96* [651], pp. 1589–1593.
- [613] K. Fazel, S. Kaiser, P. Robertson, and M. J. Ruf, "A concept of digital terrestrial television broadcasting," *Wireless Personal Communications*, vol. 2, pp. 9–27, 1995.
- [614] H. Sari, G. Karam, and I. Jeanclaude, "Transmission techniques for digital terrestrial tv broadcasting," *IEEE Communications Magazine*, pp. 100–109, February 1995.
- [615] J. Borowski, S. Zeisberg, J. Hübner, K. Koorra, E. Bogenfeld, and B. Kull, "Performance of OFDM and comparable single carrier system in MEDIAN demonstrator 60GHz channel," in *Proceeding of ACTS Mobile Communication Summit '97* [661], pp. 653–658.
- [616] P. Cherriman, T. Keller, and L. Hanzo, "Constant-rate turbo-coded and block-coded orthogonal frequency division multiplex videophony over UMTS," in *Proceeding of Globecom '98* [660], pp. 2848–2852.
- [617] J. Woodard, T. Keller, and L. Hanzo, "Turbo-coded orthogonal frequency division multiplex transmission of 8 kbps encoded speech," in *Proceeding of ACTS Mobile Communication Summit '97* [661], pp. 894–899.
- [618] Y. Li and N. R. Sollenberger, "Interference suppression in OFDM systems using adaptive antenna arrays," in *Proceeding of Globecom '98* [660], pp. 213–218.
- [619] F. W. Vook and K. L. Baum, "Adaptive antennas for OFDM," in *Proceedings of IEEE Vehicular Technology Conference (VTC'98)* [652], pp. 608–610.
- [620] ETSI, *Digital Video Broadcasting (DVB); Framing structure, channel coding and modulation for digital terrestrial television*, August 1997. EN 300 744 V1.1.2.
- [621] ETSI, *Digital Video Broadcasting (DVB); Framing structure, channel coding and modulation for cable systems*, December 1997. EN 300 429 V1.2.1.
- [622] ETSI, *Digital Video Broadcasting (DVB); Framing structure, channel coding and modulation for 11/12 GHz Satellite Services*, August 1997. EN 300 421 V1.1.2.
- [623] S. O'Leary and D. Priestly, "Mobile broadcasting of DVB-T signals," *IEEE Transactions on Broadcasting*, vol. 44, pp. 346–352, September 1998.
- [624] W.-C. Lee, H.-M. Park, K.-J. Kang, and K.-B. Kim, "Performance analysis of viterbi decoder using channel state information in COFDM system," *IEEE Transactions on Broadcasting*, vol. 44, pp. 488–496, December 1998.
- [625] S. O'Leary, "Hierarchical transmission and COFDM systems," *IEEE Transactions on Broadcasting*, vol. 43, pp. 166–174, June 1997.

- [626] L. Thibault and M. T. Le, "Performance evaluation of COFDM for digital audio broadcasting Part I: parametric study," *IEEE Transactions on Broadcasting*, vol. 43, pp. 64–75, March 1997.
- [627] B. G. Haskell, A. Puri, and A. N. Netravali, *Digital Video: An Introduction To MPEG-2*. Digital Multimedia Standards Series, Chapman & Hall, 1997.
- [628] *ISO/IEC 13818-2: Information Technology - Generic Coding of Moving Pictures and Associated Audio Information - Part 2: Video*, March 1995.
- [629] P. Shelswell, "The COFDM modulation system: the heart of digital audio broadcasting," *Electronics & Communication Engineering Journal*, vol. 7, pp. 127–136, June 1995.
- [630] M. Failli, "Digital land mobile radio communications COST 207," tech. rep., European Commission, 1989.
- [631] A. Aravind, M. R. Civanlar, and A. R. Reibman, "Packet loss resilience of MPEG-2 scalable video coding algorithms," *IEEE Transaction On Circuits And Systems For Video Technology*, vol. 6, pp. 426–435, October 1996.
- [632] G. Reali, G. Baruffa, S. Cacopardi, and F. Frescura, "Enhancing satellite broadcasting services using multiresolution modulations," *IEEE Transactions on Broadcasting*, vol. 44, pp. 497–506, December 1998.
- [633] Y. Hsu, Y. Chen, C. Huang, and M. Sun, "MPEG-2 spatial scalable coding and transport stream error concealment for satellite TV broadcasting using Ka-band," *IEEE Transactions on Broadcasting*, vol. 44, pp. 77–86, March 1998.
- [634] L. Atzori, F. D. Natale, M. D. Gregario, and D. Giusto, "Multimedia information broadcasting using digital TV channels," *IEEE Transactions on Broadcasting*, vol. 43, pp. 383–392, December 1997.
- [635] W. Sohn, O. Kwon, and J. Chae, "Digital DBS system design and implementation for TV and data broadcasting using Koreasat," *IEEE Transactions on Broadcasting*, vol. 44, pp. 316–323, September 1998.
- [636] C. Berrou and A. Glavieux, "Near optimum error correcting coding and decoding: turbo codes," *IEEE Transactions on Communications*, vol. 44, pp. 1261–1271, October 1996.
- [637] J. Goldhirsh and W. J. Vogel, "Mobile satellite system fade statistics for shadowing and multipath from roadside trees at UHF and L-band," *IEEE Transactions on Antennas and Propagation*, vol. 37, pp. 489–498, April 1989.
- [638] W. Vogel and J. Goldhirsh, "Multipath fading at L band for low elevation angle, land mobile satellite scenarios," *IEEE Journal on Selected Areas in Communications*, vol. 13, pp. 197–204, February 1995.
- [639] W. Vogel and G. Torrence, "Propagation measurements for satellite radio reception inside buildings," *IEEE Transactions on Antennas and Propagation*, vol. 41, pp. 954–961, July 1993.
- [640] W. Vogel and U. Hong, "Measurement and modelling of land mobile satellite propagation at UHF and L-band," *IEEE Transactions on Antennas and Propagation*, vol. 36, pp. 707–719, May 1988.

- [641] K. Wesolowsky, "Analysis and properties of the modified constant modulus algorithm for blind equalization," *European Transactions on Telecommunication*, vol. 3, pp. 225–230, May–June 1992.
- [642] M. Goursat and A. Benveniste, "Blind equalizers," *IEEE Transactions on Communications*, vol. COM-28, pp. 871–883, August 1984.
- [643] G. Picchi and G. Prati, "Blind equalization and carrier recovery using a "stop-and-go" decision-directed algorithm," *IEEE Transactions on Communications*, vol. COM-35, pp. 877–887, September 1987.
- [644] A. Polydoros, R. Raheli, and C. Tzou, "Per-survivor processing: a general approach to MLSE in uncertain environments," *IEEE Transactions on Communications*, vol. COM-43, pp. 354–364, February–April 1995.
- [645] D. N. Godard, "Self-recovering equalization and carrier tracking in two-dimensional data communication systems," *IEEE Transactions on Communications*, vol. COM-28, pp. 1867–1875, November 1980.
- [646] Y. Sato, "A method of self-recovering equalization for multilevel amplitude-modulation systems," *IEEE Transactions on Communications*, vol. COM-23, pp. 679–682, June 1975.
- [647] Z. Ding, R. A. Kennedy, B. D. O. Anderson, and R. C. Johnson, "Ill-convergence of Godard blind equalizers in data communications systems," *IEEE Transactions on Communications*, vol. COM-39, pp. 1313–1327, September 1991.
- [648] C.S.Lee, T. Keller, and L. Hanzo, "Turbo-coded hierarchical and non-hierarchical mobile digital video broadcasting," *IEEE Transaction on Broadcasting*, 1999. Submitted for publication.
- [649] IEEE, *Proceedings of IEEE International Symposium on Personal, Indoor and Mobile Radio Communications, PIMRC'97*, (Marina Congress Centre, Helsinki, Finland), 1–4 Sept 1997.
- [650] IEEE, *Proceedings of International Conference on Acoustics, Speech, and Signal Processing, ICASSP'80*, (Denver, Colorado, USA), 9–11 April 1980.
- [651] IEEE, *Proceeding of IEEE Global Telecommunications Conference, Globecom 96*, (London, UK), 18–22 Nov 1996.
- [652] IEEE, *Proceedings of IEEE Vehicular Technology Conference (VTC'98)*, (Ottawa, Canada), May 1998.
- [653] IEEE, *Proceedings of IEEE International Symposium on Spread Spectrum Techniques and Application (ISSSTA'98)*, (Sun City, South Africa), Sept 1998.
- [654] R. I. Damper, W. Hall, and J. W. Richards, eds., *Proceedings of IEEE International Symposium of Multimedia Technologies and Future Applications*, (Southampton, England), Prentech Press, April 1993.
- [655] IEEE, *Proceedings of International Conference on Acoustics, Speech, and Signal Processing, ICASSP'92*, March 1992.
- [656] IEEE, *Proceedings of the IEEE International Conference on Acoustics, Speech and Signal Processing (ICASSP'94)*, (Adelaide, Australia), 19–22 Apr 1994.

**BIBLIOGRAPHY**

1103

- [657] IEEE, *Proceeding of VTC'99 (Spring)*, (Houston, Texas, USA), 16–20 May 1999.
- [658] ACTS, *Proceeding of ACTS Mobile Communication Summit '99*, (Sorrento, Italy), June 8–11 1999.
- [659] ACTS, *Proceeding of ACTS Mobile Communication Summit '98*, (Rhodes, Greece), 8–11 June 1998.
- [660] IEEE, *Proceeding of Globecom'98*, (Sydney, Australia), 8–12 Nov 1998.
- [661] ACTS, *Proceeding of ACTS Mobile Communication Summit '97*, (Aalborg, Denmark), 7–10 October 1997.
- [662] IEEE, *Proc. of IEEE ICCS'96 / ISPACS'96*, (Singapore), 25–29 November 1996.
- [663] IEEE, *Proceedings of IEEE VTC '94*, (Stockholm, Sweden), June 8–10 1994.
- [664] IEEE, *Proceedings of IEEE VTC '96*, (Atlanta, GA, USA), 1996.
- [665] IEEE, *Proceedings of IEEE VTC '97*, (Phoenix, Arizona, USA), 4–7 May 1997.
- [666] IEEE, *Proc. of IEEE International Symposium on Personal, Indoor, and Mobile Radio Communications (PIMRC'96)*, (Taipei, Taiwan), 15–18 October 1996.
- [667] IEEE, *Proceedings of the IEEE International Conference on Acoustics, Speech and Signal Processing (ICASSP'96)*, (Atlanta, USA), May 7–10 1996.
- [668] *Proc. of International Workshop on Coding Techniques for Very Low Bit-rate Video (VLBV'95)*, (Shinagawa, Tokyo, Japan), November 8–10 1995.
- [669] IEEE, *Proceedings of IEEE VTC '93*, (Secaucus, NJ, USA), May 18–20 1993.